A Study of Structure, Electrical and Optical Properties of some Vanadate Glasses

by

A.A.Hosseini

B.Sc., M.Tech.

A thesis submitted to Brunel University,

Uxbridge, Middlesex, U.K.

for the degree of Doctor of Philosophy

in the Physics Department

March 1982

This work was carried out under the supervision

of C.A.Hogarth Ph.D, D.Sc., F.Inst.P.

Head of Physics Department Brunel University

To my parents

without whose encouragement and support

this work would not have been possible.

Abstract

Studies of semiconducting glasses have become of great interest in recent years because of their importance in the theory of solid state physics and in their applicability to electronic devices. Of these classes of materials the transition metal oxide glasses are much the most thoroughly studied. In these glasses the transition metal oxide e.g. V_2O_5 - TiO_2 - MoO_3, WO_3, CuO is a major constituent i.e > 50 mol%.

We start this work with a discussion about a critical review of the history, formation and modern theory of non-crystalline semiconductors in general and glassy state in particular. The aim of the experimental work in present study is to check the validity of the theories and models proposed so far to explain the origin and the nature of the charge carriers, structure, electrical and optical properties of some transition metal oxide glasses based on vanadium pentoxide.

For this purpose series of binary V_2O_5 - P_2O_5 glass samples containing 50 to 90 mol% V_2O_5 as well as ternary V_2O_5 - P_2O_5 - TeO_2 glasses containing 60 mol% V_2O_5, (40-x) mol% P_2O_5 and x mol% TeO_2 in which x varies from 5 to 35 were prepared by normal cooling from the melt. It was found that the glass forming region of the system under consideration is fairly large and in binary V_2O_5 - P_2O_5 systems, glass with up to 95 mol% V_2O_5 could be prepared.

Density measurements indicate that in binary V_2O_5 - P_2O_5 glasses the density increases linearly with increasing V_2O_5 content and in ternary V_2O_5 - P_2O_5 - TeO_2 systems density increases with increasing TeO_2 content. It was also found that the density of both systems are affected by annealing temperature.

Electron spin resonance (E.S.R.) studies show that in vanadate glasses, the vanadium exists in more than one valency

state mainly V^{5+} and V^{4+} of which V^{4+} is paramagnetic and detectable by E.S.R. This could be taken as some evidence of a hopping conduction mechanism in vanadate glasses and conduction is due to transfer of charge form V^{4+} to V^{5+} ions and this is discussed in the terms of small polaron.

It is found that the conduction in these glasses is Ohmic up to a field of the order of $4 \times 10^{5} Vcm^{-1}$ with an activation energy range from 0.31 to 0.48 e.V depending on composition and independent of temperatures in our range of temperature (above room temperature). Above this field conduction becomes non-Ohmic which is found to be due to lowering the potential barrier of the carriers at high electric field as was predicted by Poole and Frenkel. Memory switching is observed in thin blown film samples of both binary and ternary glass systems, which is associated with field-induced crystallization of a localized region and formation of conductive channel in the switched area due to self heating effect. In other words the conducting zone consists of VO_2 crystals which possess more metal-like conductivity.

Infra-red absorption spectra of these glasses revealed that some of the absorption bands of glasses and crystalline V_2O_5 are similar which is some evidence that the vanadium ions exists in six-fold co-ordination in disordered glassy systems as well as ordered crystalline V_2O_5.

The fundamental absorption edge of these glasses occurs in the short wave length region of the visible and is dependent on composition, and the fundamental absorption arises form direct forbidden transitions and occurs at a photon energy of about 1.9 - 2.6 e.V depending on composition. The absorption edge in these glasses is found to be of the same order of magnitude as that in crystalline V_2O_5.

Acknowledgement

I wish to express my deepest and sincere gratitude to my supervisor, Professor C.A.Hogarth, Head of Physics Department for his encouragement, guidance and constructive discussion throughout this study.

I would like to express my thanks to Dr.K.A.K.Lott from the Chemistry Department for his constant help and useful discussion during the E.S.R. measurements and chemical analysis.

Thanks are also due to Dr.D.Walter, Dr.S.Woodisse and Mr.C.M.Robinson for their help during the I.R. optical measurements.

I would also like to thank Mr.K.R.Schlachter and Mr.L.Lightowler for their assistance in the designing and construction of the vacuum system sample holder and other related instruments used in this work.

I wish to thank Mr.L.E.L.Chandrasekera, Mr.M.Krasso, Mr.R.Stevens, Mr.M.Varga and Mr.H.Brown of the technical staff of the Physics Department for their help during the experimental work.

I should also like to thank my colleagues and friends, especially Dr.R.Varshochi, Dr.E.Masood, Dr.I.H.I.Rashed, Mr.A.A.Higazi and Mr.N.Patel for their useful discussion.

I am especially indebted to my friend Miss.A.J.Reed for typing this thesis.

CONTENTS

Page

Chapter I

Amorphous Semiconductor Glass

1-1 General Introduction

By the introduction of new elements of the periodic system into its conventional chemical composition, glass acquired so far unexpected features which made possible its wider use ranging from glass fibre to the glass electrode or protective plates in nuclear physics.

Modern combinations of glass with other materials such as metals in machinery and electrical engineering, and with plastics in laminated products did not reduce its primary importance. On the contrary, the role of glass has been even more emphasised. Today modern technology of glass is based on the constantly developing nature of glass. To answer the question,"what is glass?" we refer to different definitions by several authors.

a) The general definition by Morey[1].

A glass is an inorganic substance in a condition which is continuous with, and analogous to the liquid state of that substance, but which as a result of having been cooled from a fused condition, has attained so high a degree of viscosity as to be for all practical purposes rigid.

b) Glass is an inorganic product of fusion which is cooled to a rigid condition without crystallization.[2]

c) There is a definition of glass in the Marshall Cavendish Encyclopedia. Glass is not solid - it is a molten liquid of materials which have been cooled to ordinary temperature when it becomes very viscous and stiff with all the normal properties of a solid.

d) Fanderbik[3] has the following definition of glass.
Its properties are to a considerable extent dependent on its thermal history (on the manner by which the glass has passed from the plastic into the rigid state).

Glasses with different compositions have different properties. It may be said of glasses in general that their properties depend on the dimensions and arrangement of ions in the silicate network. In general we can say.

I. Glasses are substances rigid at low temperature and plastic at high temperature.
II. With regard to their chemical composition they are non-stoichiometric substances.
III. They are optically isotropic.
IV. They transmit light of different wave-lengths.
V. Glasses are not crystalline and produce no sharp patterns with x-rays.
VI. They may be regarded as undercooled liquids in a metastable

state and their properties depend therefore on the thermal history of the specimen.

VII. The basic structural units consist of cations with anions co-ordinated around them with lack of periodicity.

VIII. All glasses exhibit a common characteristic such as the transformation zone between the rigid and plastic state.

IX. Due to their strong tendency to polymerization and aggregation, glass may contain groups of basic structural units arranged in various degrees of regularity.

An understanding of the phenomenon of glass formation is important for a number of reasons. First it is of scientific importance to understand the chemical, structural and other factors which define the limits within which any type of material can exist. Secondly, the problem is of practical importance when developing new glass compositions. We need some knowledge of the factors which determine the region of glass formation in the system with which we are concerned, and also of the stability of the glasses within the region. The phenomenon of glass formation is still far from being completely understood. One of the main reasons is that it is impossible at the present time to obtain sufficiently detailed information on the structure of the liquids from which glasses are produced.

1-2 The history of Glass Production

Glass is one of the most common materials in normal life. Many millions of tons are being produced every year. Although it is not known where, when or how glass was first manufactured, there is some evidence that fragments of glasses have been found mostly in Egypt where glass was manufactured around 2500 BC.

A volcanic glass called "obsidian" was created by nature a long time before man learned how to make glass. This natural glass was used to make arrow heads, knives and similar tools.

The first use of glass in architecture occurred during the time of the Roman Empire. Glass mosaic was used for the decoration of walls and was also used in the windows of houses. One of the oldest glass windows that has been found was used in the bath houses in Pompeii. It is circular glass sheets with a diameter of 5 inches.

The Roman bottle-glass industry developed and expanded after the middle of the first century. The first blown glass was for the luxury trade. Plain shapes in natural metal soon followed and for the export of perfume, small flasks were made from the beginning of the century. Apart from the flasks, the use of glass in place of pottery for the transport and storage of liquids did not become common until the next few centuries.

Recently a group of glass vessels belonging to the Sasanian period located in the Iraqi museum in Baghdad are said to come from a place called Tell Mahuz near Kirkuk in the north of Iraq.(4)

Most of the important processes for shaping glass at high temperature including blowing, drawing, moulding and casting were well established by the third century and the techniques for making and shaping articles of glass go back to Roman times.

The glass blowing technique was invented by Syrian glass-makers about the first century. This was the beginning of manufacturing of plate glass, windows and mirrors. The Syrians and Alexandrians shared the glass making industry and the first use of flat glass in architecture during the time of the Roman Empire, about the first century and they spread their techniques in the eastern empire and around the Mediteranian Sea.

Making coloured glasses for decoration and windows originated in the sixth century(5). In the twelfth century Venice became the great centre of glass making in Europe. Egyptian and Alexandrian glass-makers were the first who made specific coloured glasses by adding particular metallic oxides to the raw material, for example, copper to the molten glass to make it blue or iron oxide for a brown or black colour.

For the first time in the fourteenth century, Venetian glass-makers started to make mirrors by coating plates of glass

with tin and mercury[6]. There is evidence that different glass-making techniques came to Italy from Venice and from there to France, Spain, Portugal, Austria and Germany. By the end of the sixteenth century the Venetian technique of glass making spread to almost every country in Europe. Glass making was introduced to England before the Elizabethan reign. During the first half of the seventeenth century English factories were leading glass manufacturing in the world. A special kind of glass called lead-crystal glass was produced first in England in 1793 and by the end of the eighteenth century, England and Wales were the main countries for the production of so called lead-crystal glasses.

It can be said that classical research on glass started from the early part of the nineteenth century, when Micheal Faraday worked on optical glasses for the first time [7]. He added boric oxide in the melting of glass for the production of many new optical glasses and he was the first to describe glass as a solution of different compounds rather than a rigid chemical compound.

Winkelman and Schott were the first people who started work on the relationships between the physical and chemical properties of a glass[8].

In Britain the manufacture of pure fused silica direct from the raw material has been carried out by the Thermal Syndicate

since early in the twentieth century. Later this company spread the manufacture to West Germany and America.

Pure fused silica, the purest form of glass, is very resistant to high temperatures, thermal shock and acid attack, is a good electrical insulator and transmits ultra-violet light. It has many applications throughout the chemical, electrical and electronics industries. The raw material for this glass consists either of sand, which is translucent when fused, or quartz crystal, which is transparent when fused. This company imports sand from France and quartz crystals from Brazil. After the removal of impurities, fusion takes place at over 2,000^{o}C in a special type of electrical furnace. This company also manufactured the high temperature refactories on synthetic fused silica, the purest fused silica in the world.

The modern history of glass began in the middle of the nineteenth century[9]. In the meantime there was a search for the development of new glasses having specific physical and chemical properties. Soon after Michael Faraday, who was the first to state that glass cannot be regarded as normal chemical compounds,[10] Winkelman and Schott started to work on the properties of silicate glasses.

In the early twentieth century, Tamman[11] started to work on some of the properties of glasses, such as glass transition, viscosity relationships between crystalline rate and viscosity of

glass and the reasons for glass formation. Also at the same time, much work was done in the department of Glass Technology, Sheffield University, on the properties of commercial and laboratory glasses. About the same time Zachariasen explained why some elements are glass-formers and discussed the structure of glass in terms of chemical bonding.

It can be said that during the last thirty years, glass research progressed very rapidly. Properties such as electronic conductivity, internal friction, glass electrode surface reactions, ion exchange, phase separation, structure of glass, etc were the main topics of this research.

In 1958 Anderson[12] gave his idea about localization of the carriers in the absence of electron-phonon interaction. Miller and Abrahams[13] in 1960 suggested that the transport of the carriers is because of energy in electron-phonon interactions.

Kubo[14] suggested that the localization can be caused by a strong magnetic field. Wannier[15] suggested that a strong electric field can lead to localization. Some of the work which has been done recently on the electrical and optical properties of glasses as a semiconductor and also structure of glass are discussed.

In 1967 Kennedy and Mackenzie[16], published a paper about the role of the network-former in semiconducting oxide glasses. Electrical noise in semiconducting oxide glasses were discussed by Sayer and Prasad in 1978[17].

Mansingh and Dhawan[18] worked on molybdenum doping of semiconducting vandium phosphate glasses in 1978. Hopping conduction at high electric fields in transition metal ion glasses was discussed by Austin and Sayer[19] in 1973.

G.W.Anderson[20] published a paper in 1969 about optical absorption of vanadate glasses. In 1969 Mott[21] discussed the conduction and switching phenomena in non-crystalline materials.

1-3 The Physical Nature of Glass

Glass is melted from a batch consisting entirely of fresh raw materials. In nearly all glasses in the stage of glass-forming process, there is some rejected or waste material, often because some of the material has to be removed from the shape originally formed.

During the glass-melting process when the temperature rises to $1,300^{o}$ - $1,600^{o}C$, depending on composition, many complex physical and chemical changes occur, although in many cases the temperatures are below the individual melting points of some of the batch constituents. The initial changes include the evaporation of water contained in the batch as water of crystallization and the decomposition of carbonates, sulphates, etc with the release of CO_2, SO_2, SO_3 etc. Some of the raw materials melt as the temperature rises and liquids formed begin to dissolve the other more refractory constituents.

The final stage of melting known as refining the glass, involves the removal of residual bubbles of gas liberated by raw materials and trapped in the highly viscous molten solution.

When liquids of materials which have a viscosity about the same as that of water (.02 - 0.1 poise) at the melting temperature are cooled,rapid crystallization takes place at the melting point., even when the cooling is very rapid. A number of materials exist which melt to form very viscous liquids (10^2 - 10^8 poise). If the liquid phases of these materials are maintained for some time at a temperature a little below the freezing point it will slowly crystallize, but if instead of holding the temperature constant, we continuously cool the liquid from a temperature above the freezing point, crystallization may or may not occur, depending on the rate of cooling. In this case if the rate of cooling is very slow crystallization takes place, but if the cooling is fast it is possible to reduce the temperature to any desired extent without crystallization occurring. At the usual melting temperature glasses are highly viscous liquids. Typically, their viscosity is around 10^2 poise. As they cool their viscosity increases progressively and continuously.

1-4 Glass Transformation

A necessary condition is that the liquid should be cooled rapidly enough so that detectable nucleation and crystal growth

does not occur and in this sense glass formation is a kinetic process. It is possible to make rough estimates of the cooling rate which must be exceeded in order to encourage glass formation in particular liquids. Sargeant and Roy suggested the following formula for the rate of cooling,

$$R_c = 2 \times 10^{-6} \frac{T_m^{\,2} R}{V.\mu} \qquad (1\text{-}1)$$

Where R_c is the rate of cooling (deg/s), T_m is the thermodynamic melting temperature, R the gas constant, V the molar volume and μ is the viscosity.

Fig.(1.1) shows the changes in specific volume that would occur as a simple imaginary substance is cooled from the liquid state so as to form either a crystal or glass.

Starting from point A on the graph, where the material is in a liquid state, the volume of a given mass decreases steadily with decreasing the temperature along the line AB. If the rate of cooling is sufficiently slow and nuclei are present in the melt, crystallization will take place at the temperature T_f accompanied by a decrease in volume along the line BC. In this case at temperature T_f an abrupt change occurs in volume and in other physical properties of the material. On further cooling the crystalline material contracts along CD.

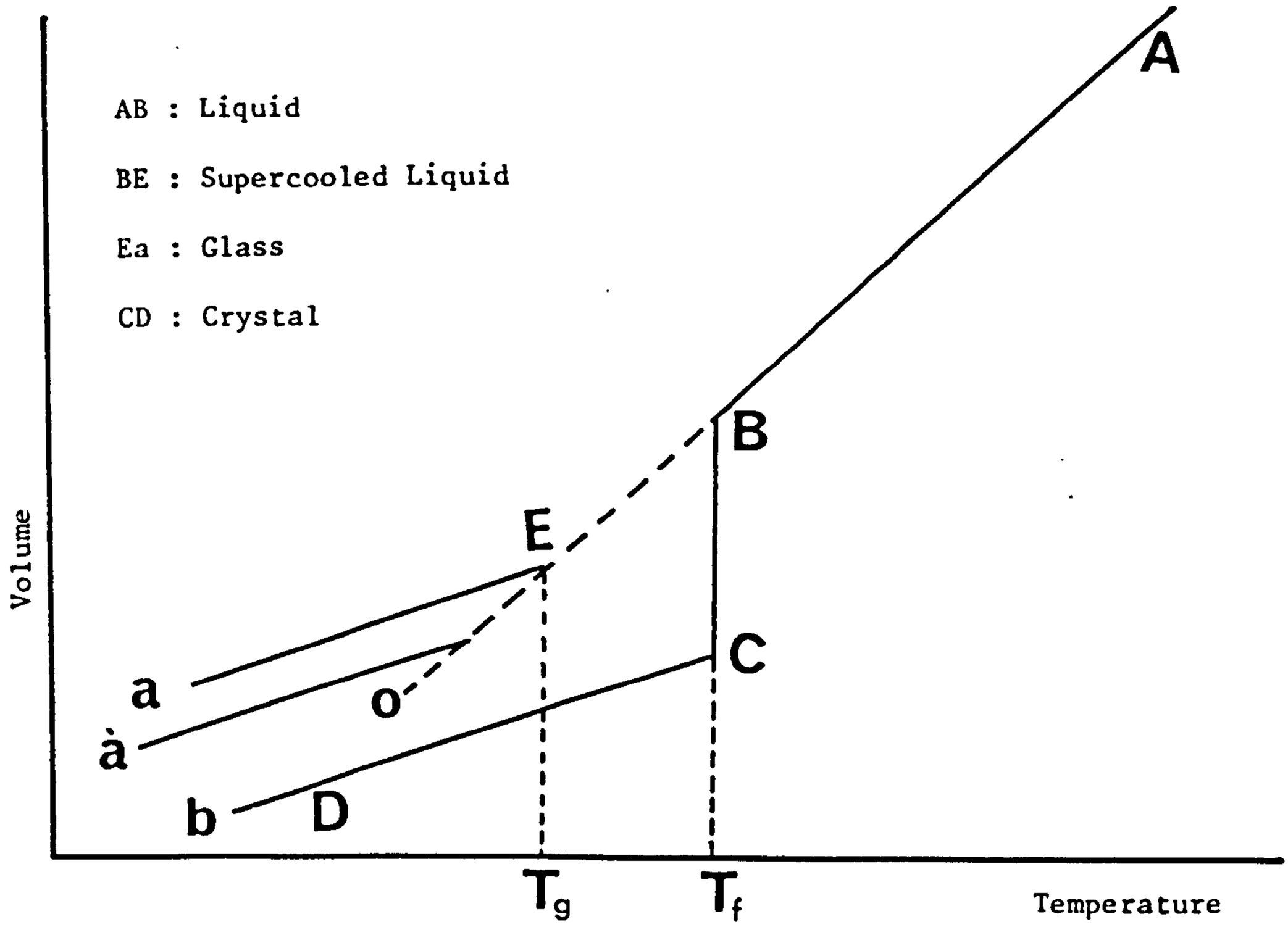

Fig.(1.1) Relation Between Glassy, Liquid and Solid State

a) glass fast cooling a') glass slow cooling b) crystal

If the liquid is cooled rapidly there is no abrupt change in volume at any temperature, instead the slope of the volume - temperature curve changes continuously over a range of temperature. As cooling continues, the volume of the now supercooled liquid decreases along the line BE which is a smooth continuation of AB. At a certain temperature T_g the volume -

temperature curve of the supercooled liquid undergoes a marked change in direction and continues almost parallel to the contraction curve of the crystalline form.

The temperature T_g at which the bend occurs is called the transformation or glass-transition temperature. The transition from the liquid to the glassy state takes place over a range of temperature. There is no clearly defined transition temperature which could be compared with the melting point of a crystalline solid.

At a low temperature the rate of change of volume with temperature is similar for both the glass and the crystalline material, but the absolute magnitude of the specific volume of the glass is much larger and it also varies with the rate at which the original liquid was cooled. Below T_g the material is described as glass. Between T_g and T_f the material is a supercooled liquid. At T_g the viscosity is extremely high (about 10^{13} poise).

An important difference between the supercooled liquid and the glass is made clear by considering what happens when the temperature of the glass is held constant at T a little below T_g. It is found that the volume decreases slowly until eventually it reaches a point O which is a smooth continuation of the curve of the supercooled liquid. It has been found that other properties of the glass also change with time around the transition

temperature. This process is known as stabilization.

1-5 Viscosity

Viscous flow in liquids can be treated as a rate process limited by potential energy barriers and the coefficient of viscosity might therefore be expected to vary with temperature (Jones)[22].

Viscosity varies with temperature according to the following equation

$$\mu = A \exp. \frac{B}{T} \qquad (1\text{-}2)$$

Where μ is the viscosity, T is the absolute temperature, A and B are constant. A can be shown to be proportional to the size of the units which flow. These units might be individual atoms or molecules according to the nature of the substance.

1-6 Working Range of Glass in Terms of Viscosity

In glass manufacture the molten glass is usually removed from the furnace at a viscosity of about 400 - 1,000 Poises, and working or shaping ceases when the viscosity reaches 10^8 poises. These are the two limiting viscosities which fix the working range of the glass.

If a molten glass with a viscosity of about 10^3 poises is at temperature T_1 and after cooling to temperature T_2, in which the viscosity is about 10^8, the working range of this glass is (T_1 - T_2).

The viscosity of glass at the melting temperature is about 10^2 poises when being pressed into a mould or drawn into tubing or rod, the viscosity is between 10^3 or 10^6. The softening point is the temperature at which the viscosity is $10^{7.6}$ Poises. The strain point is the temperature at which the viscosity is $10^{14.5}$, and the annealing point corresponds to the viscosity of $10^{13.4}$.

A series of viscosity - temperature curves for some of the glasses are shown in Fig.(1.2).

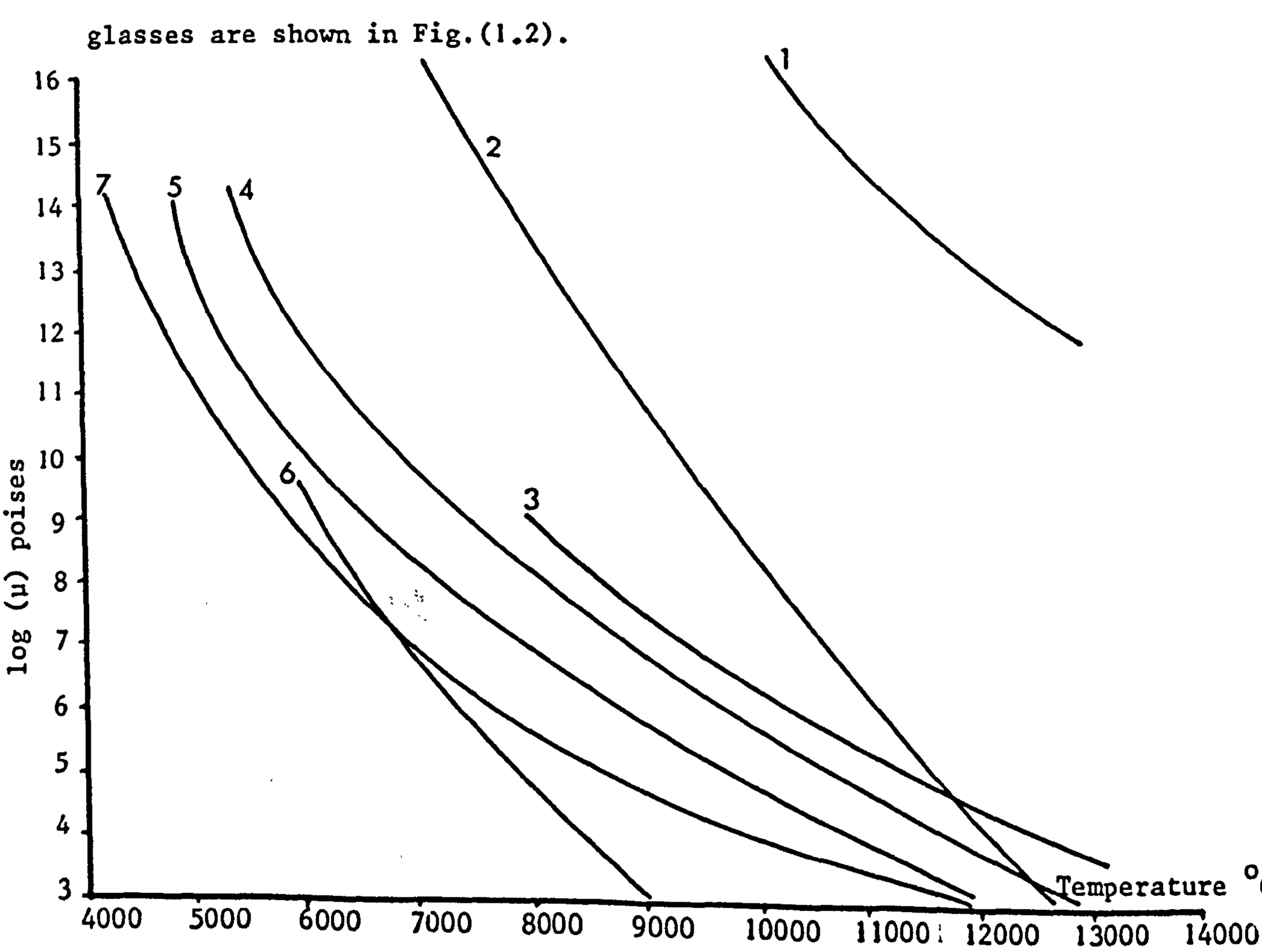

Fig.(1.2) Variation of log (μ) with Temperature for Various Glasses Listed in Table(1.1) μ is the Coefficient of Viscosity[23]

Glass	Materials	Applications
1	Fused Silica	
2	Extra Hard Alkali Free Glass	High Pressure Mercury Vapour Lamps
3	Borasilicate Glass	Chemical Apparatus
4	Borasilicate Glass	High Viscosity Lamps and Valves
5	Soft Soda Glass	Lamp and Valve Bulbs
6	Special Glass	Sodium Vapour Lamps
7	Lead Glass	Lamps and Valves

Table(1.1)

1-7 Devitrification Process in Glass

The process by which the growth of crystalline material takes place in glass is called devitrification. The devitrification process in glass should be prevented if the purpose is not the formation of glass-ceramics. If the devitrification occurs during the shaping of the glass it can lead to sudden and unpredictable change of viscosity.

Devitrification can occur for a number of reasons:-

a) Devitrification due to the selection of an unsuitable glass composition. Therefore the composition of glass should be carefully chosen so as to be resistant to devitrification.

b) Devitrification during the shaping of glass is unlikely to result in the very fine grained structure which is required, but is more likely to give rise to a coarse structure consisting of relatively few large crystals.

c) Devitrification can take place during reheating the glass. In this case the surface of the glass plays an important

role, since crystallization takes place much more rapidly at the surface than in the body of the glass. One of the reasons why crystal development commences at the surface, may be that the chemical composition of the glass at the surface differs from that of the interior. Because the loss of volatile constituents from the glass surface during melting could account for the composition difference, and those constituents which lower the surface energy tend to be concentrated at the surface.

d) The presence of gas bubbles or foreign particles within the interior of the glass could also lead to more rapid devitrification in the surrounding regions.

Preston[24] in 1940 showed that below the temperature of maximum growth, a relationship existed between the growth rate of devitrite crystals and the temperature of the liquids. This relationship is of the form

$$I = \frac{K}{\mu} (T_L - T) \qquad (1.3)$$

where I is the rate of growth, μ is the coefficient of viscosity, T_L is the liquid temperature and T is the temperature at which crystal growth rate is measured.

1-8 Annealing Process in Glass

The annealing point is the temperature at which any internal stresses will be relieved in a few minutes.

Glass is heated for a long period at a temperature somewhat lower than the normal transformation temperature for the following purposes.

a) The first purpose is to ensure uniformity in physical properties throughout the glass. It is possible by varying the rate of cooling to prepare samples of glass of a given composition having annealing temperatures differing by as much as 100 - 200°. This will lead to a large difference in physical properties - differences of at least 0.5% in density for example.

In the manufacture of high quality optical glass it is extremely important that the glass should have uniform physical properties - especially uniform refractive index - throughout the material. Cooling has therefore to be very slow in the neighbourhood of the transformation temperature (or kept constant for a few hours) so that there can be no danger of temperature difference greater than 3 - 4°C existing in the material.

b) A second purpose is to reduce the rate of subsequent contraction at room temperature. Rapidly cooled glass has a

greater tendency to contract at room temperature than slowly cooled glass, because its viscosity is at first abnormally low. This effect can be eliminated in glass of suitable composition by an annealing treatment in which the glass is heated for a long period at a temperature somewhat below the transformation temperature.

c) A third and the most important purpose is the removal of undesirable mechanical stresses which may exist between adjoining layers. Annealing treatments may be applied either as the last stage of a manufacturing operation or subsequently on the re-heated article. It can be shown that rapid cooling must lead to compressive stresses on the surface and tensile stresses in the interior layers.

Consider a sheet of glass cooling fairly quickly from a temperature above the transformation point (T_g). A temperature gradient will exist across the thickness of the specimen. since the surfaces are cooled first by the surrounding air and the interior is cooled only by conduction of heat to the surface. The surface therefore always tends to be at a lower temperature than the interior. No stresses can exist in the specimen at a temperature well above T_g, and we can say as a rough approximation that the temperature gradient will be maintained as the sheet is cooled so that there will be no stresses in the specimen when the surfaces reach room temperature. At this stage the

temperature gradient across the specimen begins to disappear in order that the interior may also reach the temperature of the surroundings. The magnitude of these stresses for a given rate of cooling depend mainly upon the expansivity, thermal conductivity and elasticity of the glass. The normal process of annealing for the removal of internal stress consists of first heating the specimen into the neighbourhood of T_g, maintaining it at the same temperature until stress relaxation is complete and finally cooling it so slowly that no further permanent strain can be introduced. After reaching a temperature somewhat below T_g, the remainder of the cooling is carried out as rapidly as may be possible without causing fracture as a result of the temporary stresses introduced.

1-9 Conditions of Glass Forming and Atomic Structure of Glass

One of the earliest attempts to discover characteristics common to glass-forming oxides was made by Goldschmidt[155] in 1926. He suggested that the ability of an oxide to form glass might be related to the way in which the oxygen ions were arranged around the cations to form the unit cell of the crystal structure.

Due to Goldschmidt[155] criterion glass-forming oxides are those for which the ratio of ionic radii R_R/R_0 lies in the range 0.2 - 0.4. Most crystals in which the ratio of their atoms lies

between 0.2 - 0.4 have four anions around each cation, the anions being situated at the corners of a tetrahedron and the cation is at the centre.

In 1932 Zachariasen[25] pointed out that the ability of an oxide to form a tetrahedral configuration could not be an absolute criterion for glass-forming ability. In the case of BeO for example, although the ratio for this oxide permits oxygen ions to form tetrahedral groupings around the beryllium ion nevertheless this oxide cannot be obtained in the glassy state.

In order to accept the fact that the interatomic forces in glasses and crystals must be similar, and that the atoms in glass oscillate about definite equilibrium positions, Zachariasen deduced that the atoms must be linked in the form of a three dimensional network in glass as in crystals. He proposed that the energy content of a substance in the glassy state must not be greatly different from that of the corresponding crystal. As a result of this for a glass-forming oxide the co-ordination number of the cation must be closely similar for crystal and glass. The only difference between the crystalline and glassy forms is that in the glassy state the relative orientation of adjacent tetrahedra is variable, whereas in crystalline forms it is constant throughout the structure. In other words, in the crystal the structured units are built up to give a regular lattice, but in the glass there is sufficient distortion of band angles to permit the structural units to be arranged in a non- periodic fashion

giving a random network.

Figure (1.3) shows the difference between the regular crystalline lattice and the random network for an oxide having the formula R_2O_3. In both cases the structural units are RO_3 triangles. Therefore glasses have short-range order since the oxygens are arranged in fairly regular polyhedra, but long-range order is absent.

Zachariasen showed that consideration of his structural energy ideas made it possible to formulate a number of rules which an oxide must obey if it is to be a glass former. These rules are as follows.

I. An oxygen atom must not be linked to more than two R atoms.

II. The number of oxygen atoms surrounding R must be small.

III. The oxygen polyhedra must share corners only and not edges or faces.

IV. At least three corners in each polyhedron must be shared.

From these conditions one can find that oxides of the formula R_2O and RO can not satisfy these rules and should not form glasses.

At the time of Zachariasen the glass-forming oxides such as SiO_2, GeO_2, B_2O_3, As_2O_3, and P_2O_5 which were the only simple oxides known to form glasses were all found to satisfy the rules. Because SiO_2, GeO_2 and P_2O_5 have structures based on RO_4

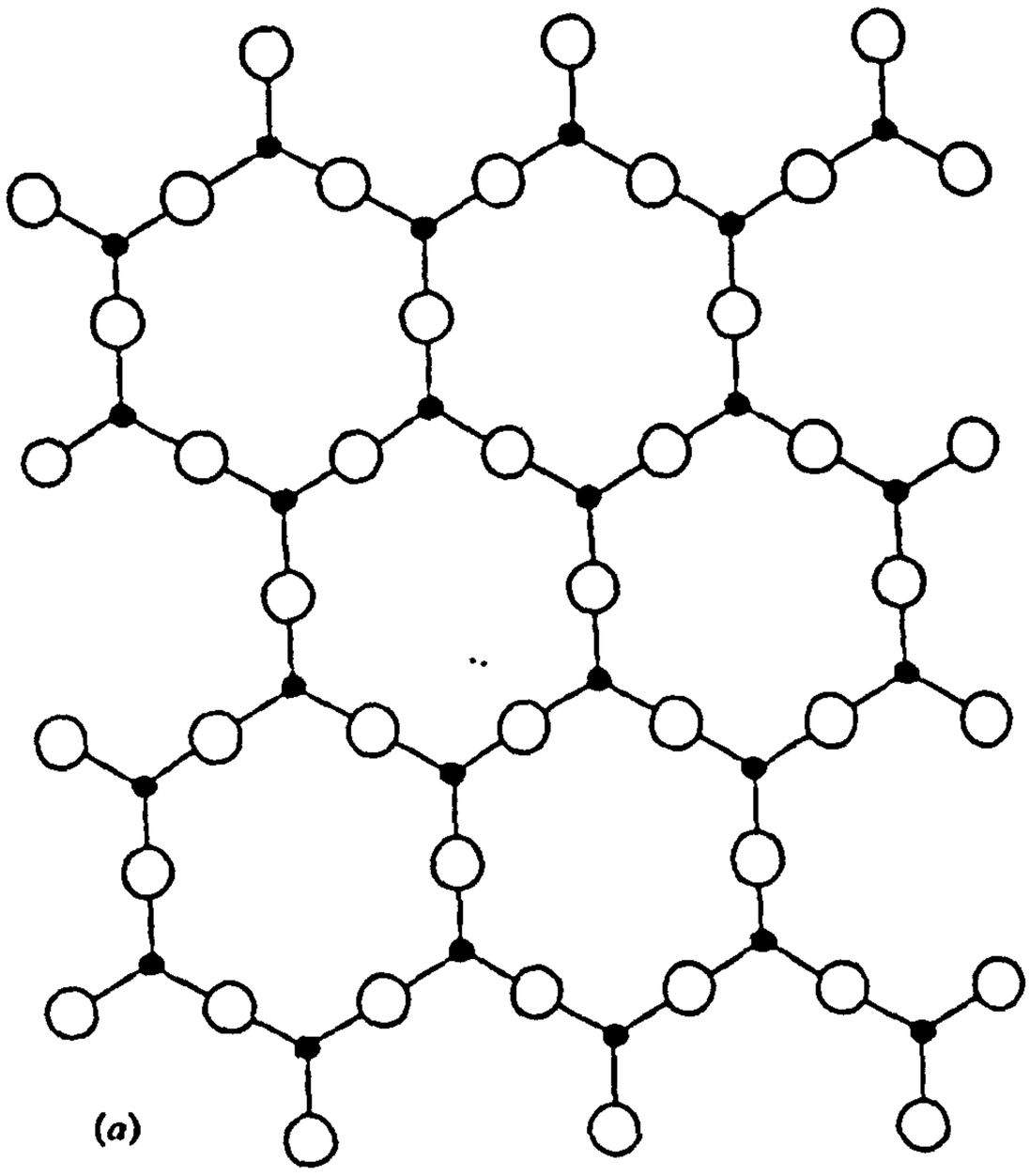

(a)

○ : Oxygen, O

● : R

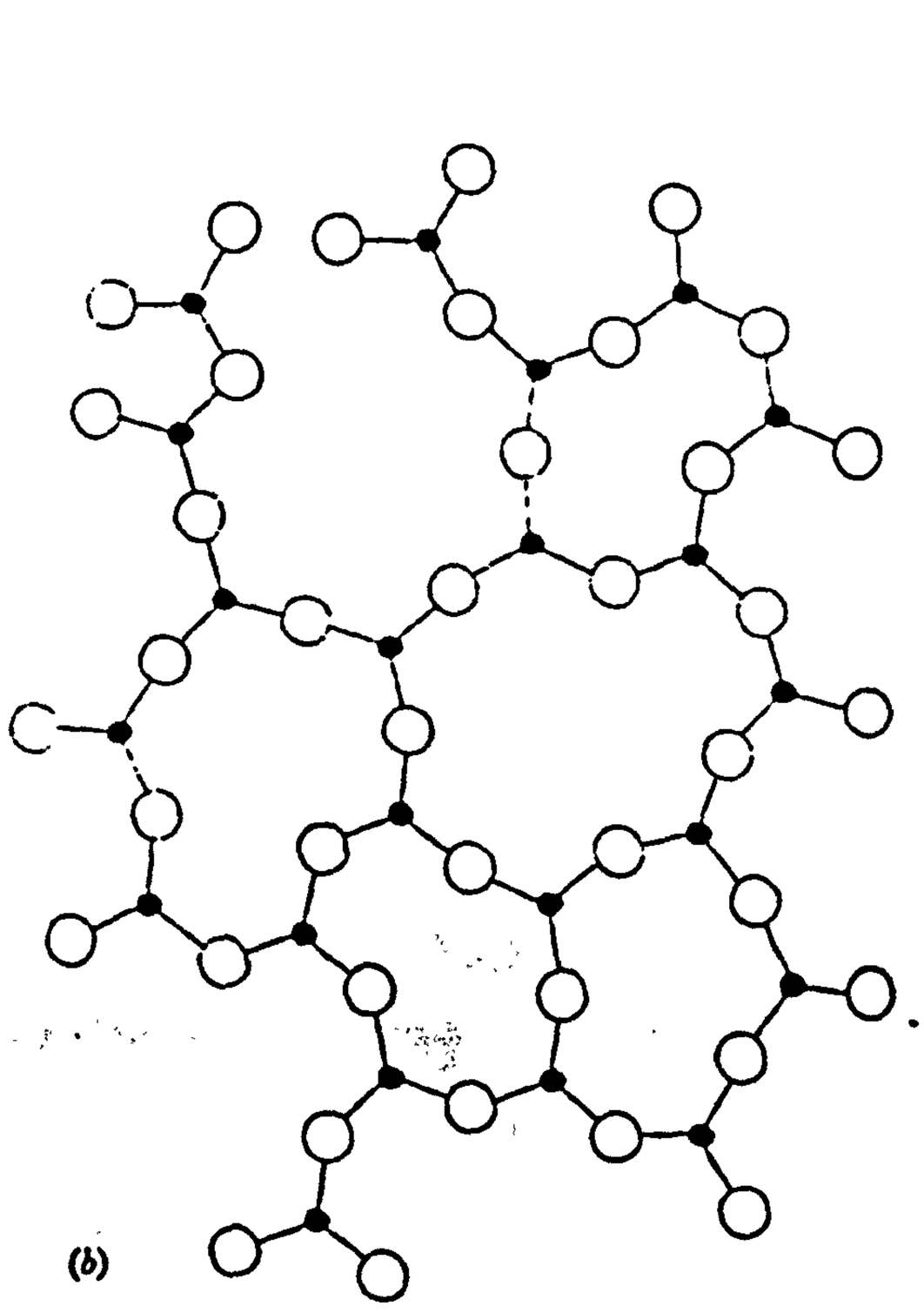

(b)

Fig.(1.3) Two-dimensional Analogue of the structure of

a) the crystal and b) the glassy state of a substance R_2O_3

tetraheda and B_2O_3 and As_2O_3 have structures based on RO_3 triangles, they are expected to form glass in accordance with Zachariasen's rules.

1-10 Glass Former and Glass Modifier

The structural elements in a crystal are arranged into a regular pattern, leaving a relatively small space between them. The structure of the crystals is therefore closed. In contrast to this the irregular network of glasses will be more open and there may be vacancies and voids. In glass such loose voids are filled with cations which have relatively large ionic radii and small charges. Such cations specifically modify the properties of glass. All cations may be divided into three groups.

a) Those taking part in the formation of the network, the so called network-formers. These are oxides which form glasses when melted and cooled, and are called glass-forming oxides or network-forming oxides, because of their ability to build up continuous three dimensional random networks. Oxides of B_2O_3, P_2O_5, SiO_2, As_2O_3 and GeO_2 belong to this group.

b) Those which are incapable of building up a continuous network or those which are found in the random voids where they modify the final properties, the so called network modifiers like NaO - CaO.

c) Those which although are not usually capable of forming a glass, can form part of a glass network.(eg. Al_2O_3)

1-11 Ionic Potential in Glass

Ions of various elements develop specific properties of glass which to a considerable extent depend on their size expressed by the ionic radii.

Although ions have no definite boundaries, but in a network and with the same number of neighbours, a definite ion will always occupy approximately spherical shape. In this sense we can speak of ionic radii, which may be thus considered as a measure of the range of influence of the ions. Cations having small radii can be surrounded in the lattice with a small number of oxygen. If the average number of oxygen surrounding a cation in a glass is called the co-ordination number, small cations with a low co-ordination number take part predominantely in the formation of the network, while ions with large radii act as modifiers. Small cations have a low co-ordination number but a larger charge (equal to valency), and for this reason they exhibit a high bond-strength to oxygen. Evaluation of the bond-strength of cations to oxygen have been estimated by various authors but show some differences. According to Pincus[26] the ratio of charge of cation to its radii (Z/r) is called the ionic potential. It represents the field of force of the charge with which an ion acts within the range of its radii. It signifies that the power of attraction between cations and oxygen increases with the charge (valency) and decreases with the increasing radius of the ions. For example a small Si ion with a large

charge (Z = 4) binds oxygen firmly, hence the melting point of fused quartz is high.

The ionic potential of boron is 15, that of phosphorus 14.5 and of silicon 9.8. Since the ionic potential of boron and phosphorus are higher than that of silicon , SiO_2 dissolves in B_2O_3 and P_2O_5, a process which plays an important part in the formation of glasses.

When the radius increases the scratch hardness and viscosity decreases and as a general rule the electrical insulating properties improve. This is particularly applicable to oxides of Pb, Ba, K, Sr. With an increasing radius or decreasing ionic potential, the bond strength decreases and also it causes an increase in thermal expansion coefficient. Table (1-2) shows the ionic potentials for a number of cations.

1-12 Co-ordination Potential

In the case of oxide melts, it can be assumed that the charge of the cation is distributed over all the co-ordinated ions. The charge per bond is equal to Z/n when n is the co-ordination number. This quantity was defined first by Pauling[28] in 1948 as the electrostatic bond-strength of the cation. Co-ordination potential of some cations are given in table (1.3).

No.	Cations	Valence	Ionic Radius	Ionic Potential
1	Li	1	0.60	1.67
2	Na	1	0.95	1.00
3	K	1	1.33	0.75
4	Rb	1	1.48	0.68
5	Cs	1	1.69	0.59
6	Be	2	0.31	6.50
7	Mg	2	0.65	3.10
8	Ca	2	0.99	2.00
9	Sr	2	1.13	1.77
10	Ba	2	1.35	1.50
11	Zn	2	0.74	2.70
12	Cd	2	0.97	2.06
13	Pb	2	1.21	1.65
14	B	3	2.20	1.50
15	Al	3	0.50	6.00
16	Sb	3	0.90	3.30
17	Si	4	0.41	9.80
18	Ti	4	0.68	5.90
19	Zr	4	0.80	5.00
20	Ge	4	0.53	7.50
21	Sn	4	0.71	5.60
22	Pb	4	0.84	4.77
23	P	5	0.34	14.70
24	Sb	5	0.62	8.10

Table (1.2) Ionic Potentials of Some Cations[27]

Ion	Charge 2	Co-ordination Number	Co-ordination Potential
Cs	1	12	1/12
Rb	1	12	1/12
K	1	8	1/8
Na	1	6	1/6
Li	1	6	1/6
Ba	2	8	1/4
Pb	2	8	1/4
Sr	2	8	1/4
Ca	2	6,8	1/3,1/4
Zn	2	6,4	1/3,1/2
Mg	2	6,4	1/3,1/2
B	3	3,4	1,3/4
Al	3	4	3/4
Si	4	4	1

Table (1.3) Co-ordination Potential For Some Ions

1-13 Types of Bonding in Inorganic Glasses

Two types of bonds have been recognized in inorganic glasses.

a) Ionic bonds (valency electron).

This type of bond occurs in the elements of group I and II in the Periodic Table whose atoms accept further electrons and form positively charged ions completing the valency

shell to an octet (with eight electrons). Ionic bonds are characteristic of elements which readily form electolytes, in glass they do not act as building stones of the lattice, but as modifiers.

b) Co-Valent Bonds

In this type of bonding atoms attain the structure of inert gases by releasing electrons. These bonds are typical of non-electrolytes and they act as a glass-former in the glass system.

The speciality of glasses is represented by the fact that they contain both types of bonds combined in a varying proportion according to the ratio of the individual elements present. The ratio of both types of bond determines the general character of the glass concerned.

In 1951 Smekal[29] suggested that the presence of mixed chemical bonds in a material is necessary if the material is to form a glass. The reason is that a random arrangement of atoms which can be maintained on cooling is incompatible with sharply defined bond lengths and bond angles. By his classification glass-forming substances with mixed bonding are divided into three classes.

I) Inorganic compounds in which the R-O bonds are partly covalent and partly ionic eg. SiO_2, B_2O_3.

II) Elements which they have chain structure with covalent bonds within the chain and Van der Waals forces between the chains eg. Se, S.

III) Organic compounds containing large molecules with covalent bonds within the molecules and Van der Waals forces between them.

Stanworth[30-33] has pointed out that from the difference between the electronegativity values of two elements, it is possible to estimate the percentage ionic character of the bonds joining them.eg. the electronegativities of oxygen and silicon are 3.5 and 1.8 respectively. The difference between the two values (1.7) corresponds to a value of 50% for the percentage ionic character of the Si-O bond. Thus we can say the smaller the difference in electronegativities, the more covalent is the bond.

Stanworth[30], for the suggestion mentioned above, used Paulings[34] values for the electronegativities of the elements. Electronegativities of some elements are given in table (1.4).

There are some problems in Stanworth's idea of using the electronegativity values to predict the type of bonds in some glasses. For example, tellurium has the same electronegativity as phosphorus, but its oxide TeO_2 cannot form glass readily. Whereas P_2O_5 can form glass.

Another problem is that although selenium readily forms a glass yet the Se-Se bond is purely covalent. Also in the former BeF_2 the Be-F bonds are at least 80% ionic.

Glass-Former		Intermediate		Modifying Oxides	
Ele	E.N	Ele	E.N	Ele	E.N
B	2.0	Be	1.5	Mg	1.2
Si	1.8	Al	1.5	Cu	1.0
P	2.1	Ti	1.6-1.5	Sr	1.0
Ge	1.8	Zr	1.6-1.4	Ba	0.9
As	2.0	Sn	1.7-1.8	Li	1.0
Sb	1.8			Na	0.9
				K	0.8
				Rb	0.8
				Cs	0.7

Table (1.4) Electronegativity Values of Elements Found in Oxide Glasses. (Stanworth)[34]

Winters[156] suggested that the ability of glass-forming could be related to the number of outer-shell P electrons per atom. The most suitable number was four, but glass could be made in the range two to four P electrons per atom. Among the elements having the most favourable number of P electorns per atom are O, S, Se, Te but nevertheless there is variation in their glass-forming ability.

1-14 Relationship Between Glass Formation and Bond Strength

Sun[35] in 1947 made a suggestion which relates glass formation conditions with bond strength. He said that the

stronger bonds cause the slower rearrangement process and hence more readily will a glass be formed. In fact he showed that the bond strengths in glass-forming oxides are particularly high. For calculating the strength of an RO bond in the oxide RO_x he used formula derived by Sun and Huggins[36] for the energy E_d required to dissociate the oxide into its constituent atoms. The strength of the single R-O bond is equal to E_d divided by the number of oxygen atoms surrounding the atom R in the crystal or glass. From his calculation it can be found that glass-forming oxides have single bond-strengths greater than 90 Kcal/mol and that the modifiers have bond-strength less than 60 Kcal/mol. It should be noted that the bond-strength for P-O, V-O, As-O and Sb-O were obtained by dividing the E_d by five instead of four, because one of the four oxygens surrounding the R atom is attached to the atom R by a double bond (the strength of double bond is equal to twice the single bond strength).

He also pointed out that although the bond strengths for V-O, As-O and Sb-O are relatively high, these oxides are not good glass-formers. He suggested that small ring formation may occur in melts of these materials which would cause easy crystallization. Table (1-5) shows the strengths of oxides calculated by Sun[35] in 1947.

1-15 Classification of Glasses

Generally glasses are classified into five groups:-

RO in RO_x	Valence	E_d/mol	Co-ordination No.	Single Bond Strength
B	3	356	3	119
Si	4	424	4	106
Ge	4	431	4	108
P	5	442	4	88-111
As	5	349	4	70-87
Ti	4	435	6	73
Zn	2	144	2	72
Pb	2	145	2	73
Al	3	317-402	6	53-67
Th	4	516	8	64
Be	2	250	4	63
Zr	4	485	8	61
Cd	2	119	2	60
Sc	3	362	6	60
La	3	406	7	58
Y	3	399	8	50
Sn	4	278	6	46
Ga	3	267	6	45
In	3	259	6	43
Th	4	516	12	43
Pb	4	232	6	39
Mg	2	222	6	37
Li	1	144	4	36
Pb	2	145	4	36
Zn	2	144	4	36
Ba	2	260	8	33
Ca	2	257	8	32
Sr	2	256	8	32
Cd	2	119	4	30
Na	1	120	6	30
Cd	2	119	6	20
K	1	115	9	13
Rb	1	115	10	12
Hg	2	68	6	11
Cs	1	114	12	10

Table (1.5) Bond Strength of Oxides Calculated by Sun[35]

I) Chalcogenide glasses; the element sulphur, tellurium, selenium are the main constituents of chalcogenide glasses. These elements are called chalcogenide elements. When these elements are mixed with any of the elements in group V in the Periodic Table glass may be formed over a wide region of composition. These glasses are semi-conductors and they are opaque in the visible region of the spectrum. Their electrical conductivity increases with the increase of atomic number of the constituent atoms.

II) Element glasses; the elements which can readily form glass are sulphur and selenium. These elements are in group V and VI of the Periodic Table. For the first time Ellis'[157] in 1963, made a vitreous form of phosphorus by heating white phosphorus to a temperature above 250°C under a pressure of 7 Kilo bars.

III) Halide glasses; in the halogen group the only halides which are accepted as glass formers are $ZnCl_2$ and BeF_2. BeF_2 has a lower melting point and is less resistant to chemical attack than are silicate glasses.

IV) Hydrogen-bond glasses; there are some oxides which can make glass because of having hydrogen bonds in their atomic structure. Potasium bisulphate glass is a member of this group. Pure water can form a glass if the vapour is condensed on a very cold surface (very fast cooling). There are a number of aqueous solutions which can form glass more readily eg. solutions of H_2O_2, HCl, $HClO_4$, NH_4OH, KOH.

V) Oxide glasses; these are the most common materials in glass

manufacturing. Because of having very strong ionic bonds they are usually good insulators. There are a few oxides which form glass readly by themselves. These oxides are SiO_2, GeO_2, B_2O_3 and P_2O_5. These oxides as mentioned before are called glass-formers. Sb_2O_3 can form glass but only when it cools very rapidly. Randell and Rooksly[37] reported that Bi_2O_3 can form glass, but later Rawson and Heynes[38] tried to do it but they where unsuccessful.

Chapter II

2-1 Theory of Electron in Amorphous Semiconductors

2-1-1 Introduction

Since about 1960 the theory of electron in non-crystalline materials has become an important part of solid-state physics. For crystalline materials the theory of conduction and valence bands and bandgaps began in the early 1930's (Bloch & Wilson), and is linked with the behaviour of electrons in a periodic field.

> If the distance 'a' between atoms in a crystalline array is increased, the overlap between the first and second energy bands for an electron decreases and eventually a gap appears between them, the two bands being the valence and the conduction bands (Mott).[39]

The study of the electrical properties of glasses as amorphous semiconductors begins with the work of Kolomets[40] on the chalcogenide glasses. He showed that these glasses appear to behave, whether in the glassy or liquid state, as intrinsic semiconductors with a bandgap of less than 2 eV, and also that their conductivities depend little on the purity or stoichiometry. In other words, for them, donors and acceptors of, as in crystalline semiconductors do not exist. As a result of this

property the conductivity increases by many orders of magnitude when crystalline, which is the main reason why chalcogenide glass shows a memory effect in switching. The lack of long-range order in amorphous materials causes low mobility for electrons in these materials and will be discussed later in more detail.

2-1-2 Classification of Amorphous Materials

As in crystalline materials the amorphous material can be classified by the type of chemical bonding. In crystalline materials five major classes of bonding were distinguished. Ionic, covalent, metallic, Van der Waals and hydrogen-bonding materials. This classification can also be used for amorphous materials.

Amorphous metals appear to have approximately the same conductivity as the corresponding crystalline materials, and the effects of long-range disorder on the electronic properties are quantitative rather than qualitative.

Amorphous metals, Van der Waals and hydrogen-bonded solids have not been studied to any great extent (because of having low melting temperatures and low cohesive energies etc.). Thus, amorphous semiconductors can be broken down into ionic and covalent materials. The ionic materials which have been studied most are the halide and oxide glasses particularly the transition-metal oxide glasses.

Covalent amorphous semiconductors break down into two classes. The first group which is perfectly covalently bonded includes Si, Ge, S, Te, Se and they are the simplest amorphous semiconductors. The second group of covalent materials include such binary materials as As_2Se_3 and GeTe as well as the multicomponent boride, arsenide and chalcogenide glasses which have been discussed in the previous chapter.

2-1-3 Order and Disorder

Classification of order and disorder in solids have been made by Seitz[41] and Cohen[42]. In general there are four types of order for materials; these are, compositional order, positional order, magnetic order and electronic order.

A perfect crystal in its ground state has perfect order although static imperfection exists for these materials. An imperfection in compositional order is an impurity, an imperfection in positional order is a defect, an imperfection in the magnetic order is a reversed spin and an imperfection in the electronic order is an excited atom.

There are also dynamic imperfections or elementary excitations which can be associated with all types of order except compositional order. Dynamic positional disorder is a result of phonons (lattice vibration), magnons (spin waves) lead

to magnetic disorder and plasmons (plasma oscillations) in metals and excitons in insulators represent types of electronic disorder. In a glass long-range order is absent and only short-range order exists i.e. the nearest neighbour atoms of a given atom are arranged in much the same way as they would be in the corresponding crystal, but beyond the nearest neighbour shell the arrangement becomes more and more distorted.

2-1-4 Radial Distribution Function

The structure of the amorphous materials are best described by radial distribution function which gives the probability of finding another atom at a given distance from an arbitrary central atom.

Fig.(2.1) shows the radial distribution function for arsenic sulphide and amorphous Ge. Note that the first peak representing the nearest neighbours to the chosen central atom is fairly well defined, but that the second, third and subsequent peaks gradually become blurred until they merge with the parabola $4\pi r^2 dr$ which is characteristic of a random structure. A completely random structure would only be realized in a hypothetical perfect gas. The local or nearest neighbour ordering in a liquid or glass is a consequence of the finite size of real atoms as compared with the extremely small dimensions of imaginary perfect gas atoms. As the temperature decreases the distribution function tends to become more peaked and the

configuration of the liquid changes, although it is still disordered.(Fig.2-2) The radial distribution function for a crystalline material would consist of a series of vertical lines separated by a distance corresponding to the interatomic spacing of crystals.

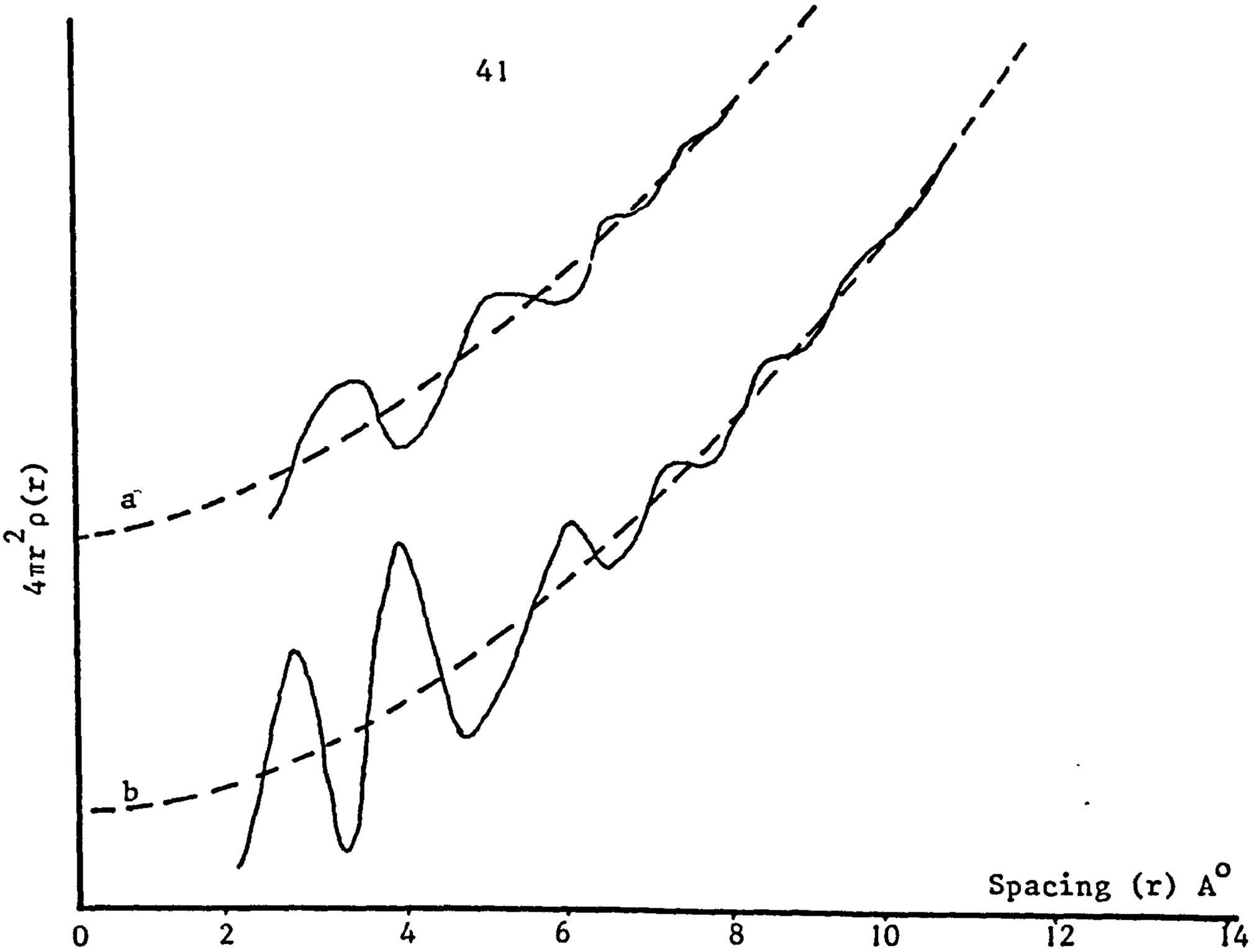

Fig.(2.1) Radial Distribution Curves for Vitreous Arsenic Sulphide and Amorphous Germanium

a) Vitreous As_2Se_3. b) Amorphous Ge.

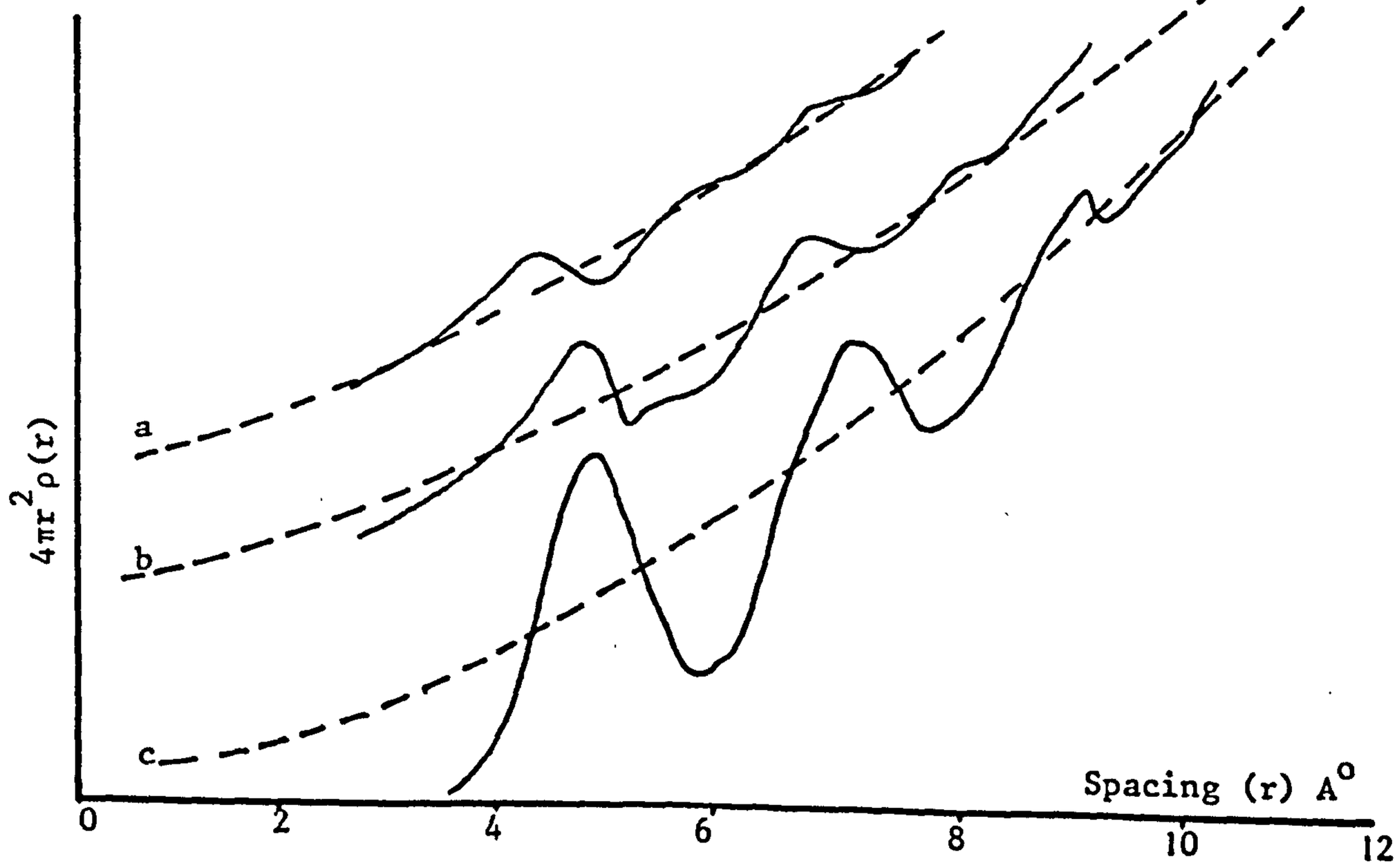

Fig(2.2) Radial Distribution Curves for Liquid Caesium at Three Different Temperatures

a) 575°C b) 300°C c) 30°C

2-2 Band Structure

2-2-1 Density of States

There is one concept that is applicable equally to both crystalline and non-crystalline materials. This is the density of electronic states which is denoted by N(E) and is defined so that N(E)dE is the number of states in unit volume for an electron in the system with given spin direction and with energy between E and E+dE then at a temperature 'T' the number of electrons in the energy range dE for each spin direction is

$$g(E) = N(E)f(E)dE \qquad (2-1)$$

Where f(E) is the Fermi distribution function given by

$$f(E) = \frac{1}{\exp\left(\frac{E-E_f}{kT}\right)+1} \qquad (2-2)$$

where E_f is the Fermi energy and is a function of temperature. This value tends to the limiting value E_F as $T\to 0$. E_F separating occupied states from non-occupied states. The form of density of states is shown for a metal and for a semiconductor or insulator in Fig.(2.3 a,b) respectively.

In a metal the states are occupied by electrons up to a limiting E_F (the Fermi energy) in a semiconductor at the absolute

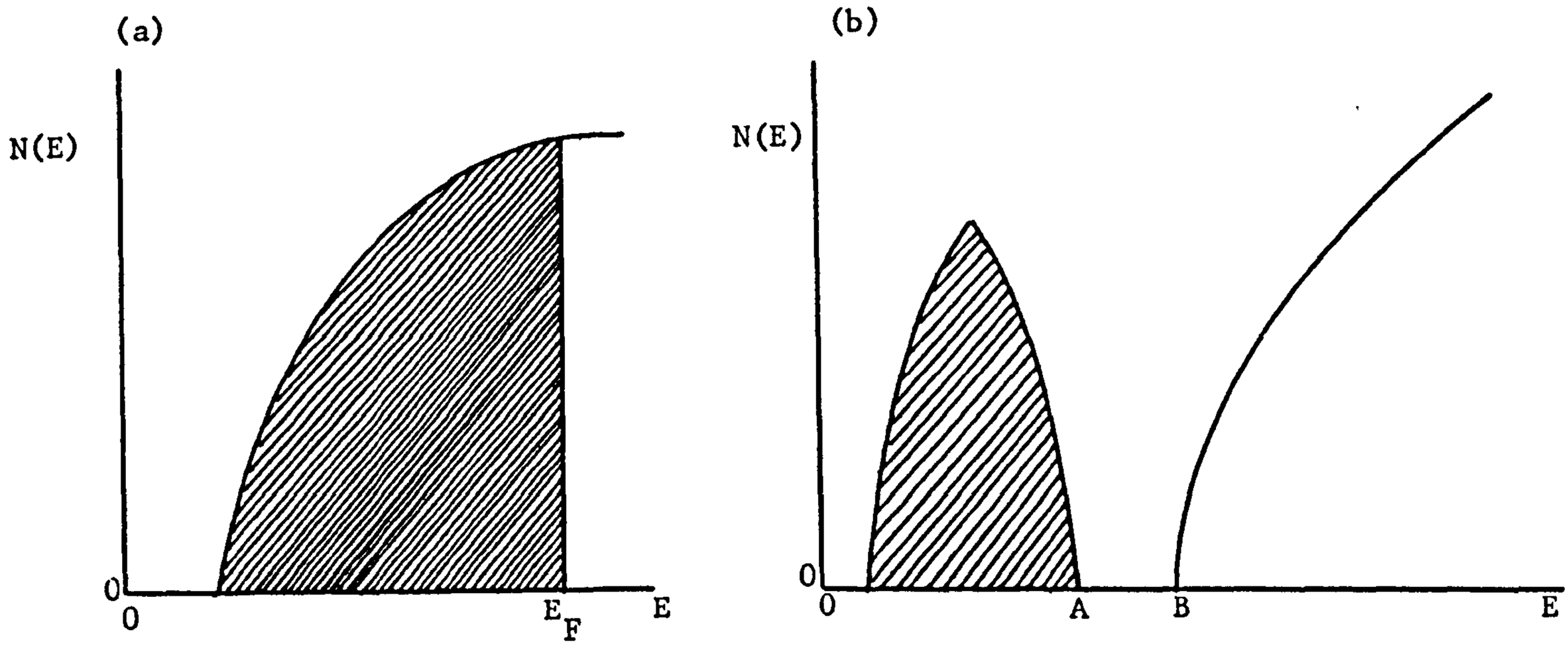

Fig.(2.3) (a) Density of states in a metal E_F is the Fermis energy.

(b) Desity of states is an intrinsic semiconductor AB is the band gap and the shaded part shows the occupied valence band.

zero of temperature a valence band is fully occupied and a conduction band empty.

The wave-function for the electrons are of the form which was introduced by Bloch

$$\Psi(x) = \exp(ikx)v(x) \qquad (2\text{-}3)$$

Where k is the wave vector, v(x) is the potential and x is a co-ordinate.

Because of the scattering of the electrons by impurities and phonons the mean free path of electron 'L' has limiting value and wave-function (2-3) for an electron is only valid over a distance L

$$kL >> 1 \qquad (2\text{-}4)$$

In other words if L is large compared with the wave-length $\frac{2\pi}{k}$ the wave function given in Eq. (2-3) is applicable for electrons. This is usually so in crystal.

In general there are two possibilities for N(E). One is that the scattering of the electron by each atom is weak, in which case the electrons are described by wave function each having wave-number k. In this case mean free path L is large and the uncertainty Δk in k given by the relation ($L\Delta k \sim 1$) is such that $\frac{\Delta k}{k} << 1$. Thus the energy of each electron is a function of (k) in the form of

$$E = \frac{\hbar^2 k^2}{2m} \qquad (2\text{-}5)$$

the Fermi surface is spherical and the density of states for the electron is given for each spin direction by the free electron formula

$$N(E) = \frac{km}{2\pi^2 \hbar^2} \qquad (2\text{-}6)$$

The second possibility is that the interaction between the electrons and atoms are strong so that $\frac{\Delta k}{k} \sim 1$. In this case the mean free path is short ($kL \sim 1$) and only in this case a gap

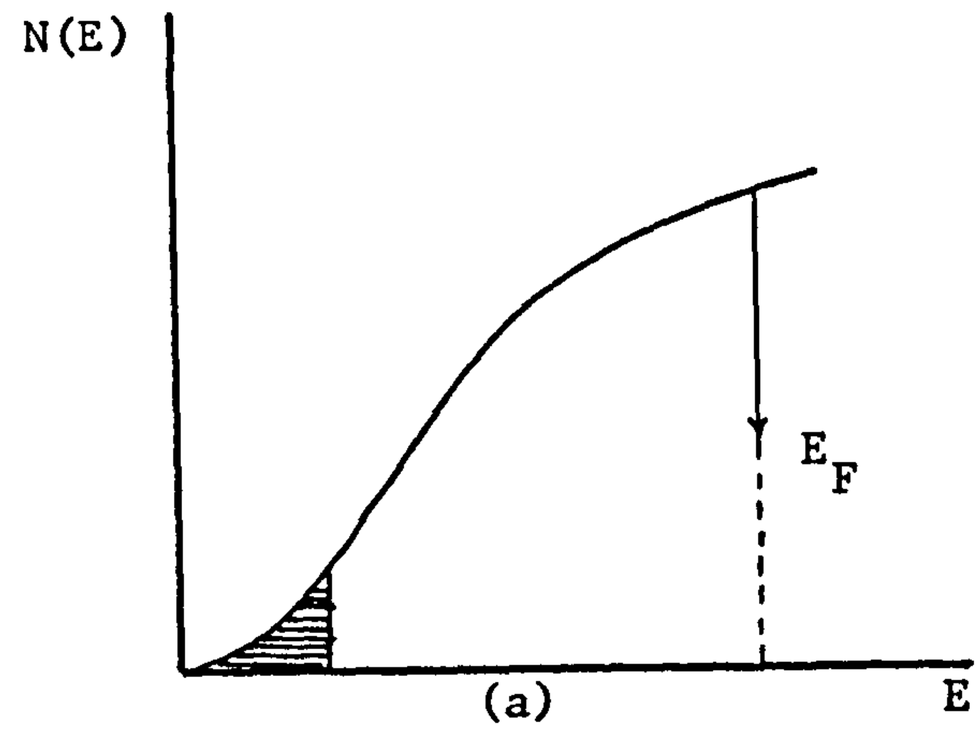

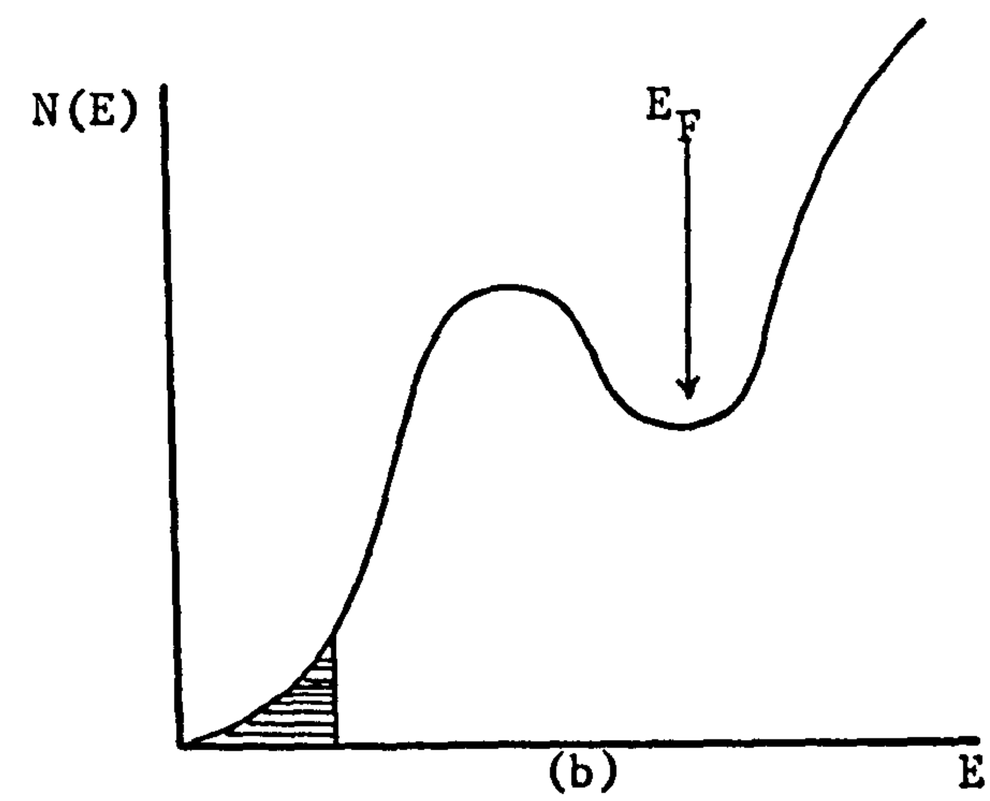

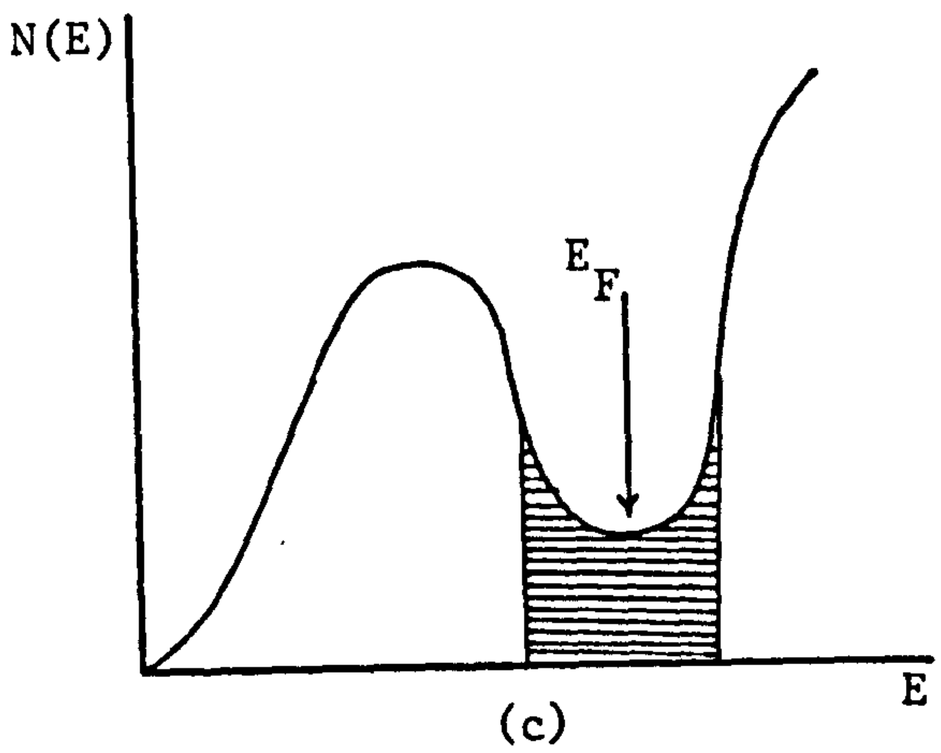

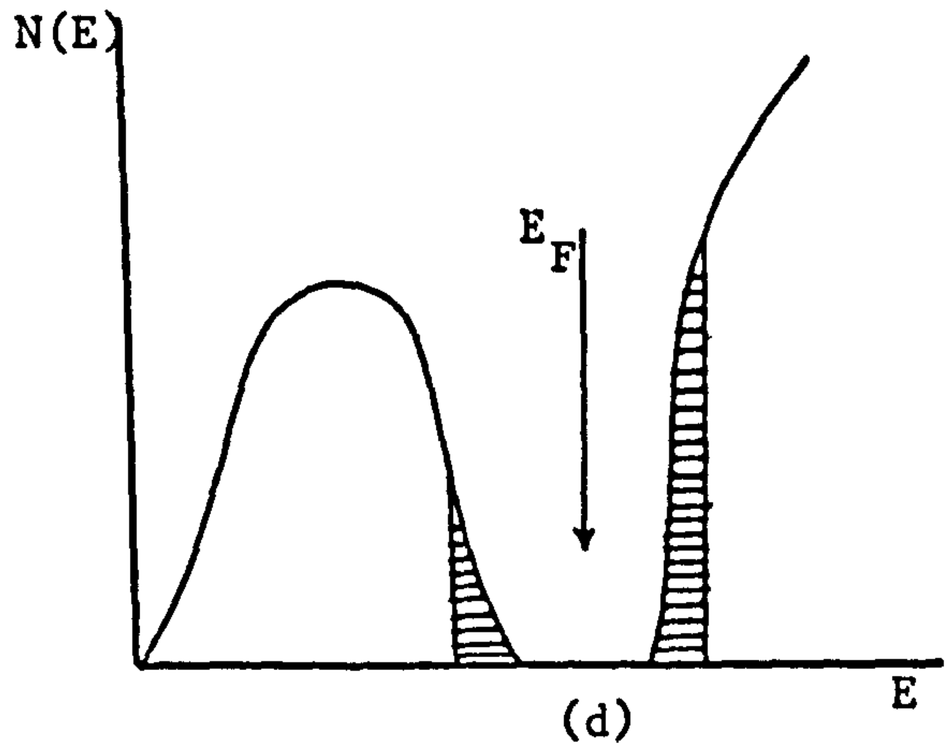

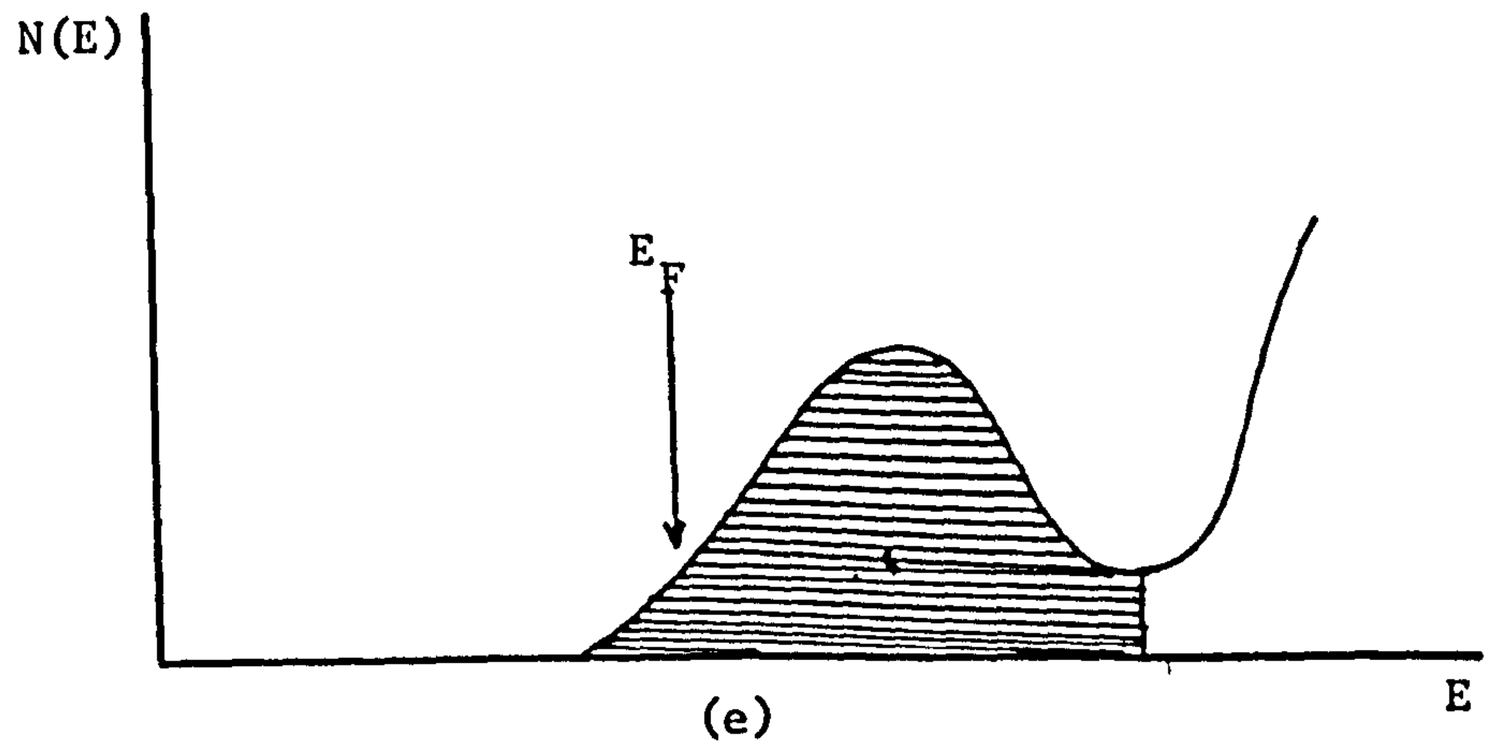

Fig.(2-4) Density of state in non-crystalline materials.[43]

Shaded regions are localized states and E_F is the Fermi energy at the absolute zero of temperature.

a)Liquid or amorphous metal. b)Semimetal. c)Semimetal with deep pseudogap. d)Insulator or intrinsic semiconductor.

e)Impurity semi-conductor.

appears between the states. In crystals (semiconductors) the form of gap is as Fig.(2.3 b). In non-crystalline material (amorphous) either this gap persists or is replaced by a minimum as in Fig.(2.4 c) which is called pseudo-gap. Such a pseudo-gap may exist in amorphous selenium or As_2Se_3 glasses. The possible forms of density of states in a non-crystalline material are illustrated in Fig.(2.4).

2-2-2 Localized States

Near the extremities of the gap, or in the pseudo-gap the wave functions are very strongly perturbed by the irregular arrangement of the atoms. Thus the direction of the electron will hardly remain constant for more than one interatomic distance. The electron will move by a sort of Brownian movement through the lattice, being deflected by every atom it passes through. The mean free path is of the order of the interatomic distance.

For the energies in the pseudo-gap, or very near to the extremities of the conduction and valence bands, the wave-function becomes localized. An electron in a localized state can be described as trapped. So this means that the absence of crystalline order produces a high density of traps. A trapped electron cannot move unless thermal energy frees it. The localization also takes place in crystalline semiconductors. Impurities or defects may give rise to electron states below the conduction band and an electron in a safe trap cannot get out

unless it receives energy from some source.

According to Mott[44] localization can occur for a given energy E for the following Reasons:-

a) A random potential at each atom[45] .

b) Fluctuation in the density of state or mean interatomic distance.

c) Absence of long-range order.

There are some definitions of the concept of localization which are believed all to be equivalent. According to Mott's definition[46], states with energy E are localized if the mean d.c. conductivity is zero at the absolute zero of temperature.

$$<\sigma_E(0)> = 0 \qquad (2\text{-}7)$$

Anderson defined[45]; the states to be localized if an electron with energy E±dE placed in a volume V large enough to satisfy the uncertainty principle, will not diffuse away.

2-2-3 Anderson Location

Anderson in 1958[45] introduced a model for certain random lattices and showed that in certain random fields, localization of the one-electron wave function can occur if the randomness of components are strong enough. For this purpose he used the tight binding approximation of ordinary energy in which the electronic energy levels of solids depend on the nature of the atoms and the

nature and the position of its neighbouring atoms.

When the tight binding approximation is applied to crystalline solids with periodic potential wells, this produces a narrow band of energy with a bandwidth of J which is dependant on the co-ordination number Z Fig.(2.5 a).

$$J = 2ZI \tag{2-8}$$

In equation (2-8) I is an overlap integral given by

$$I = \int \Phi^{*}(r - R_n)\, H\, \Phi\, (r - R_{n+1})\, d^3x \tag{2-9}$$

where $\Phi(r)$ is the atomic wave function and suffix n describes the nth well R_n its lattice site. The value of I depends on the shape of the wells and varies exponantially with R

$$I = I_o e^{-\alpha R} \tag{2-10}$$

Where I_o is a constant which depends on the depth of each well (D_o) and α is defined such that $e^{-\alpha R}$ is the rate at which the wave function on a single well falls off with distance. The value of α is given by

$$\alpha^2 = \frac{2mWo}{\hbar^2} \tag{2-11}$$

where Wo is the energy level for an electron in a single well.

In contrast to the crystalline state, where it is assumed that the potential energy is a small perturbation, in non-crystalline materials due to the lack of periodicity in the atomic structure, the potential energy function (V) is no longer a small perturbation in the Schrödinger equation given by

$$\nabla^2\psi + \frac{2m}{\hbar^2}(E-V)\,\psi = 0 \qquad (2\text{-}12)$$

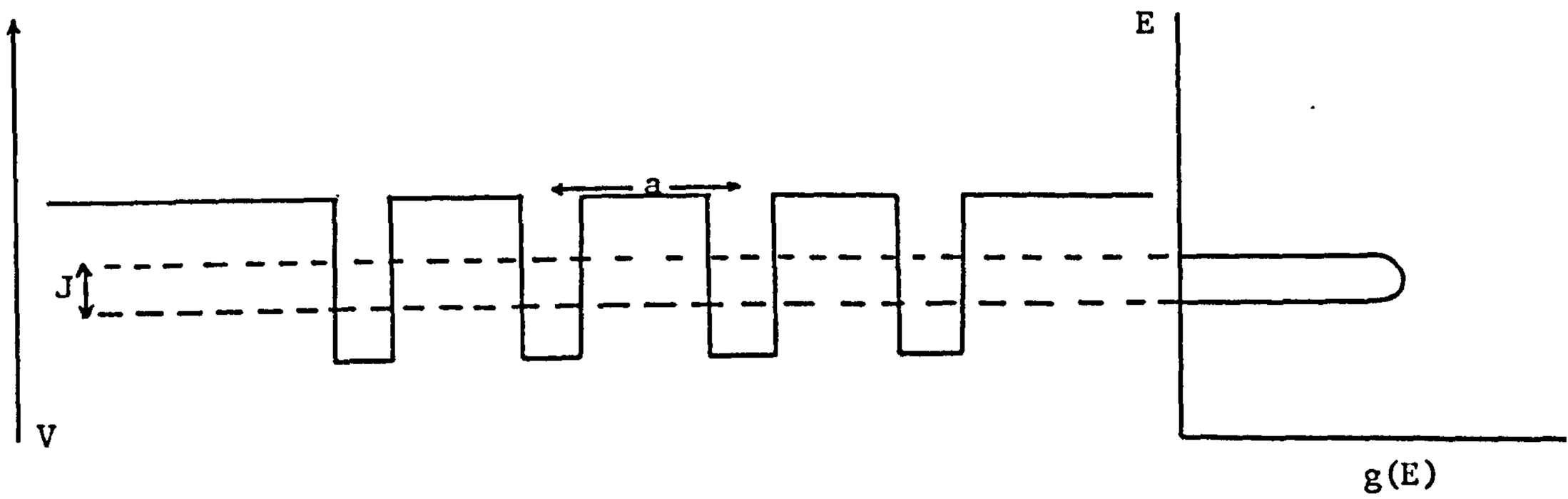

(a)

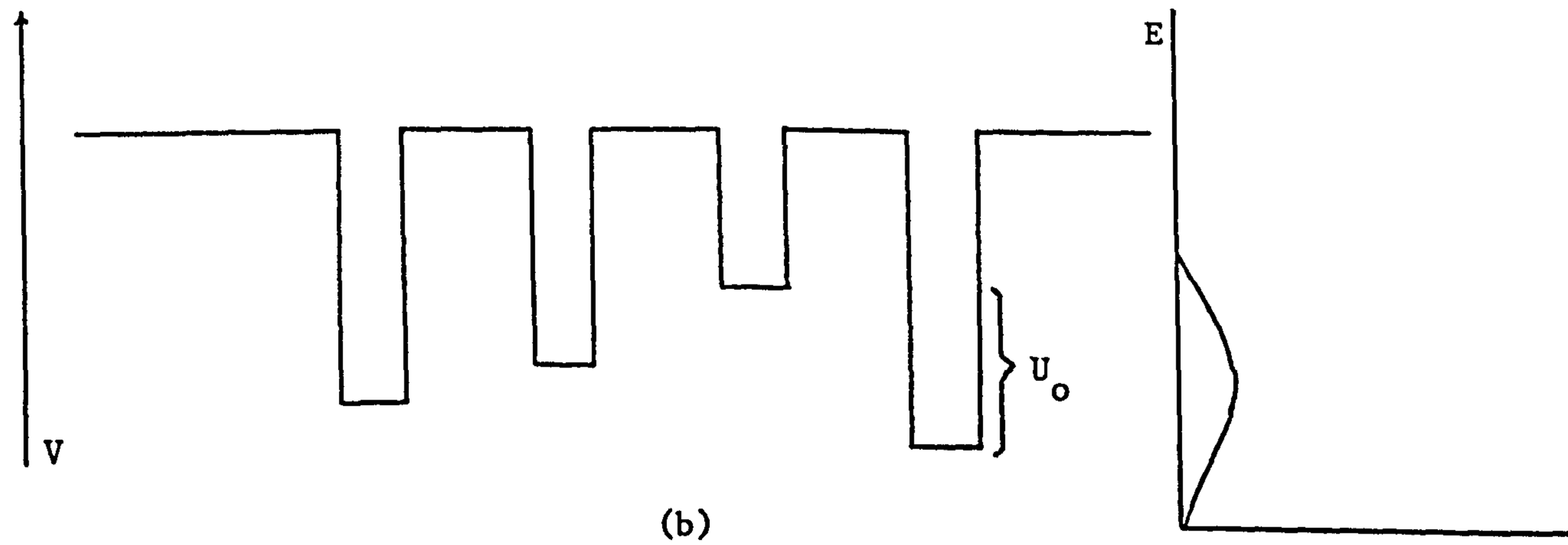

(b)

Fig.(2.5) The Potential Energy of an Electron in a Three Dimensional Lattice

a) $U_o = 0$ as in crystalline solids. b) $\frac{U_o}{J}$ large as in non-periodic amorphous materials.

A non-periodic potential can be formed in two possible ways.

a) By the displacement of each centre by a random amount which can be caused by lattice vibration or by the distortion of the long-range order.

b) By the addition of a random potential energy $\frac{1}{2}U$ to each well which causes the energy level for an electron in the well to change from W_0 to $W_0 + \frac{1}{2}U$.

Anderson considered case (b) and analysed the problem of a three-dimensional period of square wells of random depth spread over a range of U_0 where U_0 is defined as

$$< U^2 > = U_0^2 \qquad (2\text{-}13)$$

Fig.(2.5) shows two cases, one when U_0 is large, as in non-crystalline solids (2.5 b) and the other when U = 0 as in crystalline materials.

Anderson showed that the different possible modes of behaviour of an electron in the lattice can be distinguished in terms of the ratio $\frac{U_o}{J}$. Four possible modes of behaviours are expected as below:-

a) In the middle of band ($ka \sim 1$) where the minimum possible mean free path for an electron is the atomic distance 'a' (according to the rule of Joffe and Regel[47]). The sign of the wave function will vary in a random way from well to well. Fig.(2.6 a). This will happen when $\frac{U_o}{J} = \frac{7}{12}$ when Z = 6.

b) As the value of U_0 increases there will be a random fluctuation of the amplitude of ψ [48] (as well as phase) in going from well to well and this fluctuation increases with increasing the values of $\frac{U_o}{J}$. Anderson defined a critical value for $\frac{U_o}{J}$. Above which there is no diffusion at the absolute zero of temperature and the wave functions are localized. This critical value for $\frac{U_o}{J}$ depends weakly on the co-ordination number Z, according to Anderson

$$\frac{U_o}{J} \simeq 5 \quad \text{for } Z = 6$$

at $\frac{U_o}{J} \simeq 5$ states are just non-localized, and the wave function for this value is shown in Fig.(2.6 b).

c) If $\frac{U_o}{J} > 5$ states are known to be localized. In this case at low temperature conduction in amorphous semiconductors takes place by tunnelling between the localized states with a small activation energy. The activation energy in this case decreases with decreasing temperature. The wave functions of an electron for the case in which $\frac{U_o}{J} > 5$ are shown in Fig.(2.6 c,d).

d) There will be strong localization when $\frac{U_o}{J} \gg 5$ (Fig.2.6 ,d)

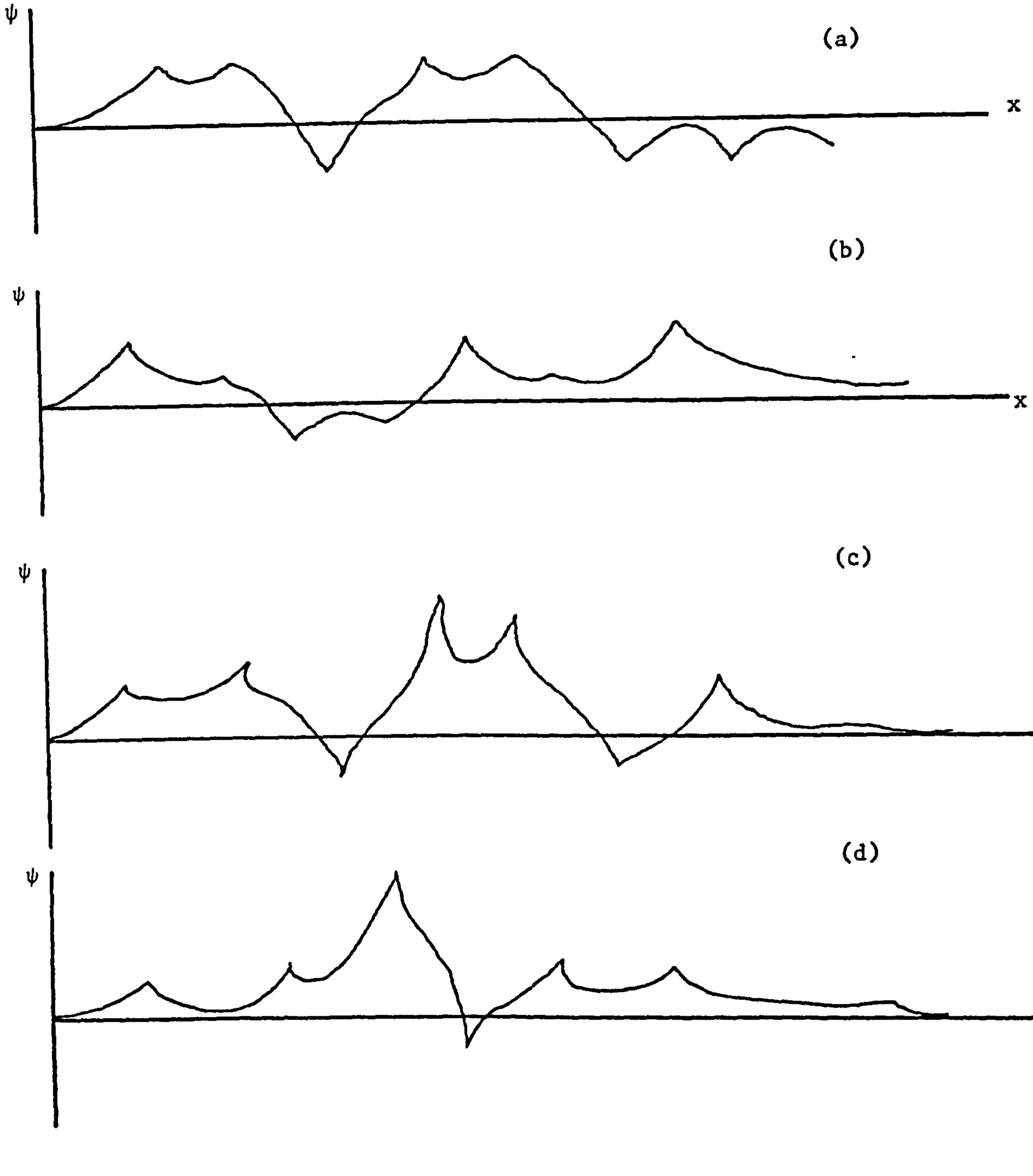

Fig.(2.6) Forms of the Wave Functions in Anderson's Model[43]

a) L^a b) States are just non-localized

c) States are just localized d) Strong localization

2-2-4 Mobility of Electrons

A general definition of mobility is the electronic velocity per unit applied electric field. ($cm^2\ V^{-1}Sec.^{-1}$) Mobility of any conduction-band state is defined as the velocity per unit field attained by an electron placed in the state, under the assumption that all valence band states remain full throughout the conduction process.

Similarly the mobility of a valence-band state can be obtained by placing a single hole in the state and evaluating the velocity per unit applied field, assuming the conduction band states to be completely empty.

For a perfect periodic crystal all states are delocalized and the mobility of any state is infinite. In real crystals, the mobility is limited by scattering arising from deviations from perfect periodicity.

In highly disordered systems, intense scattering due to large fluctuations in the one-electron potential can reduce the mobility to quite a small value despite the delocalized nature of the state. Localized state must have zero mobility if they do not spatially overlap other states with the same energy, and if overlapping localized states exist at a given energy, tunnelling between them can lead to a finite mobility.

The mobility of the states in an amorphous solid depends on

the density of state. Where the density of states is large, the mobility can be finite, where the density of state is small the mobility is essentially zero. In regions of intermediate density of states, there are some possibilities for the form of variation of mobility with energy. One possibility is that mobility gradually decreases from a finite value to zero over a wide range of energy. Fig.(2.7, a). Another possibility is that mobility falls to zero sharply, but continuously, over a narrow range of energy. Fig.(2.7, b). The third possibility is that mobility discontinuously vanishes at a single critical energy Fig.(2. 7,c).

2-2-5 Mobility Edge and Mobility Gap

According to the band model suggested by Mott and Davies[48], energy values E_c and E_v separate localized states from non-localized or extended states. The energy of this kind always exists for conduction and valence bands in non-crystalline systems, although for some materials such as liquid argon or SiO_2, E_c is very near to the band edge. There is a drop by a factor $\sim 10^3$ in the mobility as the energy crosses these values (the mobility shoulder). These energy values are called the mobility edge and the energy difference ($E_c - E_v$) defined as mobility gap (E_g) Fig.(2.8).

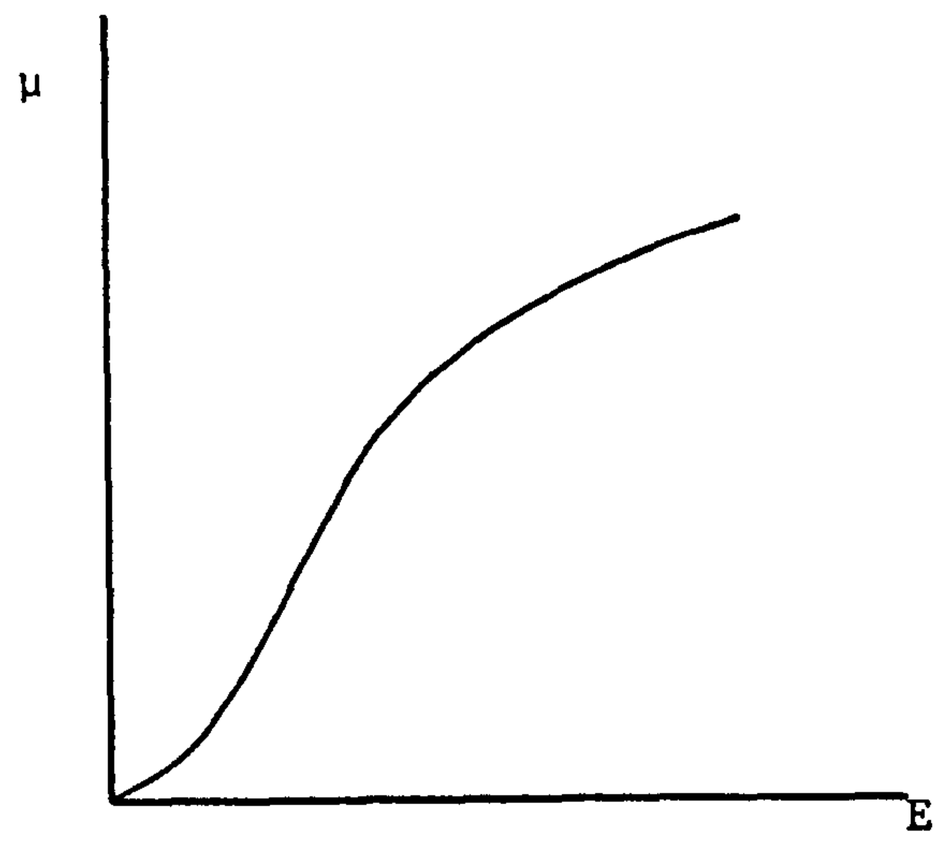

(a)

(b)

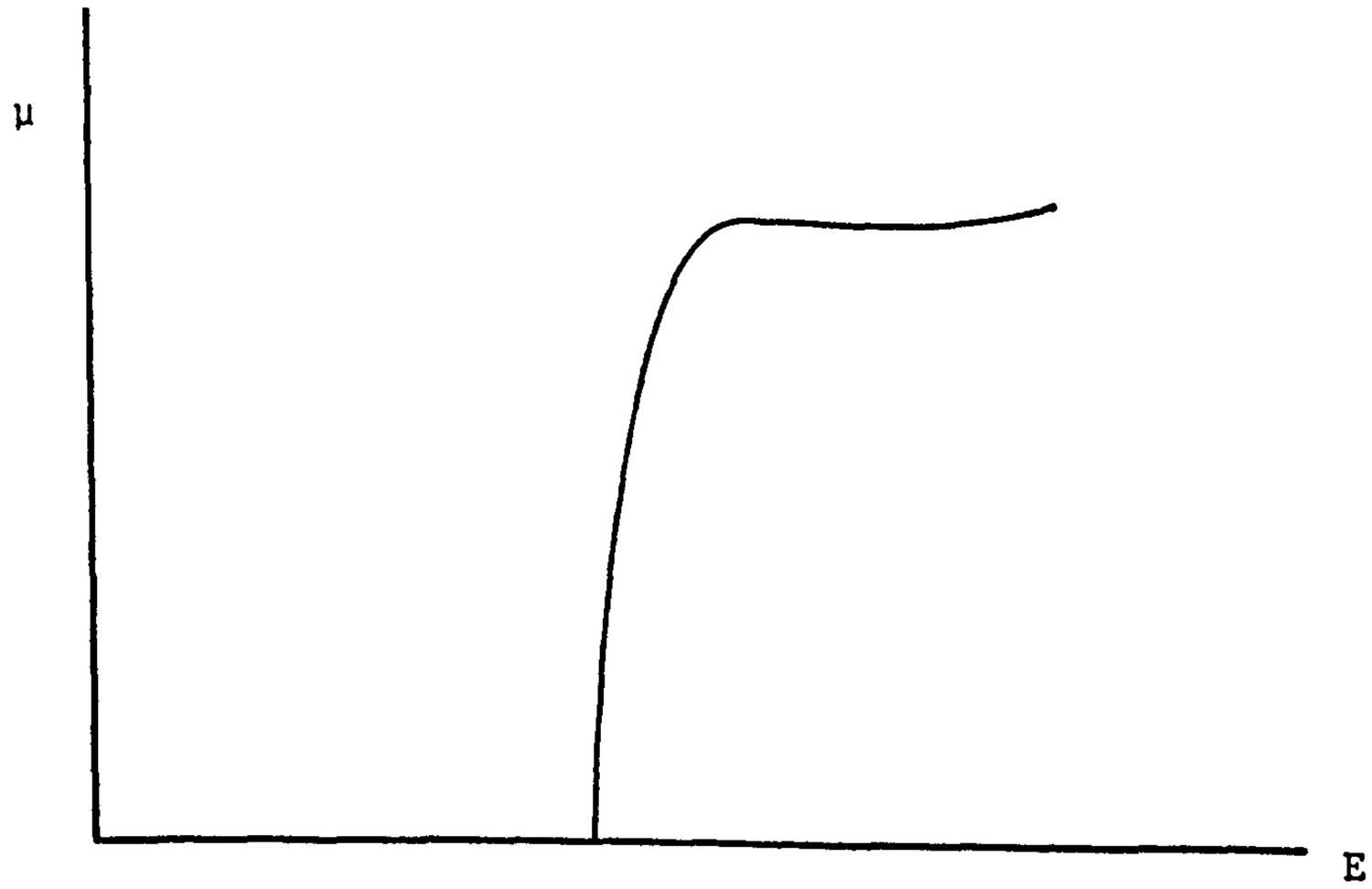

(c)

Fig.(2.7) Variation of Mobility with Energy in the Intermediate region of Density of State

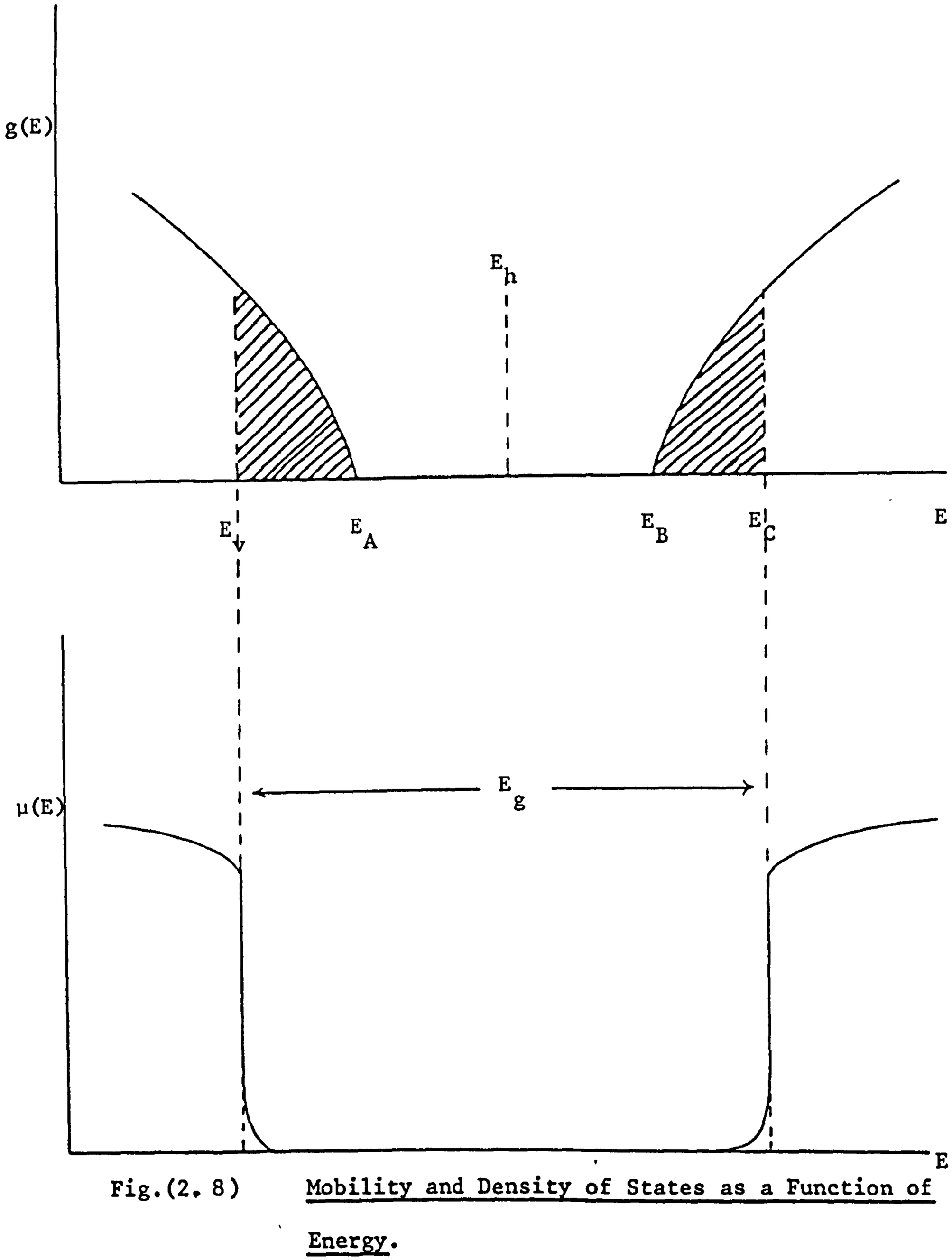

Fig.(2. 8) Mobility and Density of States as a Function of Energy.

Localized states are shown shadowed E_v, E_c are mobility edges and E_g represents the mobility gap.

2-3 Band Models in Amorphous Materials

2-3-1 Introduction

There are different opinions about the concentration and distribution of localized states in the gap of the amorphous semiconductors.

According to Bennett and Ashley[49] - and Weair[50], there are hardly any localized gap states but other experiments have suggested that densities of localized states as high as 5×10^{19} $cm^{-3}eV^{-1}$ may exist.

According to Anderson,[45] Mott[48] and Cohen[51], the states become localized near the top and bottom of the band when their density falls below about 10^{21} $cm^{-3}eV^{-1}$. An estimated concentration of 5×10^{19} $cm^{-3}eV^{-1}$ localized states in the band tail are expected when the width of the tails are about 0.1eV. This value depends on the disorder parameter. There are several band models proposed to describe the nature of the electrical conduction in disordered materials. The most important ones which concern disordered material in general and the amorphous semiconductor in particular are briefly summarized here.

2-3-2 C.F.O. Model

This model was suggested by Cohen, Fritzsche and Ovenshinsky[51] in 1969.

In this model their first assumption was that the valence and conduction bands in amorphous semiconductors have tails of localized state. They also assumed that the tails of the valence and conduction bands overlap. Fig.(2.9). Their second assumption means that an electron in a valence band in some region of the material may have a higher energy than an extra electron in a non-bridging state in another part of the material. Such electrons from the top of the valence band tail fall into spatially distinct states in the lower conduction band tail. The Fermi level E_F thus falls near the centre of the 'gap' where the density of states is near its minimum.

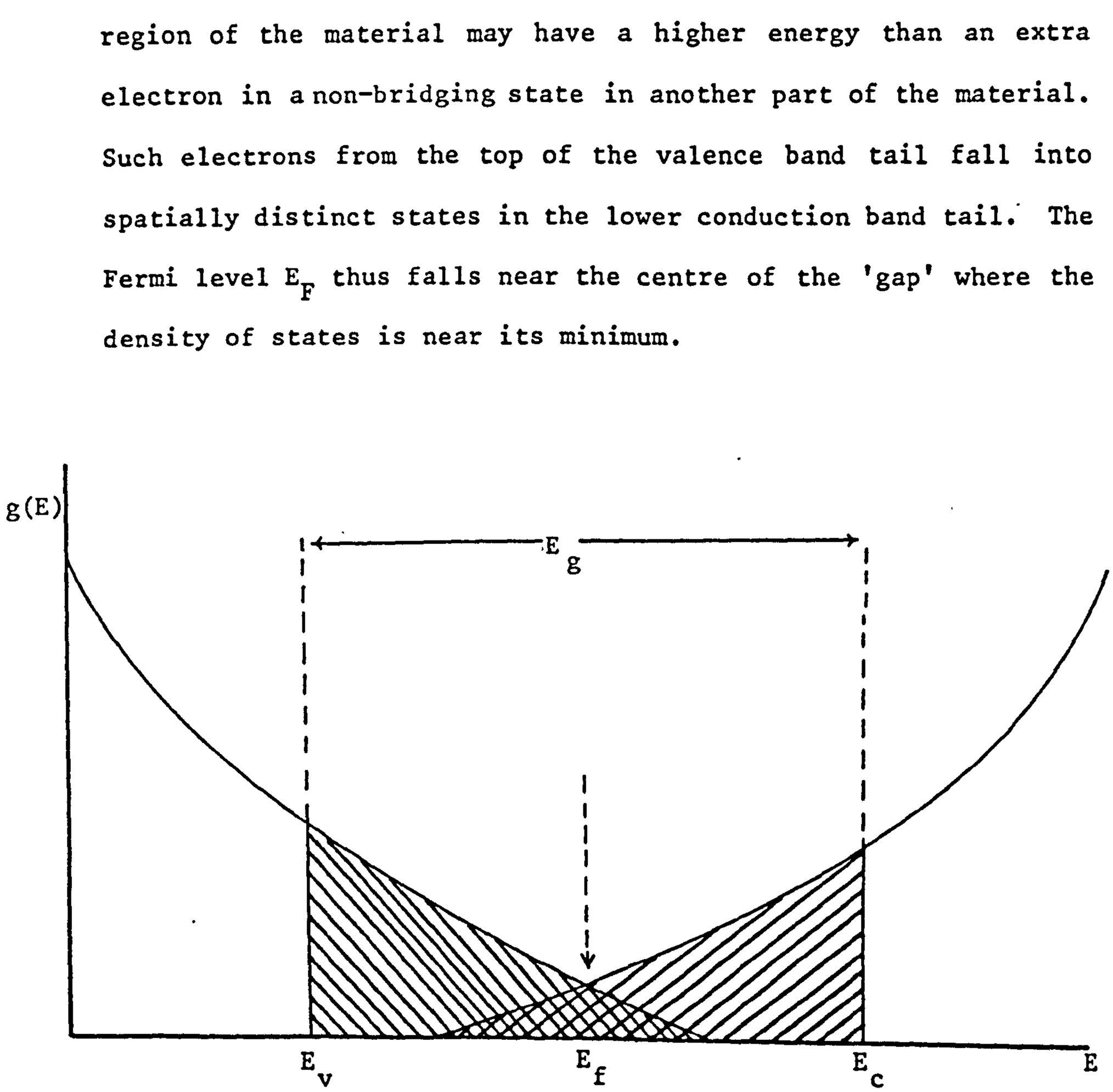

Fig.(2.9) C.F.O. Model for Density of State

E_v and E_c are the respective valence and conduction band mobility edges, E_g is the mobility gap and E_f is the Fermi energy.

An important assumption of C.F.O. model is that both the valence and conduction bands tail extensively in to the mobility gap.

2-3-3 Mott and Davis Model(52)

In the modifications which was introduced by Mott and Davis, it has been assumed that there is a distinction between the two following cases.

a) The range ΔE_c between E_c and E_A and ΔE_V between E_B and E_v where the localized states lie in the bands are due to the lack of long-range order.

b) Hypothetical tails, due to the defects in the structure.

In other words they assumed that apart from band tails, a narrow band of trapped states is present in the forbidden gap which can be attributed to dangling bonds, defects, impurities or any other deviation from a continuous random structure. The width of this trapped state is about 0.1eV. They suggested that almost all chalcogenide semiconductors contain a band of compensated level quite near the middle of the gap. Such a band can 'pin' the Fermi level so that the semiconductor is extrinsic rather than intrinsic. Fig.(2.10)

2-3-4 Mott's Model(53)

Mott suggested that dangling bands can act as donors or acceptors, giving the two broadened levels in the centre of the

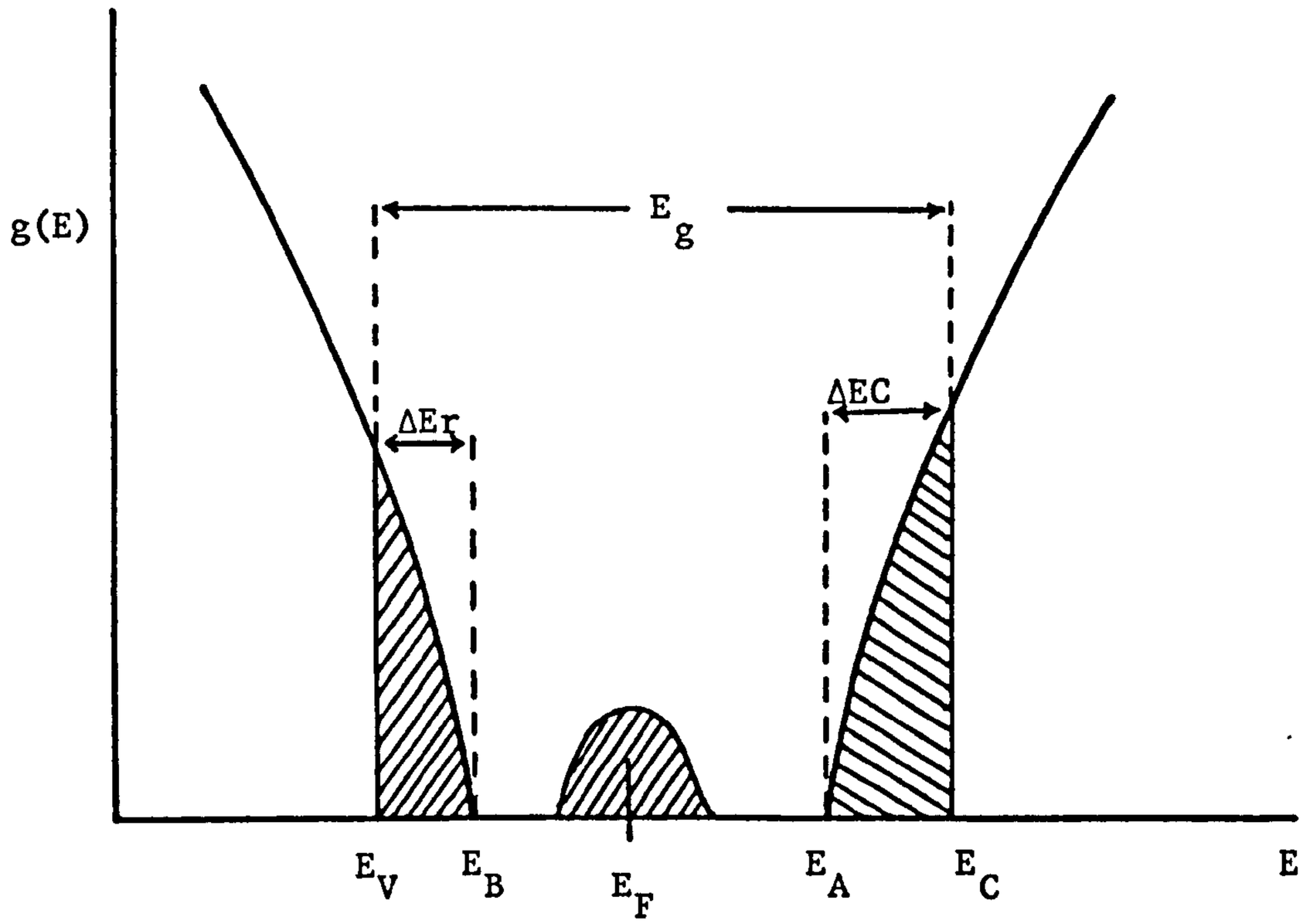

Fig.(2.10) Davis and Mott Model

E_g is the mobility gap or mobility shoulder.

gap. This model is shown in Fig.(2..11). In this model it is difficult to determine whether the material is intrinsic or extrinsic semiconductors. Mott also mentioned that states are spinless deep donors when they are neutral, and they also can act as acceptors. When they are charge they will carry a spin. If the bands of energy levels in their two capabilities overlap as in Fig.(2.11) charged states with spin are expected.

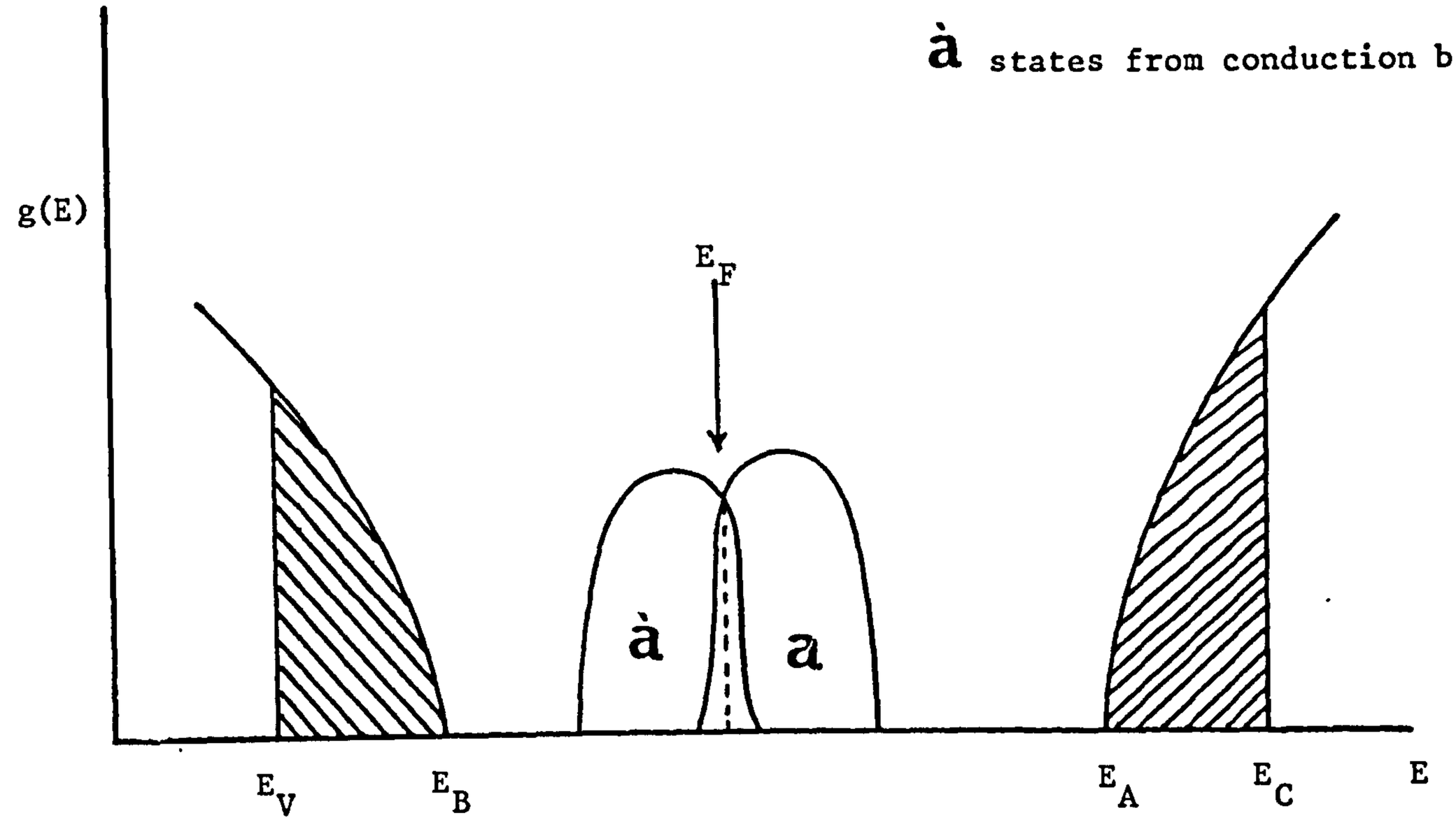

Fig.(2.11) Density of State as a function of Energy in Amorphous Semiconductor Suggested by Mott.

In this model dangling bands act as both acceptors and donors.

2-3-5 Marshall and Owen Model (54)

The main points of this model are as follows:

a) In the band structure of vitreous As_2Se_3 a band gap of approximately 2eV at $T = 0^oK$ appears between the valence and conduction band.

b) Below the delocalized states of the conduction band, and above those of the valence band, there are the usual exponential tails of localized states which are to be

expected in amorphous materials. According to Schottmiller and Tabak[55] the extension of these localized states is about 0.2eV.

c) A large concentration of 'acceptor like' localized states exist at an energy U_oeV above the mobility edge of the valence band. These are the trapping centres which limit the hole drift mobility and their density is about the same as the density of states in the valence band.

d) To explain the intrinsic behaviour of vitreous As_2Se_3 it is necessary to assume the existence of a compensating set of 'donor like' states, with about the same density as the acceptor below the mobility edge of the conduction band

The Fermi level lies half way between the two states at all temperatures to complete the compensation. If the compensation is not quite perfect, the Fermi level will lie inside the under-compensated set of levels at zero temperature and will move to a position approximately between two sets of levels at high temperature. This model is shown in Fig.(2-12)

2-3-6 The Vescan[56] and Croitoru Model[57]

In this model the acceptor and donor like levels lie nearer to the band edges than in the Davis - Mott model. They are suggested to be nearly perfectly compensated and to tail linearly

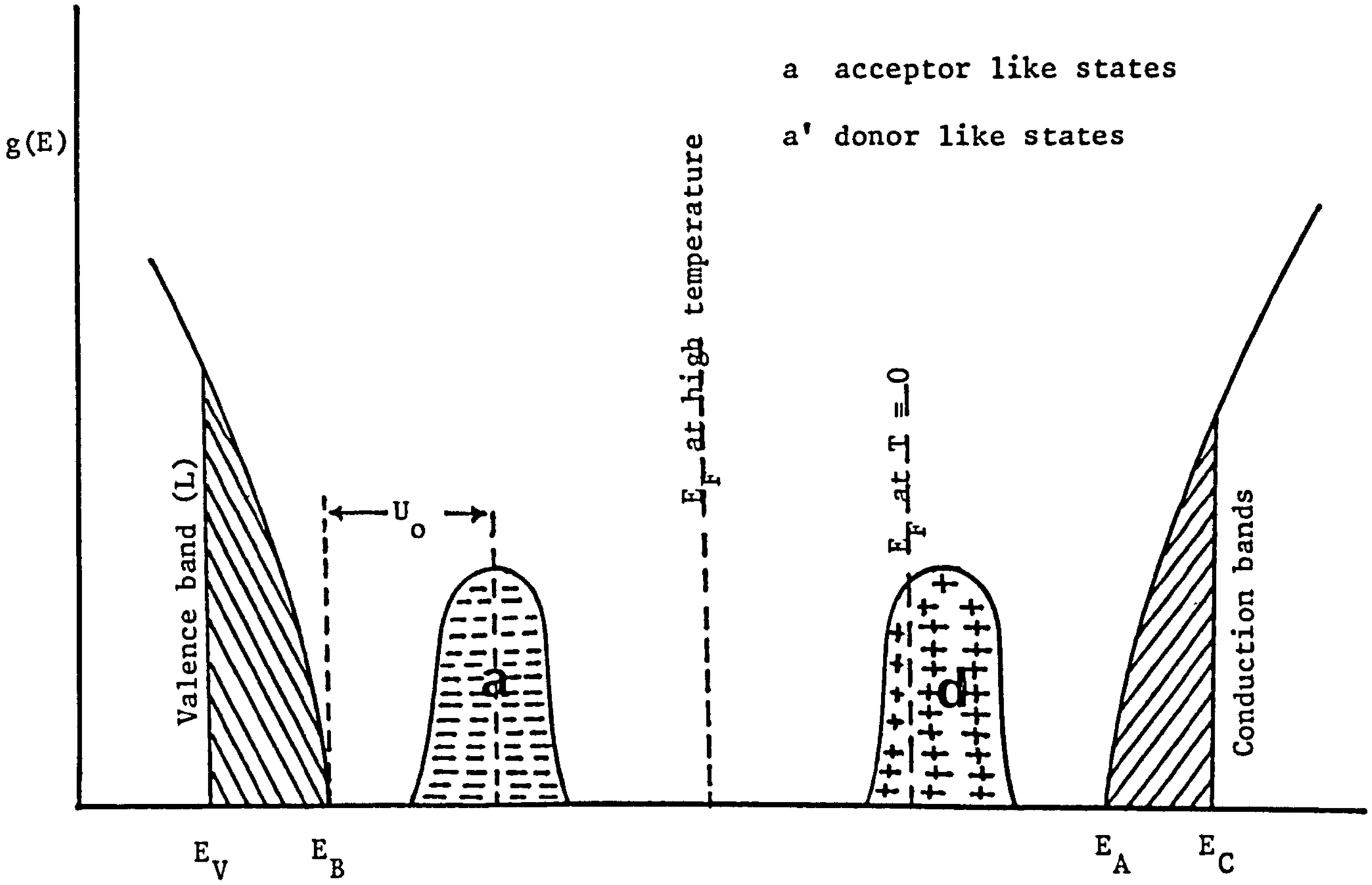

Fig.(2.12) Band Structure Model Suggested by Marshall and Owen for Vitreous As_2Se_3

towards the gap centre. At low temperatures conduction in the two tails is dominant, since the current carried in these tails have a larger separation from the Fermi level than in the case of hopping near the Fermi level, it has to be assumed that the two tails are nearly exactly symmetrical, so that the contribution of electrons and holes almost completely cancel. A sketch of the density of states distribution in this model is shown in Fig. (2.13).

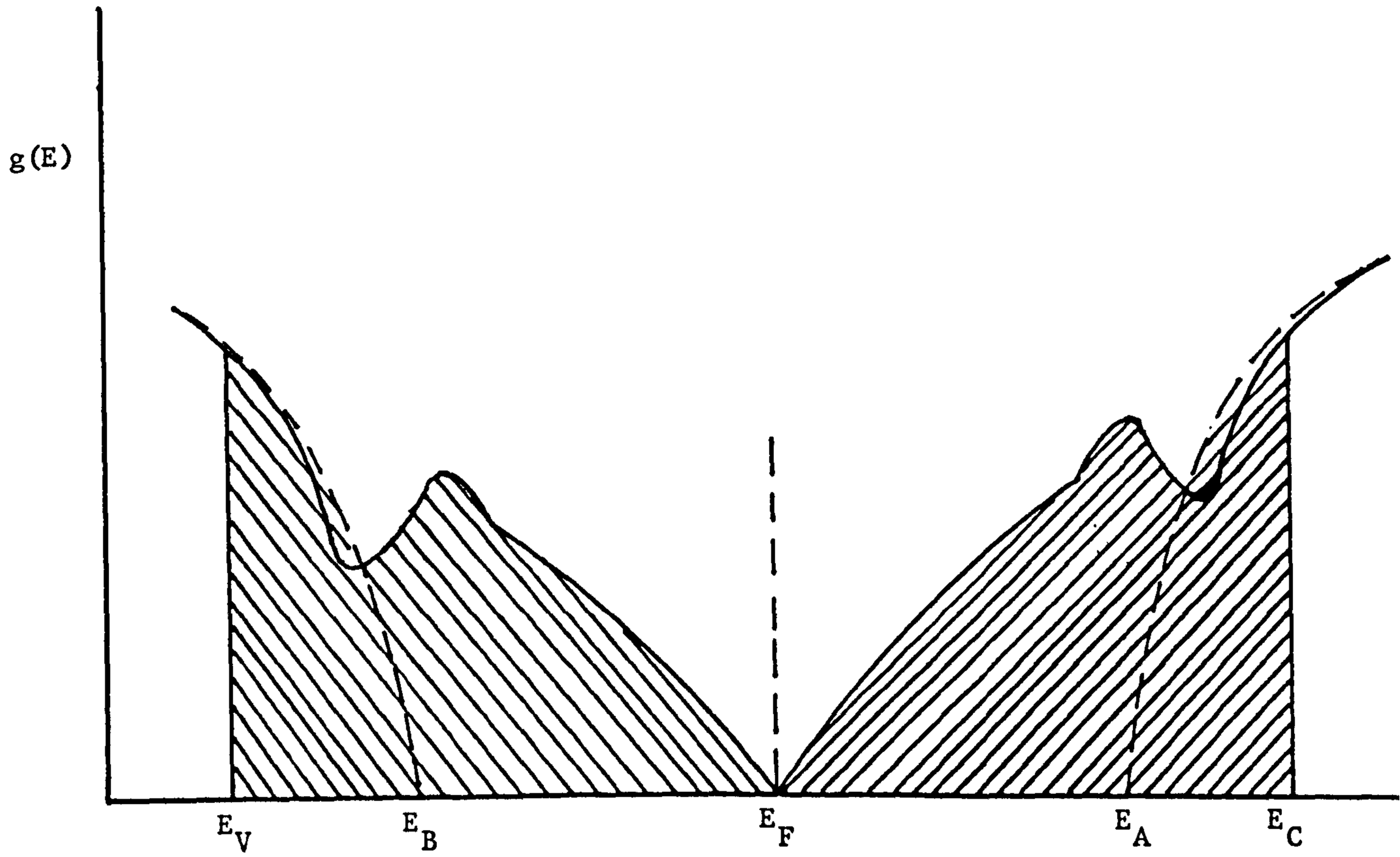

Fig.(2.13) Vescan - Croitoru Model for Density of States.

2-3-7 Madan and Spear Model[58]

This model has very recently been proposed by Madan and Spear for evaporated unannealed amorphous Si and glow discharge Si. This model differs from the Vescan - Croitoru model by its assymmetry and by the finite density of states at the Fermi energy.Fig.(2.14)

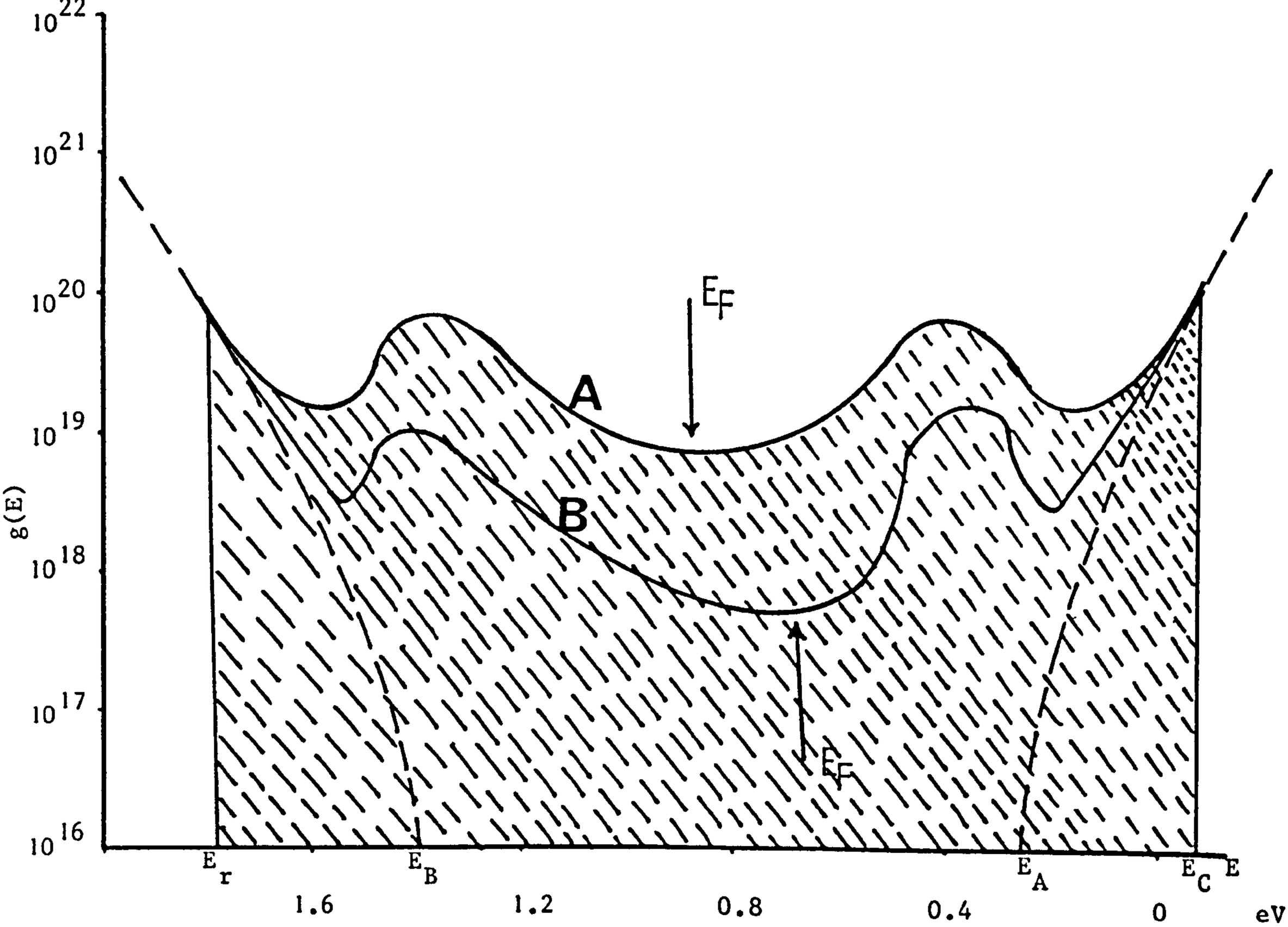

Fig.(2.14) Density of State in the Madan - Spear Model.

A Evaporated Unannealed Si

B Glow Discharge Si

Chapter III

Electrical and Optical Properties of Amorphous Semiconductors

3-1 Electrical Properties

3-1-1 Introduction

Non-crystalline materials (amorphous) may have an electronic band structure which is not much different from that of the corresponding crystal, the main difference is likely to be the tails of localized states in the forbidden gap.

Conduction can occur in bands in the non-localized region, or by hopping amongst the localized states which will be discussed later in this chapter.

In a completely pure crystalline semiconductor, conduction can only occur by excitation of carriers into the conduction band and by their subsequent relatively free motion. The carrier concentration is given by

$$n = (N_c N_v)^{\frac{1}{2}} \exp\left(\frac{-E_g}{2kT}\right) \qquad (3\text{-}1)$$

where N_c and N_v respectively, are the density of available states

in the conduction and valence bands. The conductivity in crystalline materials is given by

$$\sigma = n\mu_n e + p\mu_p e \qquad (3\text{-}2)$$

where μ is the carrier mobility and e the electric charge. Thus,

$$\sigma = (\mu_n + \mu_p) e (N_c N_v)^{\frac{1}{2}} \exp\left(\frac{-E_g}{2kT}\right) \qquad (3\text{-}3)$$

in which

$$(\mu_n + \mu_p) e (N_c N_v)^{\frac{1}{2}} = A = \text{constant} \qquad (3\text{-}4)$$

therefore

$$\sigma = A \exp\left(\frac{-E_g}{2kT}\right) \qquad (3\text{-}5)$$

E_g can be obtained from the slopes of the $\log\sigma$ v.s $\frac{1}{T}$ curves. This kind of conduction is called intrinsic conduction.

If an atom has an extra valence electron, eg. As in Ge, this atom gives rise to donor levels at the energy E_D below the conduction band edge. At T = 0 K the Fermi level lies halfway between the donors level and the conduction band and all the donors are occupied.

With increasing temperature electrons are existed to the conduction band and the carrier concentration and conductivity increases. The conductivity in this case is given by

$$\sigma = \text{constant} \exp\left(\frac{-E_D}{2kT}\right) \qquad (3\text{-}6)$$

the conduction occurs by electrons and is said to be n-type. If the donor concentration is not too high the carrier concentration becomes constant or 'saturated', because all donors are ionized before the intrinsic carrier range is reached. In this region of saturation the log σ decreases with temperature (because the mobility decreases).

Similarly to this, if an atom has an extra hole eg. B in Ge this atom introduces an acceptor level above the valence band, and when these are ionized conduction takes place through holes in the valence band. Conduction in this case is called p-type. Crystalline semiconductors are very sensitive to this kind of impurity addition and doping them with n or p type impurities makes them extremely useful materials.

According to the model which was discussed by Mott[53], conductivity in amorphous semiconductors is given by

$$\sigma = e\int g(E)\mu(E)\ f(1-f)dE \qquad (3-7)$$

where $\mu(E)$ is the mobility of carriers and $g(E)$ density of states and f is Fermi Dirac distribution function, with assuming sharp mobility edge $\mu = 0$ for $E_c<E<E_v$ if we integrate equation (3-7) we obtain

$$\sigma = e\mu_e g(E_c)kT\ \exp\frac{-(E_c-E_f)}{kT} + e\mu_h g(E_v)kT\ \exp\frac{-(E_f-E_v)}{kT} \qquad (3-8)$$

Where the two terms on the right-hand side represents the contributions from the mobile electrons and holes with density $g(E_v)$ and $g(E_c)$ and mobilities μ_e and μ_h respectively. In intrinsic crystalline semiconductors all electrons in the conduction band came from the valence band so that in the case of neutrality

$$n = p$$

this condition determines E_F in terms of the conduction and valence band parameter and the Fermi level lies at the middle of the band gap so that

$$\sigma = A \exp \frac{-(E_c - E_v)}{2kT} \qquad (3\text{-}9)$$

where $A = e\mu g(E)KT$ which is the same as Eq. (3-5)

In amorphous semiconductor $n \neq p$ because of a much larger number of electrons and holes in localized tail states, so that the situation is completely different and this is the subject which we shall discuss in this chapter.

3-1-2 D.c.Conductivity in Amorphous Semiconductors

As in crystalline semiconductors there is a possibility that electrons (or holes) will be thermally or optically activated

into the bands of non-localized levels, above some critical energy, in which they can drift in an applied electric field. In these states the carriers in a glassy semiconductor will be subject to the same collision (scattering) and trapping processes as in a crystal, but there will be at least one important additional scattering mechanism resulting from the lack of strict periodicity in the lattice. This will decrease the mean-free-path and mobility of the carrier and hence increase the resistance. The mean-free-time between collisions is called the relaxation time (τ).

In a field E the accelerating force on an electron is qE and in τ seconds it will acquire a drift velocity v which balances that force, hence

$$\frac{mv}{\tau} = qE \qquad (3\text{-}10)$$

where m is the mass of the electron.

According to the definition of mobility $\mu = \frac{v}{E}$ the mobility of electrons in these normal band states is

$$\mu_0 = \frac{q\tau}{m} = \frac{eD}{kT} \qquad (3\text{-}11)$$

where D is the diffusion coefficient.

For non-crystalline materials as for crystalline materials, the conduction mechanism is divided into two classes.

a) Conduction in which the current depends on the mobility of electrons with energies at or near the Fermi energy. This kind of conduction includes various cases of hopping conduction such as impurity conduction in crystalline semiconductors and low-temperature conduction in amorphous materials.

b) Conduction in which the conductivity due to electrons with energies near the Fermi level is small compared with conduction by electrons excited into the conduction band.

For conduction in class (a) if states are localized the probability 'p' that an electron jumps from one localized state to a given different state with higher energy depends on the following factors:-

I) The Boltzmann factor $\exp\left(\frac{-w}{kT}\right)$ where w is the energy differnce between two states.

II) ν_{ph} phonon frequency.

III) A factor depending on the overlap of the wave-function.

If the overlap is small because the localized states are far apart this factor is

$$\exp(-2\alpha R)$$

as in impurity conduction. If the overlap is large the factor

will be of the order of unity. Hence the probability is

$$P = \nu_{ph} \exp(-2\alpha R)\ \exp(-\frac{W}{kT}) \qquad (3\text{-}12)$$

Only electrons with energies equal to KT at the Fermi level are considered to be taking part in the conduction, and electrons with lower energies need more activation to hop to an empty state. The number of such electrons is

$$N(E_F)kT$$

Thus the diffusion coefficient is

$$D = PR^2\ N(E_F)kT \qquad (3\text{-}13)$$

and the conductivity from the Einstein equation is

$$\sigma = \frac{De^2N}{kT} \qquad (3\text{-}14)$$

or

$$\sigma = e^2\ PR^2\ N(E_F) \qquad (3\text{-}15)$$

R is the average distance in each hopping process.

with substituting probability from Eq.(3-12) into Eq.(3-15) the conductivity will be

$$\sigma = e^2R^2N(E_F)\nu_{ph}\ \exp(-2\alpha R)\ \exp(\frac{-W}{kT}) \qquad (3\text{-}16)$$

where w is the mean activation energy for hopping which is inversely proportional to the density of state.

For strong localization as in impurity conduction the electron will not move further than the nearest neighbour, thus

$$W = A(\frac{1}{R})^3 \, N(E_F) \qquad (3\text{-}17)$$

where A is constant and R is interatomic distance. If localization is weak

$$W = B(\frac{2m\Delta E}{\hbar^2})^{3/2} N(E_F) \qquad (3\text{-}18)$$

where $\Delta(E)$ is the range of energy which E(F) lies Fig.(3.1) illustrates the mechanism of thermally activated hopping conduction by electrons in states near the Fermi energy. The thermally activated electron hops from state (A) below the Fermi energy to one above (B).

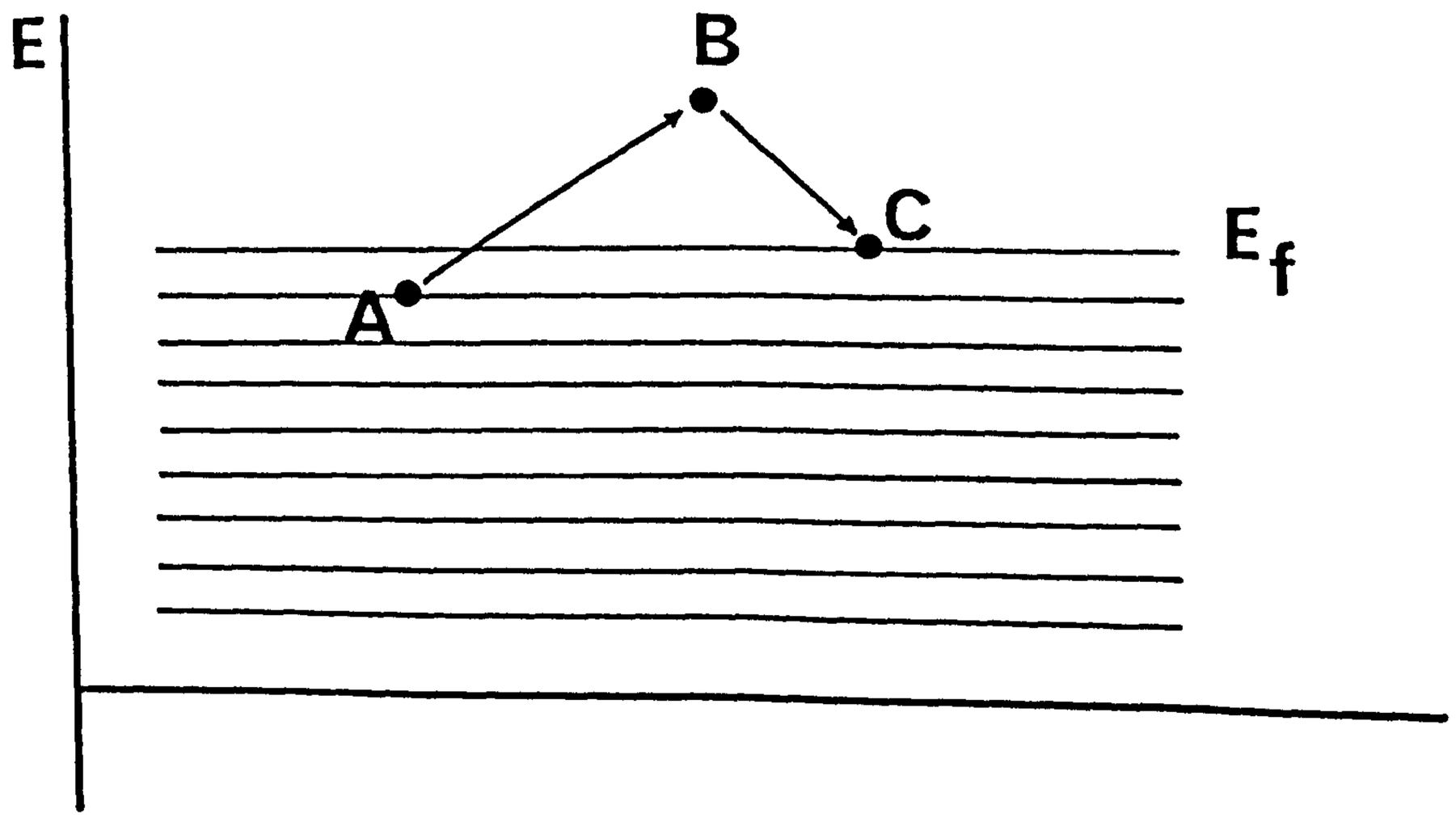

Fig.(3.1) Thermally Activated Hopping Processes in Conduction Mechanisms

As we mentioned earlier in this chapter, the probability p per unit time that this occurs depends on Boltzmann factor $\exp(\frac{-W}{kT})$,phonon frequency ν_{ph} and overlap of the wave function. Hopping mobility μ is given by[43]

$$\mu = (\nu_{ph} \frac{ea}{kT}) \exp(\frac{-W}{kT}) \qquad (3\text{-}19)$$

3-1-3 Temperature Dependence of d.c. Conductivity

Considering models for the density of states and mobilities as mentioned in the last chapter, four mechanisms of electrical conduction can be distinguished for an amorphous semiconductor.

1) Conduction due to carriers excited beyond the mobility shoulders into non-localized (extended) states. The main current is carried by holes. In this case the conductivity is given by

$$\sigma = \sigma_0 \exp \frac{-(E_f - E_v)}{kT} \qquad (3\text{-}20)$$

where the σ_0 is conductivity at T = 0K is expected to be given by

$$\sigma_0 = 0.06 \frac{e^2}{\hbar a_E} \qquad (3\text{-}21)$$

In general σ_0 lies between 10^2 and 10^3 $\Omega^{-1}cm^{-1}$ depending on co-ordination number and the distance between the states eg. for $z = 6$ and $a_E = 4A^o$ is about $350\Omega^{-1}cm^{-1}$. It can also be given by

$$\sigma_0 = e\, N(Ev)kT\mu_0 \qquad (3\text{-}22)$$

where μ_0 is the mobility in extended states which is proportional to $\frac{1}{T}$.

2) Conduction due to carriers excited into localized states at the band edges (E_A or E_B). Here also the main current is carried by holes and conduction is by hopping hence

$$\sigma = \sigma_1 \exp \frac{-(E_f - E_B + \Delta W_1)}{kT} \qquad (3\text{-}23)$$

where $\Delta W1$ is the activation energy for hopping and σ_1 is estimated to be a factor of $10^2 - 10^4$ less than σ_0.

3) Conduction due to carriers hopping between localized states near the Fermi energy eg. conduction in heavily doped semiconductors (impurity conduction) and the conductivity is given by

$$\sigma = \sigma_2 \exp \frac{-\Delta W_2}{kT} \qquad (3\text{-}24)$$

where σ_2 is less than σ_1 and ΔW_2 is the hopping energy and it is equal to half of the band width.

4) At low temperature, eg. when kT is less than the band width, hopping will not take place between the nearest neighbours, but there will be a variable range of hopping and the conductivity is then given by

$$\sigma = \sigma_2' \exp\left(\frac{-B}{T^{\frac{1}{4}}}\right) \qquad (3\text{-}25)$$

where

$$B = 2\left[\frac{a^3}{kN(E_F)}\right]^{\frac{1}{4}} \qquad (3\text{-}26)$$

in which a is the distance between the states. A plot of $\ln\sigma$ vs. $\frac{1}{T}$ for the different regions mentioned above is shown in Fig.(3.2)

The total conductivity for all the processes mentioned above is obtained as an integral over all available energy states

therefore

$$\sigma = \int \sigma(E)\, dE \qquad (3\text{-}27)$$

or

$$\sigma = \int e\, N(E)\, \mu(E) kT\, \frac{df(E)}{dE} \qquad (3\text{-}28)$$

where f(E) is the Fermi - Dirac function.

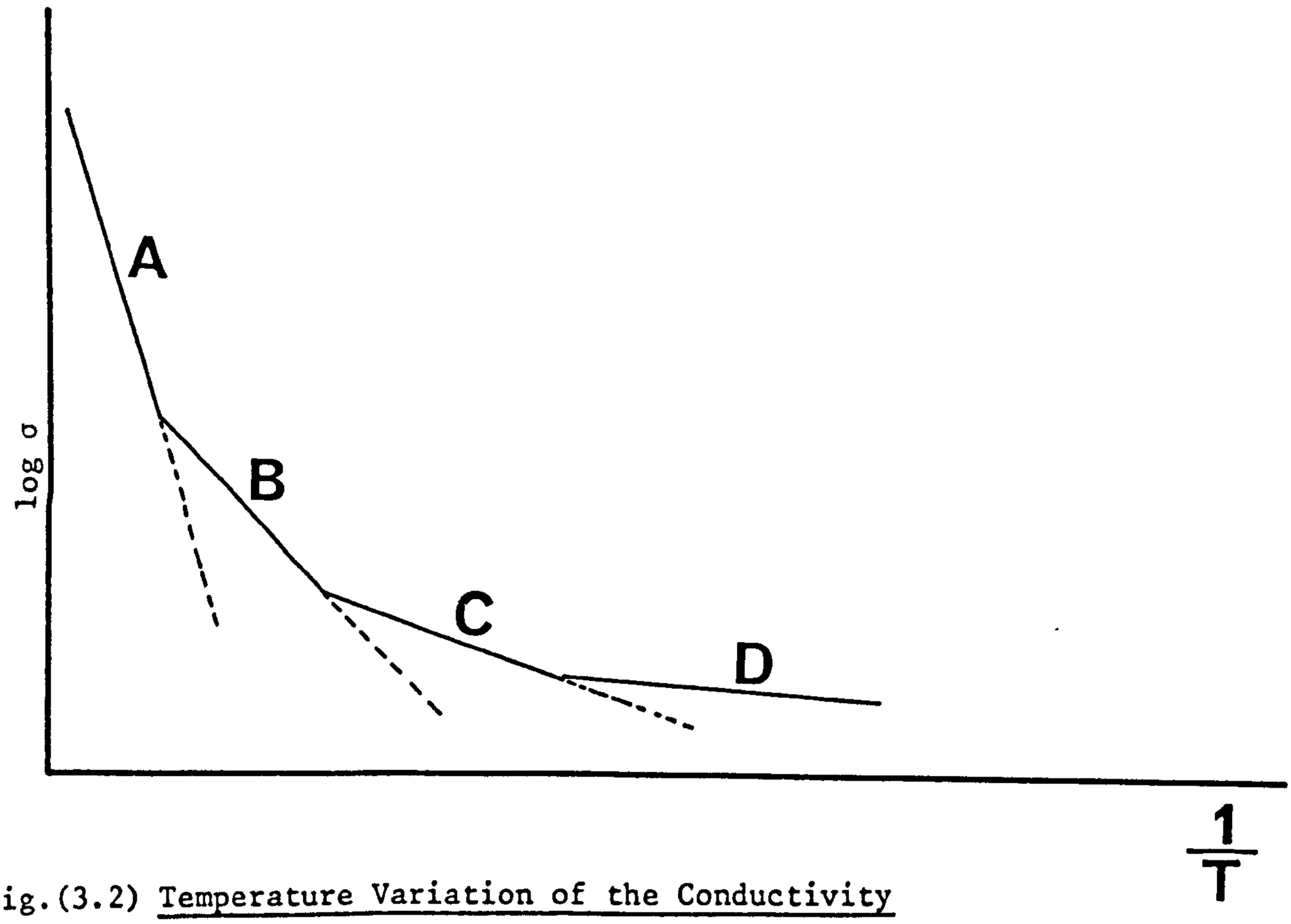

Fig.(3.2) Temperature Variation of the Conductivity

Slopes of the curves are the activation energy.

A. $\sigma = \sigma_0 \exp \frac{-(E_c - E_f)}{kT}$

B. $\sigma = \sigma_1 \exp \frac{-(E_A - E_F + W_1)}{kT}$

C. $\sigma = \sigma_2 \exp \left(\frac{-W_2}{kT}\right)$

D. $\sigma = \sigma'_2 \exp \left(\frac{-B}{T^{\frac{1}{4}}}\right)$

3-1-4 A.C. Conductivity

Pollak and Geballe[59] were the first who observed a frequency-dependent conductivity $\sigma(\omega)$ in a hopping system for compensated crystalline silicon in the impurity conduction range. The dependence could be shown as

$$\sigma(\omega) = A(\omega)^n \qquad (3.29)$$

Where A is constant, ω is the angular frequency and n was found to have a value close to (0.8) and to be weakly dependent on temperature.

Pollak in several papers,[60,61,62] by using this theory, analysed the hopping motion of electrons between pairs of localized sites and also extended this to hopping over many sites.

The theory of this phenomenon was reviewed by Jonscher [158] and he pointed out that this type of frequency dependence is found not only in disordered glassy and amorphous solids, but also in molecular solids. He also found that the carriers involved are not necessarily electrons, but may be polarons, protons or ions.

It has been found that n is not a constant for all systems as was assumed by many authors, but is a function of temperature

and is close to unity at low temperature and decreases with increasing temperature. There are many other theoretical treatments of the frequency dependent of conductivity in hopping systems eg. Mott[39], Austin and Mott[63], Davis and Mott[52] and the more recent theory is that of Scher and Lax [64-65] who have extended the d.c. conduction theory of Miller and Abrham[13] to a.c. conduction.

According to Mott and Davis three mechanisms of charge transport which can contribute to d.c. conductivity in amorphous semiconductors can be applied to the a.c. conductivity as follows.

a) The conduction by carriers excited to the non-localized (extended) states near band edges. For these carriers a.c. conductivity is given by

$$\sigma(\omega) = \frac{\sigma(0)}{1+\omega^2\tau^2} \qquad (3\text{-}30)$$

Where τ is the relaxation time defined earlier in this chapter ($\sim 10^{-15}$s). A decrease in $\sigma(\omega)$ as ω^{-2} is not expected below the frequency $\sim 10^{15}$HZ. We have to note that in the electrical range of frequency up to 10^7HZ no frequency dependence of the conductivity associated with carriers in non-localized states is expected.

b) Conduction by carriers excited into the localized states at the edges of the valence and conduction band.

The temperature dependence of the a.c. conductivity should be the same as that of the carriers concentrated at the band edge, so that for the conduction band it should increase as

$$\exp \frac{-(E_A - E_F)}{kT} \qquad (3\text{-}31)$$

The frequency dependence of a.c. conductivity is expected to be as

$$\omega \left(\mathrm{Ln} \frac{\nu_{ph}}{\omega}\right)^4 \qquad (3\text{-}32)$$

Where ν_{ph} is the phonon frequency.

c) Hopping transport by electrons with energy near the Fermi level. The conductivity in this process is expected to increase with frequency as $\omega \left(\mathrm{Ln} \frac{\nu_{ph}}{\omega}\right)^4$ but the exponential dependence on the temperature is absent. $\sigma(\omega)$ is proportional to T if kT is small compared to the width of the occupied part of the defect band and independent of T if kT is large.

The frequency dependence of conductivity was formulated by

Austin and Mott[66] as below

$$\sigma(\omega) = 1/3\ \pi e^2\ kT\left[N(E_F)\right]^2 \alpha^{-5} \omega \left(\mathrm{Ln}\frac{\nu_{ph}}{\omega}\right)^4 \qquad (3\text{-}33)$$

It has been assumed that in this formula hopping is between pairs of centres, in other words the multipile-hopping processes can be neglected[67].

Fig.(3.3) shows the frequency dependence of the conductivity for three different conduction mechanisms mentioned above.

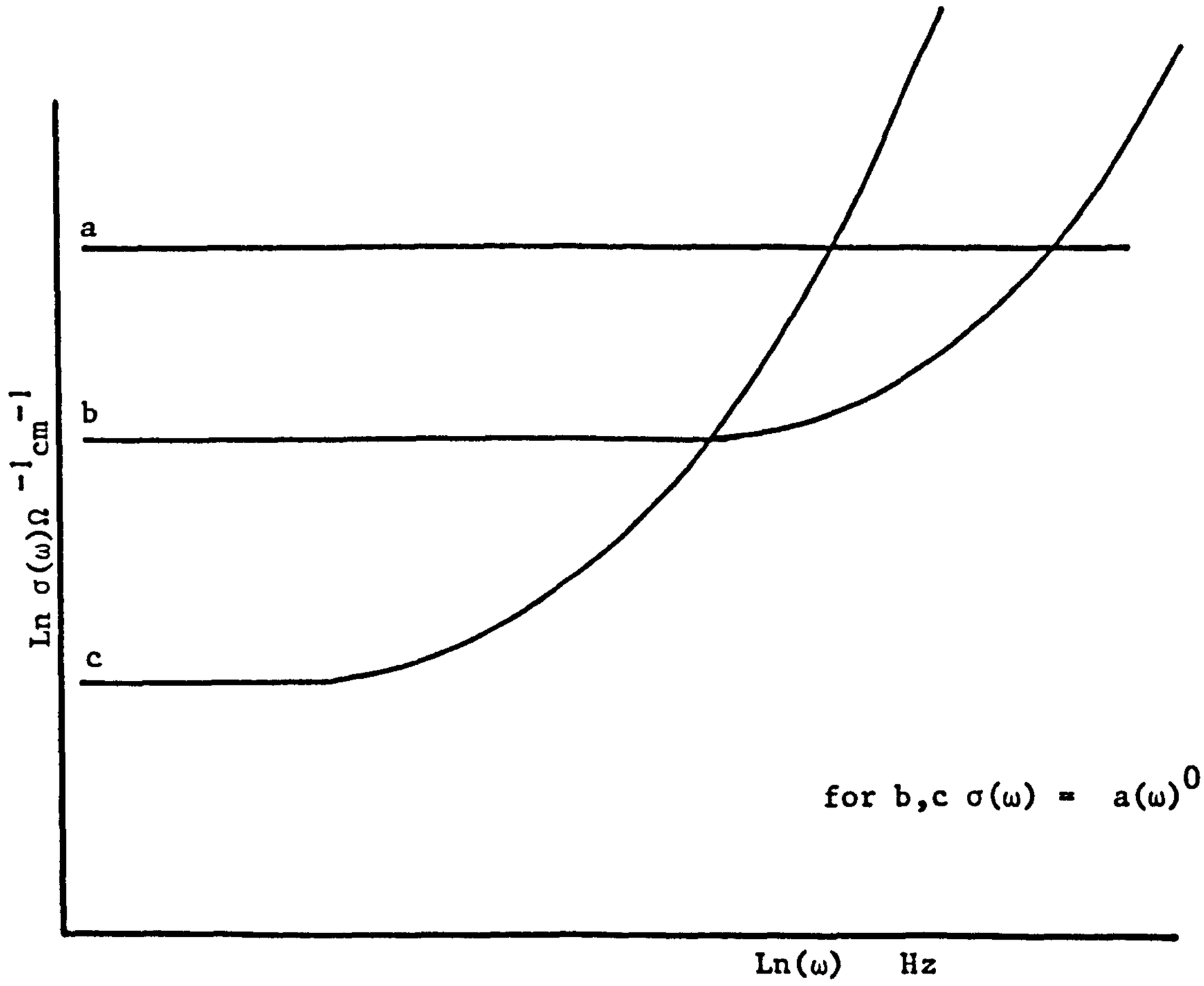

Fig.(3.3) Frequency dependence of a.c. Conductivity[43]

Typical temperature dependence of a.c. conductivity for a vitreous state is shown in Fig.(3.4)

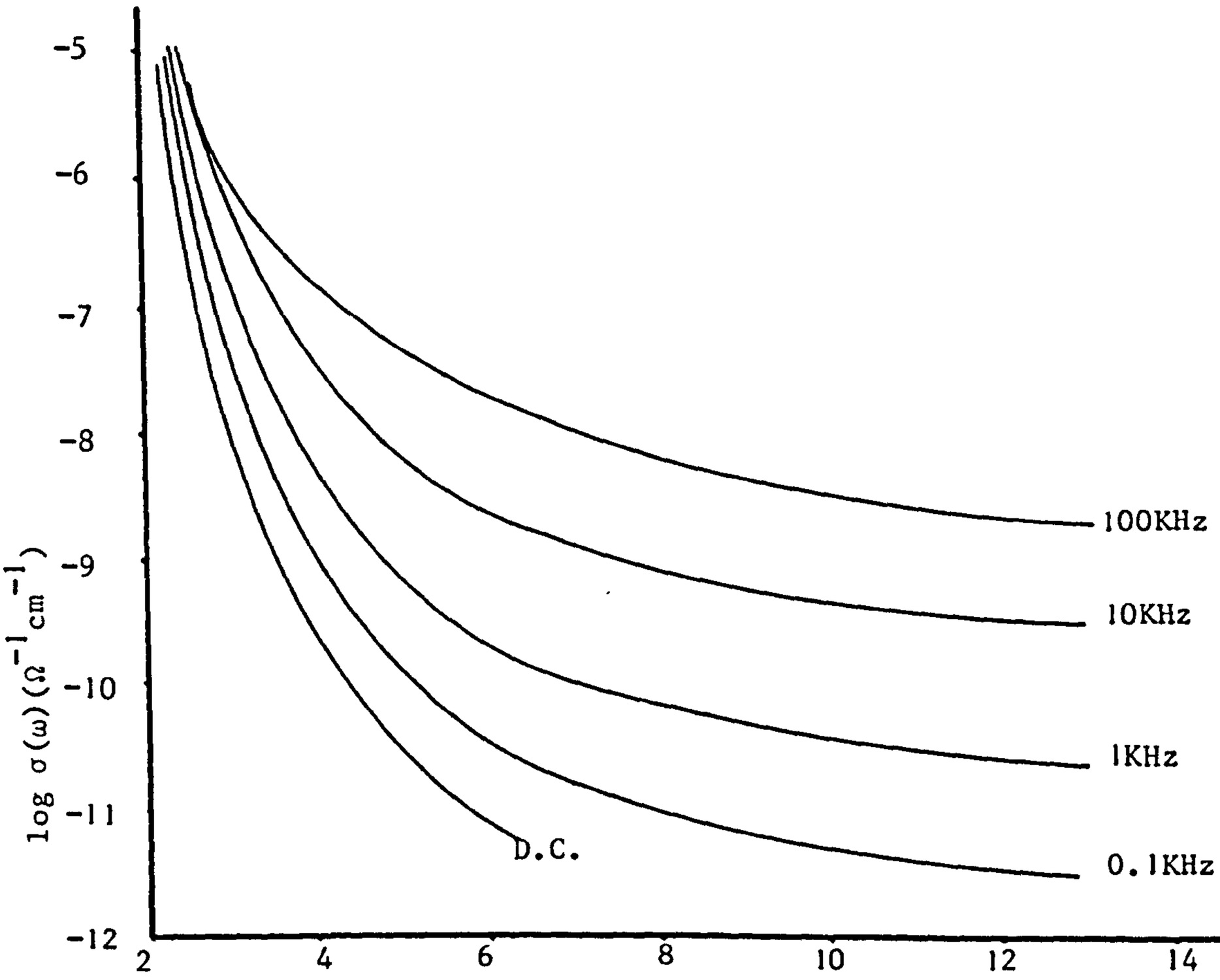

Fig.(3.4) Temperature dependence of Conductivity for Vitreous States[68]

3-1-5 High Electric Field Effect

If a sufficiently high electric field be applied to a semiconductor material sooner or later there will be a deviation from linearity in the current - voltage characteristic which is refered to as non-Ohmic conductivity.

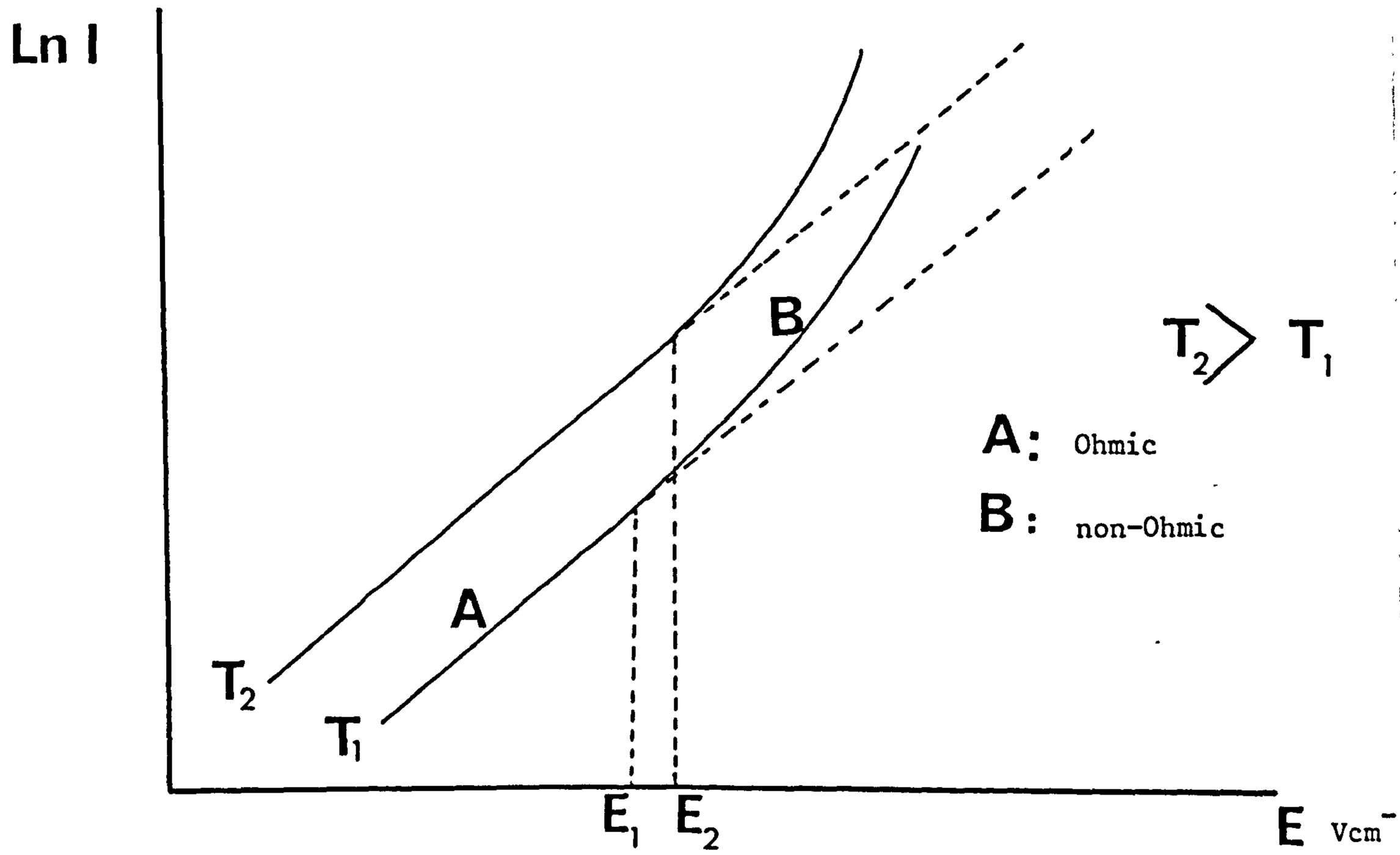

Fig.(3.5) Current - Voltage Characteristic at Low and High Electric Field at Different Temperature

The effects of high field can be thermal or electrical. The former arise because of the fact that interactions between electrons and phonons (lattice Vibration) exist in all materials. When electrons are accelerated by the field, they can always emit phonons, thus giving up some of this excess energy to the ion cores. This increases the temperature of the material, and effect known as Joule heating.

Electronic non-Ohmic effects arise because of changes in the response of the electrons in the material to the electric field itself at a constant temperature. In general the non-Ohmic characteristic due to high field can be classified into two classes as in the following.

a) Behaviour in which the free carrier density is enhanced by field emission from traps and charged centres. In the model of Poole and Frenkel, the material is assumed to contain neutral impurity centres and the field-emission current is given by[69]

$$J = A\ (\theta\ \text{Cosh}\ \theta - \text{Sinh}\,\theta\ )\,\theta^{-2} \qquad (3\text{-}34)$$

where A is constant and θ is given by

$$\theta = \frac{(\frac{eE}{\pi k})^{\frac{1}{2}}}{kT} \qquad (3\text{-}35)$$

It has been assumed that the field alters the equilibrium free carrier concentration and the conductivity is enhanced as

$$\sigma(E) = \sigma_{(o)}\ (1 + \theta\ \text{Sinh}\ \theta - \text{Cosh}\ \theta)\ \theta^{-2} \qquad (3\text{-}36)$$

The physical basis of Poole-Frenkel effect is the lowering of the Coubombic potential barrier when it interacts with an electric field, and thermal excitation of electrons from traps into the conduction band.

The Poole-Frenkel effect applies on donor sites, acceptor sites and traps as well as in the valence band.

b) Behaviour in which the mobility becomes field dependent.

In some amorphous semiconductors charge transport occurs in states close to mobility edge which divides localized states (tails) from non-localized or extended states. Mott pointed out that in a high field, carriers trapped in localized states just below the mobility edge will be released by tunnelling into the extended states above the mobility edge, thus their mobility increases.

Marshall and Miller observed a field dependent mobility of the form

$$\mu_{(E)} \propto \mu_0 \exp \frac{eaE}{kT} \qquad (3\text{-}37)$$

for chalcogenide glasses which extends down to low fields $\sim 10^3$ Vcm^{-1} or less. In contrast to chalcogenides the transitional metal oxide glasses show Ohmic behaviour at fields up to $\sim 10^5$ Vcm^{-1}. At higher fields the conductivity varies as

$$\sigma(E) = \sigma(0)\frac{\text{Sinh } \frac{eaE}{2kT}}{\frac{eaE}{2kT}} \qquad (3\text{-}38)$$

where a is the jump parameter which is larger than ion spacing for a hopping model the sinh term implies a departure from Ohmic behaviour at high fields.

3-1-6 Switching Phenomena

One of the most important factors to achive a drastic change in the physical properties of the material is the possibility of controlling the short-range order parameters of amorphous semiconductors.

In switching phenomena two different cases should be distinguished as follows.

a) Those phenomena which do not involve a change in the structure of a material, which implies that the atomic arrangement remains essentially undisturbed.

b) Those phenomenon which are associated with a structual change. Threshold switching is an example of case 'a' and for case 'b', memory switching is typical in some materials. A structural change can be achieved either locally by a current pulse or over a large area by exposing the material to a light image.

3-1-7 Threshold and Memory Switching

Fig.(3.6 a,b) shows the characteristics of threshold and memory switch. When a low voltage is applied to a semiconductor the conduction is Ohmic (up to field of the order of 10^4 v/cm for chalcogenide glasses); under this field the semiconductor is in its high resistance state which is known as the 'off state'.

If the value of the applied field increases sufficiently (above 10^4 v/cm) non-Ohmic processes become evident and the current rises exponentially with applied voltage but the semiconductor is still in its high resistance state. At a critical value of field ($\sim 10^5$ v/cm for chalcogenide glasses) the sample switches from high resistance to a low resistance which is known as the 'on state' and current increases rapidly.

The actual switching is extremely rapid occurring in less than 5×10^{-5} sec. Switching from high resistance (off state) to low resistance (on state) is common for both types of switching which occur at a critical voltage V_t (threshold voltage) when applied voltage is increasing gradually from low to high voltage, or after a delay time T_D when voltage pulse V_P larger than V_t is applied. The delay time T_D decreases rapidly as the applied voltage V_P is increased beyond V_t. For $V_P > 1.2V_t$ it decreases exponentially as [70]

$$T_D = T_{D_0} \exp(-\beta V_P) \qquad (3\text{-}39)$$

where β is constant.

The principal difference between the two devices is the existance in the threshold switch of a holding current value I_h below which the low resistance state (on state) can not be maintained. ie when the current falls below this voltage the threshold switch returns to its high resistance (off state). In

contrast the memory switch retains a low-resistance state even when the current approaches zero or becomes negative.

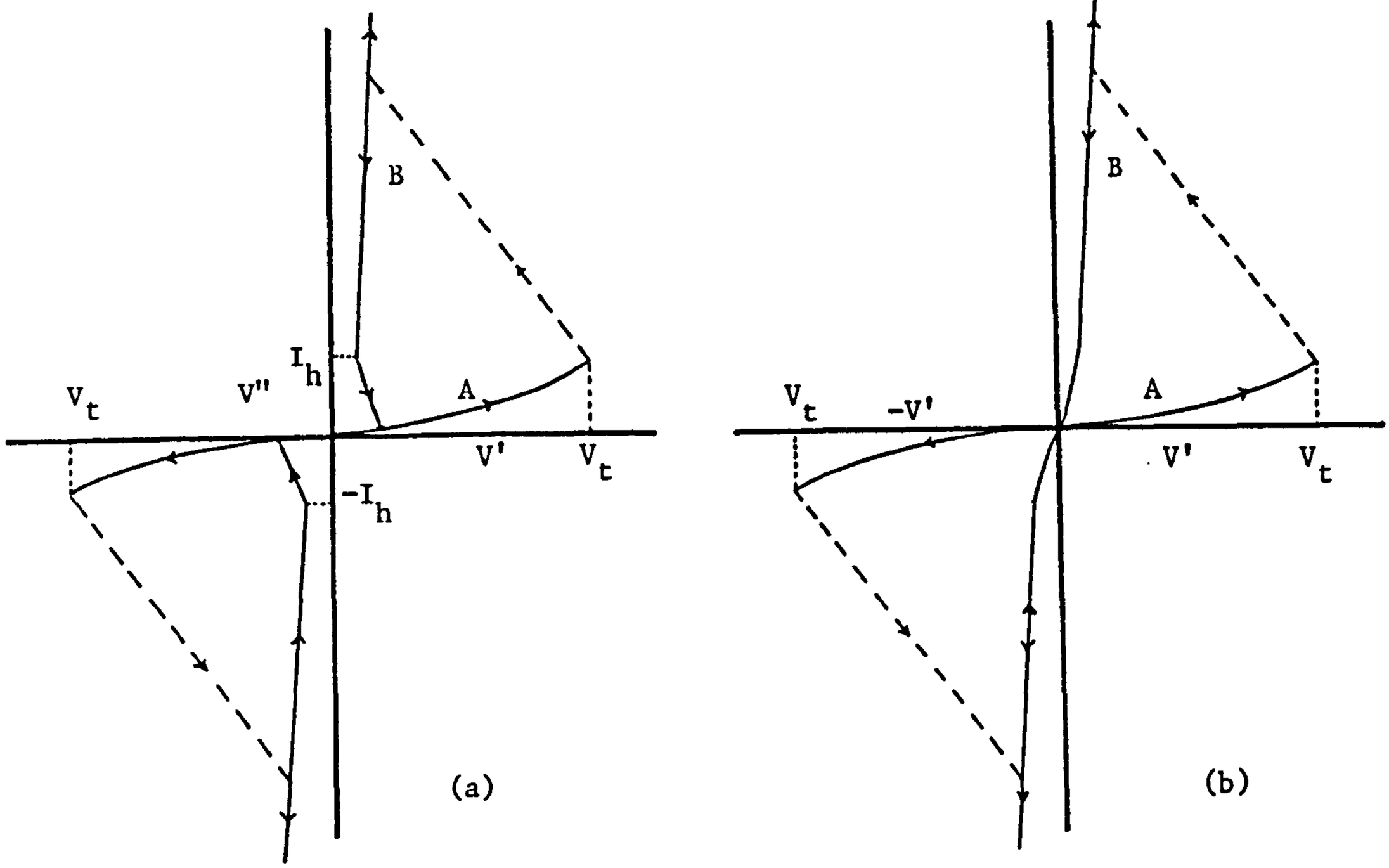

Fig.(3.6) Typical I - V Characteristic of a) Threshold and b) Memory Switching Device

A and B are the regions for off and on states respectively.

The memory switch retains its low resistance state only after it has been kept in this state for a sufficient period of time, the lock-on time 'T_{LO}' to set the memory state. If the set pulse V_P is shorter than $T_D + T_{LO}$ then the memory switch reverts to its high resistance as if it were a threshold switch. After lock-on the memory switch is in a permanent low resistance (conductive) state. The lock-on period represents the time needed to allow the material in the current channel to devitrify.

The switching threshold voltage (V_t) increases nearly linearly with electrode separation up to separation of about 2 microns and less fast for larger separation. V_t decreases generally with increasing temperature although threshold-type switching has been observed in semiconducting metals of Te with Se or S several hundred degrees above the melting point.

3-1-8 Phonons (Lattice Vibration) and Polarons

Lattice vibrations which are called phonons affect the properties of materials (electrical and optical) in various ways.

a) In non-crystalline materials as well as in crystals, scattering of electrons by phonons increases the resistivity. In amorphous semiconductors since the mean-free-path of the carrier is already of the order of the lattice parameter due to disorder, the effect of phonon scattering is likely to be small, but it may be more important in non-crystalline solid metals. In non-crystalline semiconductors an electron with energy near E_C is scattered once every 10^{-15} sec. and these collisions can be elastic or inelastic. The probability per unit time that an electron loses a quantum of energy $\hbar\omega_0$ to a phonon with angular frequency ω_0 is normally not greater than $\omega_0(\sim 10^{-12}\text{sec.}^{-1})$. Thus the rate of loss of energy is often $\hbar\omega_0^2$.

b) Thermally activated hopping.

In thermally activated hopping an electron can jump from one

localized state to another, only when the energies of the two states are different, and this happens as a result of exchanging energy with phonons. Electrons jump between two localized states with difference W_D, and electron exchanges this energy with phonon. Two different cases must be distinguished I. If $W_D < \hbar\omega_0$ and II. $W_D > \hbar\omega_0$, where ω_0 is the highest phonon frequency and we will come to this later.

c) Formation of polaron, which is in fact as a result of distortion of the lattice around the localized electron. The polaron is an electron which moves through the lattice so slowly that there is sufficient time for the cage surrounding its host ion to relax into a new configuration appropriate to the altered charge on the central ion. This produces a change in the energy level scheme on the host ion in which the electron can be said to be self trapped.

The polaron binding energy is the magnitude of the alteration in the electron energy level. In fact a polaron is formed from the electron and the lattice distortion which it carries with it through the solid.

The size of the polaron is determined by the ratio of the electron overlap to the polaron binding energy. Thus the polaron is large when the electron overlap is large compared to the polaron binding energy, and small when the ratio of overlap to polaron binding energy is small. A small polaron can be formed in two cases I.in the case of strong

localization, and II. in the case of a charge coupling between the electron and the lattice. A study of the conductivity as a function of temperature of glasses containing transtional metal oxides suggests that the charge carrier is well described by a small polaron. The theory of conduction by small polarons has been developed by Holstein[71] and Friedman[72].

Polaron theory has been derived in various limits, depending on the strength of the electron-phonon interation, the extent of the lattice distortion, and band-width of the electron.

Fröhlich[73] showed that the extent of the lattice distortion induce by an electron of effective mass m* is

$$\delta_p = \left(\frac{\hbar}{2m^*\omega_o}\right)^{\frac{1}{2}} \qquad (3\text{-}40)$$

where ω_0 is an average longitudinal optical phonon frequency and $\delta_p = r_p$ is called the radius of the polaron. He concluded if r_p is much larger than the interatomic spacing the polaron is called large, and if the opposite condition obtains it is called a small polaron.

d) The effect of polaron formation on transport properties.

3-1-9 Single Lattice Processes

In the case of some crystalline materials (Ge, Si), the wave function of an electron in a donor centre has an extent large compared with the lattice parameter. Thus the distortion of the lattice which it produces is small and is usually negligible. For electrons in deep traps this may not be true. A simple way of developing the theory of polaron motion in a molecular lattice has been given by Austin and Mott[66]. They considered the energy of a diatomic molecule as a function of some configurational co-ordination 'q' which can be the distance between nuclei. The minimum energy is supposed to be at $q = 0$. If we assume that the energy of a moleclue is Aq^2. For small value of q and an electron (or hole) is placed on the molecule, the total energy is then

$$Aq^2 - Bq \qquad (3\text{-}41)$$

where $-Bq$ is the energy of an extra electron on the molecule, Fig.(3.7) Value of (3-41) has its minimum when $q = q_0$ then

$$B/2A = q_o \qquad (3\text{-}42)$$

The energy of the system is lowered by Bq_0 with the substituting (3-42) into (3-41) we can determine the distortion energy of the system

$$Aq_0^2 - 2Aq_0^2 = -Aq_0^2 = W_P \qquad (3\text{-}43)$$

This energy which is as a result of polorization is called polaron energy.

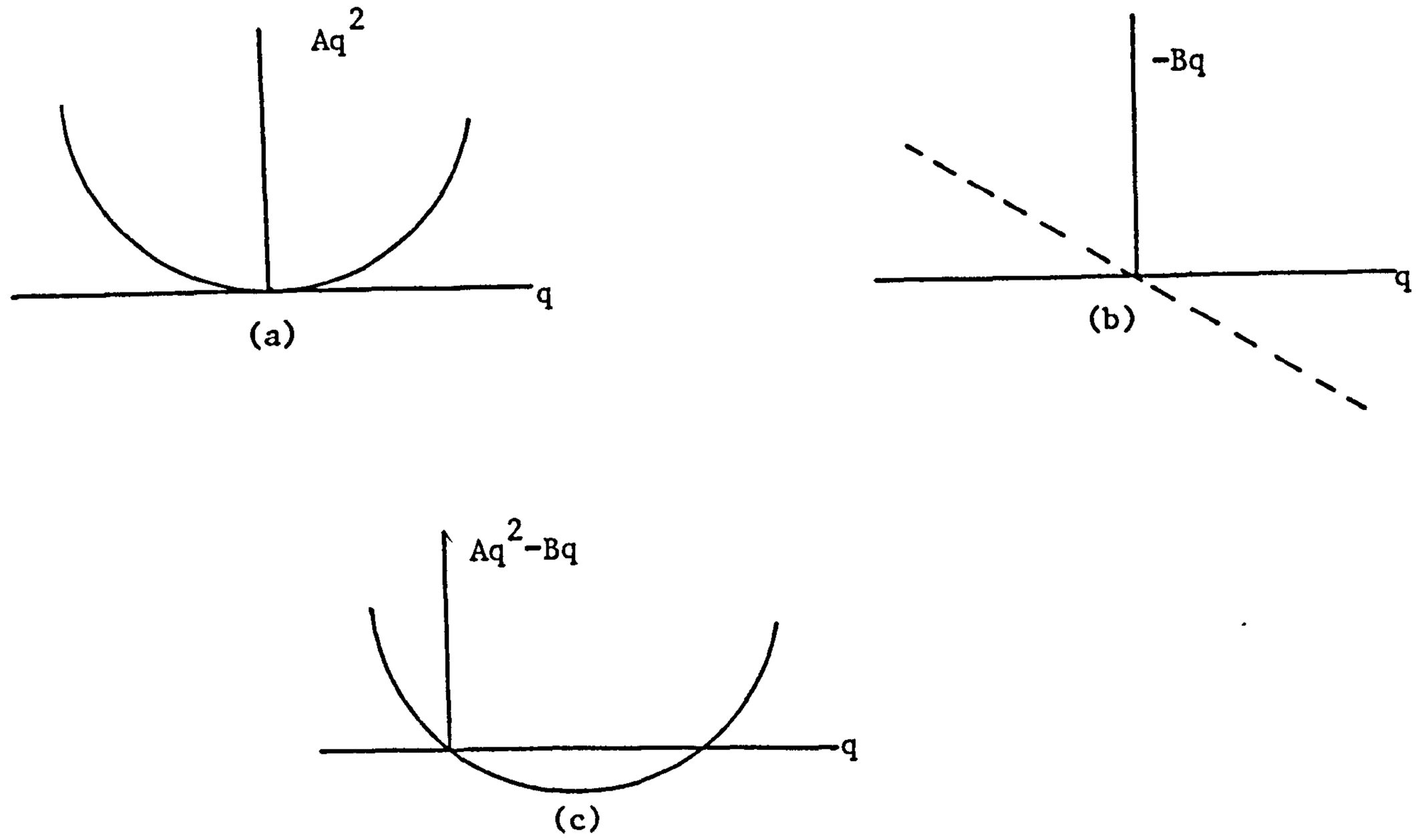

Fig.(3.7) The Energy of an Electron as a Function of a Configuration Parameter q[43]

For a polar lattice, we consider a trap with radius r_0 which is neutral when empty. When an electron comes into this trap, before the surrounding ions are displaced, the potential energy of (another) electron at a distance r is

$$V_p = \frac{e^2}{\varepsilon_\infty r} \quad r>r_0 \tag{3-44}$$

where ε_∞ is the high frequency dielectric constant. After the ions are displaced the potential energy becomes $\frac{e^2}{\varepsilon r}$ therefore an electron forms a potential well for itself which is equal to Fig.(3.8)

$$V_p(r) = \frac{-e^2}{\varepsilon_p r} \qquad (r>r_o) \tag{3-45}$$

$$V_p(r) = \frac{-e^2}{\varepsilon_p r_0} \qquad (r<r_o) \tag{3-46}$$

where

$$\frac{1}{\varepsilon_p} = \frac{1}{\varepsilon_\infty} - \frac{1}{\varepsilon_o} \tag{3-47}$$

and the energy of the system is lowered by[43]

$$W_p = \frac{1}{2}\ \frac{e^2}{\varepsilon_p r_o} \tag{3-48}$$

which is due to polarization.

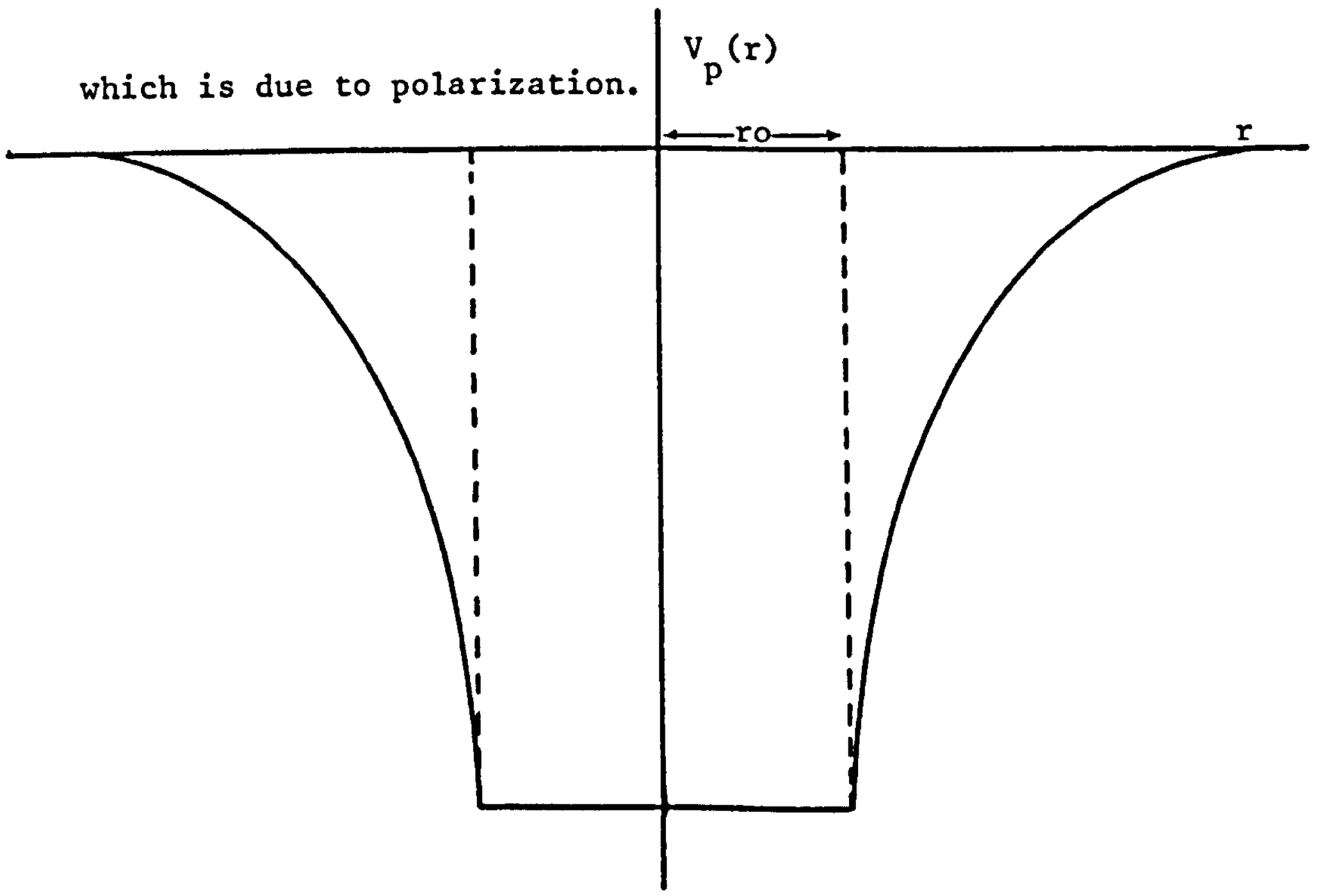

Fig.(3.8) Potential Well Due to Polarization of an Ion Lattice Around a Trapped Electron[43]

3-1-10 Multiphonon Processes

Now we consider that an electron is hopping from one molecule to another with configuration co-ordinations q_1 and q_2. This is a transition in which several phonons are simultaneously emitted or absorbed and may give a larger transition probability when a single phonon hop. We have two localized states with energy difference W_D. The electron energies on either molecule must be identical, then,

$$B(q_1 - q_2) = W_D \tag{3-49}$$

if the electron is initially on molecule 2, the energy required to produce such a state is

$$A(q_1)^2 + A(q_2 - q_0)^2 \tag{3-50}$$

or
$$A(q_2 + \frac{W_D}{B})^2 + A(q_2 - q_0)^2 \tag{3-51}$$

and it is minimum when

$$q_2 = \frac{q_0}{2} - \frac{W_D}{2B} \tag{3-52}$$

from (3-52) and (3-51) the minimum energy required for an electron to hop from one state to another is

$$W = \tfrac{1}{2} W_P + \tfrac{1}{2} W_D + \frac{W_D^2}{8W_P} \tag{3-53}$$

or $$W = W_H + \tfrac{1}{2} W_D + \frac{W_D^2}{16 W_H} \tag{3-54}$$

where $$W_H = \tfrac{1}{2} W_P = \frac{e^2}{4\varepsilon_p r_o} \tag{3-55}$$

when W_D is small, term $\frac{W_D^2}{16W_H}$ is negligible then

$$W = W_H + \tfrac{1}{2} W_D \tag{3-56}$$

W_H is hopping activation energy for small polarons which is approximately half of the polaron binding energy W_P and W_D is called disorder energy. Eq.(3-55) is valid only in a model in which the electron on one molecule does not affect the value of q for the other. In other words in polar materials in which two polarization wells overlap and can affect each other it is not valid.

For polar lattices if the distance R through which the electron must be transfered is not large compared with r_p Eq.(3-55) must be modified as[66]

$$W_H = \frac{e^2}{4\varepsilon_p}\left(\frac{1}{r_p} - \frac{1}{R}\right) \tag{3-57}$$

where $\frac{1}{\varepsilon_p} = \frac{1}{\varepsilon_\infty} - \frac{1}{\varepsilon_0}$ and ε_∞, ε_0 are high and low frequency dielectric constants respectively and r_p is the polaron radius given by[74]

$$r_p = \tfrac{1}{2}\left(\frac{\pi}{6N}\right)^{1/3} \tag{3-58}$$

where N is the number of sites per unit volume.

The probability per unit time for an electron hops from one site to another is given by

$$P = \lambda \exp\left(-\frac{W}{kT}\right) \tag{3-59}$$

Two cases are distinguished.

a) The adiabatic case, in which the sites are close enough together for the electron to tunnel several times forwards and backwards during a time of the order of 10^{-12}sec.(a time in which the excited states persist). In this case $\lambda = \frac{1}{2\pi}\ \omega_0$ where λ is the frequency of an optical phonon. The activation energy W_H is given by

$$W_H = \tfrac{1}{2}\ W_P - J_P \tag{3-60}$$

where J_P is the polaron band width in adiabatic case, J_P is some how that (Holstein)[75]

$$J_P > (2kTW_H)^{\frac{1}{2}}\ \left(\frac{\hbar\omega_0}{\pi}\right)^{\frac{1}{2}} \tag{3-61}$$

b) The non-adiabatic case, in which the chance for an electron to make a transition between sites during lattice vibration is small. In this case for temperature $T > \frac{1}{2}\theta_D$ where θ_D is the Debye temperature defined by

$$\hbar\omega_0 = K\theta_D \tag{3-62}$$

λ is given by

$$\lambda = \pi^{\frac{1}{2}} \left(\frac{J_0}{2h}\right) (W_H kT)^{-\frac{1}{2}} \exp(-2\alpha R) \tag{3-63}$$

where α is the decay of the wave function, R is the site separation and $J_0 \exp(-\alpha R)$ is the overlap integral between sites. In this case the polaron hopping energy W_H is approximately equal to half the polaron binding energy W_P.

$$W_H \approx \tfrac{1}{2} W_P \tag{3-64}$$

and the polaron hopping probability is given by

$$P \sim \exp(-2\alpha R) \exp^{\frac{-(W_H + \frac{1}{2}W_D)}{kT}} \tag{3-65}$$

At high temperature the hopping is a multiphonon process and at $T < \frac{1}{4}\theta_D$ the single phonon process dominates. At the lowest temperature the jump probability is given by

$$P \sim \exp(-2\alpha R) \exp\left(\frac{-W_D}{kT}\right) \tag{3-66}$$

The mobility of the carrier in the case of an adiabatic process is given by Emin and Holstein[76] as

$$\mu = 4/3 \left(\frac{ea^2\omega_0}{kT}\right) \exp \frac{-(W_H - J)}{kT} \tag{3-67}$$

and for the non-adiabatic case, the mobility according to Holstein and Friedman[77] is given by

$$\mu = 3/2 \frac{ea^2J^2}{kT\hbar} \left(\frac{\pi}{kTW_H}\right)^{\frac{1}{2}} \exp \frac{-W_H}{kT} \qquad (3\text{-}68)$$

Mott[78] suggested the following formula for the conductivity of a transitional metal oxide in the non-adiabatic region.

$$\sigma = \nu C(1-C) \frac{Ne^2R^2}{kT} \exp(-2\alpha R) \exp\left(\frac{-W}{kT}\right) \qquad (3\text{-}69)$$

where N is the number of sites per unit volume, ν is the jump frequency, R is the transitional-metal ion separation and C is the fraction of sites occupied by an electron or ratio of the concentration of reduced transition-metal ion to the total transitional metal ion concentration. In the next chapter we will discuss the conduction in transitional metal oxides glasses in more detail.

3-2 Optical Properties of Amorphous Semiconductors

3-2-1 Introduction

Optical absorption in solids or liquids can occur by various mechanisms, all of which involve coupling of the electric vector of incident radiation to dipole moments in the material and a consequent transfer of energy. In any particular range of the spectrum, the photon energy will be absorbed by either the lattice or by the carriers.

Analysis of the absorption spectra in the lower energy part gives information about the atomic vibrations, and higher energy part of the spectrum gives a knowledge about electronic states in the normal material.

In the absorption process at the higher energy parts of the spectrum, the electron is excited from a filled to an empty band by the photon absorption and the consequence is a marked sharp increase in the absorption coefficient $\alpha(\omega)$, particularly for crystalline samples. The onset of this rapid change in $\alpha(\omega)$ is called the fundamental absorption edge and the corresponding energy is defined as the optical energy gap. The optical absorption coefficient $\alpha(\omega)$ and the a.c. conductivity are related to each other by

$$\alpha(\omega) = \frac{4\pi\sigma(\omega)}{n_o c} \tag{3-70}$$

where n_0 is the real refractive index and c the velocity of light and (ω) is the angular frequency of the incident radiation.

3-2-2 Different Processes in Optical Absorption

In general there are three kinds of absorption as following.

a) Free carrier absorption: This kind of absorption is observed in metals and semiconductors whenever there is a sufficient densities of free carrier (n) in a single band. It is frequency dependant and follows the Drude-Lorentz relation

$$\sigma(\omega) = \frac{\sigma(0)}{1+\omega^2\tau^2} \qquad (3\text{-}71)$$

where $\sigma(\omega)$ is the a.c. conductivity at frequency (ω) and $\sigma(0)$ is d.c. conductivity and τ is the relaxation time or time between scattering events. If the effective mass of the carrier is m* then

$$\sigma(0) = \frac{ne^2\tau}{m^*} \qquad (3\text{-}72)$$

where n is the density of free carrier states

when $\omega\tau << 1, \sigma(\omega) \rightarrow \sigma(0)$ and when $\omega\tau >> 1, \sigma(\omega)$ is proportional to the square of the wavelength of the incident radiation i.e.

$$\sigma(\omega) \propto \frac{1}{\omega}2 \qquad (3\text{-}73)$$

b) Lattice absorption: Lattice vibration in solids and liquids give rise to absorption of radiation normally in the infra-red region of the spectrum. This kind of absorption can occur in covalent materials under 'single phonon' processes, and in ionic and covalent crystals under multi phonon processes. In amorphous materials, lattice absorption processes are retained to a degree which depends on the material, but the fine structure present in the spectra of corresponding crystalline materials is absent.

c) Electronic interband absorption: In this process the electron is excited from filled to empty state by photon absorption which is very important in semiconductors. Optical absorption played an important role in investigating certain features of the electronic band-structure of crystalline semiconductors and we shall consider here what effect disorder can have.

In the region of the spectrum where the photon energy is of the order of energy gap ($\sim E_g$), there should be a rapid increase in optical absorption as a function of frequency, because electrons are excited across the energy gap of the crystal and photons of the corresponding frequency are absorbed. In crystals the absorption process is governed by two conservation processes, I. K conservation or momentum conservation, and II. Energy conservation. If k_i and k_f are the initial and final wave numbers of the electron and k the wave number of the photon of

frequency ω we may have,

$$k_f = k_i + k \qquad (3-74)$$

thus

$$E(k_f) = E(k_i) + \hbar\omega \qquad (3-75)$$

In semiconductors the wave length of the photon corresponding to the absorption edge is very large compared with lattice spacing and the k conservation rule is therefore $k_f \simeq k_i$. Transitions in this condition are called 'direct transition' and absorption coefficient $\alpha(\omega)$ is given by

$$\alpha(\omega) = \text{const } (\hbar\omega - E_g d)^{\frac{1}{2}} \qquad (3-76)$$

In the region $\hbar\omega < E_g d$, α is expected to rise very rapidly with frequency. In-direct optical transitions involving the absorption or emission of a phonon may also occur in crystalline materials eg Si and Ge and the absorption coefficient is then given by

$$\alpha(\omega) = \text{const } (\hbar\omega - E_g i)^2 \qquad (3-77)$$

In the case of direct transitions the gap $E_g d$ will not necessarily correspond to the thermal gap E_g obtained from the temperature variation of the conductivity, but in the case of indirect transitions, since phonon participation is required, the indirect optical gap, $E_g i$ will normally be close to the thermal gap E_g.

In the case of vitreous-semiconductors both localized and non-localized states are involved. For non-localized states Tauc[79] assumes that the electronic wave-function are only slightly perturbed compared with crystal and absorption coefficient which is

$$\alpha = \text{const } P_{if}^2 \int N_c(E)\, N_v(E + \hbar\omega)\, dE \qquad (3\text{-}78)$$

where p_{if} is the probability of transitions between initial and final states and $N_c(E)$ and $N_v(E)$ are the density of states in the conduction and valence bands respectively. Therefore the absorption coefficient will be in the form of

$$\alpha(\omega) = \text{const } (\hbar\omega - E_g)^2 \qquad (3\text{-}79)$$

According to the Tauc assumption, optical transitions between two localized states are not likely to contribute effectively to the absorption since they are spatially separated. Transitions between occupied states in valence-band tails and non-localized empty states in the conduction-band play a very important role.

There are uncertainties concerning the nature of the exponential absorption edges in amorphous semiconductors. Tauc suggested that such an edge can arise from interband transitions involving the tails of the localized states where the density of states falls off exponentially with energy. At a photon energy higher than that of which the exponential behaviour is observed

in chalcogenide glasses, which do not exhibit exponential absorption edges, the absorption occurs by the excitation of electrons across the gap into to the band.

* In amorphous semiconductors the shape of the absorption edge is not sharp and most important feature of the optical absorption processes is that the k conservation rule breaks down and k is not a good quantum number. The optical absorption coefficient for non-crystalline semiconductors can be deduced from a.c. conductivity given by[48]

$$\sigma(\omega) = \frac{2\pi e^2 \hbar^3 \Omega}{m^2} \quad \frac{N_e N(\hbar\omega+E)}{\hbar\omega} \quad (D_E)^2 dE \qquad (3\text{-}80)$$

where Ω is the volume of the specimen, D_E matrix element for optical transition N(E) is the density of states function. If we substitute $\sigma(\omega)$ into the Eq.1 (3-66) $\alpha(\omega)$ will be

$$\alpha(\omega) = \frac{8\pi^2 e^2 \hbar^3 \Omega}{n_o e m^2} \quad \frac{N(E)N(E+\hbar\omega)}{\hbar\omega} \quad (DE)^2 dE \qquad (3\text{-}81)$$

Davis and Mott assume that D_E has the same value whether or not the initial or final states are localized. They also assume that the density of states at the band edges are linear functions of the energy and that the transition for which both initial and final states are localized are improbable. Their assumptions are different from those of Tauc, mentioned above. Their assumption leads to

$$N(E_c) = N(E_v) \rightarrow E_c - E_A = E_B - E_V = \Delta E \qquad (3\text{-}82)$$

where ΔE is the width of the tail of the localized states in the band gap. According to these assumptions Eq.(3-81) can be simplified to the form of [43]

$$\alpha(\omega) = \frac{4\pi}{n_o C} \sigma_o (\hbar\omega - E_o)^2 / \hbar\omega \Delta E \qquad (3\text{-}83)$$

where

$$\frac{4\pi}{n_o C} \times \frac{\sigma_o}{\Delta E} = A = \text{Const} \qquad (3\text{-}84)$$

and σ_o is the electronic conductivity obtained by extrapolation of $\ln \sigma$ v.s $\frac{1}{T}$ given by

$$\sigma_o = \frac{2\pi^3 \hbar^3 a}{m^2} N(E)^2 \qquad (3\text{-}85)$$

thus

$$\alpha(\omega) = A (\hbar\omega - E_{opt})^2 / \hbar\omega \qquad (3\text{-}86)$$

under the assumption that the matrix element D_E is independent of energy and conduction and valence band edges are parabolic, this can also lead to Eq.(3-86) and in this case

$$E_{opt} = E_A - E_B \qquad (3\text{-}87)$$

There are some exceptions, as following.

a) For amorphous Se [43] absorption coefficient is as

$$\alpha(\omega) = \text{const} \frac{\hbar\omega - E_{opt}}{\hbar\omega} \qquad (3\text{-}88)$$

b) Some multicomponent materials have absorption coefficient as[80]

$$\alpha(\omega) = \text{const} \frac{(\hbar\omega - E_{opt})^3}{\hbar\omega} \qquad (3\text{-}89)$$

In general, conditions of Eq.(3-86) give the absorption coefficient for indirect inter-band transitions in non-crystalline materials, where E_{opt} defines the optical gap obtained by extrapolation of the absorption curve $(\alpha\hbar\omega)^{\frac{1}{2}}$ vs. $\hbar\omega$ for $(\alpha\hbar\omega)^{\frac{1}{2}} = 0$. An example of absorption whose functional dependence of photon energy is given by Eq.(3-86) for different materials is shown in Fig.(3.9).

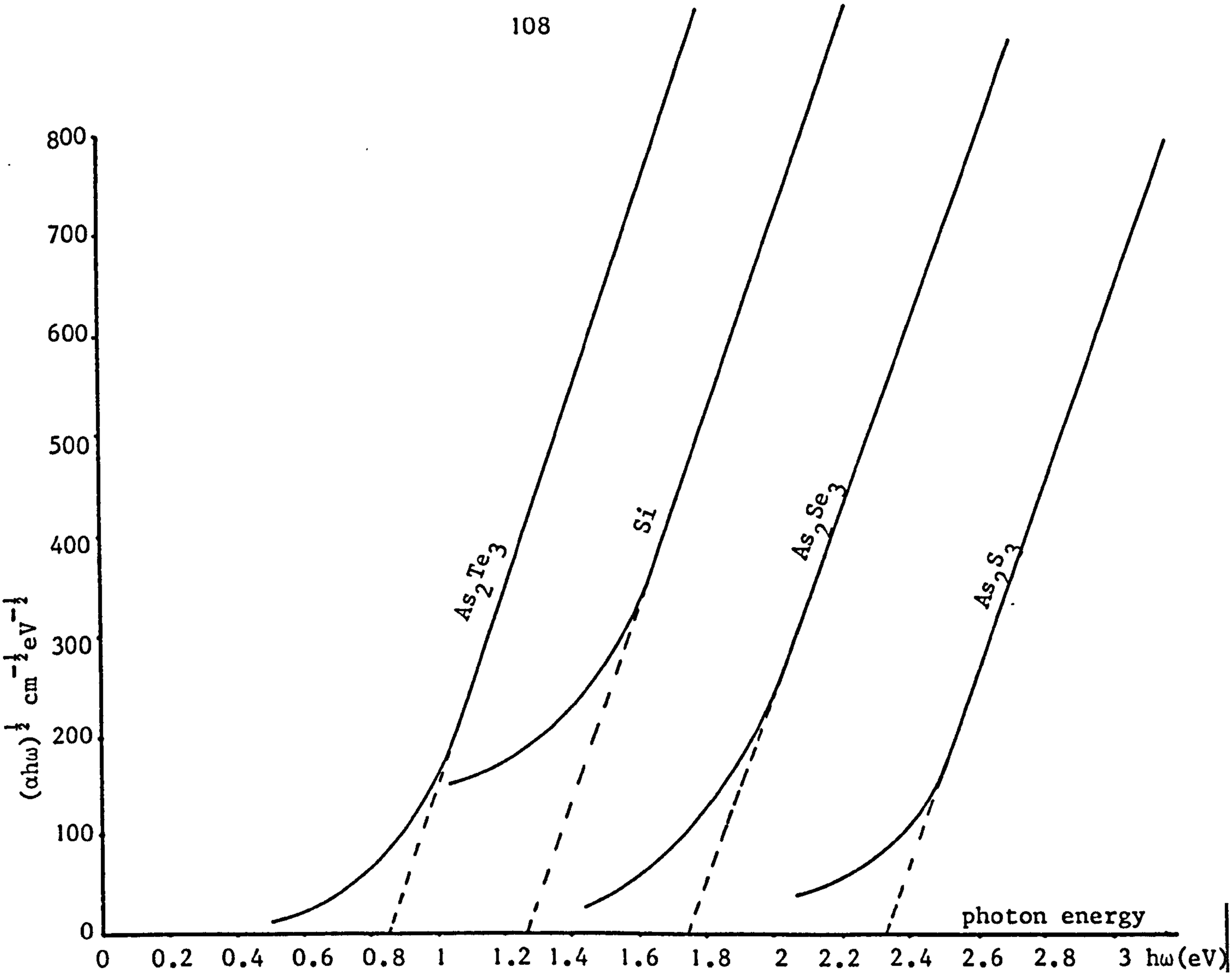

Fig.(3.9) Absorption Edge for Some Materials Whose Functional Dependence on Photon Energy is Given by

$\alpha = A(\hbar\omega - E)^2/h\omega$.

The slopes of intercepts for those materials vary somewhat according to the method of preparation[48].

Chapter IV

Review of Previous Work on Vanadium Phosphate Glasses

4-1-1 Introduction

Transition-metal-oxide glasses are the kind of glasses in which the transition-metal-oxides e.g. Fe_2O_3, TiO_2, MnO_2, MnO_3, WO_3, CuO or V_2O_5 etc. are or can be major constituents i.e. 50 mol percent. Of these the vanadium phosphate (V_2O_5, P_2O_5) are much the most thoroughly studied. These glasses show semiconducting behaviour when the transition metal ion has more than one valence state, for example as V^{+4} and V^{+5} ions in the vanadates.

In 1954 Denton, Rawson and Stanworth[81] for the first time suggested that vanadium-phosphate glasses are n-type semiconductors. Since then many studies have been made on the electrical properties of vanadate glasses which have confirmed that they are indeed n-type semiconducting glasses with an activation energy for conduction that varies between 0.2 - 0.44 eV, depending on composition.

The optical properties of vanadate glasses have received considerably less attention than the electrical properties. An early work on these glasses shows that some of them are

transparent in the infra-red between 1.5 and 5μm but that all are opaque in the visible for samples of thickness greater than 1.5mm. In general the characteristics of these glasses can be classified as follows.

I) The d.c. conductivity of these glasses varies as exp $-W/kT$ over the temperature 100 - 700K. At T > 300K the value of the activation energy ranges from ≃ 0.44 eV in vanadate glasses to 1.2 eV in glasses with Ni, Co or Ca ions.

II) W decreases with decreasing temperature in vanadate glasses from ∿0.44 eV to 0.05 eV. In contrast W in the crystals is constant.

III) The mobility 'μ' is smaller and activation energy is larger than in the corresponding crystal.

IV) The a.c. conductivity is of the form $\sigma \propto (\omega)^n$ (where $n \simeq 0.85$) and is almost independent of temperature at frequency > 10^8Hz.

V) The static dielectric constant is large (20 -40) in the vanadate glasses and increases with vanadium content.

The most striking characteristic of vanadium phosphate glasses are observed at low temperatures where the activation energy for d.c. conduction is found to be temperature dependent and the a.c. conductivity is approximately a linear function of

frequency.

Killias[82] interpreted the variation in activation energy as being due to thermally activated hopping in a system which has a distribution of jump distances, and Schmid[83-84] has formulated a model which assumes that polarons move by random hopping at high temperature and by tunnelling along chains of equal energy sites at low temperature.

Schakenberg[85] has considered the general case of polaron hopping when $\Delta W \neq 0$. In the low temperature range $T < \theta_D/4$ (where θ_D is Debye temperature defined as $k\theta_D = \hbar\omega_0$ and ω_0 is the mean optical phonon frequency), charge carrier transport should be an acoustical one-phonon-assisted hopping process, having an activation energy ΔW, while in the high temperature range $T > \theta_D/2$ optical multiphonon processes should determine the conductivity and the activation energy should be of the form of $W_H + \Delta W$ where W_H is the polaron hopping energy. The value of ΔW is predicted to be given by the Miller-Abrahams[13] energy as

$$\Delta W = \left(\frac{e^2}{4\pi\varepsilon_o \varepsilon_o r_o}\right) k \qquad (4-1)$$

Where r_o is the average distance between transition metal ions, ε'_o is the static dielectric constant and k is a constant.

According to Schmid[84] there is a break in the $\log \sigma$ v.s $\frac{1}{T}$ curve at a temperature of roughly $\theta_D/2$ and virtually no temperature dependence is found at lower temperatures.

4-1-2 Structure of Vanadate Glasses

There are three forms of oxide for phosphorus, namely P_2O_3, P_2O_4 and P_2O_5; among them only the pentoxide (P_2O_5) can form a glass. Crystalline phosphorus pentoxide is in three forms, hexagonal, orthorhombic and tetragonal. All three structures are based on a PO_4 tetrahedron, in which a phosphorus atom is at the centre and four oxygen atoms are at the corners. The hexagonal form consists of discrete P_4O_{10} molecules, and is thus a molecular crystal held together by Van der Waals' interactions. The orthorhombic form is made of rings of PO_4 tetrahedra, the inter-ring forces again being of the Van der Waals type. The tetragonal form is a layer structure consisting of a ring of six PO_4 tetrahedra. Crystalline V_2O_5 has a complex orthorhombic structure in which VO_5 pyramids link together partly at the corners and partly at the edges to form two-dimensional layers. Each VO_5 pyramid consists of a central V^{5+} ion. The similar structure of vanadium pentoxide containing VO_4 tetrahedra may be found in vanadate glasses, but structurally they will not be equivalent to the corresponding phosphates, because of the presence of vanadium in a lower valency state.

The structural information on vanadium phosphate glasses has been determined mainly from infra-red absorption (I.R.), nuclear magnetic resonance (N.M.R.) and electron spin resonance (E.S.R.). One of the first techniques used to try to determine the structure of these glasses was infra-red absorption, and the most

complete study is that of Anderson and Compton[20]. They studied V_2O_5 - P_2O_5 glasses containing 70% and 80% mol percent V_2O_5. In the 70% V_2O_5 sample vibrational absorption peaks were observed near 360, 420, 680, 900, 1010, and 1100cm^{-1} and in the 80% V_2O_5 sample the peaks occurred near 330, 435, 635, 810, 1010 and 1085cm^{-1}. Except for the peaks near 1010^{-1} the absorption bands were very broad and overlapped each other, they also found out that the positions of the peaks were independent of temperature in the range from 77 to 300K.

According to Anderson[20] and Conlon[86], crystalline V_2O_5 has vibrational absorption peaks near 915, 1040, 1260 and 1275cm^{-1} and the peak at 1040cm^{-1} is sharp. It has been reported that the vanadium-oxygen (V-O) stretching frequency is in the 1025 - 1050cm^{-1} range for compounds in which the vanadium atoms are totally ionized to[87] V^{+5}, while the presence of V^{+4} ions appears to reduce the stretching frequency in the 900 - 1020cm^{-1} range[109].

Anderson[20] and Compton suggested that the vibrational band near 1010cm^{-1} in the vanadium phosphate glass is due to V-O stretching vibrations. Also Chapman[88] suggested that crystalline phosphate compounds exhibit strong vibrational peaks between 1100cm^{-1} and 1400cm^{-1} and these peaks appear to be shifted into the 1020 to 1100cm^{-1} region in phosphate glasses Corbridge[89].

From the data given by Chapman and Corbridge mentioned above, Anderson and Compton[20] concluded that the 1085 to 1100cm^{-1} peaks in the vanadium phosphate glass is due to P-O stretching frequency.

N.M.R. and E.P.R. spectra of several vanadium phosphate glasses have been investigated by Landsberger and Bray[90]. They could locate and separate the V^{5+} nuclear magnetic resonance lines. From the N.M.R. data they suggested that two types of VO_5 units exist in glass. One is a VO_5 unit similar to that in crystalline V_2O_5 and the other is a VO_5 unit with a PO_4 unit substituted for the apex oxygen Fig.(4.1).

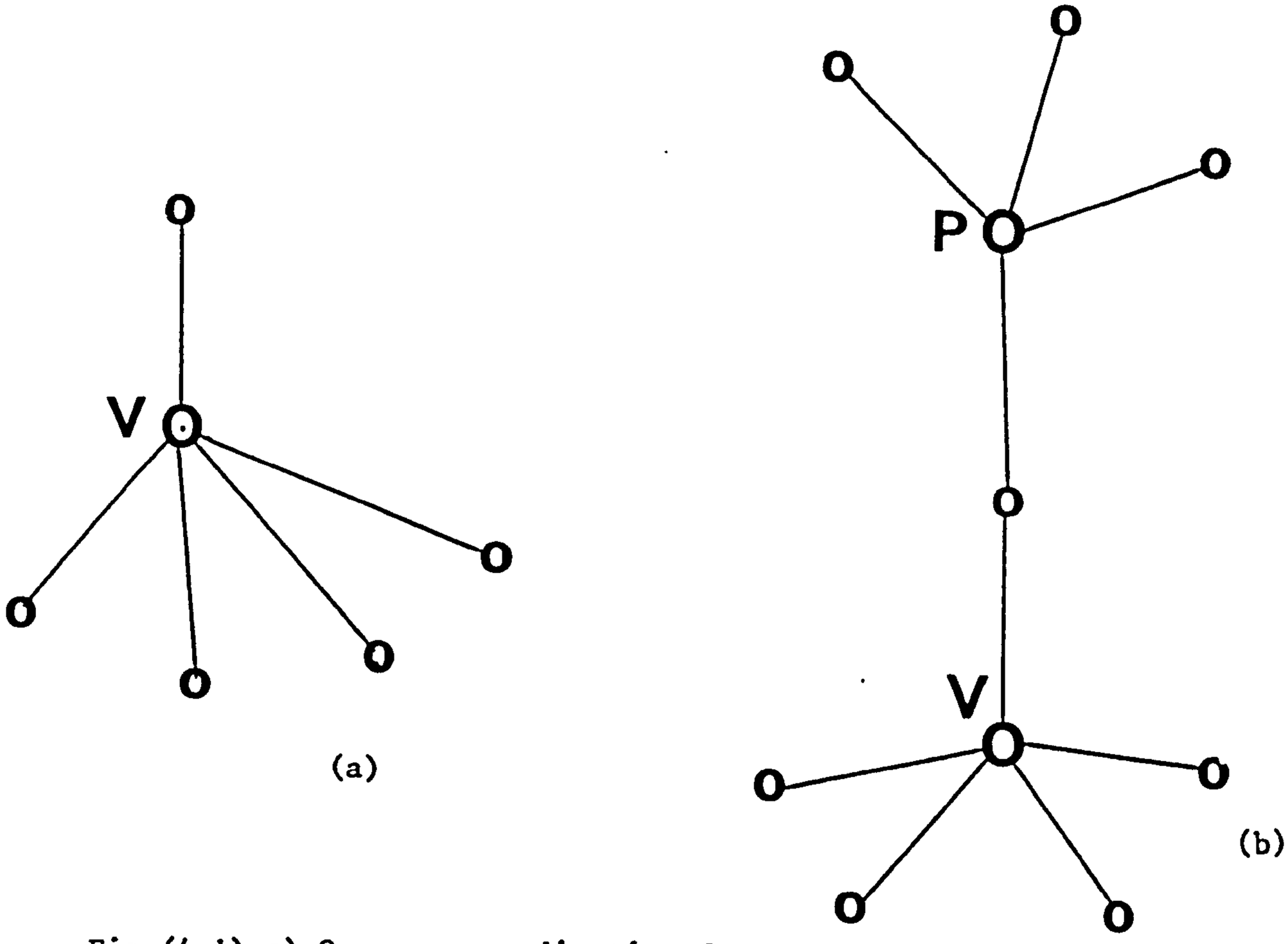

(a) (b)

Fig.(4.1) a) Oxygen co-ordination for Vanadium in V_2O_5

b) Substituting of PO_4 to apex oxygen. Landsberger and Bray[90].

Landsberger and Bray[90] could detect a resonance line due to the V^{4+} site in their N.M.R. experiment and from this resonance they suggested that the conduction electrons are localized at V^{4+} ions for a period of time at least comparable to the lifetime of the nuclear state. This was because if the electrons were non-localized and spent a little time on vanadium sites, then all the vanadium nuclei would be of the diamagnetic form e.g. V^{5+} and no N.M.R. signal due to the paramagnetic ion V^{4+} would be detected. Landsberger and Bray[90] also studied the E.S.R. spectra of vanadium phosphate glasses in order to determine the ratio of V^{4+} ions to V^{5+} ions as a function of composition, and they found that in a glass with 53% V_2O_5 and 47% P_2O_5 about one third of the vanadium atoms were quadruply ionized and the ratio of V^{4+} to V^{5+} decreased with increasing V_2O_5 percentage.

Lynch[91] et al used E.S.R. to measure the ratio of V^{4+}/V^{5+} over a temperature range from 77 to 333K and found that the spin concentration is independent of temperature. This illustrates the fact that the average number of paramagnetic sites is unchanged over this temperature range, and since electrical conductivity is an exponential function of temperature, then carrier concentration is independent of temperature and only the mobility is dependent on temperature. This result is very important in discussion of the electrical conduction of these glasses.

4-2 Electrical Properties

4-2-1- Conduction Mechanisms

The characteristic feature of the electronic structure of the transition elements is the filling up by electron of an inner d-level.

Pure stoichiometric V_2O_5 will normally be at best a semi-insulator; the 3d levels are unoccupied and the band gap will be 2 eV or more.

Conduction will occur more readily however in the non-stoichometric V_2O_x (x = 5-n and n = 1, 2, 3) in which some of the V^{5+} will occur in a lower valence state $V^{4+}(3d^1)$, $V^{3+}(3d^2)$ or $V^{2}(3d^3)$. Some d electrons are then available for conduction, but in contrast to the lower oxides there is no evidence for the formation of a d-level band probably because the V-V separation is somewhat greater in V_2O_5 than in the other oxides.

Fig.(4.2) shows a band model for a vanadium or other transition-metal-oxide glass. In this model there will be localized states in the energy gap, a fraction C of which will be occupied by electrons (corresponding to V^{4+}) and a fraction (1-C) therefore empty (V^{5+}). These localized states separated from the conduction band by an average energy E, will be distributed over a range of energy W_D because of the randomly fluctuating potential field of the disordered structure.

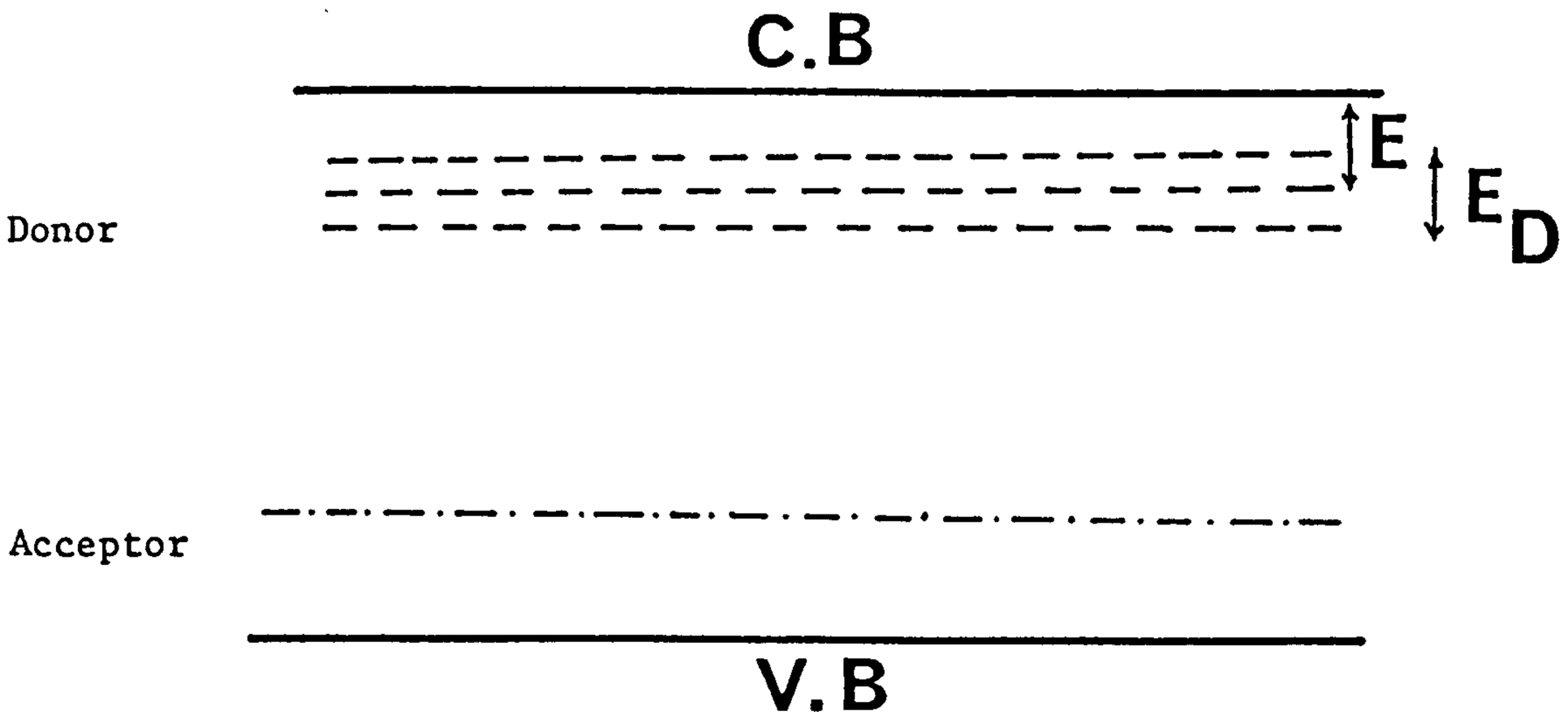

Fig.(4.2) Energy Band Model for T.M.O.Glasses

Conduction occurs by an electron hopping directly between occupied (V^{4+}) and unoccupied (V^{5+}) sites or,

$$V^{4+} \text{ —— } 0 \text{ —— } V^{5+} \longrightarrow V^{5+} \text{ —— } 0 \text{ —— } V^{4}$$

Lower valence states may also take part of course, e.g. V^{3+} or V^{2+}, but in glasses in which V_2O_5 is a major constituent, evidence is that the reduced vanadium is present mainly as V^{4+}. For the mechanism shown schematically above one would expect the conductivity to go through a maximum when there are equal numbers of V^{4+} and V^{5+} ions e.g. when $C = \frac{V^{4+}}{V^{5+}+V^{4+}} = 0.5$, but experimentally there is very little evidence on this point. Linsley[92] found that the maximum in conductivity occurred for a value of C between 0.1 and 0.2. Materials in which electronic conduction depends in this way upon the presence of ions in different valence states are known as mixed-valence semiconductors.

The mobility in a hopping process is given by[39]

$$\mu = \frac{\nu e a^2}{kT} \qquad (4\text{-}2)$$

where a is the jump distance, ν the jump frequency and T is the absolute temperature. In the case of mixed-valence semiconductors this must be multiplied by (1-C) the probability of an adjacent site being unoccupied, and for the jump frequency we can write

$$\nu = \nu_0 \exp(-2\alpha a) \exp(-W_D/kT) \qquad (4-3)$$

in which ν_0 will correspond roughly to a phonon frequency ($\sim 10^{12}$Hz) and α is the tunnelling probability given by

$$\alpha = \left(\frac{2mE}{\hbar}\right)^{\frac{1}{2}} \qquad (4-4)$$

Thus;

$$\sigma = ne\mu = \frac{\nu_o n e^2 a^2 (1-C)}{kT} \exp(-2\alpha a) \exp -W_D/kT \qquad (4-5)$$

where n is the carrier concentration. If N_o is the total number of sites (occupied or unoccupied) in a solid of volume V*, then $n = \frac{N_o}{V^*} C$ since C is the probability that one of these sites is occupied. If the number of sites in volume a^3 (a is the jump distance) is n_o, then $n_o = \frac{n}{a^3}C$, thus

$$\sigma = \frac{n_o \nu_o e^2}{a} \frac{C(1-C)}{kT} \exp(-2\alpha a) \exp -W_D/kT \qquad (4-6)$$

where $\frac{n_o \nu_o e^2}{a}$ = constant.

In a polar material such as a transition-metal oxide, the

extra charge introduced by an electron or hole on a particular site will tend to distort or polarize the surrounding ions. In this case the (W_D) disorder energy in Eq.(4-6) is displaced by W which is given by (see chapter 3)

$$W = W_H + \tfrac{1}{2}W_D \qquad (4\text{-}7)$$

where W_H is hopping activation energy for small polarons and is approximately half of the polaron binding energy W_P ($W_H = \frac{1}{2}W_P$) Therefore conductivity for transitional-metal oxide glasses will be

$$\sigma = \text{constant}\frac{C(1-C)}{kT} \exp(-2\alpha a) \exp(-W/kT) \qquad (4\text{-}8)$$

where the polaron hopping energy is W_H and the polaron disorder energy is W_D. Therefore W decreases with decreasing temperature. From Eq.(4-8) we expect the conductivity to be zero when C is 0 (the fraction of V^{4+} for example) or one, and to go to maximum at $C = \frac{1}{2}$.

4-2-2 d.c.Electrical Conductivity

Stanworth, Rawson and Denton[81],[93] were almost the first who studied the electrical properties of vanadium phosphate glasses. They considered that the specific conductivity for these glasses with high V_2O_5 content is of the order of $10^{-5}\,\Omega^{-1}cm^{-1}$ at room temperature, and the activation energy was found to be in the range of 0.35 to 0.4 eV.

Janakirama - Rao[94] studied complex glasses in the V_2O_5 - P_2O_5 - GeO_2 system and found ordinary semiconductors behaviour in the temperature range 200 to 500K with activation energy in the 0.2 to 0.4 eV range decreasing with increasing V_2O_5 content.

Schmid[84] found similar behaviour in the V_2O_5 - P_2O_5 system in the 200 to 300K range with σo of the order of $10^{-1}\ \Omega^{-1}cm^{-1}$ and activation energy varying from 0.24 eV to 0.44 eV, but he obtained breaks in the conductivity curves below 150K. Ioffe[95] et al studied P_2O_5 - V_2O_5 and P_2O_5 - V_2O_5 - BaO glasses and they found that the electrical conductivity mainly depends on the ratio of V_2O_5/P_2O_5 and not on the BaO content.

Nester and Kingery[96] worked on glasses containing up to 90 mol percent V_2O_5 and they found that the activation energy varies from 0.29 eV to 0.44 eV and is proportional to $(1/\varepsilon_\infty - 1/\varepsilon_o)$ where ε_∞ and ε_o are the high and low frequency dielectric constants respectively.

The more recent work on vanadium phosphate glasses has been done by Linsley et al[92]. They found that at any constant composition the conductivity increased initially with increasing V^{4+}/V^{5+} ratio., but then exhibited a maximum near the point at which the V^{4+} ions represents between 10% and 20% of the total vanadium ions, depending on the composition of the glass. Linsley et al measured the conductivity for a series of glasses containing 50 to 90 mol percent V_2O_5 at different temperatures. In these glasses they used a reducing agent to control the

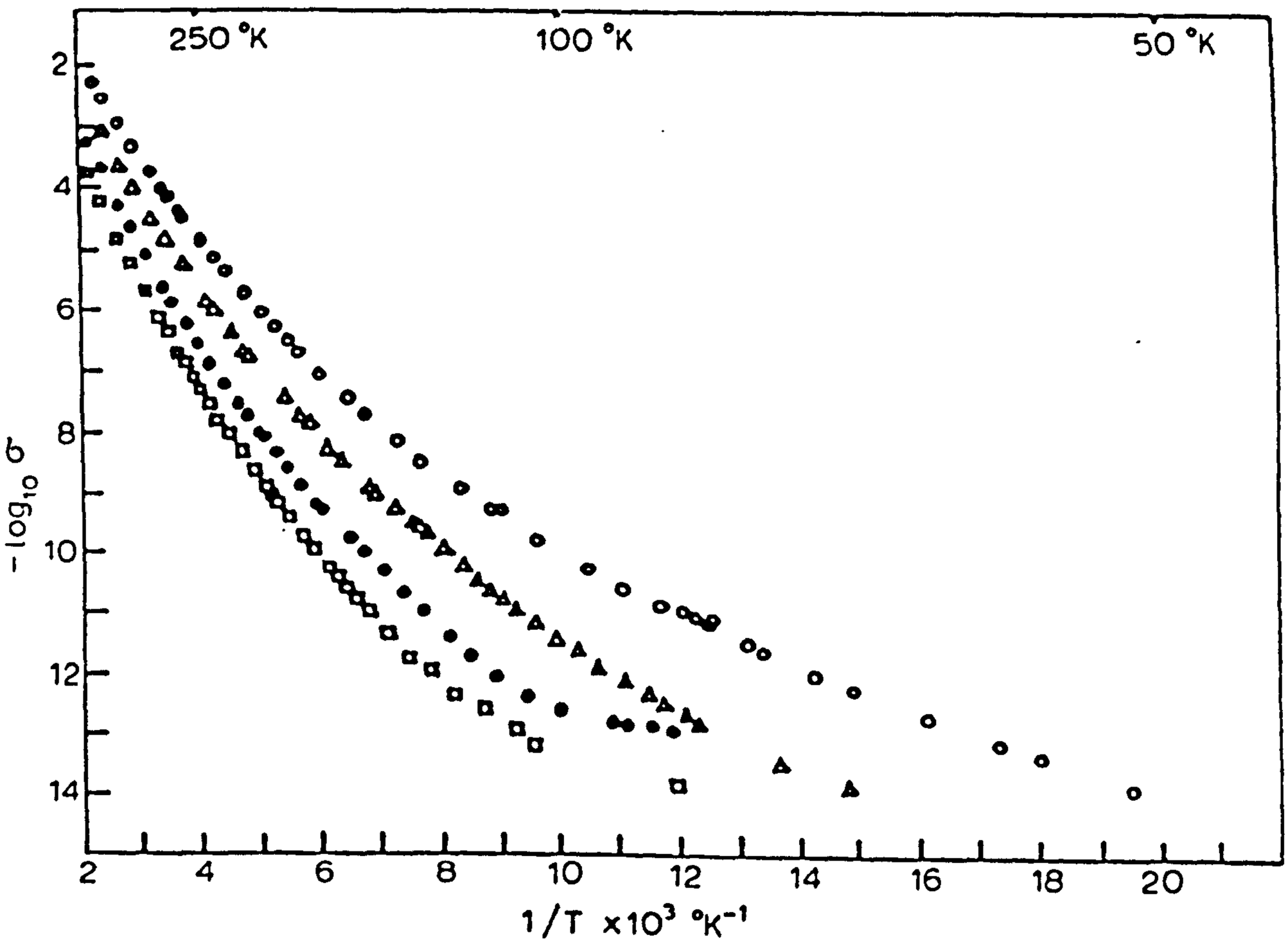

Fig.(4.3) Conductivity as a function of temperature for vanadium phosphate glasses (o)90% V_2O_5; (Δ)80% V_2O_5; (●)70% V_2O_5; (□)60% V_2O_5; (Linsley et al [92])

V^{4+}/V^{5+} ratio at constant composition. Their results are shown in Fig.(4.3).

These curves become considerably more linear on a Ln σ v.s $T^{-1/4}$ plot, but since the maximum temperature was 50k

no conclusion can be made. Linsley et al also found the value of σ_0 of the order of 10 $\Omega^{-1}cm^{-1}$ which is higher than previous work (Schmid)[84].

Grechanik[97] et al studied the preparation and electrical properties of ternary oxide glasses containing $V_2O_5 - P_2O_5 - RO_x$ where RO_x represents nearly 35 different oxides they found the activation energy in the 0.32 to 0.6 eV range and the room temperature conductivity was of the order of 10^{-4} to $10^{-1}\Omega^{-1}cm^{-1}$ depending on composition.

Hamllen[98] et al investigated the correlation between electrical properties and the thermal history of the vanadate glasses, particularly between the liquids temperature and the annealing range. For this purpose they made a series of glasses containing V_2O_5 and metaphosphate from $R(PO_3)_x$ of the metal oxides. This had the advantage of introducing into the melt the more stable metaphosphate rather than other more highly volatile compounds of P_2O_5. Various series of glasses with $Pb(PO_3)_2$, $LiPO_3$, KPO_3, $Ba(PO_3)_2$ and $Na(PO_3)_2$ were made to determine the maximum $\frac{V_2O_5}{R(PO_3)x}$ ratio that would produce a glass. They found that V_2O_5 with $Al(PO_3)_2$ and $Mg(PO_3)_2$ cannot make glasses.

Hamllen et al[98] found that the resistivity of these glasses decreased with increasing ratio of $\frac{V_2O_5}{R(PO_3)_x}$. A typical curve of resistvity versus composition for $V_2O_5 - Ba(PO_3)_2$ is shown in Fig.(4.4).

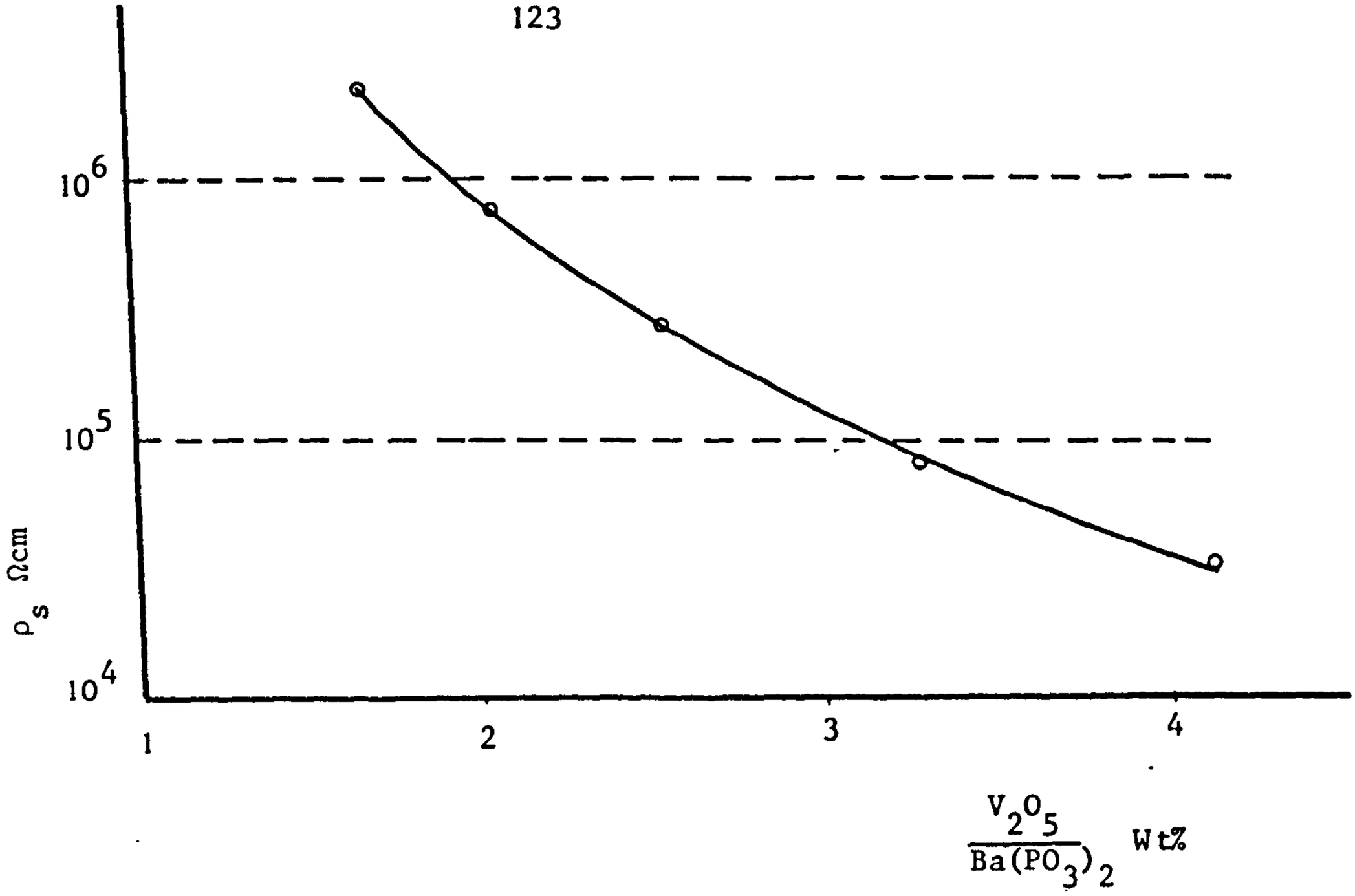

Fig.(4.4) Variation in Specific resistance, ρ_s, with V_2O_5 Content at 40°C.

They also measured the resistivity of these glasses at different temperatures and they found that the resistivity decreases on a smooth curve until a temperature just above the annealing range, and above this temperature there is a relatively larger decrease in resistivity and they concluded that the thermal history of these glasses above the annealing and below the liquids temperature strongly affected the electrical characteristic.

Carly[99] et al compared the conductivity of $V_2O_5 - P_2O_5$ and $WO_3 - P_2O_5$ glasses and found that for both glasses conductivity increases with an increasing amount of transition metal oxide. They also investigated the conductivity of these glasses when P_2O_5 is replaced by one of the oxides B_2O_3, SiO_2, GeO_2, TeO_2, and

they found that for vanadate glasses the conductivity increases with increasing concentration of these oxides, and for tungstate glasses the conductivity increases with increasing B_2O_3, SiO_2 and GeO_2 concentrations and slowly decreases with increasing TeO_2 concentration. The most striking result was for the addition of V_2O_5 to tungstate glasses. The conductivity-composition curves for the tungstate glasses with V_2O_5 added show that on replacement of only 1.5 mol percent V_2O_5 for P_2O_5 the conductivity decreases from 10^{-7} to $10^{-11}\ \Omega^{-1}cm^{-1}$, and further addition of V_2O_5 causes the conductivity to be restored. The reason is difficult to explain without quantitative spectral analysis to establish which valence states of vanadium and tungsten are present. It is suggested that V^{4+} ions either strongly reduce the W^{6+} ions or further reduce the lower state in the base glasses, and improvement in conductivity above 1.5 mol% V_2O_5 could result from $V^{4+} \longrightarrow V^{5+}$ and or $W^{5+} \longrightarrow W^{6+}$ transition.

Several authors[84-100-102] tried to apply the theory of the small polaron (see Chapter III) to vanadate glasses in order to explain some of the features of the electrical conductivity. The polaron model predicts that a departure from a linear $\log \sigma$ vs. $\frac{1}{T}$ plot should occur at $T<\frac{1}{2}\theta_D$ where θ_D is the Delye temperature which is about 300K. According to the polaron model the activation energy for electrical conductivity W consist of two terms, namely polaron hopping energy W_H which is roughly half of the polaron binding energy W_P, and the disorder energy W_D. At high temperature $T>\frac{1}{2}\theta_D$ activation energy is $W = W_H + \frac{1}{2}W_D$ and at low

temperature $T<1/4\,\theta_D$ activation energy is of the order of disorder energy $W = W_D$ and in the intermediate region activation energy varies with temperature.

Greaves[103] describes the low temperature conduction in terms of Mott variable range hopping and high temperature conduction according to non-adiabatic small polaron.

4-2-3 A.C.Conductivity

The a.c. conductivity of vanadate glasses has been studied by many authors. Linsley[92] and Schmid[104] showed that the a.c. conductivity of V_2O_5 - P_2O_5 glasses is independent of frequency at high temperature and low frequencies. They also found that a.c. conductivity is essentially independent of temperature at high frequency $>10^8$Hz. At low temperatures a linear increase in a.c.conductivity with frequency was observed in the 10^3 to 10^5 Hz region, but above 10^6 Hz the a.c.conductivity appears to be proportional to ω^2.

Mansingh[105] and Tandon measured the a.c. conductivity and dielectric constant for a series of V_2O_5 - P_2O_5 glasses at different temperatures and over the frequency range 100 Hz to 100 KHz. Their results are shown in Fig.(4.5,6). They concluded that at high temperature the total conductivity σ_{tot} which is the sum of a.c. and d.c. conductivities ($\sigma_{tot} = \sigma_{ac} + \sigma_{dc}$) is equal to the d.c. conductivity and at low temperature the a.c. conductivity is given by

$$\sigma(\omega) = A\omega^{s}$$

where A and s are constant and the value of s varies from 0.85 to 0.95.

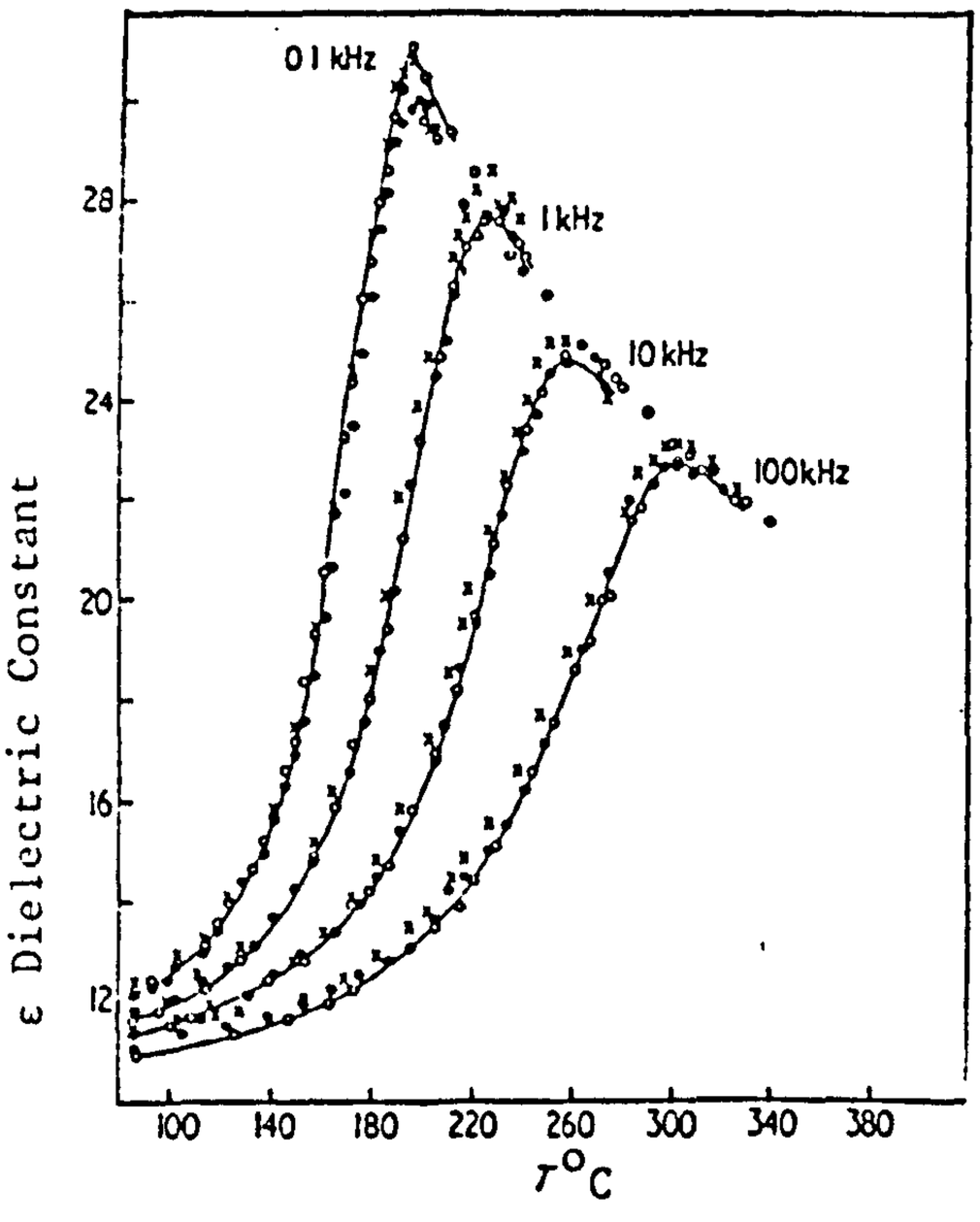

Fig.(4.6)

Temperature dependance of dielectric constant measured at different fixed frequencies and for different annealing as Fig.(4.5).[105]

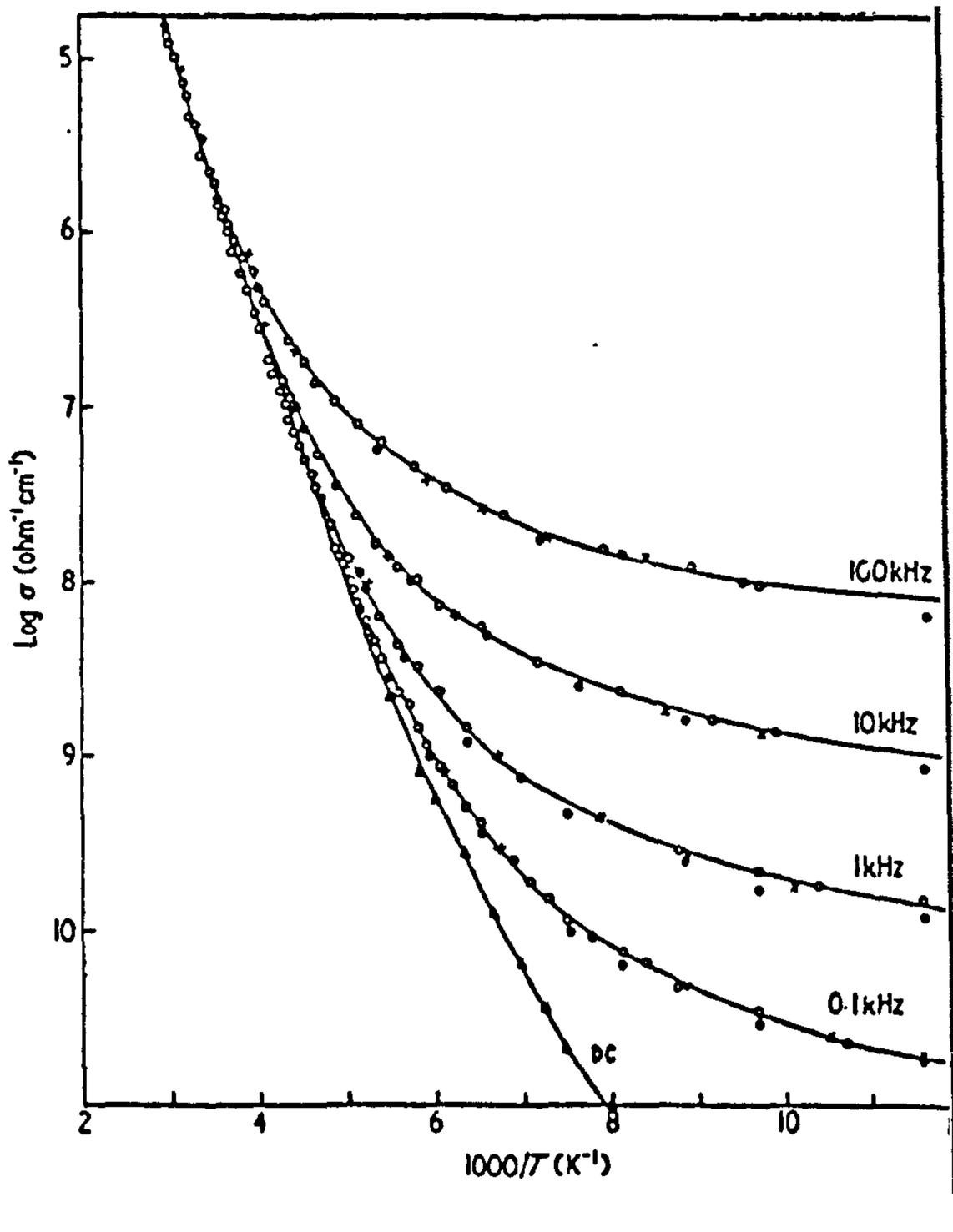

Fig.(4.5)

A.c.conductivity v.s inverse temperature for various fixed frequencies and different annealing.

unannealed o annealed for 5 hours at 150°C

x annealed for 1 hour at 300°C.[105]

From dielectric measurements Mansingh and Sayer[106] found that the dielectric loss ε'' which is proportional to the difference between σ_{tot} and σ_{dc} for a given frequency e.g. $\omega\varepsilon'\varepsilon'' = \sigma_{tot} - \sigma_{dc}$ shows a peak which shifts to higher temperature for higher frequency. Mansingh and Tandon[128] also studied the effect of annealing on the a.c. conductivity and dielectric constant and they found that the annealing temperature and annealing time have no effect on a.c. conductivity and dielectric constant.

4-3 Optical Properties of Vanadate Glasses

As we mentioned before the optical properties of vanadate glasses have received less attention than the electrical properties and most of the studies were concentrated on infra-red regions.[81-94-95] Infra-red measurements provide information regarding local vibrational modes which can be compared with phonon energies calculated from electrical data.

Janakirama - Rao[107] studied the infra-red spectra of binary and ternary composition in the glassy state and in the devitrified crystalline state in the system GeO_2 - P_2O_5 - V_2O_5 and compared the results with the infra-red spectra of crystalline V_2O_5. He indicated that the fundamental vibration frequency of the V - O bond occurred at wave number $1015cm^{-1}$ and concluded that the normal vibration frequency of the V - O bond seen in crystalline V_2O_5 at wave number $1015cm^{-1}$ persists in all the spectra indicating that the V^{5+} ion exists in octahedral co-ordination in all these compositions.

Janakirama - Roa[107] also found that the infra-red spectra of V_2O_5 - GeO_2 in the glassy state and in the crystalline state are almost identical, which means that the V^{5+} ion does not change co-ordination from the crystalline state to the glassy state. In the system V_2O_5 - P_2O_5 with low concentrations of P_2O_5 the V - O absorption bond shifts from $1015cm^{-1}$ to $1005cm^{-1}$ which can be attributed to the environmental influence of the P^{5+} ion which has a higher charge density than the V^{5+} ion and

consequently attracts the bonding electrons nearer to the P^{5+} core, thereby weakening the V - O bond.

Janakirama - Rao[107] also found that in the spectrum for glass GeO_2 - P_2O_5 (80 mol% GeO_2 - 20 mol% P_2O_5) in which vanadium is absent, the absorption bond at wave number 1015cm^{-1} disappears. This shows that it is due to the V - O bond vibration.

Sayers et al[108] studied the infra-red absorption for series of vanadate glasses in the 2000 to 200cm^{-1} range. Absorption spectra from 2000 to 600cm^{-1} are shown in Fig.(4.6) and from 600 to 200cm^{-1} in Fig.(4.7).

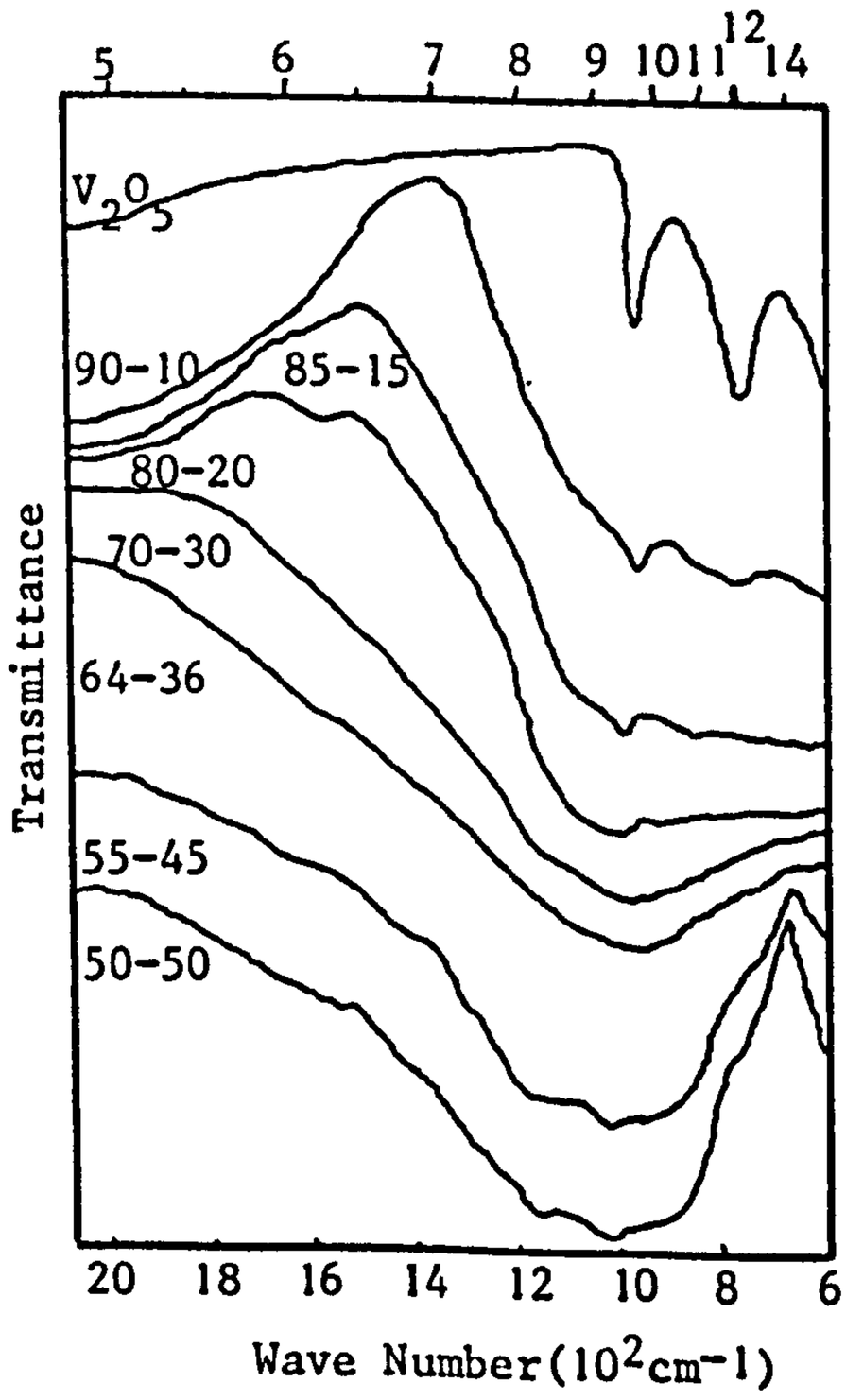

Fig.(4.6) Optical Transmittance 2000 to 600cm^{-1} for Glasses of Different Composition[108]

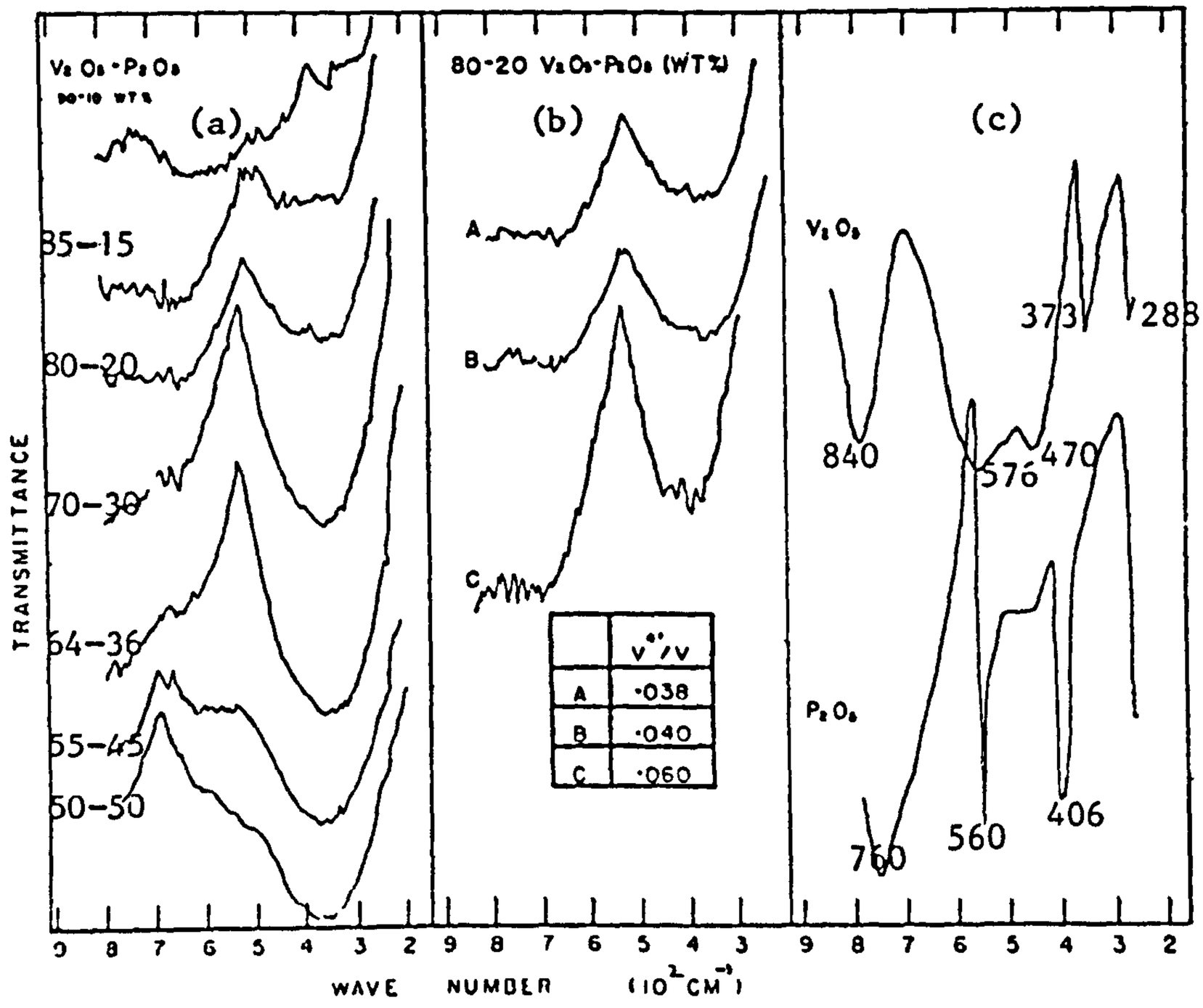

Fig.(4.7) Optical Transmittance From 600 to 250cm^{-1} (108)

a)glasses of different composition,

b)80% V_2O_5 : 20% P_2O_5 glasses having different V^{4+} concentrations,

c)V_2O_5 and P_2O_5.

They observed a peak at 1015cm^{-1} in both crystalline V_2O_5 and the glasses and this is attributed to the V - O stretching frequency of the V_2O_5 structural unit, which agrees with the work of Janakirama - Rao previously mentioned in this section.

Sayer et al[108] also observed a broad absorption bond at about 380cm^{-1} with an intensity which is related to the phosphate content for glasses of different compositions and to the V^{4+} concentration for glasses of the same composition but different V^4 content.

Anderson[20] and Compton studied the optical absorption of vanadate glasses based on the system V_2O_5 - P_2O_5 for a series of glasses in the $20cm^{-1}$ to $25,000cm^{-1}$ range at room and liquid-nitrogen temperatures. The samples of composition 70 -80 and 87.5 mol% V_2O_5 were blown films of thickness 1 - 2μm. They observed vibrational absorption peaks at about 360, 420, 680, 1010 and $1100cm^{-1}$ for 70 mol% V_2O_5 glasses. Absorption peaks were observed at about 330, 435, 810, 1007 and $1085cm^{-1}$ in the 87.5 mol% V_2O_5 glasses. They also observed absorption tails extending from the lower energy peaks to $20cm^{-1}$ for 70 mol% V_2O_5 and $33cm^{-1}$ for 87.5 mol% V_2O_5 samples. There were no noticable temperature effects on spectra slope and peak positions. They also measured the absorption spectra for crystalline V_2O_5 at room and liquid nitrogen temperatures and found absorption peaks at 1038 and $1277cm^{-1}$ at room temperature and 915, 1040 and $1274cm^{-1}$ at liquid nitrogen temperature.

Anderson and Compton[20] concluded that the peaks at about $1010cm^{-1}$ in glasses are due to V -O stretching vibration and peaks at about $1090cm^{-1}$ were due to P - O vibrations. They also observed a broad absorption tail between the fundamental absorption edge of the glasses in the short-wave length region of the visible and at about $4,000cm^{-1}$, which is responsible for the dark black colour of bulk samples.

Anderson and Compton[20] suggested that the absorption coeffient fits the conditions for the direct forbidden transitions given by

$$\alpha = A\,(\hbar\omega - E_g)^{2/3}/\hbar\omega \qquad (4\text{-}9)$$

much better than it fits the conditions for direct allowed transition which is given by

$$\alpha = A'(\hbar\omega - E_g)^{\frac{1}{2}} \qquad (4\text{-}10)$$

where E_g is the optical gap and A, A' are constant. The value of E_g was found to be 2.38 and 2.41 eV for 87.5 mol% V_2O_5 at room and liquid nitrogen temperature respectively and 2.47 and 2.51 eV for the70 mol% V_2O_5 films at room and liquid nitrogen temperature respectively.

Chapter V

Preparation and Structural Investigation of $V_2O_5 - P_2O_5$ and $V_2O_5 - TeO_2 - P_2O_5$ Glasses

5-1 Introduction

The properties of transition-metal oxide glasses mainly depend upon the two factors (a) total concentration of the transition metal oxide and (b) the ratio of ions in the low and high valence states e.g. V^{4+}/V^{5+}.

These factors are influenced by many other factors arising from the existence of other oxides (glass formers) and the thermal history involving both the temperature of melting and the cooling schedule. These factors are the following.

I) A verage V - V separation.

For the same molecular percentage of V_2O_5 in different glass systems e.g. $V_2O_5 - P_2O_5$ and $V_2O_5 - B_2O_3$, there will be different densities and hence different V - V separations resulting in different distributions of the vanadium ions and the structure of the glasses.

II) The oxidation-reduction potential of the melt from which the glass is prepared will be different in the presence of BaO or P_2O_3 or acidic P_2O_5 oxides and this will alter the ratio of low to high valence transition-metal ions.

III) The nature of the other oxides will affect the polarizability of the glass network and hence the polaron hopping energy W_H in Eq.(3-51).

IV) The presence of other transition-metal oxides in the glass e.g. WO_3 and TiO_2 will affect the oxidation-reduction equilibrium and if present in large amounts they may also enter into the conduction process.

V) The oxidation-reduction potential of the melt and hence the ratio of low to high valence states will depend on the temperature of the melt and to some extent on the rate of cooling.

VI) The density of glass, in common with other physical properties of glass depends on the thermal history of glass and this will alter the metal-metal separation.

At the present time the knowledge about the structure of the transition-metal oxide glasses in general, is very little, and there are many questions about the structure of these glasses. For example, optical absorption measurements on some V_2O_5 - GeO_2 - P_2O_5 [107] glasses have shown that the vanadium is in sixfold octahedral co-ordination with oxygen ions (VO_6), but in contrast, electron spin resonance studies have been interpreted in terms of tetrahedral co-ordination.

5-2 Glass Preparation

The binary system based on V_2O_5 - P_2O_5 with 50 to 90 mol percent V_2O_5 and ternary system based on V_2O_5, P_2O_5, TeO_2 with keeping V_2O_5 constant at 60 mol percent and replacing P_2O_5 with TeO_2 were prepared from the powders of these oxides as shown in Table (5.1).

The oxides used in making these glasses were supplied from B.D.H. chemicals. The weighing of the oxides was carried out using an electric balance of the type Oertling with an accuracy of 0.2mg. For each composition the amount of oxides was estimated from the molecular weight of the oxide times the percentage of that oxide. For example

$$m_{V_2O_5} = M_{V_2O_5} \times \text{Mol\% } V_2O_5 \qquad (5\text{-}1)$$

The sensitivity of P_2O_5 to humidity causes errors during the weighing of materials therefore we tried to minimize these errors by weighing the material as quickly as possible.

In our experiments we used alumina crucibles for making thick samples and platinum crucibles for making thin blown films for optical absorption and high field conductivity measurements.

Firstly a cleaned and dried crucibles (cleaned with white spirit) was weighed and then P_2O_5 was introduced and it was weighed again. Vanadium pentoxide was added to P_2O_5 in the crucibles and weighed again and in the case of ternary glasses

TeO_2 was added and weighed again. All glasses were prepared from 30 to 50 gram quantities, initially heated in an electric furnace at $400^{o}C$ for one hour to minimize the tendency of P_2O_5 to evaporate and then raising the temperature of the furnace gradually up to the melting point. It was found that the softening temperatures of V_2O_5 - P_2O_5 glasses decrease rapidly with increasing V_2O_5 content and range from about $600^{o}C$ for glasses containing 50 mol percent V_2O_5 to about $400^{o}C$ for glasses containing 90 mol percent V_2O_5.

Glasses were melted for a period of two hours, and during this time the glass melts were stirred by an alumina rod several times in order to get a homogeneous melt.

The homogeneous melt was cast into a stainless steel cylindrical shaped mould having 3cm diameter and 0.3cm depth as shown in Fig.(5.1). Glass samples were then replaced in the annealing furnace and annealed at $200^{o}C$ for two hours to relieve them from any excess mechanical stresses. After annealing the glasses, the furnace was switched off and the sample was allowed to cool down to room temperature gradually.

It was found that glass preparation history, such as melting temperature, melting time, annealing time and rate of cooling could affect the properties of glasses. Therefore we tried to keep all these parameters as constant as possible. All glasses were examined for crystallinity by x-ray powder-diffraction and

showed no discrete lines which would be characteristic of crystalline pattern (see Fig.(5.2,a), but only diffuse holes which are characteristic of amorphous structures. Fig.(5.2b,c) shows x-ray diffraction photographs of V_2O_5 - P_2O_5 and V_2O_5 - P_2O_5 - TeO_2 glasses. X-ray diffraction examination was carried out for all samples and no crystalline pattern was observed in their photographs.

For resistivity measurements, glass disks with 3cm diameters and 1.5 to 3mm in thickness were ground in a machine and then polished with a fine lapping paper using 6 microns diamond paste. We used white spirit for lubrication during polishing and cleaning the sample surface from contamination after polishing.

Gold electrodes (for some experiments silver or copper) were vacuum-deposited in both sides of samples and to avoid surface charge effects a guard ring was deposited on one side of the sample as is shown in Fig.(5.2).

Samples were further annealed to 150°C for two hours after the vacuum deposition of electrodes in order to get a good Ohmic contact. The Ohmic contacts were checked by measuring the I - V characteristic which gives a straight line at low fields, up to 10^5 V/cm. A good Ohmic contact was not normally obtained without the proper annealing of the samples before and after the electrode deposition.

The glass samples used in optical experiments and high field electrical conductivity measurements were blown films having a thickness of about four microns. For this purpose we immersed one end of an alumina tube with a diameter of 2 to 5mm into the glass melt and blew gently from the other end of the tube. All blown film samples were annealed at 200°C for two hours.

Phosphate glasses are highly water absorbing therefore samples should be kept under high vacuum in a desiccator containing a water absorbant material such as silica gel.

5-3 Density Measurements

The densities of the annealed and polished samples after cleaning with white spirit were determined by weighing them in atmosphere and in a liquid. The liquid used was eythyl-methyl ketone with a density of the order of $0.803 gcm^{-3}$ at room temperature.

According to Archimedes' principle the density of sample can be determined from the following formula.

$$\rho_g = \rho_L \frac{M_1}{M_1 - M_2} \qquad (5\text{-}2)$$

where ρ_g and ρ_L are the density of sample and liquid respectively and M_1 and M_2 are the weights of the sample in atmosphere and liquid respectively.

We found that in the binary glass system V_2O_5 - P_2O_5 the density of glass increases with increasing V_2O_5 content and in the ternary system V_2O_5 - P_2O_5 - TeO_2 the density increases with increasing TeO_2 content. Table (5.2)

The variations of density with V_2O_5 content for V_2O_5 - P_2O_5 glasses and with TeO_2 content for V_2O_5 - P_2O_5 - TeO_2 glasses are shown in Fig.(5.4) and (5.5) respectively. It has been found that the temperature of melting and annealing can affect the structure of the glass resulting in a change in physical properties including density. We measured the density of 75% - 25%(V_2O_5 - P_2O_5) and for the ternary system V_2O_5 - P_2O_5 - TeO_2 (60 mol% - 20 mol% - 20 mol%) samples annealed at different temperature, and found that in both glasses the density increases with increasing the annealing temperature, which means that the average interatomic spacing decreases with annealing and the structure becomes more compact. Variation of density with annealing temperature for V_2O_5 - P_2O_5 and V_2O_5 - P_2O_5 - TeO2 glasses are shown in Fig.(5.6) and (5.7) respectively.

The molar volumes for both binary and ternary systems were determined from the following formula.

$$V = \frac{\Sigma x_n y_n}{\rho} \qquad (5-3)$$

where x_n and y_n are the mol percent and molecular weight of the constituent oxides in the glass composition respectively. Results obtained for V_2O_5 - P_2O_5 and V_2O_5 - P_2O_5 - TeO_2 glasses are shown in Fig.(5.8) and (5.9). Results of density measurements can be summarized as following.

I) Density of V_2O_5 - P_2O_5 glasses increases with increasing transition-metal oxide content in glass.

II) Density of V_2O_5 - P_2O_5 glass increases with replacing P_2O_5 with TeO_2 in glass system and density increases with increasing TeO_2 content.

III) Density of both binary V_2O_5 - P_2O_5 and ternary V_2O_5 - P_2O_5 - TeO_2 glasses increase linearly with increasing annealing temperature it means glass annealed at higher temperature becomes more compact.

IV) Molar volume of V_2O_5 - P_2O_5 glass increases with increasing transition metal oxide content.

V) Molar volume in V_2O_5 - P_2O_5 - TeO_2 system decreases with increasing TeO_2 content.

Molar volume per ion pair was also calculated for binary system V_2O_5 - P_2O_5 from the following formula

$$V^* = \frac{2\Sigma x_n y_n}{\rho \Sigma x_n z_n}^{o} \qquad (5-4)$$

where z^o_n is the number of atoms in chemical formula of constituent oxide e.g. z^o_n is 7 for V_2O_5 or P_2O_5. Variation of V* v.s V_2O_5 content in binary system V_2O_5 - P_2O_5 is shown in Fig.(5.10).

The average transition metal ion spacing R is also calculated for V_2O_5 - P_2O_5 glasses from the following formula[96]

$$R = (\frac{1}{N})^{1/3} \qquad (5\text{-}5)$$

where N is the transition metal ion concentration which can be determined from the formula given by

$$N = \frac{\rho_g W\%.A}{AW.100} \qquad (5\text{-}6)$$

where ρ_g is density of glass, W% the weight percent of vanadium ions in glass, A is Avogadro's number and AW.is the atomic weight of vanadium.

Calculated values for R and N in both binary and ternary systems are given in Table (5.3). Variation of transition metal ion concentration and transition metal ion spacing v.s V_2O_5 content for binary system V_2O_5 _ P_2O_5 are shown in Figs.(5.11) and (5.12) respectively and for ternary system v.s TeO_2 content are shown in Figs.(5.13) and (5.14). These figures show that T.M.I. concentration in binary system increases with increasing V_2O_5 content and in ternary system increases with increasing TeO_2 content. In binary system T.M.I. spacing decreases nearly linear with increasing V_2O_5 content and decreases with TeO_2 content in ternary system as shown in Figs.(5.12) and (5.14).

5-4 Electro Spin Resonance

As we mention earlier in this chapter, the electronic conduction in transition metal oxide glasses results from electron transfer from a transition metal ion with the lower valency to an ion with a higher one. If such conduction occurs, the nominal carrier concentration is determined by the fraction of transition metal ions in the reduced valence state, while the mobility and other electronic properties are strongly influenced by the crystal structure and by the effects of defects and impurities. Therefore the interpretation of the semiconductivity in these glasses requires a knowledge of the valence state of the transition metal ions that are present in the glass.

The electron spin resonance (E.S.R.) technique provides a useful method for determining the concentration of a paramagnetic species present in the glass. The unreduced ions $(V)^{5+}$ are diamagnetic and hence cannot be detected directly by E.S.R. technique while the reduced ions V^{4+} which are paramagnetic and have spin $S = \frac{1}{2}$ can be detected directly by E.S.R. leading to a single resonance line influenced by nuclear hyperfine interactions. The combined effect of this interaction and the interaction of adjacent paramagnetic centres in an amorphous material result in a line shape which should be characteristic of each glass.Fig.(5.15)

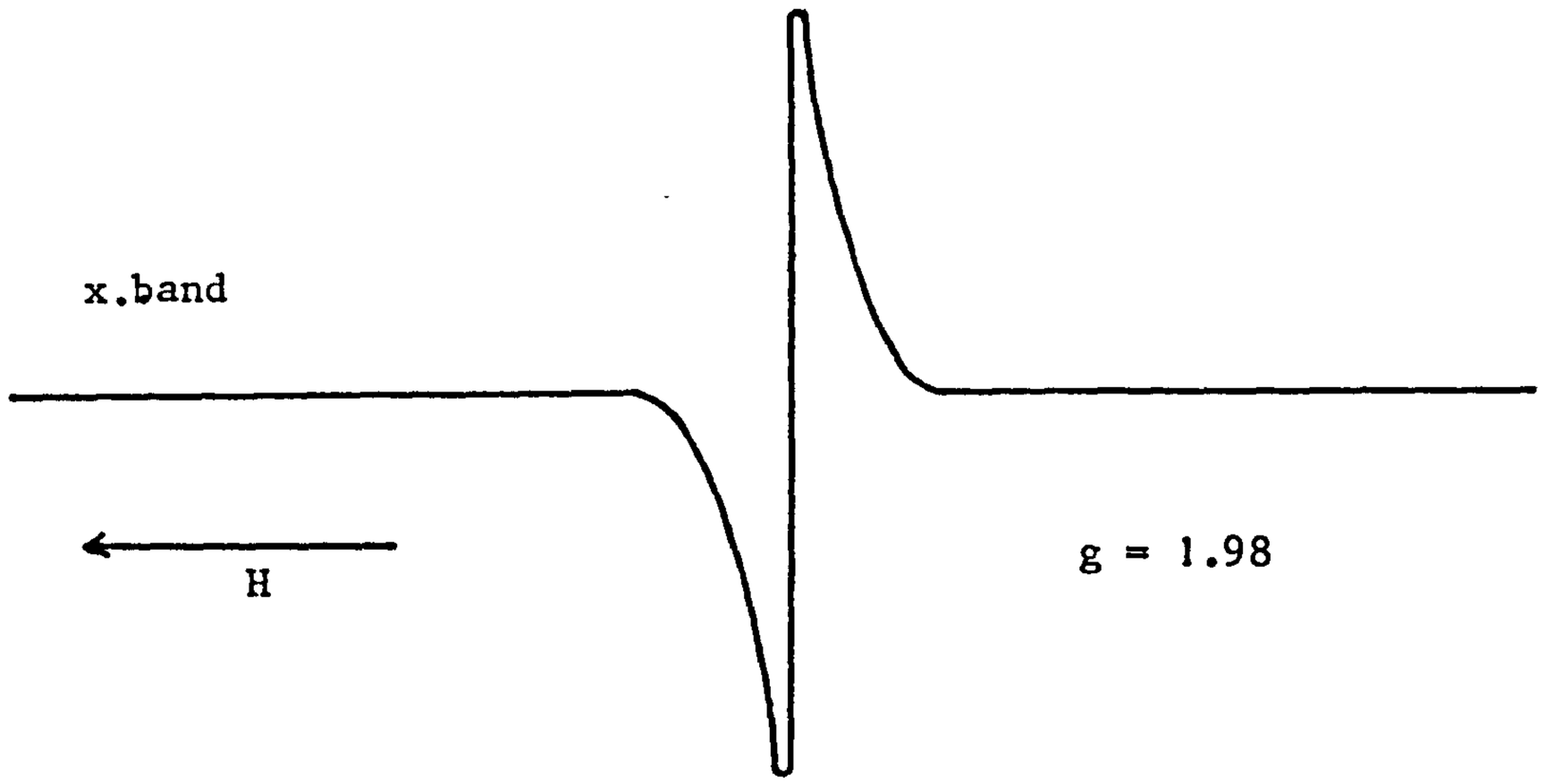

Fig.(5.13) Typical E.S.R. Spectra for amorphous material

The E.S.R. spectral intensity is determined by the concentration of paramagnetic ions $(V)^{4+}$ present in each glass. If the fraction of paramagnetic ions is n_4 which refers to the V^{4+} ions, the quantity n_4 can be determined for each glass from the intensity of the resonance given by[90]

$$I = K\, W^2 H \qquad (5\text{-}7)$$

where I is the intensity of resonance, W is the peak-to-peak width, H is the peak-to-peak height of the resonance and K is a constant depending on the line shape and the assumption was made that all x-band resonances have the same line shape and can be described by the same value of K.

A standard Varian-silica tube contained the glass sample in the form of powder and was held in a rectangular cavity. The measurements were carried out on an x-band Varian E3 spectrometer

having a modulation frequency of 100KHz. The integrated intensity of the E.S.R. signal is proportional to the number of paramagnetic spin $(V)^{4+}$ per unit sample length. The fraction of vanadium ions that are in the V^{4+} state is then

$$n_4 = a \frac{I}{W\%\rho} \qquad (5\text{-}8)$$

where n_4 represents the concentration of V^{4+} ions, a is constant, W% is the weight percent of vanadium in the glass and ρ is the mass per unit length of sample in the tube.

The spin concentration can be determined by double integration of the E.S.R. spectra and comparison with Varian standard spin sample which in the case of vanadate glasses is ammonium vanadyl oxalite $(NH_4)_2VO(C_2O_4)_2\ 2H_2O$ which is convenient.

The integrated area under the absorption curves were found for both the standard ammonium vanadyl salt and the unknown sample of vanadate glasses. The integrated area under the spectra of the standard solution enabled us to determine the V^{4+} spin density of standard solution and this value can be used to calculate the spin density of the unknown sample. The V^{4+} spin of the sample is determined from the following formula

$$n^{4+} = \frac{A_1}{A_2} \frac{m}{M} A \qquad (5\text{-}9)$$

where n^{4+} is the number of V^{4+} spin for one cm of sample in the

tube with 3mm diameter, A_1 and A_2 are the integrated area under the spectra of the sample and standard solution m is the weight of the standard solution and M is the molecular weight of the standard solution and A is the Avagadro number.

The ratio of reduced valence state to total vanadium concentration(V^{4+}/V_{total}) can also be determined by conventional chemical analysis. This technique is limited to room temperature. One of the disadvantages of this method is the sensitivity to other transition metal ions which may be present as impurities and possible changes in the ion ratio which may be induced by the process of desolving the material.

In this technique the reduced valence concentration V^{4+} is determined by desolving the glass in weak sulphuric acid and titration with potassium permanganate. The total amount of vanadium is determined by the complete reduction of vanadium ions to the V^{4+} state with sulpuric dioxide, and titration with potassium permanganate.

5-5 E.S.R.Results and Discussion

The absorption spectra of vanadium phosphate glasses containing 50 to 90 mol percent V_2O_5 and ternary system V_2O_5 - P_2O_5 - TeO_2 containing 60 mol percent V_2O_5 are shown in Figs.(5.15) and (5.16) respectively. Fig.(5.17) shows the

absorption spectra of ammonium vanadyle oxalite which we used as standard. The existence of only a single resonance line, means that the reduced valency states only belong to V^{4+} ions and the reduced valency states below the first reduced state are negligible (V^{3+} and V^{2+}). The ratio of the reduced valency states to total vanadium ions $V^{4+}/V_{tot.}$ present in glasses have been determined from E.S.R. intensity measurements and chemical analysis (titration) as a function of glass composition for both binary and ternary systems. These values are given in Table (5.4).

We found that the fraction of the reduced valency states decreases with increasing the transition metal oxide content in binary glass system and also decreases with increasing TeO_2 content in ternary V_2O_5 - P_2O_5 - TeO_2 glass system.

Variations of reduced valency state to total vanadium ion ($C = V^{4+}/V_{tot}$) with transtion metal oxide concentration in V_2O_5 - P_2O_5 and with TeO_2 content in V_2O_5 - P_2O_5 - TeO_2 glasses are shown in Figs.(5.18) and (5.19). In these figures results from E.S.R. and chemical analysis are shown for comparison.

We also found that the reduced valency concentration depends strongly on the atmosphere under which the glass is prepared. It has been assumed[90] that two V^{4+} sites are formed for each PO_4 unit that is substituted for the apex oxygen of a VO_5 unit.

Lynch[91] et al found that the paramagnetic spin

concentration is independent of temperature over a temperature range from 77 K to 400 K and they concluded that the temperature dependence of electrical conductivity in this temperature range arises from a change in the effective carrier mobility rather than a change in the carrier concentration.

Sayer et al in their 1972 paper[102] reported that this may be interpreted either on the assumption that all electron sites are similar and that no site energy differences exist such that $W \ll kT$ ($T \sim 77K$), or that electrons are localized in sites whose energy differs from the average by an amount such that $W \gg kT$ ($T \sim 400K$). So that no detectable redistribution occurs over the temperature range considered.

5-6 Discussion

It has been reported[81] that glass can be formed from the system V_2O_5 - P_2O_5 if the mol percent of P_2O_5 (glass former) is higher than 5%. Chemical analysis has shown an increasing loss of oxygen from the melts as the phosphate content increases. It should be noted that wet chemical analysis alone cannot distinguish exactly the various oxidation states of vanadium because of reactions between the various vanadium ions e.g. $V^{3+} + V^{5+} \rightleftarrows 2V^{4+}$. But chemical analysis and E.S.R. results can be interpreted together to provide more correct information about the states of different valency as has been suggested by Harper and McMillan[110].

Magnetic susceptibility studies of these glasses show that antiferromagnetic exchange interaction exists between vanadium ions in the glass[91]. Since V^{5+} ions are diamagnetic and since the concentration of V^{2+} and V^{3+} in the glass are very small, the antiferromagnetic coupling must be predominately between V^{4+} ions. Such antiferromagnetic coupling reduces the intensity of the resonance line in E.S.R. experiments and thus the apparent concentration of V^{4+}. This effect causes error in determining the value of C (ratio of reduced valency state to total vanadium ion $\frac{V^{4+}}{V_{tot}}$) and this error is proportional to the concentration of V^{4+} and the values of $\frac{V^{4+}}{V_{tot}}$ for the glasses with high V^{4+} contents will be too small.

For glass containing a large concentration of reduced ions, exchange coupling between V^{4+} and V^{3+} ions is also possible which would tend to change the resonance line and resulting change in the value of $C = \frac{V^{4+}}{V_{tot}}$. The similarity between the infra-red spectra of crystalline V_2O_5 and the V_2O_5 - P_2O_5 glasses suggests a structural similarity between these materials (see next chapter).

Janakirama-Rao[107] suggested that the vanadium co-ordination is octahedral in both crystalline V_2O_5 and the glassy system. According to Bachman et al[111] the crystalline V_2O_5 structure consists of distorted trigonal bipyramids with a vanadium ion in octahedral co-ordination at the centre of each pyramid. The oxygen atoms on the basal corners of the pyramid link to other pyramids so that sheets of VO_5 units are formed.

In the glasses containing P_2O_5, PO_4 tetrahedra replace the non-bridging oxygen at the apex of the pyramid, and the sheets are twisted to accommodate the PO_4 units and maintain the randomness of the glass. At higher P_2O_5 content these sheets degenerate into chains and ribbons of VO_5 pyramids which are bonded to PO_4 tetrahedra. With increasing concentration of V_2O_5, the concentration of V^{4+} ions and thus the exchange coupling between V^{4+} ions decreases and leads to a decrease in concentration of VO_5 units with PO_4 tetrahedra replacing the apex oxygens.

The P^{5+} ions have a greater charge density in comparison with V^{5+} ions. Therefore the tetrahedral P - O interatomic

distance is much smaller than the octahedral V - O interatomic distance. Thus when the concentration of P_2O_5 increases it produces volume expansion which leads to a reduction in the density of glass. Fig.(5.4).

Chapter VI

Optical Properties of V_2O_5 - P_2O_5 and V_2O_5 - P_2O_5 - TeO_2 Glasses

6-1 Introduction

The energy of a molecule can be separated into three parts,

I) the rotation of the molecule as a whole

II) the vibration of the constituent atoms

III) the motion of the electrons in the molecule.

If a molecule is placed in an electromagnetic field e.g. light, a transfer of energy from the field to the molecule will occur only when Bohr's frequency condition is satisfied,

$$\Delta E = E_2 - E_1 = h\nu \qquad (6\text{-}1)$$

where ΔE is the difference in energy between two quantized states, h is Planck's constant, ν is the frequency of the light. If E_2 is a quantized state of higher energy than E_1, the molecule absorbs radiation when it is excited from E_1 to E_2 and emits radiation of the same frequency as given by Eq.(6-1) when it reverts from E_2 to E_1.

Because rotation levels of molecules are relatively close to each other, transitions between these levels occur at low frequency (long wave lengths) and pure rotational spectra appear

in the range between 10^2 - $10^4\mu m$ ($1cm^{-1}$-10^2cm^{-1}). The separation of vibrational energy levels is greater, and the transitions occur at higher frequency (shorter wave lengths) therefore pure vibrational spectra are observed in the range between 10^2 - $1\mu m$ (10^4cm^{-1} to 10^2cm^{-1}).

Finally electronic energy levels are usually far apart and electronic spectra are observed in the range between 10^4cm^{-1} and 10^5cm^{-1} ($1\mu m$ - $10^{-1}\mu m$). Thus as a general rule pure rotational spectra are observed in the microwave and far infra-red regions pure vibrational spectra are observed in the infra-red and pure electronic spectra are observed in the visible and ultra-violet region.

Infra-red spectroscopy has been used in studying the structure of gases, molecules and organic substances. This technique has also been used for structural investigation of glassy materials but the application of this method is limited mainly because of the complicated nature of the glassy state. The study of semiconducting amorphous materials such as glasses by means of analysing the optical absorption edge provides useful information about the optical transition mechanisms and hence some ideas concerning the band structure of the glassy materials.

6-2 Infra-red Spectroscopy

This is a useful method providing information such as quantitative and qualitative analysis in the calculation of

various physical constants in the determination of the structure of compounds and in many other areas.

An infra-red spectrogram is a two-dimensional presentation on a sheet of paper of the absorption characteristics of a molecule. These absorption characteristics appearing on the spectrogram as bands or peaks can be described in terms of three variables, position, intensity and shape. The first two of these can be expressed in numbers while the third is usually expressed in words. *The position of the spectra on the x axis where the band appears is expressed in terms of energy (ergs), frequency (sec^{-1}) wavelength (microns) or wave number (cm^{-1}). Intensity is a measure of the quantity of energy absorbed, and is measured by shape. It is determined from the y axis. The band shape is usually described as broad, narrow, sharp, etc.

The application of infra-red spectroscopy to the identification of inorganic compounds has been somewhat less successful, mainly because many simple inorganic compounds such as the borides, silicides, do not absorb radiation in the region between 4000 and 6000cm^{-1}. Another problem is the possible chemical reaction (cation exchange) between the inorganic compound and the infra-red window material or support medium.

6-3 Sample Preparation and Experimental Procedure

Glass samples of the composition 50 to 90 mol% V_2O_5 for the binary V_2O_5 - P_2O_5 system and 5 to 35 mol% for the ternary V_2O_5 -

P_2O_5 - TeO_2 system as are listed in Table (5.1) were ground in a clean mortar to a fine powder. A few milligrams of glass powder were mixed and ground with the KBr (B.D.H.Chemicals Ltd.). KBr pellets, transparent to light, were formed by pressing the mixture at 10 to 15 tons for a few minutes under vacuum.

Infra-red absorption spectra of these samples (annealed at 200°C for two hours) were determined by using a Unicam SP2000 double beam recording infra-red spectrophotometer, at room temperature, in the wavelength region 2.5 - 25μm ($4000cm^{-1}$ - $400cm^{-1}$).

6-4 Experimental Results and Discussion

Vibrational absorption peaks observed for V_2O_5 - P_2O_5 and V_2O_5 - P_2O_5 - TeO_2 glasses are listed in Tables(6.1) and (6.2). Figs.(6.1) and (6.2) show the vibrational absorption spectra for the binary and ternary system respectively. From these figures one can see that with the exception of the peaks at about 1005 - $1010cm^{-1}$, these peaks are quite broad and overlap. Thus the exact location of them is not possible and the values given in Tables(6.1) and (6.2) are the average of several experiments on two or three samples for each composition.

Anderson[20] measured the absorption spectra of 70 mol% V_2O_5 sample in the range 20 - $300cm^{-1}$ using an interfrometer spectrophotometer and reported that no new absorption peaks appear at longer wavelengths. The vibrational absorption bands

in the range 300 to 2000cm^{-1} could be due to a number of reasons such as bridging and non-bridging oxygen ions which are doubly and singly bonded, to the high and low states of vanadium ions, to phosphate ions and possibly due to some combination of these reasons.

It has been reported[10] that the V^{5+} ion exists in sixfold co-ordination in crystalline V_2O_5. It is also recognised[12] that as long as the co-ordination of a cation remains constant, the infra-red spectra of a given compound are similar. If the composition of vanadium pentoxide in their glassy state and in their crystalline state give rise to similar absorption bands corresponding to that of the V - O band vibration in crystalline V_2O_5, it would indicate that V^{5+} ion in the glassy state are also in sixfold co-ordination.

The infra-red spectra for crystalline V_2O_5 are also shown in Fig.(6.3). Crystalline V_2O_5 exhibits vibrational absorption peaks at 280, 370, 480, 660, 800, 915, 1040, 1260, 1275cm^{-1} and the peak at 1040 is relatively sharp. It has been reported[12] that this peak is due to the vanadium - oxygen stretching frequency. It is also observed that the vanadium - oxygen stretching for compounds in which the vanadium atoms are totally ionized to V^{5+}, is in the 1025 - 1005cm^{-1} range and the presence of V^{4+} ions appears to reduce the V - O stretching frequency to the 900 - 1020cm^{-1} range. From these data and comparing the vibrational spectra of V_2O_5 in the crystalline state and of V_2O_5

- P_2O_5 in the glassy state one can conclude that the peaks at $1010cm^{-1}$ in the glassy state is due to V - O stretching frequency.

The V - O absorption band shifts to longer wavelengths for glasses with high percentage of P_2O_5. This could be due to the influence of the P^{5+} ion which has a higher charge density than the V^{5+} ion and therefore attracts the bonding electrons near to the P^{5+}which leads to weakening of the V - O band. The absorption spectrum for P_2O_5 is also shown in Fig.(6.3) and in this spectrum the peak at 1010 disappears which leads to the fact that this peak is associated with the V - O stretching frequency.

From Figures (6.1) and (6.2) it is obvious that the normal vibrational frequency of the V - O band seen in crystalline V_2O_5 at wave number 1040 is shifted to longer wavelengths as the V_2O_5 content decreases and can be seen in all the spectra of the glassy state, indicating that the V^{5+} ion exists in sixfold co-ordination in the glassy state as well as crystalline V_2O_5. Phosphate ions introduce weak vibrational absorption in some phosphate glasses in the range 1020 - $1100cm^{-1}$ and in some crystalline phosphate networks in the range 1150 - $1400cm^{-1}$[20] therefore the broad absorption spectra between 1080 - $1150cm^{-1}$ could be due to phosphorous - oxygen vibration as has been reported by Janakinama-Rao[10].

We found that on replacing P_2O_5 with TeO_2, as the

concentration of TeO_2 increases (decreasing P_2O_5) the intensity of the vibration at a frequency $1010cm^{-1}$ due to V - O bands becomes weaker and shifts to larger wavelengths which could possibly be due to a smaller influence of the P^{5+} ion which has a higher charge density.

From Fig.(6.2) one can see that a peak appears at about 810 - $820cm^{-1}$ which is not found in the spectra of V_2O_5 - P_2O_5 glasses, and the intensity of this peak increases with increasing TeO_2 content. A similar absorption peak was observed in the spectra of TeO_2, Fig.(6.3) at about $830cm^{-1}$. Therefore this absorption peak could possibly be due to the Te - O stretching frequency.

Anderson and Compton[20] studied the optical absorption properties of V_2O_5 - P_2O_5 glasses containing 70 and 87.5 mol% V_2O_5 and observed vibrational peaks at 360, 420, 680, $1010cm^{-1}$ in the 70 mol% V_2O_5 glasses and the absorption peaks about 330, 435, 635, 810, $1007cm^{-1}$ and $1085cm^{-1}$ in 87.5 mol% V_2O_5 glass. From observation of a sharp absorption peak at $1038cm^{-1}$ in crystalline V_2O_5, Anderson and Compton[20] concluded that the peak at about $1010cm^{-1}$ is due to the V - O stretching frequency. Sayer et al[108] observed an absorption band at $1015cm^{-1}$ in both crystalline V_2O_5 and P_2O_5 - V_2O_5 glasses and suggested that this peak is due to the V - O stretching frequency. Sayer et al have also observed an absorption peak at about $380cm^{-1}$. The intensity of this peak appears to increase with P_2O_5 content and also

depends on the V^{4+} concentration of the same composition but different reduced valence state ratio. With considering that this band is not a feature of either pure V_2O_5 or P_2O_5, Sayer et al suggested that this absorption peak is due to the formation of a localized structure or the creation of V^{4+} sites in the glass.

6-5 Absorption Edge of Vanadium Phosphate Glasses

6-5-1 Introduction

In transition metal oxide glasses in general, and in vanadate glasses in particular, a photon with a certain range of energy could be absorbed by transition metal ion present in glass by two different processes.

I) Absorption may be due to internal transition between the d shell electron and

II) Absorption may be due to a transfer of electron from a neighbouring atom to the transition metal ion and vice versa.

The first process is known as the ligand field absorption and the second process relates to a charge transfer band.

The study of optical absorption and particularly the absorption edge is a useful method for the investigation of optically-induced transitions and for the provision of information about the band structure and energy gap in both crystalline semiconductors and non-crystalline materials. The principle of this technique is that a photon with energies greater than the band gap energy will be transmitted. The absorption edge in many disorder materials follows the Urbach[114] rule given by

$$\alpha(\omega) \propto \exp\ (\frac{\hbar\omega}{\Delta E}) \qquad (6\text{-}2)$$

where $\alpha(\omega)$ is the absorption coefficient at an angular frequency

of $\omega = 2\pi\nu$ and ΔE is the width of the tail of localized states in the band gap.

There are two kinds of optical transition at the fundamental edge of crystalline and non-crystalline semiconductors, direct transition and indirect transition. Both kinds involve the interaction of an electromagnetic wave with an electron in the valence band, which is raised across the fundamental gap to the conduction band.

For direct optical transition from the valence band to the conduction band it is essential that the wave vector for the electron be unchanged. In the case of indirect transition the interactions with lattice vibration (phonon) takes place, thus the wave vector of the electron can change in the optical transition and the momentum change will be taken or given up by phonons. If the minimum of the conduction band lies in a different part of k space then the maximum of the valence band, a direct optical transition from the top of the valence band to the bottom of the conduction band is forbidden. In this case, indirect transitions in which a phonon is emitted or absorbed occur and the absorption coefficient for indirect transition is of the order of 10 to $10^3 cm^{-1}$ as compared with 10^4 for direct transitions.

Mott and Davis[43] suggested the following expression for direct transitions

$$\alpha = B \frac{(\hbar\omega - E_{opt})^n}{\hbar\omega} \qquad (6\text{-}3)$$

where n = ½ or 3/2 depending on whether the transition is allowed or forbidden, and for indirect transition the expression given by Mott and Davis is as following

$$\alpha = \frac{(\hbar\omega - E_{opt} + \hbar\omega_{ph})^n}{\hbar\omega} \Big/ \left[\exp\left(\frac{\hbar\omega_{ph}}{kT}\right) - 1\right] + \frac{(\hbar\omega - E_{opt} - \hbar\omega_{ph})^n}{\hbar\omega} \Big/ \left[1 - \exp\left(\frac{\hbar\omega_{ph}}{kT}\right)\right] \qquad (6\text{-}4)$$

the two terms on the right hand side of Eq.(6-4) represent contributions from transitions involving absorption and emission respectively, which have different coefficients of probability and temperature dependence.

It has been suggested by Anderson and Compton[20] that the fundamental absorption edge of the vanadate glasses and crystalline V_2O_5 near 2.5 eV fits the condition for direct forbidden transition in which the absorption coefficient is given by

$$\alpha = B (\hbar\omega - E_{opt})^{3/2} / \hbar\omega \qquad (6\text{-}5)$$

where α is the absorption coefficient, E_{opt} is the optical gap and B is constant.

A broad absorption tail extends from the absorption edge to the lattice vibration absorption band at about 1400cm^{-1} in glass but not in crystalline V_2O_5 which is the reason for the black

colour in vanadate glasses. The fundamental absorption edge shifts to higher energies with increasing P_2O_5 content and occurs at higher energies than that of crystalline V_2O_5.

It has been reported by many authors[90-91-106-108] that this broad absorption tail and the optical band gap energy E_{opt} may be related to the high concentration of V^{4+} ions in vanadate glasses.

6-5-2 Sample Preparation and Experimental Technique

Thin blown films of some glasses listed in Table(5.1) were prepared by dipping a silica tube into the molten material and gathering a small amount of glass melt on the end of the tube and blowing it into the air. The optical absorption edge of these glasses after annealing at 200°C for two hours was measured in the wavelength range of 200 - 700mμm using a Perkin - Elmer model 137U.V spectrometer at room temperature.

The general formula for the optical absorption coefficient $\alpha(\omega)$ is given by

$$\alpha(\omega) = \frac{1}{L} \text{Ln} \frac{I_0}{I_t} \qquad (6\text{-}7)$$

where $\alpha(\omega)$ is the absorption coefficient (cm^{-1}) I_0 and I_t intensity of incident and transmitted light and L is the thickness of the sample (cm).

6-5-3 Results and Discussion

The optical absorption spectra for V_2O_5 - P_2O_5 and V_2O_5 - P_2O_5 - TeO_2 glasses as a function of wavelength are shown in Figs.(6.4) and (6.5). These figures show that firstly, in contrast to crystalline V_2O_5 there is no sharp absorption edge and this is a characteristic of the glassy state, and secondly the position of the fundamental absorption edge shifts to higher energy with increasing P_2O_5 content as was reported by Anderson.

The absorption coefficient $\alpha(\omega)$ was determined at different photon energies, near the absorption edge for V_2O_5 - P_2O_5 and V_2O_5 - P_2O_5 - TeO_2 glasses and the quantity $(\alpha\hbar\omega)^{2/3}$ is plotted vs. photon energy $(\hbar\omega)$ as has been suggested by Anderson for direct forbidden transitions. Figs.(6.6) and (6.7) show the linear dependence of $(\alpha\hbar\omega)^{2/3}$ on photon energy $(\hbar\omega)$ for both binary and ternary glass systems, which tends to deviate from linearity at low photon energy. E_{th} is defined as the onset of the photon energy at which the linear relationship between $(\alpha\hbar\omega)^{2/3}$ and $\hbar\omega$ is observed. Values of E_{th} are found from Figs.(6.6) and (6.7) for both binary and ternary glass and are plotted against the P_2O_5 content in Figs.(6.8) and (6.9) respectively. These figures show that the value of E_{th} shifts towards higher energies as the P_2O_5 content decreases and this shift is a linear function of the P_2O_5 content. The values of optical gap E_{opt} are obtained by extrapolation of the linear region of the plots of $(\alpha\hbar\omega)^{2/3}$ vs. $\hbar\omega$ in Figs.(6.6) and (6.7) to

$(\alpha h\omega)^{2/3} = 0$ and these values for $V_2O_5 - P_2O_5$ and $V_2O_5 - P_2O_5 - TeO_2$ glasses are given in Table(6.3). We found that the values of E_{opt} increase with increasing P_2O_5 content which as we saw in chapter (V) was the reason for the increasing V^{4+} ion concentration in glass. It has been established that the concentration of the non-bridging oxygen ions decreases with increasing P_2O_5 content. This is due to the increase in V^{4+} ion concentration with P_2O_5 content. Because the charged non-bridging oxygens associated with the V_2O_5 network would introduce 2p like energy levels which are higher than those of bridging oxygen ions therefore E_{opt} increases with increasing V^{4+} ion concentration or P_2O_5 content (with a decrease in concentration of non-bridging oxygen).

Variations of E_{opt} with P_2O_5 content for both $V_2O_5 - P_2O_5$ and $V_2O_5 - P_2O_5 - TeO_2$ glasses are shown in Figs.(6.10) and (6.11) respectively. In Fig.(6.12) and (6.13) the variation of E_{opt} is plotted vs. the ratio of reduced valence state to total vanadium ion concentration ($C = V^{4+}/V^{5+}$) for both glass systems.

The value of B in Eq.(6-5) can be determined from the slope of the linear part of curve $(\alpha h\omega)^{2/3}$ vs. $h\omega$ in Figs.(6.6) and (6.7). These values for $V_2O_5 - P_2O_5$ and $V_2O_5 - P_2O_5 - TeO_2$ are found and listed in Table (6.3). It was found that the value of B in these glasses increases with increasing P_2O_5 content. The dependence of B on P_2O_5 content in both glass systems are shown in Figs.(6.14) and (6.15).

In vanadate glasses as the P_2O_5 content increases the separation distance between oxygen ions increases firstly because the oxygen content decreases (due to decrease in non-bridging oxygen concentration) and secondly because the density of V_2O_5 - P_2O_5 glasses decreases with increasing P_2O_5 content. This causes more localization of p like electrons on the oxygen ions and this localization could be the reason that the absorption occurs at higher energies.

In many crystalline and non-crystalline semiconductors the absorption coefficient $\alpha(\omega)$ depends exponentially on photon energy ($\hbar\omega$). The exponential dependence is known as the Urbach[114] rule and is given by the following expression

$$\alpha(\omega) = B' \exp\left(\frac{\hbar\omega}{\Delta E}\right) \qquad (6\text{-}8)$$

where B'is constant and ΔE is the width of the band tails of the localized states. The origin of the exponential dependence of absorption coefficient on photon energy $\hbar\omega$ is not clearly known. Tauc[118] has suggested that it arises from electronic transitions between localized states where the density of localized states is exponentially depandent on energy. But Mott and Davis[52] reported that this explanation is not valid for all disordered materials since the slope of the observed exponential behaviour remains unchanged for many crystalline and non-crystalline materials. Figs.(6.16) and (6.17) show the variation of $Ln\alpha(\omega)$ with photon energy $\hbar\omega$ for some V_2O_5 - P_2O_5 and V_2O_5 - P_2O_5 - TeO_2 glasses respectively. The values of ΔE in

Eq.(6.8) are calculated from the slope of the straight line of these curves are given in Table (6.3). Mott and Davis[48] reported that the values of ΔE for a range of amorphous semiconductors are very close together in value and lie between 0.046 and 0.066 eV. For highly disordered crystalline GeTe ΔE is reported by Lewis[115] to be 0.1 eV and in the case of molybdeum phosphate glasses Austin[116] et al reported the value of ΔE as high as 0.16 eV. Recently Moridi[117] reported for copper-calcium-phosphate glasses that the value of ΔE varies between 0.66 and 1.06 eV depending on the copper concentration. For glasses investigated in the present work the exponential behaviour is observed and the values of ΔE varies between 0.31 and 0.68 eV depending on the composition.

Tauc et al[118] explain the behaviour of the Urbach rule in terms of two contributions to the absorption coefficient for liquid sulphur. The first part arises because of the electron-hole interaction; which causes the optical edge to show an exponential dependence on photon energy. The second part consists of low energy of the absorption spectrum which increases with polymerization.

In the case of vanadate glasses as well as in crystalline V_2O_5, the exponential dependence of absorption coefficient $\alpha(\omega)$ on photon energy $\hbar\omega$ Figs.(6.16) and (6.17) suggests that these materials obey the Urbach rule.

The electrical properties of some vanadate glasses are being

studied in the present work and some results are given in the next section. The activation energy values at high temperature (W) for some of these glasses were found from the slope of the log σ vs. $\frac{1}{T}$ curves and are given in Tables(7.2) and (7.8). The values of $E_{el} = 2W$ for these glasses are given in Table(6.3) and plotted vs. E_{opt} for $V_2O_5 - P_2O_5$ and $V_2O_5 - P_2O_5 - TeO_2$ glasses as shown in Figs.(6.18) and (6.19) respectively. From these figures a simple correlation is found between E_{el} and E_{opt} for $V_2O_5 - P_2O_5$ glasses as

$$E_{el} = 0.97\ E_{opt} - 1.37 \qquad (6\text{-}9)$$

and a similar relationship was found for $V_2O_5 - P_2O_5 - TeO_2$ in empirical form as

$$E_{el} = 0.39\ E_{opt} - 0.09 \qquad (6\text{-}10)$$

Nunoshita et al[119] found a similar relationship for Si - As - Te glasses as the contents of Si and Te are varied.

Chapter VII

Electrical Properties of $V_2O_5 - P_2O_5$ and $V_2O_5 - P_2O_5 - TeO_2$ Glasses

7-1 Introduction

From the magnitude of the electrical conductivity and the temperature dependence of the conductivity in vanadate glasses one can readily classify these glasses as semiconductors. Stanworth[120] et al were the first to note this behaviour in their attempts to determine to what extent vanadium oxide could be considered as a glass former.

Vanadate glasses belong to a class of materials known as narrow-band semiconductors as well as certain other transition metal oxide glasses. According to Morin[121], the 3d conduction band is quite narrow and this causes charge carriers to have very high effective mass. This being the case, the charge carriers can be treated as localized charges which jump from site to site. Since the bonding in these solids is largely ionic, lattice relaxation occurs around the localized carriers.

In the 3d glasses, we expect the 3d bands to form localized states in the Anderson[122] senses and any polaron hopping energy (W_H) will be increased by a disorder term (W_D). There is good evidence for this type of model in 3d glasses, but it is difficult to determine the size of the (W_D) term exactly.

Lattice relaxation leads to the trapping of the carrier because of its associated deformation potential. As a result of trapping, free charge carriers require an appreciable thermal activation energy of formation, and this gives rise to the observed exponential temperature dependence of electrical conductivity. According to Mott and Gurney[123] the strength of trapping of carriers should be proportional to $\left(\frac{1}{\varepsilon_\infty} - \frac{1}{\varepsilon_o}\right)$ where ε_∞ and ε_o are the high frequency dielectric and static dielectric constant respectively.

The electrical conductivity of transition metal oxide glasses has been studied by several authors[123-128], and it has been established that the conduction in these materials is due to transitions of electrons from a low valence state to a high valence state.

In vanadium phosphate glasses (V_2O_5 - P_2O_5) the predominant valence statesof vanadium are V^{4+} and V^{5+} and the valence states lower than V^{4+} are negligible and V^{4+} ions share fivefold co-ordination with surrounding oxygens similar to the situation in crystalline V_2O_5 [90,91]. The interaction of electrons with ions is so strong as to produce localization and formation of small polarons. As we saw in the last chapter the amount of V^{4+} decreases as the V_2O_5 concentration increases. Apparently V_2O_5 decomposes irreversibly in the melt and the loss of oxygen increases with the amount of P_2O_5 in the composition.

It has been found that the paramagnetic spin concentration V^{4+} in these glasses is relatively insensitive to temperature

between 77 and 400 K[20]. This leads us to suppose that semi-conduction in these glasses is not due to excitation of carriers across the band gap, but to thermally activated hopping between vanadium ions of varying valency.

It has also been found that there is a break in the log σ v.s 1/T curve at a temperature of roughly $\theta_D/2$ (where θ_D is the Debye temperature defined by $k\theta_D = \hbar\omega_o$ in which ω_o is the mean optical phonon frequency) and virtually no temperature dependence at lower temperature[83].

This effect has been interpreted by many authors. Schamakenberg[129] has considered that in the low temperature range $T<\theta_D/4$ charge carrier transport should be via an acoustical one phonon assisted hopping process having an activation energy ΔW, while in the high temperature range $T>\theta_D/2$, optical multiphonon processes should determine the conductivity, and the activation energy should be of the form of $W_H + \Delta W$, where W_H is the polaron hopping energy. In this chapter we shall discuss some electrical properties of binary system ($V_2O_5 - P_2O_5$) glasses as well as glasses of the ternary system containing TeO_2. For this purpose we carried out the following experiments.

I. D.c. conductivity measurement for a series of $V_2O_5 - P_2O_5$ glasses containing 50 to 90 mol% V_2O_5, at different temperatures.

II. Activation energy measurement.

III. Checking the Ohmic contact for all samples from the observation of linear I-V characteristic.

IV. Effect of time on the resistivity of samples in order to determine the kind of conduction (electronic or ionic).

V. Composition dependence of conductivity and activation energy.

VI. Dependence of electrical properties on the transition-metal-ion concentration and transition-metal-ion spacing.

VII. Mobility measurement and temperature dependence of mobility.

VIII. Effect of ratio of reduced valence concentration to the total valence state ($C = V^{4+}/V_{tot}$) on the electrical properties.

IX. Effect of electrode material on the electrical properties.

X. In order to study the effect of replacing P_2O_5 with TeO_2 on the electrical properties of the glass we repeated the experiments mentioned above for a series of glasses containing 60 mol% V_2O_5 (40-x) mol% P_2O_5 and x mol% TeO_2 where x varies from 5 to 35 mol%.

XI. High electric field effect and switching phenomena for both the binary and ternary system.

In general we found that the electrical properties of vanadium phosphate glasses are governed by many factors which include the following.

a) The concentration of the transition metal oxide.

b) The ratio of the concentrations of reduced valence states to total valence states.

c) Average separation distance of the transition metal ions.

d) Thermal history. It has been found that the annealing temperature and annealing time can have effects on the magnitude of the conductivity of a semiconducting glass. The melting temperature of $V_2O_5 - P_2O_5$ and $V_2O_5 - P_2O_5 -$

TeO_2 glasses influences the ratio of V^{4+}/V_{tot} and thus the conductivity of these glasses.

e) The atmosphere under which the glass is prepared has an effect on the ratio of $C=\frac{V^{4+}}{V_{tot}}$ valency states therefore the electrical conductivity of these glasses is affected by atmosphere.

7-2 Sample Preparation

A series of glasses containing 50 to 90 mol% V_2O_5 was prepared by using the method mentioned earlier (chapter V). Glasses annealed at 200°C for two hours were ground and polished to discs about 2 to 3mm in thickness, using a flexibox grinding machine. Grinding was carried out using 400 grade silicon carbide powder with Mobil oil as lubricant. The samples were polished using a diamond wheel with diamond paste (grade, 6) and with paraffin as a lubricant. Diamond paste was removed from the samples with white spirit supplied by B.D.H. Chemicals and they were dried under compressed air.

After cleaning the samples the evaporation of gold elctrodes was carried out in an Edwards (12") coating unit at a pressure of 10^{-5} torr. Before the deposition of electrodes the samples were again annealed at 200°C for one hour to remove the volatile contamination. On one side of the sample the electrode was 9mm in diameter and on the other side was a 6mm diameter gold electrode. It is preferred to use a guard-ring electrode in order to eliminate the surface leakage and to measure the true

bulk conductivity of glasses. Fig.(7.1) shows the gold electrode deposited sample with the guard-ring arrangement used. After the electrode deposition, samples were annealed at 200°C for one hour in order to harden the electrodes and to achieve a good ohmic contact, and were then cooled to room temperature gradually.

Silver and copper electrodes were deposited for some samples using the method mentioned above, in order to study the effect of electrode material on the electrical conductivity. Samples were stored in a desiccator under vacuum, containing a water absorbing material until the tests were begun.

7-3 Experimental Techniques

Ohmic contacts and the absence of barrier layer formation were checked by the observation of linear I - V characteristics. The circuit used for measuring the I - V characteristic and resistances of the samples is illustrated in Fig.(7.2). As is shown in Fig.(7.3) the sample is placed between two copper cylinders surrounded by a heater which is a wire-wound furnace in cylindrical form.

Two thermocouples A(chromel/alumel) and B(copper/constantin) were used for measuring the temperature of both sides of the sample in order to ensure that these temperatures were the same. The temperature was controlled by using a Eurotherm temperature controller. A typical sample holder used for low field electrical measurements is shown in Fig.(7.4). All electrical measurements were carried out under a vacuum of 10^{-5} torr in

order to prevent atmospheric effects such as arise from humidity. Apparatus used for d.c. electrical measurements is shown in Fig.(7.5). A Keithley regulated high voltage power supply model 241 was used as a voltage source which could provide a stabilized d.c. voltage up to 1000 volts with an accuracy of the order of 0.05%. The current was measured by a Keithley model 610 C electrometer capable of measuring currents as low as 10^{-14} amps.

7-4 D.C. Conductivity Results for $V_2O_5 - P_2O_5$ Glasses

A typical I - V characteristic for glass number 106 in table (5.1) (75 mol% V_2O_5 - 25 mol% P_2O_5) at different temperatures, is shown in Fig.(7.6). In this figure log V is plotted vs log I. The I - V characteristics were measured for all samples listed in Table(5.1) at different temperature. The main purpose of the I - V characteristic is to ensure that the voltage applied for the conductivity measurements at different temperature are linear with the currents across the sample, and therefore Ohm's law can be applied through the whole range of measurements.

The value of resistance (R) was measured from the slope of the I - V characteristic according to Ohm's law (R = V/I). The conductivity (σ) and resistivity (ρ) of the samples were calculated from the relation

$$\sigma = \frac{1}{\rho} = \frac{L}{A} \cdot \frac{1}{R} \qquad (7\text{-}1)$$

where σ is the conductivity ($\Omega^{-1}cm^{-1}$), ρ is the resistivity (Ωcm), L thickness of sample (cm), A is the deposited electrode area (cm^2) and R is the resistance of the sample which is the slope of the log V vs. log I.

The d.c. electrical conductivity for V_2O_5 - P_2O_5 glasses with different compositions as listed in Table(5.1) were measured over the temperature range 293-473 K. The values of σ for these glasses at different temperatures are given in Table(7.1). The variations of log σ as a function of reciprocal temperature for these glasses are shown in Fig.(7.7). This figure shows that the conductivity increases with increasing temperature over a considerable range of temperature. From Fig.(7.7) one can see that the log σ vs. $\frac{1}{T}$ gives a good straight line over a temperature range 293-473 K. This can be taken as evidence that the activation energy for V_2O_5 - P_2O_5 glasses in this temperature range is independent of temperature.

The d.c. activation energy can be determined from the slope of the straight line obtained from log σ vs. $\frac{1}{T}$ using equation

$$\sigma = \sigma_0 \exp\left(\frac{-W}{kT}\right) \qquad (7\text{-}2)$$

The values of the slopes and the activation energies for V_2O_5 - P_2O_5 glasses are given in Table(7.2). The variation of activation energy with transition metal oxide content for V_2O_5 - P_2O_5 glasses is shown in Fig.(7.8). This figure shows that the

activation energy for these glasses decreases with increasing transition metal oxide content.

In Fig.(7.9) the conductivities of V_2O_5 - P_2O_5 glasses are plotted against the V_2O_5 content at different temperatures which shows that the conductivity in these glasses increases with increasing transition metal oxide content.

Time dependences of the conductivity for V_2O_5 - P_2O_5 glasses are shown in Fig.(7.10), and it can be seen that the conductivity is constant and time independent which is the evidence for electronic conduction.

Variation of activation energy as a function of transition metal ion spacing (R) is shown in Fig.(7.11) which indicates that with increasing ion spacing the activation energy increases and this leads to a reduction in conductivity according to the general formula given by Mott for d.c. condcutivity (chapter IV)

$$\sigma = \nu_{ph} \frac{Ne^2R^2C(1-C)}{kT} \exp(-2\alpha R) \exp(\frac{-W}{kT}) \qquad (7-3)$$

In order to study the effect of different electrode materials and determine any surface dependence, we measured the conductivity for samples with different electrode materials. Three samples of composition 104 (65 mol% V_2O_5 - 35 mol% P_2O_5) had electrodes deposited of gold, silver and copper and the conductivities were measured for these samples at different temperatures. The

results for samples with Ag and Cu electrodes are shown in Fig.(7.12) and (7.13) respectively. These figures show that there is no significant change in conductivity of glass with these different electrode materials. This is some evidence that the measured values for conductivity represent the bulk conductivity of the glass and are independent of any surface phenomena.

It was found that the conductivity of V_2O_5 - P_2O_5 glasses increases with increasing transition-metal-ion concentration, and decreases with increasing transition-metal-ion spacing. Fig.(7.14) and (7.15) show the dependence of conductivity for these glasses on T.M.I. concentration and T.M.I. spacing respectively. It was also found that in these glasses the conductivity decreases with increasing activation energy. The dependence of conductivity on the activation energy is shown in Fig.(7.16).

As we mentioned before, in vanadate glasses as well as in many other transition metal oxide glasses, the interaction between the electrons and the lattice is sufficiently strong to produce small polarons. The value of the polaron binding energy W_p can be determined from the following formula[130].

$$W_p = \frac{e^2}{2\varepsilon_p r_p} \qquad (7\text{-}4)$$

Where ε_p is the effective dielectric constant given by

$$\frac{1}{\varepsilon_p} = \frac{1}{\varepsilon_\infty} - \frac{1}{\varepsilon_o} \qquad (7\text{-}5)$$

in which ε_∞ and ε_o are the high frequency and static dielectric constants. r_p in Eq.(7-4) is the polaron radius which can be determined from the following equation[131]

$$r_P = \frac{1}{2}\left(\frac{\pi}{6N}\right)^{1/3} \qquad (7\text{-}6)$$

where N is the number of sites per unit volume. It should be mentioned that if the distance (R) through which the electron must be transformed is not large compared with the polaron radius (r_p), then Eq.(7-4) is not valid and must be replaced by [100]

$$W_P = \frac{e^2}{2\varepsilon_p}\left(\frac{1}{r_p} - \frac{1}{R}\right) \qquad (7\text{-}7)$$

The calculated values of polaron radius and polaron binding energy W_p (which is approximately twice the activation energy) for vanadate glasses are given in Table(7.6). It was found that the conductivity of $V_2O_5 - P_2O_5$ glasses decreases with increasing polaron radius (r_p). The dependence of conductivity and the activation energy on polaron radius are shown in Figs.(7.17) and (7.18) respectively.

The mobility of the carriers can be determined when the conductivity and carrier concentration n(which is equal to the volume concentration V^{4+} ions in the n-type semiconductors) is known from the following formula (see chapter III).

$$\mu = \frac{\sigma}{ne} \qquad (7\text{-}8)$$

where e is the electron charge. Tabulated results for a temperature range from 293 to 473 K are given in Table(7.4). Fig.(7.19) shows the temperature dependence of the mobility for glasses containing 50 to 90 mol% V_2O_5. This figure shows that the mobility of V_2O_5 - P_2O_5 glasses increases with increasing temperature and a plot of log μ vs. $\frac{1}{T}$ is a straight line.

The variation of the electron mobility with V_2O_5 content for V_2O_5 - P_2O_5 glasses at different temperature is shown in Fig.(7.20). From this figure one can see that the mobility of electrons for these glasses increases with increasing V_2O_5 content.

Mott[132] suggested that the band gap in the amorphous state is replaced by a minimum called a pseudogap and he concluded that the single particle state becomes localized with the electron moving by thermally activated hopping process. The small polaron studying by Holstein[133] lead to the conclusion that at temperature above $\frac{1}{2}\theta_D$ where θ_D is Debye temperature, the electron states would become localized and the conduction is then described via a hopping of an electron and the mobility is described by

$$\mu = \nu_{ph}\, a^2 \frac{e}{kT} \exp\left(\frac{-W_H}{kT}\right) \qquad (7\text{-}9)$$

where ν_{ph} is the polaron frequency, a the mean separation between the ions and W_H is the activation energy for the hopping process.

If at high temperature the thermally activated process is

dominant, then by using Eq.(7-9) a plot of $\log \mu T$ vs. $\frac{1}{T}$ should yield as straight line, i.e.

$$\log \mu T \propto \frac{1}{T} \qquad (7\text{-}10)$$

A plot of $\log \mu T$ vs. $\frac{1}{T}$ is shown in Fig.(7.21) which shows the linear dependance of $\log \mu T$ on $\frac{1}{T}$.

7-5 D.C.Conductivity Results for Glass Containing TeO_2

In order to study the effect of replacing P_2O_5 with TeO_2 on the electrical properties of these glasses, we prepared series of glasses containing 60 mol% V_2O_5 and 5 to 35 mol% TeO_2 as are listed in Table(5.1). The experimental technique was the same as for V_2O_5 - P_2O_5 glasses.

The I - V characteristic measurement was carried out for all samples listed in Table(5.1) and showed a linear dependence of log V on log I which is an evidence for good Ohmic contact and conduction. Typical I - V characteristics for glass No. 204 (60 mol% V_2O_5 - 20 mol% P_2O_5 - 20 mol% TeO_2) at different temperatures are shown in Fig.(7.22).

The resistivities of the samples are measured at different times in order to find the kind of conduction. Plots of resistivity vs. time for these glasses are shown in Fig.(7.23) and demonstrate that the resistivity of these glasses is independent of time, which is a characteristic of electronic conduction.

D.C. conductivities for V_2O_5 - P_2O_5 - TeO_2 glasses were

measured at different temperatures and are listed in Table(7.7). Fig.(7.24) shows the variation of log σ vs. $\frac{1}{T}$ for these glasses which shows that the conductivity increases with temperature over the temperature range from 293 to 473 K, and a plot of log σ vs. $\frac{1}{T}$ gives a straight line. This is evidence that in this range of temperature, the activation energy which is determined from the slope of these lines do not change with temperature. Fig.(7.25) shows a plot of log σ vs. $\frac{1}{T}$ for some of these glasses as well as glass No.103(60 mol% V_2O_5 - 40 mol% P_2O_5) for comparison. We found that the conductivity of these glasses increases with increasing TeO_2 content over our range of temperature. The dependence of the conductivity on TeO_2 content is shown in Fig.(7.26).

The activation energy was measured from the slope of the log σ vs. $\frac{1}{T}$ curve Fig.(7.24), and the values are listed in Table(7.8). The activation energy in the present results was found to decrease slightly with increasing TeO_2 concentration. Dependence of the activation energy on the TeO_2 concentration is shown in Fig.(7.27).

The transition metal ion spacing (T.M.I.) and concentration were measured for these glasses and are listed in Table(7.8). Variation of T.M.I. concentration and T.M.I. spacing with TeO_2 concentration are shown in Fig.(7.28) and (7.29) respectively. These figures show that with increasing TeO_2 concentration, the T.M.I. concentration N decreases and the T.M.I. spacing increases, which is possibly due to the different size of the structural units of the PO_4 tetrahedra and TeO_6 octahedra.

The mobility(μ)of the carriers for glasses containing TeO_2 was measured at different temperatures and the values are listed in Table(7.9). Fig.(7.30) shows the variation of a log μ with $\frac{1}{T}$ and clearly shows the exponential dependence on the temperature. The present results show that the mobility of the carriers for glass containing TeO_2 increases with increasing TeO_2 content. A plot of log μ vs. TeO_2 concentration is shown in Fig.(7.31).

As we mentioned in the last section, in vanadate glass at high temperature the thermally activated hopping is dominant, therefore by using Eq.(7-10) a plot of log μT vs. $\frac{1}{T}$ should give a straight line. Values of μT at different temperature for these glasses are given in Table(7.10) and are plotted vs. $\frac{1}{T}$ in Fig. (7.32). From this figure one can see that log μT is an exponential function of temperautre.

7-6 Conduction Mechanism and Discussion of the D.C.Conductivity Results

The general condition for semiconducting behaviour in transition metal-oxide glasses is that the transition metal ion should exist in more than one valence state so that conduction can take place by the transfer of electrons from low to high valence states.

$$V^{4+} \text{——} O \text{——} V^{5+} \text{——} O \text{——} V^{4+}$$

All interpretations of the electrical conduction process in vanadate glasses involve the transfer of localized electrons between the constituent vanadium ions.

In these models V^{4+} is considered to consist of a V^{5+} core plus an excess electron that is easily transfered to any essentially equivalent V^{4+} ion in the material with or without the necessity of phonon assistance. In other words, conduction takes place by an electron hopping directly between occupied (V^{4+}) and unoccupied (V^{5+}) sites. Lower valency states of vanadium (V^{3+}, V^{2+}) may also exist but we found from E.S.R. results that their contribution is not significant (chapter V).

It has been reported by Janakirama-Rao[94] that two possible mechanisms of conduction may be considered in transition metal oxide glasses in general, and vanadate glasses in particular. (I) Conduction by electron released by partial dissociation of the oxygen anion according to $O^{2-} \longrightarrow O^{-} + e^{-}$ and (II) Conduction by electron exchange between vanadium cations of different valence occupying equivalent position in adjacent VO_6 octahedra. The first mechanism becomes significant at high temperature because O^{2-} dissociation of the first electron requires high energy.

Vanadate glasses belong to a class of materials known as narrow band semiconductors. The 3d conduction band in these materials is quite narrow and this causes charge carriers to have

very high effective mass. In this case charge carriers can be treated as localized charges which jump from site to site.

Janakirama-Rao[94] interpreted the conduction mechanism in vanadate glases as follows. In crystalline V_2O_5, VO_6 octahedra form a three-dimensional structure of long-range order. Infra-red date show that in the glassy state the co-ordination of cations remains constant, (since the infra-red spectra of a given compound are similar,. See chapter VI). Therefore the continuous sheets, ribbons or chains of VO_6 octahedra provide the conduction path for the electron. As the V_2O_5 content decreases in the glass the VO_6 groups change progressively from sheet structure to ribbon structure and then to chain structure, depending on the number of oxygens shared by the VO_6 octahedra. Conductivity decreases as the number of VO_6 octahedra decreases.

Experiment shows that a glass containing 95 mol% V_2O_5 is almost as conductive as crystalline V_2O_5 and a glass with 5 mol% V_2O_5 has very low conductivity, because the VO_6 octahedra are isolated and as a result can not provide a continuous path for electrons.

Experimental work[94] on a series of vanadate glasses containing GeO_2 supports this mechanism of conduction mentioned above. It was found that the conductivity of these glasses decreases gradually when the V_2O_5 content decreases to approximately 10 mol% and below this concentration of V_2O_5 the

conductivity of these glasses sharply decreases and their conductivity is less than $10^{-10}\,\Omega^{-1}cm^{-1}$ even at 200°C. The abrupt decrease of electronic conductivity can be due to the isolation of VO_6 octahedra (which were inferred from the infra-red spectrum) or chains of these octahedra.

Mott[100] has suggested the following formula for the conductivity of vanadate glasses

$$\sigma = \nu_{ph} \frac{Ne^2R^2C(1-C)}{kT} \exp(-2\alpha R) \exp(\frac{-W}{kT}) \qquad (7\text{-}11)$$

where R is the site spacing, α is the tunnelling probability, N is the number of sites, C is the fraction of sites occupied by electrons, ν_{ph} is the phonon frequency and W is the activation energy.

Since there is a strong interaction between electron and lattice the activation energy W is the result of polaron formation with binding energy W_p (See chapter III) and at energy difference W_D which might exist between the initial and final sites is due to variation in local arrangement of ions. According to Austin and Mott[66]

$$W = W_H + \tfrac{1}{2}W_D \qquad \text{for } T > 1/2\theta_D$$
$$W_H = \tfrac{1}{2}W_P \qquad (7\text{-}12)$$

and
$$W = W_D \qquad \text{for } T < 1/4\theta_D$$

where θ_D defined by $\hbar\omega = k\theta_D$ is a temperature characteristic of

the average optical phonon frequency (or Debye temperature).

According to equation (7-12) a departure from linearity of the $\log \sigma$ vs. $\frac{1}{T}$ takes place at temperature below $1/2\,\theta_D$ and below this temperature disorder energy is considered to indicate the low temperature activation energy. The disorder energy is related to a phonon frequency by the following expression

$$W_D = K\theta_D = \hbar\omega \qquad (7\text{-}13)$$

In vanadate glasses the Debye temperature θ_D was found to be of the order of $\sim 600K$[101] ($\frac{1}{2}\,\theta_D = 300K$) and above this temperature the activation energy is temperature independent and $\log \sigma$ vs. $\frac{1}{T}$ yields a straight line Fig.(7.7).

In the polaron model the activation energy is reported to be $W = W_H - J$ where J is a polaron band width related to the electron wave function overlap on adjacent sites. Holstein[77] derived an expression for the mobility in the case of non-adiabatic hopping as following

$$\mu = 3/2\ \frac{ea^2J^2}{kT}\left(\frac{\pi}{kTW_H}\right)^{\frac{1}{2}}\ \exp\left(\frac{-W_H}{kT}\right) \qquad (7\text{-}14)$$

and in the case of adiabatic hopping the mobility was suggested by Emin and Holstein[75] to be

$$\mu = 4/3\frac{ea^2\omega_o}{kT}\ \exp\left[\frac{-(W_H-J)}{kT}\right] \qquad (7\text{-}15)$$

Emin and Holstein also suggested the following condition for hopping in the adiabatic region

$$J > \left(\frac{2kTW_H}{\pi}\right)^{1/4} \left(\frac{\hbar\omega_o}{\pi}\right)^{1/2} \qquad (7\text{-}16)$$

and the condition for the small polaron to exist is given as

$$J \leqslant \frac{1}{3} W_H \qquad (7\text{-}18)$$

An estimated value for polaron band width is suggested by Mott and Davis[48] as

$$J \simeq e^3 \left[\frac{N(E_F)}{\varepsilon_p^3}\right]^{\frac{1}{2}} \qquad (7\text{-}18)$$

where $N(E_F)$ is the density of states near the Fermi level which is approximately of the order of $10^{21} cm^{-3} eV$, ε_p is the polaron dielectric constant. Taking $\varepsilon_p \simeq 5$, a value of 0.09 is obtained for J. Sayer and Mansingh assumed that the variation in activation energy is due to the variation in J and they found that the value of J to be of the order of 0.15 eV for vanadate glasses.

Disorder energy was discussed by Greaves[124] and he suggested that at high temperature the d.c. conductivity can be given by

$$\sigma T^{\frac{1}{2}} = A \exp\left(\frac{-W}{kT}\right) \qquad (7\text{-}19)$$

where W is the activation energy at high temperature given by

$$W = \left(\frac{W_D + 2W_p}{8W_p}\right)^2 \qquad (7\text{-}20)$$

in which W_D is the disorder energy and W_P is the polaron binding energy. Therefore the slope of the log $T^{\frac{1}{2}}$ vs. $\frac{1}{T}$ line can yield the disorder energy W_D if W_P is known. The polaron binding energy (W_P) can be determined from the formula suggested by Mott[100]

$$W_P = \frac{e^2}{2\varepsilon_p r_p} \qquad (7\text{-}21)$$

where ε_p is the effective dielectric constant given by

$$\frac{1}{\varepsilon_p} = \frac{1}{\varepsilon_\infty} - \frac{1}{\varepsilon_o}$$

where ε_o and ε_∞ are the static and high frequency dielectric constant. r_p in Eq.(7-21) is the polaron radius and can be determined from the following expression[74]

$$r_p = \tfrac{1}{2}\left(\frac{\pi}{6N}\right)^{1/3} \qquad (7\text{-}22)$$

where N is the number of sites per unit volume. Using a formula suggested by Greaves[124] for conductivity at high temperature, the plot of log $\sigma T^{\frac{1}{2}}$ vs. $\frac{1}{T}$ from the present results for glasses containing 50, 70 and 90 mol% V_2O_5 are shown in Fig.(7.33). In

this figure a change in the slope was found at about 400 K for vanadium phosphate glasses and is less than the value of 415 K obtained by Greaves[124].

At high temperature, the phonon frequency can be determined from Eq.(7-11) by ignoring the tunnelling term exp ($-\alpha R$)(because at high temperature a thermally activated process is dominant) Calculated values of the phonon frequency for V_2O_5 - P_2O_5 and V_2O_5 - P_2O_5 - TeO_2 glasses are given in Tables(7.6) and (7.8) respectively.

The interaction between electron and polaron which causes localization is defined by a coupling constant γ which can be determined from the formula

$$\gamma = \frac{W_p}{\hbar\omega_o} \qquad (7\text{-}23)$$

calculated values of γ for V_2O_5 - P_2O_5 and V_2O_5 - P_2O_5 - TeO_2 are also given in Tables(7.6) and (7.8). From these tables one can see that with increasing T.M.I. concentration, the polaron binding energy and also the coupling constant decreases, resulting in a decrease in activation energy and an increase in the conductivity of the glass.

It is difficult to interpret the variation of the conductivity with glass composition in vanadate glass since the activation energy (W), reduced valence ratio (C), T.M.I.

concentration N, and jump parameter (α) all vary with the percentage of the transition metal oxide in glass. According to Eq.(7.11) we expect the conductivity to be zero when C is 0 and to go through a maximum at C = ½. But experimental evidence shows that a maximum in the conductivity occurs at a ratio of V^{4+}/V_{tot} having a value of much less than ½.

The maximum conductivity for these glasses was found for a reduced T.M.I. ratio between 0.1 and 0.2 by Linsley et al.[92]. Generally the conductivity for these glasses increases with increasing T.M.I. concentration. Increase of activation energy and thus a decrease in the conductivity with reduced valence ratio could be due to a correlation effect of V^{4+} and V^{2+} ions. In other words, V^{4+} and V^{2+} ions can be paired antiferomagnetically in vanadate glasses and this would increase the energy which is required for electron hopping to take place between the pairs.

Another possible reason for the variation of conductivity with composition could be the strong influence of short range order. The growth of crystallites and devitrification in the glass matrix with composition, can lead to long range order resulting in an increase in the conductivity. Fig.(7.7) shows that the conductivity of glass at any temperature is smaller in glass with higher activation energy (lower V_2O_5 content) which is consistent with Eq.(7-11). This leads to the fact that the thermal activation energy for conduction dominates the factor

which determines the conductivity, and the tunnelling factor $\exp(-2\alpha a)$ dose not vary rapidly with site spacing 'a' and glass composition.

The E.S.R. data in the present work shows that the V^{4+}/V_{tot} ratio of $V_2O_5 - P_2O_5$ glasses decreases with increasing V_2O_5 content Fig.(5.18). On the other hand the electrical conductivity of these glasses increases with increasing V_2O_5 content Fig.(7.9). This could be interpreted as follows.

In a glass with lower V_2O_5 concentration, the VO_5 sheets degenerate into ribbons and chains. With reducing V_2O_5 content the number of V-O-V conduction paths in the glass will decrease and therefore conductivity decreases. Since the number of conduction paths is proportional to the V_2O_5 content, conductivity should increase with increasing V_2O_5 content (V^{5+} concentration). From Fig.(7.11) the activation energy at high temperature increases with site spacing. Killias[82] suggested the following expression for the variation of activation energy due to site spacing

$$\Delta W = \Delta W a_o + B\Delta a \qquad (7\text{-}24)$$

where Wa_o is the activation energy corresponding to the average site spacing a_o, B is constant and Δa is the random variation in the site spacing. In this model Killias assumed nearest neighbour hopping with energy W_H and fluctuations in W_H due to

random variation in'a' which generates random potentials of magnitude $\alpha\Delta a$. This model was discussed by Austin and Garbett[134] and they suggested that if the random potentials are large the Killias model cannot be applied.

The present work shows that the electrical conductivity and the activation energy, as well as other physical properties for vanadate glasses appear to be affected slightly by replacement of P_2O_5 with TeO_2. Figs.(7.7) and (7.24) show the dependence of $\log\sigma$ on $\frac{1}{T}$ for glasses of the V_2O_5 - P_2O_5 and V_2O_5 - P_2O_5 - TeO_2 systems. This dependence is linear in both systems, the electrical conductivity increases with temperature and the slope of the straight line (the activation energy) decreases with increasing V_2O_5 content. The dependence of $\log\sigma$ on $\frac{1}{T}$ is similar for the two systems, but the curve of the system containing TeO_2 is displaced. With the same amount of V_2O_5, the electrical conductivity of glasses containing TeO_2 is higher than the electrical conductivity of a binary V_2O_5 - P_2O_5 glass system. Fig.(7.25).

The similarity of these curves suggests that the increase in conductivity (decrease in activation energy) is due to increase of the ratio of vanadium to phosphorus in the glass. Dependence of the activation energy on the V_2O_5/P_2O_5 ratio for glasses containing TeO_2 is shown in Fig.(7.34). This figure shows that the activation energy decreases from 0.44 eV for glass containing 60 mol% V_2O_5 and 40 mol% P_2O_5 to 0.38 eV for a glass containing 60 mol% V_2O_5 - 10 mol% P_2O_5 and 30 mol% TeO_2.

Chapter VIII

High Electric Field Effect and Switching Phenomena in $V_2O_5 - P_2O_5$ and $V_2O_5 - P_2O_5 - TeO_2$ Glasses

8-1 Introduction

The semiconductor glasses often show marked deviation from normal semiconductor behaviour, e.g. non-Ohmic conduction under the influence of temperature and or in a strong electric field. The application of a high electric field to a free carrier system may influence both the mobility of the carriers and the number of available carriers. The mobility of the carrier may be influenced by the change in the effective energy distribution of the carriers, which would be described in terms of a rise of carrier temperature T_c above the lattice temperature. There are various conduction mechanisms at high electric field.

In the model of Schottky the emission of electrons occurs from the metal contact at negative potential into the high electric field obtainable across thin insultating films. In this model when electron is at a distance (r) from the surface of a metal a positive charge will develop inside the metal and is known as image charge, the effect of image charge is that it changes the shape of the potential barrier. The effect of high electric field not only lowers the height of the potential barrier, but also increases the emission current.

At sufficiently high electric field the coulombic barrier becomes thin and conduction at the Fermi level occurs due to tunnelling through the barrier rather than over it.

In the model proposed by Poole[135] and Frenkel[136], if a crystalline or amorphous semiconductor contains donors or traps in which the binding energy of an electron is E_b, the effect of the high electric field E is to lower the ionization energy of the centre by $\Delta\phi$ given by

$$\Delta\phi = \beta E^{\frac{1}{2}}/kT \qquad (8-1)$$

where β is the field-lowering coefficient given by

$$\beta = \left(\frac{e^3}{\pi\epsilon\epsilon_o}\right)^{\frac{1}{2}} \qquad (8-2)$$

in which the ϵ is relative dielectric constant and ϵ_o is the permittivity of the free space.

The physical basis of this effect is the lowering of Coulombic potential barrier when it interacts with the electric field, and the thermal excitation of electrons from traps into the conduction band.

In the derivation of the formula (8-1) it is assumed that there is no tunnelling through the barrier at high temperature. As the temperature is lowered tunnelling through the barriers

rather than excitation over the barrier can take place. The reduction in height of the coulombic barrier $\Delta\phi$ due to the Poole - Frenkel effect in a uniform electric field is found to be twice that due to the Schottky effect at a neutral barrier[137].

The effect of high electric field on the mobility of the carriers was discussed by Mott[48]. He assumed that if the hopping mobility of the carrier is of the form

$$\mu = \frac{ea^2\nu_{ph}}{kT} \exp(-2\alpha a) \exp\left(\frac{-W}{kT}\right) \qquad (8\text{-}3)$$

in which hopping is to nearest neighbour sites, an electric field should reduce the activation energy (W) to W-eaE. It should also increase the tunnelling factor $e^{-2\alpha a}$, but calculations of the effect have not been made.

The effect of high electric field in polaronic conduction in low mobility solids, such as amorphous semiconductors in general and glassy systems in particular is of considerable interest. A small polaron may be considered to form on a neutral centre. The effect of a high electric field may be considered in two terms. Firstly the field may enhance the supply of electrons from donors to the medium, and their further transport between donor centres may then proceed the polaronic transport. Secondly, the field may affect the hopping probability of the polarons themselves, by causing a lowering of the potential barrier of the short range field between nearest neighbours.

Application of sufficiently high electric field to a disordered material sooner or later leads to deviations from linearity in the resultant current. Such deviations are indicative of non-Ohmic conductivity.

It was found that in contrast to many other disordered systems, the transition metal oxide glasses show Ohmic behaviour at fields up to about $10^5 Vcm^{-1}$ and at higher fields the conductivity varies as[125]

$$\sigma(E) = \sigma(0) \frac{\text{Sinh } \frac{eaE}{2kT}}{\frac{eaE}{2kT}} \qquad (8-4)$$

where $\sigma(0)$ is the Ohmic conductivity and 'a' is the site separation and the sinh term implies a departure from the Ohmic behaviour at a field $E = \frac{kT}{ea}$. The estimated value of 'a' can be determined by measuring the field at a point in which the non-linear behaviour of I - V characteristic occurs.

In this chapter the attempt is to examine glass samples of composition $V_2O_5 - P_2O_5$ as well as $V_2O_5 - P_2O_5 - TeO_2$ in order to study the effect of high electric field on these glasses. This will be followed in the next section with an investigation of the possible switching effect in binary and ternary glass systems.

8-2 Sample Preparation and Measuring Techniques

Thin blown films of the glasses listed in Table(5.1) were

prepared using the method described in section (6-2-2). The thicknesses of the samples were measured using a Sigma Comparator. Silver paste was used as the electrode material and the samples, after painting on the electrodes, were annealed at 100°C for two hours.

Figs.(8.1) and (8.2) show the sample holder device, cooling and heating system, and Fig.(8.3) illustrates the circuit used to observe the I - V characteristic. The two high resistance (1MΩ each) were used as current limiters across the sample at high electric field. The measurements were carried out by using stabilized d.c. voltage supply model 241 as a power supply and a Keithley 610C electrometer for measuring the current. Experiments were carried out under a vacuum of 10^{-5} torr.

8-3 Experimental Results and Discussion

A typical voltage-current characteristic is shown in Fig.(8.4) for glass No.104 and in Fig.(8.5) for glass No.204 and similar curves were obtained for samples of other compositions listed in Table(5.1).

Under present work it was found that for vanadium phosphate glasses at fields below $4 \times 10^{5} Vcm^{-1}$ the conduction is Ohmic and plots of log V vs. log I gives straight lines. The departure from linearity and the appearance of non-Ohmic behaviour occurs at fields above $4 \times 10^{5} Vcm^{-1}$.

It was also found that with increasing temperature the linear region extends to higher values of field as has been observed generally for oxide glasses. A similar characteristic has been observed for glass containing TeO_2 but the departure from linearity in the I - V characteristic occurs at a field slightly less than $4 \times 10^5 Vcm^{-1}$.

In order to analyse the basis of this behaviour we first examined the effect of the sample thickness and electrode material on the conductivity of our samples and we found that the conductivity is independent of these factors which suggests that the space-charge-limited conduction and Schottky emission do not determine the conductivity and consequently the field dependence was property of the bulk material.

Secondly we determined the value of β in Eq.(8-2) from the slope of the log I vs. $V^{\frac{1}{2}}$ curves and compared the figure with the theoretical value of β calculated from Eq.(8-2).

Figs.(8.6) and (8.7) show the plot of Log I vs. $V^{\frac{1}{2}}$ for $V_2O_5 - P_2O_5$ and $V_2O_5 - P_2O_5 - TeO_2$ glasses respectively. These figures show that the dependence of log I on $V^{\frac{1}{2}}$ is linear at high fields and the value of β obtained from the slope of the linear part of these curves is about 1.37×10^{-4} $eV(cmV^{-1})^{\frac{1}{2}}$ sec^{-1} for $V_2O_5 - P_2O_5$ glasses. Theoretical values of β calculated from Eq.(8.2) are $\beta_{PF} = 1.02 \times 10^{-4}$ and $\beta_s = \frac{1}{2}\beta_{PF} = 0.51 \times 10^{-4}$ eV $(cm^{-1})^{\frac{1}{2}} sec^{-1}$. This calculation shows that the experimental value of β fits to the Poole - Frenkel formula much better than the Schottky effect.

The value of jump parameter (a) in Eq.(8-4) is calculated by measuring the field at the point at which departure from linearity in plots of log I vs. log V occurs and an average of 21 A^{o} was found for a which is nearly 5 times greater than the results of E.S.R. and chemical analysis (see chapter V). Austin and Sayer[125] reported the similar enhancement factor for V - V spacing for V_2O_5 - P_2O_5 glasses and they concluded that this factor is a characteristic of any individual glassy system depending on the structure of glass. However many authors[138] have suggested that a modification to the formula

$$\sigma = \sigma(0) \frac{\mathrm{Sinh}\frac{eaE}{2kT}}{\frac{eaE}{2kT}} \qquad (8\text{-}5)$$

is necessary in order to explain the experimental results for value of (a) and concluded that the sinh law is only applicable in a small range of electric field.

8-4 Switching Phenomena in Vanadate Glasses

8-4-1 Introduction

It was known for many years that when the interelectrode distances in samples of amorphous semiconductors (glass) are reduced to sufficiently small values (a few μm), the current-voltage characteristics are no longer governed by Ohm's law after a certain threshold voltage has been reached. At this point breakdown takes place and the conductance of the sample

appears to increase abruptly. This phenomenon is described as a switching effect, which has many potentially useful applications in electronics.

Two kinds of switching have been recognised, threshold[139,140,141] and memory[142] switching. In both types of device the switching process occurs when an increasing applied voltage exceeds the threshold voltage V_{th}, or after a delay time t_D when a voltage pulse V_p larger than V_{th} is applied.

The switching process takes place very rapidly within a switching time $t_s \leq 10^{-10}$ sec. However there is a delay time t_D typically about 10μsec at the threshold voltage and the delay time decreases exponentially with over voltage[143]. It has been reported[144] that if the applied voltage is about 50% above threshold voltage, the delay time will be reduced to 10^{-9} sec. The voltage dependence is also composition-dependent. Sugi et al[145] reported that the decrease in delay time is proportional to the inverse square of the over voltage.

In the case of threshold switch, during the switching process the atomic arrangement and structure of the sample do not change permanently, and on the contrary, in the case of memory switching the switching process is associated with a structural change.

When the low voltages are applied to a device with 1 - 50μm

thickness sandwiched between two electrodes, the conduction is Ohmic. Above fields of about 10^4 to $10^5 Vcm^{-1}$ a non-Ohmic characteristic becomes evident and the current rises exponentially with applied voltage[140]. Switching occurs at a critical field generally of the order of $\sim 10^5 Vcm^{-1}$ from the high resistance (off state) to low resistance (on state). As long as a holding voltage V_h is maintained across the device the material remains in the conducting state. In the case of threshold switching if the holding voltage is removed the device switches back to the resistive state (off state) in about 5×10^{-7} sec.

The switching process is entirely reversible and independent of polarity. The threshold voltage decreases with increasing temperature and it has been reported[147] that the threshold voltages appear to increase exponentially with glass transition temperature[148] for a large number of disordered material.

A typical memory switch behaves initially like a threshold switch. At low fields the conductivity is low and obeys Ohm's law until the applied voltage reaches the threshold voltage. Above this voltage after a delay time, there is rapid switching from high resistance (off state) to low resistance (on state). After switching if the current is quickly reduced below a critical value, the device will switch back to the high resistance state, exactly like a threshold switch. But if the device is held in the conductive state for about 10^{-3} sec, it will remain highly conductive, even after the external field is

removed. This time is called the lock-on time (t_L). Memory switched material can be returned to the original high resistance (off state) by applying a short intense current pulse of either polarity.

8-4-2 Sample Preparation and Experimental Procedures

Thin blow films of glass samples of some compositions listed in Table(5.1) were prepared using the method described in section (6-2-2).

Glass No.104 (65 mol% V_2O_5 - 35 mol% P_2O_5) and glass No.205 (60 mol% V_2O_5 - 15 mol% P_2O_5 - 25 mol% TeO_2) were prepared and two terminal devices were made by using silver paste as the electrode material. The cross sectional area of the silver paint was 0.2 - 0.3cm^2.

The sample holder and the cooling and heating systems are shown in Fig.(8.1) and (8.2), Fig.(8.3) illustrates the circuit used to observe the I - V characteristics. The two 1M Ω variable resistors were used to limit the current across the device in the on state. Experiments were carried out in both air and under a vacuum of 10^{-5} torr.

8-4-3 Experimental Results and Discussion

A typical I - V characteristic of memory switching for glass No.104 is shown in Fig.(8.8) and similar characteristics were

observed for glasses with various compositions as listed in Table(5.1). As the applied voltage increases in the high resistance state, the conduction is Ohmic at low field and the current becomes increasingly non-Ohmic at higher field as we saw earlier in this chapter (high electric field effect).

When the applied voltage exceeds a threshold voltage V_{th}, the device switches from high resistance to an ordered state. Thus a rapid current increase and a large decrease in voltage drop across the sample occurs. As the applied voltage increases further the current continues to increase and in the case of our samples the log V vs. log I curve after switching was linear as is shown in Fig.(8.8). The device remains in its conductive state even when the current decreases to zero which is characteristic of a memory switch. The switched device can be returned to its high resistance state by applying a high d.c. pulse (0.2 - 1mA).

It was found that the threshold voltage is not reproducible and depends on the external switching condition as was reported by Drake et al[149]. For all devices the first switching voltage was much higher than for the subsequent switching. All glasses with different thicknesses show a similar switching effect and it seems that the on state of devices is nearly independent of the sample thickness. Fig(8.8). In any event the current in the on state is largely determined by the high volume series resistors.

We found that the threshold voltage decreases with

increasing temperature. Fig.(8.8), (8.9) and (8.10) show memory switch for glass No.104 at three different temperatures. Variation of threshold voltage with temperature is shown in Fig.(8.11).

It is known that during a memory switching process, a crystalline channel is formed between the electrode at the switching voltage leading to the low resistance state. The high current re-setting pulse succeeds in melting the crystalline material and cools it rapidly to a glassy state. Decreasing the threshold voltage with increasing temperature supports the idea that a thermally produced crystalline filament is responsible for switching. As the temperature is increased molecular re-arrangement and relaxation becomes easier in the glass, which causes further formation of the crystalline filament.

To observe the existence of a conduction channel at the on state, contact points between electrodes and samples were removed to a place just close to the switched area and it was found that this part of the sample is in high resistance (off state rather than being in the on state).

It has been suggested by Saji and Kao[150] that the filament formed by the application of a threshold voltage in the case of threshold switching may consist of a mixture of amorphous and crystalline regions in the switching area, but the filament responsible for memory switching may consist of crystalline

region only as has been observed by Moridi and Hogarth[151]. Cohen et al[152] suggested that the memory action occurs by switching initially to a filamentary threshold on state and maintained current causes the slow crystallization to take place and a memory state to be formed.

Chunghi et al[153] reported that the I - V characteristics of vanadate glasses in the switching process can be interpreted by thermal effects. As the voltage in the high resistance state is increased, the current becomes increasingly non-Ohmic due to self-heating. The conductivity increases and an internal temperature rise yields a collapse of the current into a filament at a critical temperature at which devitrification takes place. Thus the irreversible switching action occurs once on the surface of the glasses,if the filament is devitrified completely during the delay and switching time, and the structure is not reversible.

The observation of a devitrified filament formed after switching reveals that the switching action is associated with a phase transition from a disordered glassy state to an ordered devitrified state due to self-heating effects.

Drake and Regan[154] worked on switching phenomena of V_2O_5 - P_2O_5 - CuO glasses and reported that these glasses exhibit different switching properties depending upon the glass composition and switching arrangements. They found that glasses

with high vanadium content exhibit two types of switching, memory and threshold, dependent upon the switching circuit and glasses made with a lower vanadium content do not show threshold switching properties but show a memory effect.

Chapter IX

Summary and Conclusion

In the present work it was found that the technical properties of binary V_2O_5 - P_2O_5 and ternary V_2O_5 - P_2O_5 - TeO_2 glasses are very similar. They could be melted easily with softening point in the range from 300 - 600°C and in the boiling point range from 800 - 1200°C depending on composition. With increasing V_2O_5 content the softening and boiling point were found to increase. The glass had low values of viscosity (compared with chalcogenide glasses) and a strong tendency to crystallization. The chemical durability of V_2O_5 - P_2O_5 glasses deteriorates with increasing V_2O_5 content and glasses with a high percentage of V_2O_5 (80 mol% V_2O_5) are soluble in cold water.

In vanadate glasses V_2O_5 decomposes irreversibly in the melt, and the loss of oxygen increases with the amount of P_2O_5 in the composition. This results in a non-stoichiometric oxide where part of the V^{5+} ions are reduced to a lower oxidation state, mostly V^{4+} ions, which have a 3d' configuration. In V_2O_5 - P_2O_5 glasses the predominant valency states of vanadium are V^{4+} and V^{5+} and the amount of V^{4+} decreases with increasing V_2O_5 content, Table (5.4). Vanadium ions in different oxidation states yield semiconducting properties due to a hopping process of the unpaired 3d electrons from V^{4+} to V^{5+} ions[161-162].

The densities of both binary and ternary systems were found

to increase with decreasing P_2O_5 content, Fig.(5.4) and Fig.(5.5) and also with increasing of the annealing temperature, the density increases which means that the average interatomic distance decreases with annealing and structure becomes more compact, Fig.(5.6) and (5.7).

The values of T.M.I. concentration (N) and T.M.I. spacing (R) were found to be composition dependent and in both systems an increase in theP_2O_5 content increases the average T.M.I. spacing which is very important in relation to electrical and optical properties of these glasses. One of the important factors in the electrical and optical properties of these glasses is the ratio of low valence state to total vanadium ions ($C = \frac{V^{4+}}{V^{+}_{tot}}$). This ratio was determined by chemical analysis and E.S.R. experiments (Chapter V) and are listed in Table (5.3). It was found that this ratio depends on composition and increases with increasing P_2O_5 content. The E.S.R. results show that in the binary V_2O_5 - P_2O_5 glass system, C decreases with increasing V_2O_5 content Fig.(5.18), while the electrical conductivity increases with increasing V_2O_5 content. In fact as the V_2O_5 content decreases the VO_5 sheets degenerate into ribbons and chains and thus the number of V-O-V conduction paths in glass decreases. Since the number of conduction paths is proportional to the V_2O_5 content the conductivity of these glasses increases with increasing V_2O_5 content.

It has been reported that[112-160] so long as the

co-ordination number in a system in both vitreous state and in their devitrified crystalline state remains unchanged, then their infra-red spectra will give rise to similar absorption bands. The infra-red experiments show that there are similarities between spectra of crystalline V_2O_5 and glasses based on V_2O_5 Figs.(6.1) - (6.3), which leads to the fact that V^{5+} ions in these glasses exist in six-fold co-ordination as well as in crystalline V_2O_5 as is reported by Janakirama Rao[94]. From the infra-red experiments it is also found that the V-O stretching frequency occurs at a wave number of $\sim 1010 cm^{-1}$.

It appears that there is an exponential absorption edge in the visible spectral range $1.9 < \hbar\omega < 2.6$ eV Figs.(6.6) and (6.7) which could be explained as due to the exponential distribution of localized states in the forbidden gap. The carrier concentration in the localized levels (band tails) depends upon the total number of available sites which in the case of vanadium phosphate glasses is difference between V^{5+} and V^{4+} ions. It is also found that the fundamental absorption edge of these glasses near 2.5 eV fits the conditions for direct forbidden transition suggested by Anderson[20] as

$$\alpha(\omega) = \frac{(\hbar\omega - E_g)^{3/2}}{\hbar\omega}$$

The electrical conductivity of V_2O_5 is known to be due to the hopping of small polorons[101]. The hopping probability is proportional to $\exp(\frac{-W_H}{kT})$ where W_H is the activation energy for

the hopping process. In the case of amorphous V_2O_5, this activation energy becomes

$$W = W_H + \tfrac{1}{2}W_D$$

where W_D represents the mean energy difference between the d' energy levels of neighbouring ions and is due to local fluctuations of the crystal field. This fluctuation is larger in the amorphous oxide than in the crystalline one, leading to a localization of the polaron (Anderson localization[12]).

It has been generally recognized that there are two parallel conduction mechanisms in transition metal oxide glasses such as vanadate glasses, namely (I) tunnelling, which is charge transfer between equivalent sites without alteration in the phonon occupation numbers and (II) hopping, in which the charge site transfer takes place through a simultaneous exchange of energy with the lattice. The first mechanism is dominant at low temperatures and the second mechanism is the characteristic of conduction at high temperatures, and the electrical conductivity of these glasses is an exponential function of inverse temperature. The polaron model predicts that a departure from a linear log σ vs $\frac{1}{T}$ plot should occur below a temperature of $\frac{1}{2}\theta_D$ where θ_D is the Debye temperature given by $\hbar\omega = k\theta_D$ and ω is the mean frequency of the optical phonon. The value of θ_D for vanadate glasses was known to be of the order of $\sim 600^{o}K$[101].

From the value of the σ conductivity at room temperature

(10^{-6} - 10^{-4} Ω^{-1} cm^{-1}) one can classify these glasses as semiconductors and the lack of time dependence of resistivity for these glasses is evidence for electronic conduction. The activation energy for electrical conduction above room temperature varies from ∿0.31 to 0.48 eV for glasses containing 90 to 50 mol% V_2O_5.

It is found that the value of activation energy (W) for conduction is less than half the optical gap (E_g) which can be taken as evidence that the hopping process does not take place only across the mobility gap, but is possibly from one or more trapping levels to the conduction band.

The concentration of charge carriers in these glasses is approximately equal to the concentration of V^{4+} ions which is found to be of the order of 1.2×10^{21} to 4.8×10^{21} cm^{-3}. From the conductivity and concentration of charge carriers mobility of the carrier is estimated (Table (7.2)-(7.7)) which at high temperature increases exponentially with temperature.

Nester and Kingery[96] reported that photoconductivity is not observed in vanadate glasses which suggests that the transition probability for an electron jump is not altered when the sample is illuminated, this could be explained as follows. The absorption of a photon of energy $h\nu$ by an electron causes it to be elevated to a higher energy states. This electron can remain

in this excited state for a finite time, after which it returns to the original state. But if the lifetime of the optically-excited state is shorter than the period of the lattice vibration (due to low mobility), then a charge transfer will not take place. In other words, the electron becomes trapped at the same site from which it was optically excited to the higher energy state.

The high electric field experiments show that at fields below $\sim 4 \times 10^{5} Vcm^{-1}$ the conductivity is Ohmic Fig.(8.4) and (8.5) but above this field behaviour becomes non-Ohmic and this was found to be due to a lowering of the potential barrier at high electric field. The Ohmic region of the I - V characteristic tends to be extended to higher fields as the temperature rises, Fig.(8.4) and (8.5). The value of the jump parameter (a) in equation (8-4) was found for $V_2O_5 - P_2O_5$ glasses to be of the order of $21A^{o}$ which is five times higher than actual V - V ion spacing determined from chemical analysis and E.S.R. data.

These glasses show memory switching phenomena independent of electrode material Fig.(8.8) and (8.12) and threshold voltage decreases with increasing temperature Fig.(8.9) and (8.10) and depends on the thickness of the samples. Thicker samples of the same composition switch at higher voltages. The threshold voltage is not reproducible and depends on the external condition as has been previously reported by Drake[149]. It is

believed that during the switching action a devitrified filament (conducting channel) forms after the first switching and this reveals that the switching action is associated with a phase transition from a disordered glassy state to an ordered devitrified state due to self heating effect and the conducting zone consists of VO_2 crystals which possess a more metal-like conductivity.

Our experiments show that replacing of P_2O_5 with TeO_2 increases the conductivity of these glasses by a small amount which could be due to change in the ratio of reduced valence state to total vanadium ions ($C = \frac{V^{4+}}{V_{tot}}$).

In general there are no abrupt changes in electrical and optical properties of these glasses when P_2O_5 is replaced by TeO_2. This behaviour could be interpreted by the lack of sensitivity of amorphous semiconductors to impurity in contrast to crystalline semiconductors. In crystalline materials impurities are foreign particles in the lattice, excess of one constituent leading to departure from stoichiometry in compounds and possible other defects. Such impurities are important in crystalline materials because they produce additional levels in the energy spectra of the valence electrons. These levels raise the conductivity sharply and a discontinuity in log σ vs. $\frac{1}{T}$ may take place, and indicate the transition to conduction by means of new carriers with lower activation energy. These phenomena are not generally applicable to glassy semiconductors since their structure is defined to be lacking in long-range order.

However, more study is required to investigate the structural change of these glasses when P_2O_5 is replaced by other oxides such as TeO_2.

REFERENCES

1 G.W.Morey Preparation of Glass.
Reinhold Publication Corp. New York (1954)

2 Glass Ind. 26 (1945) pp.417

3 M.Fanderlik Sklar a Keramik 4 (1954) pp.14

4 C.Clairmont The Glass Vessels. The Excavation at Dura Europos Final Report (1963) pp.57

5 F.J.Maloney Glass in Modern World (1967)

6 R.Persson Flat Glass Technology
Butterworth London - New York (1969)

7 M.Faraday Trans. Roy. Soc. London 1 (1930)

8 E.C.Marboe The Constitution of Glass II
Inter. Science Publication (1962)

9 The New Britannica Encyclopedia 15th ed. 8 pp.181

10 W.A.Weyl The Constitution of Glass I pp.249

11 G.Tamman Der Glaszustand (Leonard Voss Leipzig) (1973)

12 P.W.Anderson Physic. Rev. 109 (1958) pp.1492

13 A.Miller & E.Abrahams Phys. Rev. 120 (1960) pp.745

14 R.Kuba J. Phys. Soc. Japan 12 (1961) pp.570

15 G.H.Wannier Phys. Rev. 117 (1960) pp.423

16 T.N.Kennedy & J.D.Mackenzie Phys. & Chem. of Glasses 8 (1967) pp.169

17 M.Sayer & E.Prasad J. of Non-Cryst. Solids 33 (1979) pp.345

18 A.Mansingh & A Dhawan J. of Non-Cryst. Solids 33 (1979) pp.351

19 I.G.Austin & M.Sayer J. Phys. C. Solid State Phys. 7 (1974) pp.905

20 G.W.Anderson & W.D.Compton J. of Chem. Phys. 52 (1970) pp.6166

21 N.F.Mott Contemp. Phys. 10 (1969) pp.125

22 G.O.Jones Glass 2nd Ed. Chapman and Hall (1971) pp.70

23 J.H.Dickson Glass Scientific and Technical London New York (1951) pp.38

24 E.Preston J. Soc. Glass Tech. 15 (1940) pp.262

25 W.H.Zachariasen J. Amer. Chem. Soc. 54 (1928) pp.3841

26 A.G.Pincus Ceramic Age 39 (1948) pp.38

27 J. Amer. Chem. Soc. 49 (1927) pp.49

28 L.Pauling Nature of Chemical Band and Stucture of Molecules and Crystals (1948)

29 A.Smekal J. Soc. Glass Technology 35 (1951) pp.411

30 J.E.Stanworth J. Soc. Glass Tech. 30 (1946) pp.54

31 J.E.Stanworth J. Soc. Glass Tech. 32 (1948) pp.154

32 J.E.Stanworth J. Soc. Glass Tech. 32 (1948) pp.366

33 J.E.Stanworth Nature 169 pp.581

34 L.Pauling The Nature of the Chemical Band 2nd Ed. (1945) pp.450

35 K.H.Sun J. Amer. Ceram. Soc. 30 (1947) pp.277

36 K.H.Sun & M.K.Huggins J. Phys. Colloid Chem. 51 (1947) pp.438

37 J.T.Randall & H.P.Rooksby J. Soc. Glass Tech. 17 (1933) pp.287

38 H.Rawson & M.S.R.Heynes J. Soc. Glass Tech. 41 (1957) pp.347

39 N.F.Mott Conduction in Non-Crystalline Materials Phil. Mag. 19 (1969) pp.835

40 B.T.Kolomiets Phys. Status Solidi 7 (1974) pp.359

41 F.Seitz J. Phys. Chem. 57 (1953) pp.737

42 M.H.Cohen Lecture at the N.A.T.O. School on Amorphous Semiconductors Belgium (1969)

43 N.F.Mott & E.A.Davis Electronic Processes in Non-Cyrstalline Materials 2nd Ed. Oxford Univ. Press (1979)

44 N.F.Mott Conduction in Non Crystalline Materials J. Non-Cryst. Sol. 8-10 (1972) pp.1

45 P.W.Anderson Phys. Rev. 109 (1958) pp.1492

46 N.F.Mott Phil. Mag. 17 (1968) pp.1259

47 A.F.Joffe & A.R.Regel Prog.Semiconduction 4 (1960) pp.237

48 N.F.Mott & E.A.Davis Electronic Processes in Non-Crystalline Materials 1st Ed. Oxford Univ. Press (1971)

49 J.M.Benton & E.J.Ashly J. Phys. Rev. B2 (1970) pp.397

50 D.J.Weaire J. Non-Cryst. Solids 6 (1971) pp.181

51 M.H.Cohen, H.F.Fritzsch & S.R.Ovshinsky Phys. Rev. Lett 22 (1969) pp.1065

52 E.A.Davis & N.F.Mott Phil. Mag. 22 (1970) pp.903

53 N.F.Mott J. Non-Cryst. Solids 8-10 (1972) pp.1

54 J.M.Marshall & A.E.Owen Phil. Mag. 24 (1971) pp.1281

55 J.Schottmiller & M.D.Tabak J. Non-Cryst. Solids 4 (1979) pp.80

56 L.Vescan Phys. State Solid B 54 (1972) pp.735

57 N.Croitoru Phys. State Solid B 48 (1971) pp.429

58 A.Madan & W.E.Spear Private Communication (1973)

59 M.Pollak & T.H.Geballe Phys. Rev. 122 (1961) pp.1745

60 M.Pollak Phys. Rev. 133 (1964) pp.A-465

61 M.Pollak Phys. Rev. 138 (1965) pp.A-1822

62 M.Pollak Phil. Mag. 23 (1971) pp.519

63 G.I.Austin & N.F.Mott Advance Phys. 18 (1969) pp.81

64 H.Scher & M.Lax J. Non-Cryst. Solids 8-10 (1972) pp.497

65 H.Scher & M.Lax Phys. Rev. 7B (1973)

66 I.G.Austin & N.F.Mott Advance Phys 18 (1969) pp.41

67 M.Pollak Phil. Mag. 23 (1971) pp.519

68 A.Mansingh & R.P.Tandon J. Phys. C. Solid State Phys. 9 (1971) pp.1809

69 R.M.Hill Phil. Mag. 23 (1971) pp.59

70 H.Fritzsche Electronic and Structual Properties of Amorphous Semiconductors Ed.P.G.le Comber & J.Mort Academic Press London New York (1973)

71 T.Holstein Ann Phys. 8 (1959) pp.325

72 C.Friedman Phys. Rev. 135 (1964) pp.232

73 H.Frohlich Advance Phys. 3 (1954) pp.325

74 V.N.Bagamalov & E.K.Kudinov Sov. Phys. Solid State 9 (1968) pp.2502

75 T.Holstein Ann Phys. 8 (1959) pp.343

76 D.Emin & T.Holstein Ann Phys. 53 (1969) pp.439

77 T.Holstein & L.Friedman Ann Phys. 21 (1963) pp.494

78 N.F.Mott Adv. Phys. 16 (1967) pp.49

79 J.Tauc Optical Properties of Solids (North Holland Amsterdam) (1970) pp.123

80 N.F.Mott Phil. Mag. 22 (1970) pp.7

81 E.P.Denton, H.R.Rawson & J.E.Stanworth Nature 173 (1954) pp.1030

82 H.R.Killias Phys. Lett 20 (1966) pp.5

83 A.P.Schmid J. Appl. Phys. 40 (1969) pp.4128

84 A.P.Schmid J. Appl. Phys. 39 (1968) pp.3140

85 J.Schnakenberge Phys. Status Solidi 28 (1968) pp.623

86 D.C.Conlon & W.P.Dalbe J. Chem Phys. 35 (1961 pp.752

87 D.N.Sathyanarayana & C.C.Potel J. Inorg. Nucl. Chem. 30 (1968) pp.207

88 A.C.Chapman Spectra Chem. Acta. 20 (1964) pp.937

89 D.E.C.Corbridge & E.J.Lowe J. Chem Soc. 493 (1954)

90 F.R.Landsberger & D.J.Bray J. Chem. Phys. 53 (1970) pp.2757

91 G.F.Lynch, M.Sayer & M.Segel J. Appl. Phys. 42 (1971) pp.2587

92 G.S.Linsly, A.E.Owen & F.M.Hayatee J. Non-Cryst. Solids 4 (1970) pp.208

93 J.E.Stanworth, R.E.Baynton & H.Rawson J. Ele. Chem. Soc. 104 (1957) pp.237

94 B.H.V.Janakirama-Rao J. Amer. Ceram. Soc. 48 (1965) pp.311

95 A.V.Ioffe, I.V.Patrina & S.V.Poberovskaya Sov. Phys. Solid State 2 (1960) pp.609

96 H.H.Nester & W.D.Kingery Proc. VII Inter. Congr. on Glass Brussels (1965) pp.106

97 L.A.Grechanik & N.V.Pelrovykh Sov. Phys. Solid State 2 (1960) pp.1908

98 D.P.Hamllin, R.A.Weidel & G.E.Blair J. Amer. Ceram. Soc. 46 (1963) pp.499

99 R.H.Caley & M.Krishna Murthy. J. Amer. Ceram. Soc. 53 (1970) pp.254

100 N.F.Mott J. Non-Cryst. Solids 1 (1968) p.1

101 M.Sayer, A.Mansingh, J.M.Reyes & G.Rosenbalatt J. Appl. Phys. 42 (1971) pp.28 57

102 M.Sayer & A Mansingh Phys. Rev. B 6 (1972) pp.4629

103 G.N.Greaves J. Non-Cryst. Solids 11 (1973) pp.427

104 A.P.Schmid J. Non-Cryst. Solids 4 (1970) pp.232

105 A.Mansingh, J.K.Vaid & R.P.Tandon J. Phys. C. Solid State Phys. 8 (1975) pp.1023

106 A.Mansingh, J.M.Reyes & M.Sayer J. Non-Cryst. Solids 7 (1972) pp.12

107 B.H.V.Janakirama-Rao J. Amer. Ceram. Soc. 49 (1966) pp.605

108 M.Sayer, A.Mansingh, J.M.Reyes & G.F.Lynch 2nd Inter. Conf. on Conduction in Low Mobility Materials Elial - Israel Taylor and Francis (1971) pp.115

109 F.Vratny J. Inorg. Nucl. Chem. 21 (1961) pp.77

110 H.Harper & P.W.McMillan Phys. & Chem of Glasses 15 (1974) pp.148

111 H.G.Bachmann, F.R.Ahmed & W.H.Barnes Crystal Structure of Vanadium Penoxide Z.Kristallogr 115 (1961) pp.110

112 F.Dachille & R.Ray J. Amer. Ceram. Soc. 42 (1959) pp.78

113 R.A.Nyquist & R.O.Kagel Infra-red Spectra of Inorganic Compounds Academic Press New York London (1971)

114 F.Urbach Phys. Rev. 92 (1953) pp.1324

115 J.E.Lewis J. Non-Cryst. Solids 15 (1974) pp.352

116 I.G.Austin, M.Sayer & R.S.Sussman Amorphous and Liquid Semiconductors Taylor and Francis London (1973) pp.1343

117 G.R.Moridi Ph.D. Thesis Brunel University Middx. U.K. (1975)

118 J.Tauc & M.Zanini J. Non-Cryst. Solids 23 (1977) pp.349

119 M.Nunoshita, H.Arai, T.Taneki & Y.Hamakawa J. Non-Cryst. Solids 12 (1960) pp.339

120 J.E.Stanworth, E.P.Denton & H.Rawson Chem. Abstr. 54 (1960) pp.17 83

121 F.J.Morin Oxides of 3d Transition Metals (Bell Telephone Monograph U.S.A.) (1958) pp.3116

122 P.W.Anderson Phys. Rev. 109 (1958) pp.1492

123 N.F.Mott & R.W.Gurney Electronic Processes in Ionic Crystals Oxford London (1950)

124 G.N.Greaves J. Non-Cryst. Solids 11 (1973 pp.427

125 I.G.Austin & M.Sayer J. Phys. C. Solid. State Phys. 7 (1974) pp.905

126 P.K.Chaudhari & S.S.Li Phys. State Solidi A 24 (1974) pp.231

127 P.H.Caley & M.K.Murthy J. Amer. Ceram. Soc. 53 (1969) pp.254

128 A.Mansingh, J.K.Vaid & R.P.Tandon J. Phys C. Solid State Phys. 8 (1975) pp.1023

129 J.Schnakenberge Phys. Status Solidi 28 (1968) pp.623

130 N.F.Mott & I.G.Austin Adv. Phys. 18 (1969) pp.41

131 V.N.Bogamalove,E.K.Kudinove & A.Firsov Sov. Phys. Solid State 9 (1968) pp.2502

132 N.F.Mott Advance Phys. 16 (1967) pp.49

133 T.Holstein Phys. Rev. 124 (1961) pp.1329

134 I.G.Austin & E.S.Garbett Proc, 13th Session of Scottish University Summer School in Physics Academic Press London (1973) pp.393

135 H.W.Poole Phil. Mag. 22 (1961) pp.112

136 J.Frenkel Phys. Rev. 54 (1938) pp.64

137 K.Moorjani & C.Feldman J. Non-Cryst. Solids 4 (1970) pp.248

138 J.P.Lacharme & J.O.Isard J. Non-Cryst. Solids 27 (1978) pp.381

139 S.R.Ovshinsky Phys. Rev. Lett 21 (1968) pp.1450

140 R.R.Shanks J. Non-Cryst. Solids 2 (1970) pp.504

141 D.R.Haberland Solid State Electronics 13 (1970) pp.207

142 E.J.Evans, J.H.Helbers & S.R.Ovshinsky J. Non-Cryst. Solids 2 (1970) pp.334

143 A.Csillay & H.Jager J. Non-Cryst. Solids 2 (1970) pp.123

144 B.T.Kolomiets, B.A.Lebedov and I.A.Taksami Sov. Phys. Semiconductors 3 (1969) pp.621

145 M.Sugi, M.Kikuchi & K.Tanaka Solid State Communication 7 (1969) pp.1805

146 J.E.Hall J. Non-Cryst. Solids 2 (1970) pp.125

147 S.Lizima, M.Sugi, M.Kikuchi & K.Tanaka Solid State Communication 8 (1970) pp.153

148 M.Regan & C.F.Drake Mat. Res. Bull. 7 (1972) pp.1559

149 C.F.Drake, I.F.Scandal & A Engel Phys. Status Solidi 32 (1969) pp.193

150 M.Suji & K.C.Kao J. Non-Cryst. Solids 18 (1975) pp.275

151 G.R.Moridi & C.A.Hogarth Int. J. Electronics 44 (1978) pp.297

152 M.H.Cohen, R.G.Neale & A Paskin J. Non-Cryst. Solids 8-10 (1972) pp.885

153 R.C.Chunghi & S.W.Yoon J. of Korean Phys. Soc. 7 (1971) pp.87

154 M.Regan & C.F.Drake Mat. Res. Bull. 6 (1971) pp.487

155 V.W.Goldschmidt Geochemische Verteilungsgesetze der Element viii vid. A.Kad

156 A.Winter J. Amer. Ceram. Soc. 40 (1957) pp.54

157 R.C.Ellis Inorg. Chem. 2 (1963) pp.22

158 A.K.Jonscher J. Non-Cryst. Solids 8 (1972) pp.293

159 J. of Glass Studies (XV) pp.9

160 W.Bruegel Introduction to Infra-red Spectroscopy Translations from German John Wiley & Sons Inc. New York (1962) pp.228

161 V.A.Ioffe & I.B.Patrina Phys. Status Solidi b 40 (1970) pp.389

162 J.Hamers, E.Bactens and J.Vennick Phys. Status Solidi a 20 (1973) pp.381

Tables and Graphs

Glass No	V_2O_5 mol%	P_2O_5 mol%	TeO_2 mol%	Softening temp ^oC	Colour
101	50	50	0	595	Black*
102	55	45	0		"
103	60	40	0		"
104	65	35	0		"
105	70	30	0		"
106	75	25	0		"
107	80	20	0		"
108	85	15	0		"
109	90	10	0	420	"
201	60	35	5	555	"
202	60	30	10		Black**
203	60	25	15		"
204	60	20	20		"
205	60	15	25		"
206	60	10	30		"
207	60	5	35	435	"

Table (5.1) Glass Composition for Binary $V_2O_5 - P_2O_5$ and Ternary $V_2O_5 - P_2O_5 - TeO_2$ Systems

* Blown films of $V_2O_5 - P_2O_5$ glasses 2-10$\mu$are dark green

**Blown films of $V_2O_5 - P_2O_5 - TeO_2$ glasses 2-10μ are dark brown

Glass No.	Density(ρ) gm cm^{-3}	Molar Vol cm^{+3}	Molar Vol per ion pair	% of T.M.I. content	Composition
101	2.87_4	56.33	16.10	32.18	50%-50% V_2O_5 - P_2O_5
102	2.89_2	56.58	16.17	34.14	55%-45% " "
103	2.90_2	57.16	16.33	37.22	60%-40% " "
104	2.91_0	57.69	16.42	39.08	65%-35% " "
105	2.93_2	57.94	16.55	42.02	70%-30% " "
106	2.94_5	58.37	16.68	44.62	75%-25% " "
107	2.96_0	58.74	16.78	47.22	80%-20% " "
108	2.97_0	59.22	16.92	49.31	85%-15% " "
109	2.98_2	59.65	17.04	52.64	90%-10% " "
201	2.91_8	57.21_9	16.83	35.92	60%-35%-5% V_2O_5-P_2O_5-TeO_2
202	2.99_8	56.08_8	16.91	35.10	60%-30%-10% " " "
203	3.11_7	54.20_7	16.94	33.90	60%-25%-15% " " "
204	3.21_2	52.78_3	17.03	33.75	60%-20%-20% " " "
205	3.35_0	50.54_6	17.09	33.45	60%-15%-25% " " "
206	3.43_0	50.00_9	17.16	33.25	60%-10%-30% " " "
207	3.51_0	49.02_8	17.51	32.90	60%-5%-35% " " "

Table (5.2) Density and Molar Volume of V_2O_5 - P_2O_5 and V_2O_5 - P_2O_5 - TeO_2 Glasses

Glass No.	T.M.I. cm^{-3} concentration $Nx10^{22}$	T.M.I. spacing A^{o} R	C. chemical Analysis	C. E.S.R.
101	1.09_2	4.50_7	0.43_7	0.39_3
102	1.16_6	4.40_9		
103	1.27_5	4.28_1	0.28_3	0.26_0
104	1.34_3	4.20_7		
105	1.45_5	4.09_3	0.18_0	0.18_9
106	1.55_2	4.00_9		
107	1.65_1	3.92_7	0.08_1	0.11_0
108	1.72_9	3.86_7		
109	1.85_4	3.77_8	0.05_1	0.05_7
201	1.23_8	4.32_0	0.33_1	0.36_7
202	1.24_3	4.31_6	0.28_9	0.31_2
203	1.24_8	4.31_0		
204	1.28_1	4.27_1	0.24_3	0.28_5
205	1.32_3	4.24_5		
206	1.34_7	4.20_3	0.20_8	0.24_1
207	1.36_4	4.18_5	0.17_1	0.21_3

Table (5.3) Transition Metal ion Concentration and Transition Metal ion Spacing for V_2O_5 - P_2O_5 and V_2O_5 - P_2O_5 - TeO_2 glasses.

Glass No.	Total V in 100gr of Glass	T.M.I. concentration $x10^{22} cm^{-3}$	v^{4+} concentration $x10^{21} cm^{-3}$		$C = \frac{v^{4+}}{v_{tot}}$	
			Chemical	E.S.R.	Chemical	E.S.R.
101	32.18	1.092	4.77	4.297	0.437	0.393
103	37.22	1.275	3.61	3.135	0.283	0.260
105	42.02	1.455	2.62	2.751	0.180	0.189
107	47.22	1.561	1.32	1.684	0.080	0.110
109	52.64	1.854	1.22	1.055	0.055	0.057
201	35.92	1.238	4.10	4.51	0.331	0.36
202	35.10	1.243	3.59	3.96	0.289	0.31
204	33.75	1.281	3.11	3.62	0.243	0.28
206	33.45	1.347	2.80	3.25	0.208	0.24
207	32.91	1.364	2.33	2.80	0.171	0.21

Table (5.4) Reduced Valency States Results From Titration and E.S.R. for $V_2O_5 - P_2O_5$ and $V_2O_5 - P_2O_5 - TeO_2$ Glasses

Annealing Temp. °C	Density gr. cm^{-3}	
	Glass No.106	Glass NO.204
105	2.91_4	3.18_0
200	2.94_5	3.21_0
250	2.97_0	3.25_0
300	3.01_2	3.28_0

Table (5.5) Density of Glasses No.106 and 204 at Differeut Annealing Temperatures

glass No.		WAVE NUMBER cm^{-1}							
101	360	390	–	1015	1180	–	–	–	–
102	360	400	600	1010	1190	–	–	–	–
103	360	400	–	1015	1190	–	–	–	–
104	360	410	–	1010	1190	–	–	–	–
105	350	430	600	110	1180	–	–	–	–
106	350	430	620	1015	1180	–	–	–	–
107	350	430	640	1015	1200	–	–	–	–
108	345	640	1015	1180	–	–	–	–	–
109	335	435	680	1015	1180	–	–	–	–
V_2O_5	280	370	480	660	800	915	1040	1260	1275

Table (6.1) Position of Peaks in Infra-red Absorption Spectra in $V_2O_5 - P_2O_5$ Glasses at Room Temperature

Glass	WAVE NUMBER CM^{-1}					
201	300	420	590	820	1015	-
202	300	410	600	810	1010	1150
203	300	-	600	810	1010	1160
204	300	410	600	810	1015	1160
205	300	410	600	810	1010	1160
206	300	410	620	820	1010	1170
207	300	410	630	820	1010	1140
TeO_2	230	350	660	830	-	1150
P_2O_5	270	410	570	760	-	1230

Table (6.2) Position of Peaks in the Infra-red Absorption Spectra for $V_2O_5 - P_2O_5 - TeO_2$ Glasses

Glass No.	E_{op} e.V	E_{el} e.V	E_{th} e.V	A x 10^3 $cm^{-2/3} e.V^{-1/3}$	C	E e.V
101	2.43	0.98	2.65	3.70	0.44	0.39
103	2.32	0.88	2.55	3.44	0.28	
105	2.21	0.76	2.42	3.33	0.18	
107	2.12	0.68	2.35	3.10	0.08	0.54
109	2.02	0.62	2.24	2.80	0.05	0.61
201	2.44	0.86	2.68	4.95	0.33	0.41
202	2.38	0.84	2.59	4.82	0.29	
204	2.30	0.78	2.50	4.67	0.24	0.35
206	2.13	0.74	2.33	4.56	0.21	
207	2.10	2.22	2.39	4.38		0.31

Tabel (6.3) Values of some Physical Parameters for V_2O_5 - P_2O_5 - TeO_2 Glasses

TK / Gl.No.	293	323	348	373	398	423	448	473
101	2.1×10^{-6}	1.3×10^{-5}	4×10^{-5}	1.5×10^{-4}	3.8×10^{-4}	1.1×10^{-3}	2.2×10^{-3}	3.5×10^{-3}
103	5.8×10^{-6}	2.4×10^{-5}	9×10^{-5}	2×10^{-4}	5.5×10^{-4}	1.2×10^{-3}	2.5×10^{-3}	4.6×10^{-3}
105	1.8×10^{-5}	6×10^{-5}	1.6×10^{-4}	4×10^{-4}	1×10^{-3}	1.7×10^{-3}	3×10^{-3}	5.5×10^{-3}
107	3.7×10^{-5}	1.1×10^{-4}	3×10^{-4}	6.9×10^{-4}	1.3×10^{-3}	2.3×10^{-3}	3.9×10^{-3}	6.9×10^{-3}
109	7×10^{-5}	2×10^{-4}	6×10^{-4}	1×10^{-3}	1.8×10^{-3}	2.9×10^{-3}	5.2×10^{-3}	8×10^{-3}

Table (7.1) Values of σ for V_2O_5 - P_2O_5 Glasses with Different Composition at Different Temperatures

Glass No.	Slope of log vs. 1/T x 1000	E Activation Energy e.V	R T.M.I.Spacing A^{o}
101	2.48	0.489	4.51
103	2.225	0.439	4.28
105	1.91	0.378	4.11
107	1.75	0.339	4
109	1.58	0.308	3.78

Table (7.2) Slope of log σ vs. $\frac{1}{T}$ and Activation Energy for $V_2O_5 - P_2O_5$ Glasses with Different V_2O_5 Content

T	Electrode Material		
	Au	Ag	Cu
293	$1.1\times10^{-5}\ \Omega^{-1}cm^{-1}$	$1.2\times10^{-5}\ \Omega^{-1}cm^{-1}$	$1\times10^{-5}\ \Omega^{-1}cm^{-1}$
323	$4\times10^{-5}\ \Omega^{-1}cm^{-1}$	$3.7\times10^{-5}\ \Omega^{-1}cm^{-1}$	$3.4\times10^{-5}\ \Omega^{-1}cm^{-1}$
348	$1.3\times10^{-4}\ \Omega^{-1}cm^{-1}$	$1.1\times10^{-4}\ \Omega^{-1}cm^{-1}$	$1.2\times10^{-4}\ \Omega^{-1}cm^{-1}$
373	$3\times10^{-4}\ \Omega^{-1}cm^{-1}$	$2.8\times10^{-4}\ \Omega^{-1}cm^{-1}$	$2.4\times10^{-4}\ \bar{\Omega}^{1}cm^{-1}$
398	$8\times10^{-4}\ \Omega^{-1}cm^{-1}$	$7\times10^{-4}\ \Omega^{-1}cm^{-1}$	$6.3\times10^{-4}\ \Omega^{-1}cm^{-1}$
423	$1.6\times10^{-3}\ \Omega^{-1}cm^{-1}$	$1.8\times10^{-3}\ \Omega^{-1}cm^{-1}$	$1.7\times10^{-3}\ \Omega^{-1}cm^{-1}$
448	$3\times10^{-3}\ \Omega^{-1}cm^{-1}$	$2.7\times10^{-3}\ \Omega^{-1}cm^{-1}$	$3.3\times10^{-2}\ \Omega^{-1}cm^{-1}$
473	$5.2\times10^{-3}\ \Omega^{-1}cm^{-1}$	$4.7\times10^{-3}\ \Omega^{-1}cm^{-1}$	$5.7\times10^{-2}\ \Omega^{-1}cm^{-1}$

Table (7.3) Values of Conductivity for 65% - 35% ($V_2O_5 - P_2O_5$) Glasses with Different Electrode Materials Measured at Different Temperature

Glass No.	V^{4+} = n $x10^{21} cm^{-3}$	$\mu\ cm^2 V^{-1}\ sec^{-1}$				
		T = 293	T = 323	T = 373	T = 423	T = 473
101	4.77	$9.13x10^{-10}$	$5.65x10^{-9}$	$6.52x10^{-8}$	$4.78x10^{-7}$	$1.52x10^{-6}$
103	3.61	$3.35x10^{-9}$	$1.32x10^{-8}$	$1.15x10^{-7}$	$6.92x10^{-7}$	$2.65x10^{-6}$
105	2.62	$1.43x10^{-8}$	$4.71x10^{-8}$	$3.18x10^{-7}$	$1.35x10^{-6}$	$4.37x10^{-6}$
107	1.32	$5.84x10^{-8}$	$1.73x10^{-7}$	$1.08x10^{-6}$	$3.62x10^{-6}$	$1.09x10^{-5}$
109	1.22	$1.19x10^{-7}$	$3.41x10^{-7}$	$1.71x10^{-7}$	$4.95x10^{-6}$	$1.37x10^{-5}$

Table (7.4) Values of Mobility for V_2O_5 - P_2O_5 Glasses at Different Temperatures

Glass No.	V^{4+} = n $x10^{21} cm^{-3}$	$\mu T cm^2 V^{-1}\ sec^{-1} T$				
		T = 293	T = 323	T = 373	T = 423	T = 473
101	4.77	$2.66x10^{-7}$	$1.83x10^{-6}$	$2.43x10^{-5}$	$2.02x10^{-4}$	$7.20x10^{-4}$
103	3.61	$9.82x10^{-7}$	$4.26x10^{-6}$	$4.28x10^{-5}$	$2.93x10^{-4}$	$1.25x10^{-3}$
105	2.62	$4.20x10^{-6}$	$1.52x10^{-5}$	$1.18x10^{-4}$	$5.71x10^{-4}$	$2.10x10^{-3}$
107	1.32	$1.17x10^{-5}$	$5.55x10^{-5}$	$4.02x10^{-4}$	$1.53x10^{-3}$	$5.15x10^{-3}$
109	1.22	$3.48x10^{-5}$	$1.10x10^{-4}$	$6.37x10^{-4}$	$2.10x10^{-3}$	$6.48x10^{-3}$

Table (7.5) Values of μT for V_2O_5 - P_2O_5 Glasses at Different Temperatures

Glass No.	W e.V	W_p e.V	r_p A^o	$\nu_p \times 10^{-12}$ Hz	γ
101	0.48	0.96	1.82	3.14	75.66
103	0.41	0.82	1.73	3.92	50.62
105	0.38	0.76	1.65	4.67	37.34
107	0.34	0.68	1.61	6.31	26.08
109	0.31	0.62	1.52	8.18	18.30

Table (7.6) Values of Some Physical Parameters for V_2O_5 - P_2O_5 Glasses

TK / Gl.No.	293	323	348	373	398	423	448	473	$\frac{V_2O_5}{P_2O_5}$
103 60-40	5.8×10^{-6}	2.4×10^{-5}	9×10^{-5}	2×10^{-4}	5.5×10^{-4}	1.2×10^{-3}	2.5×10^{-3}	4.6×10^{-3}	1.5
201 60-35-5	8×10^{-6}	3×10^{-5}	1.1×10^{-5}	2.8×10^{-4}	7.1×10^{-4}	1.5×10^{-3}	2.8×10^{-3}	5.2×10^{-3}	1.7
202 60-30-10	1×10^{-5}	5×10^{-5}	1.4×10^{-4}	3.2×10^{-4}	8.5×10^{-3}	1.9×10^{-3}	3.4×10^{-3}	6.5×10^{-3}	2
204 60-20-20	2.1×10^{-5}	8×10^{-4}	2×10^{-4}	5.6×10^{-4}	1.3×10^{-3}	2.5×10^{-3}	4.5×10^{-3}	8×10^{-3}	3
206 60-19-30	3.1×10^{-5}	1.3×10^{-4}	3.2×10^{-4}	7.9×10^{-3}	1.7×10^{-3}	3.6×10^{-3}	5.2×10^{-3}	9.5×10^{-3}	6

Table (7.7) Values of Conductivity for Glasses Containing TeO_2 at Different Temperatures

Conductivity Values for (60-40) mol% $V_2O_5 - P_2O_5$ is also given for Comparison

Glass No.	$C = \frac{V^{4+}}{V_{tot}}$	Slope $\frac{1}{T}$ log σ vs. α	W e.V	N_{22} x10^{22}	R_o A^o	r_p A^o	W_p e.V	ν_{Ph} x10^{12} Hz	γ
201	0.33	2.17	0.43	1.23	4.32	1.74	0.86	4.15	50.72
202	0.29	2.16	0.42	1.25	4.31	1.73	0.84	4.92	41.31
204	0.24	1.98	0.39	1.28	4.27	1.72	0.78	6.11	33.27
206	0.21	1.91	0.37	1.34	4.19	1.69	0.74	7.47	26.56

Table (7.8) Values of some Physical Parameters for V_2O_5 - P_2O_5 - TeO_2 Glasses

T Gl.No.	293 K	323 K	373 K	423 K	473 K
201 60-35-5	3.35×10^{-9}	1.30×10^{-8}	1.15×10^{-7}	6.92×10^{-7}	2.65×10^{-6}
202 60-30-10	5.80×10^{-9}	2.90×10^{-8}	1.80×10^{-7}	1.10×10^{-6}	3.80×10^{-6}
204 60-20-20	1.40×10^{-8}	5.36×10^{-8}	3.70×10^{-7}	1.60×10^{-6}	5.36×10^{-6}
206 60-10-30	2.31×10^{-8}	9.67×10^{-8}	5.80×10^{-7}	2.60×10^{-6}	7.10×10^{-6}

Table (7.9) Values of Mobility for Glasses Containing TeO_2 at Different Temperature

T Gl.No.	293 K	323 K	373 K	423 K	473 K
201 60-35-5	9.80×10^{-7}	4.20×10^{-6}	4.30×10^{-5}	2.90×10^{-4}	1.30×10^{-3}
202 60-30-10	1.70×10^{-6}	9.40×10^{-6}	6.70×10^{-5}	4.70×10^{-4}	1.80×10^{-3}
204 60-20-20	4.10×10^{-6}	1.70×10^{-5}	1.40×10^{-4}	6.80×10^{-4}	2.50×10^{-3}
206 60-10-30	6.80×10^{-6}	3.10×10^{-5}	2.20×10^{-4}	1.10×10^{-3}	3.40×10^{-3}

Table (7.10) Values of μT for Glasses Containing TeO_2 at Different Temperature

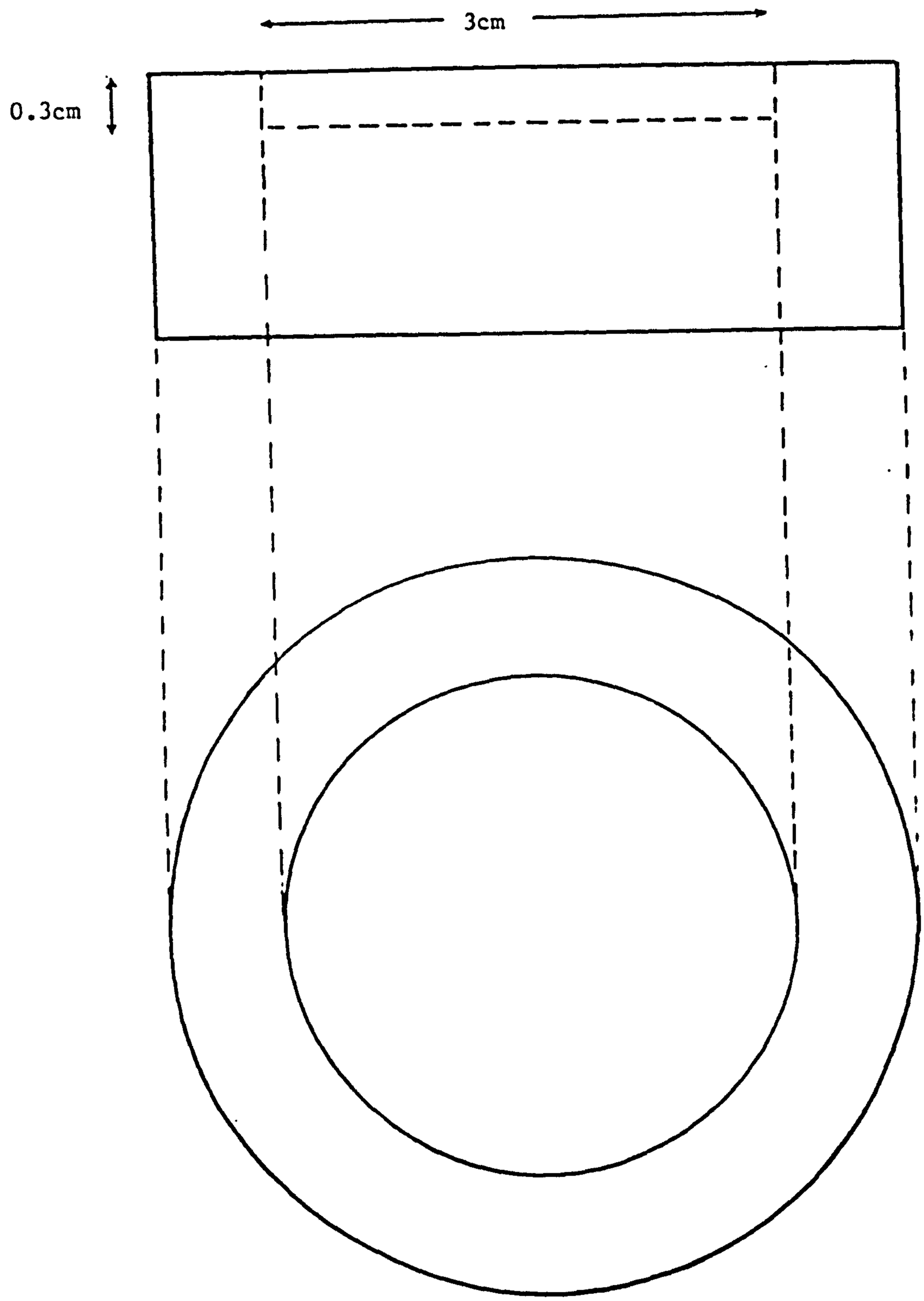

Fig.(5.1) Diagram of Cylindrical Shape Mould used in Bulk

Sample Preparation Processes

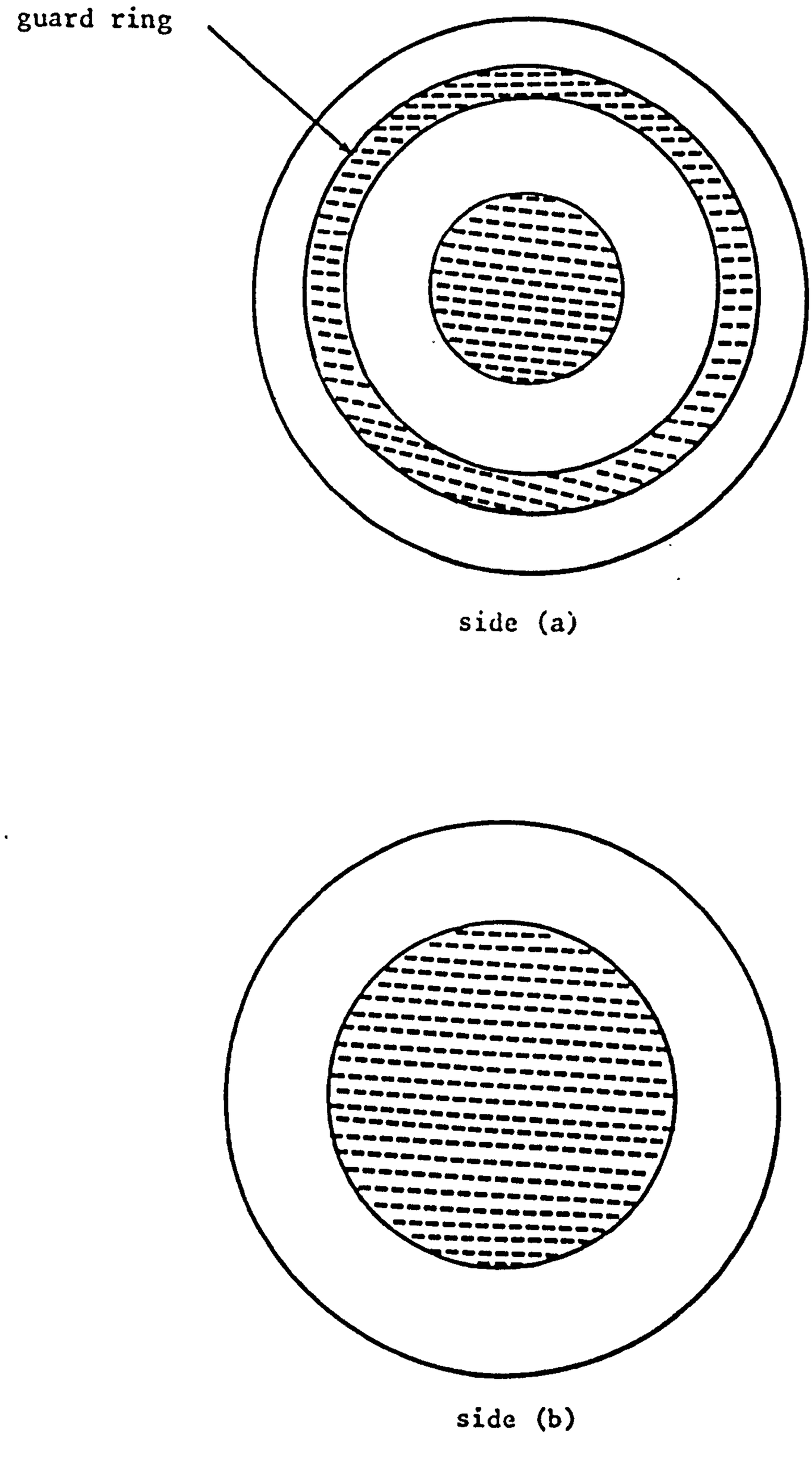

Fig.(5.2) Typical Electrode Deposited Sample with Guard Ring for Electrical Measurement at Low Electric Field. Shaded Region Represents the Deposited Area.

(a)

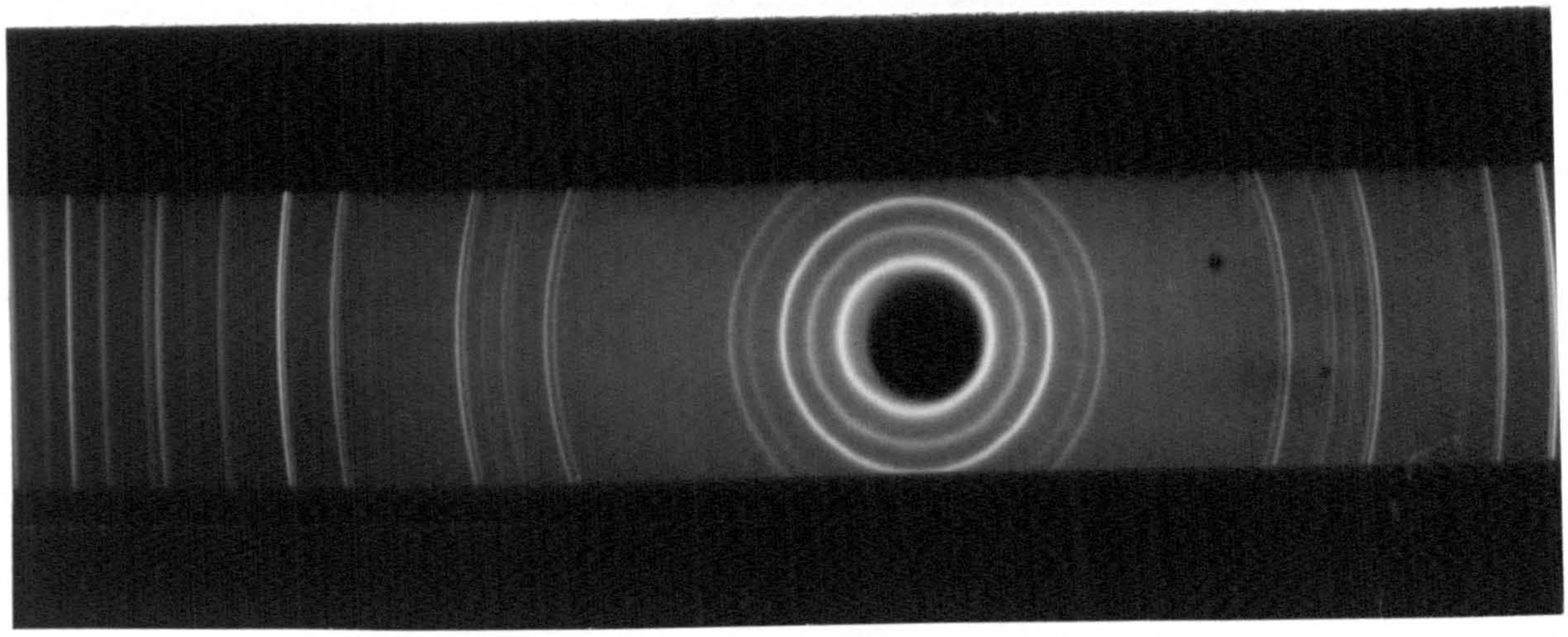

(b)

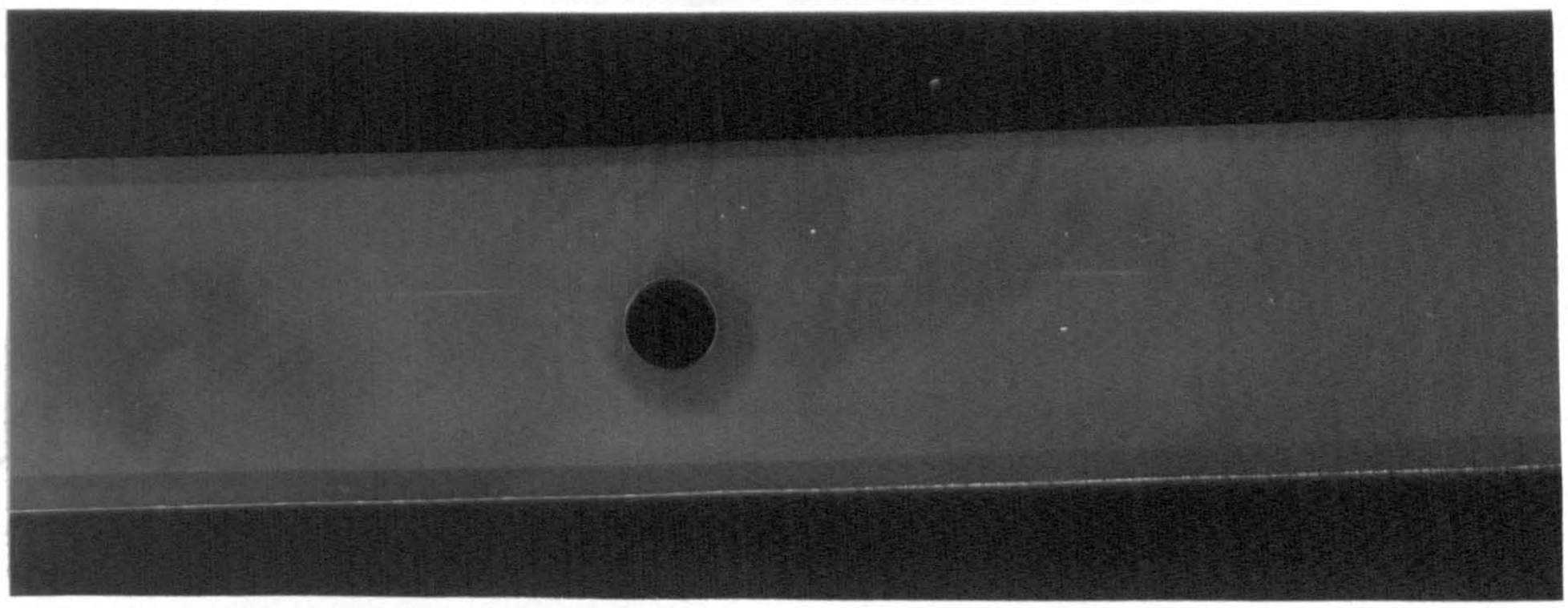

(c)

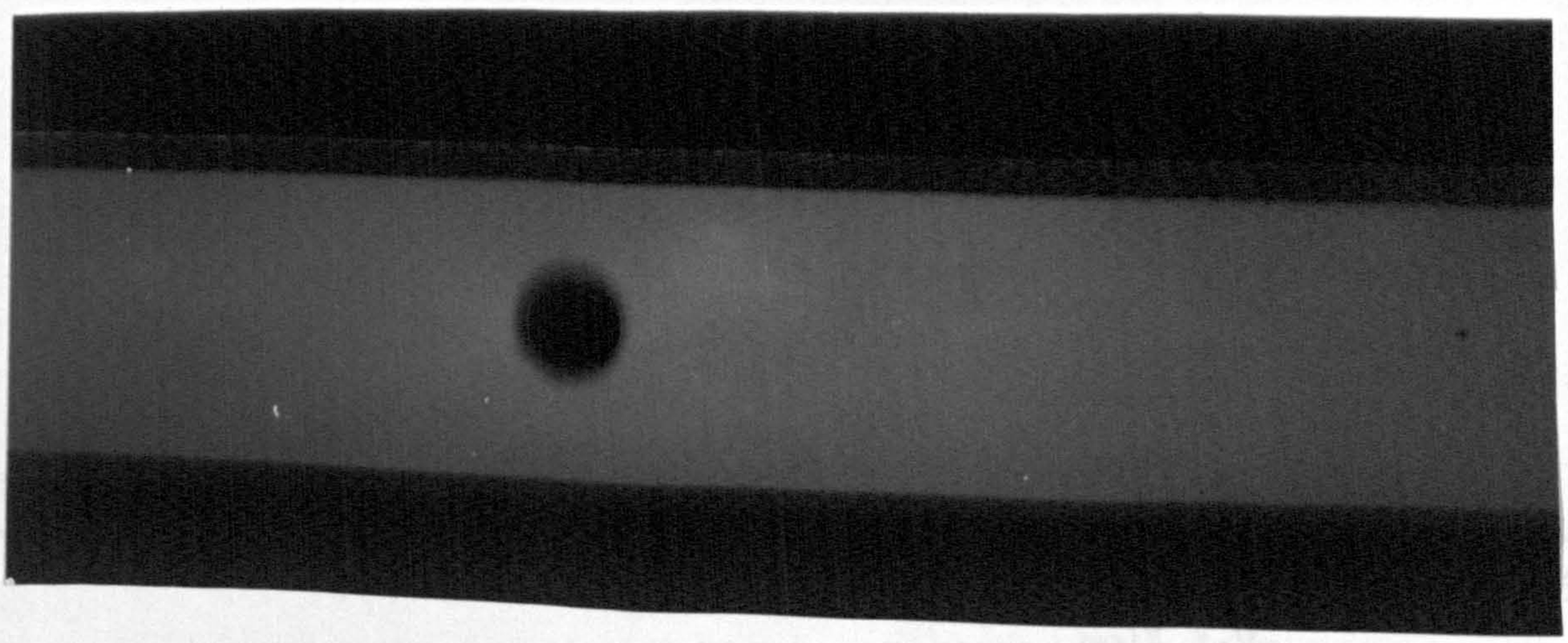

Fig.(5.3) Typical X-ray Photograph of a) Crystalline Material b) $V_2O_5 - P_2O_5$ Glass c) $V_2O_5 - P_2O_5 - TeO_2$ Glass

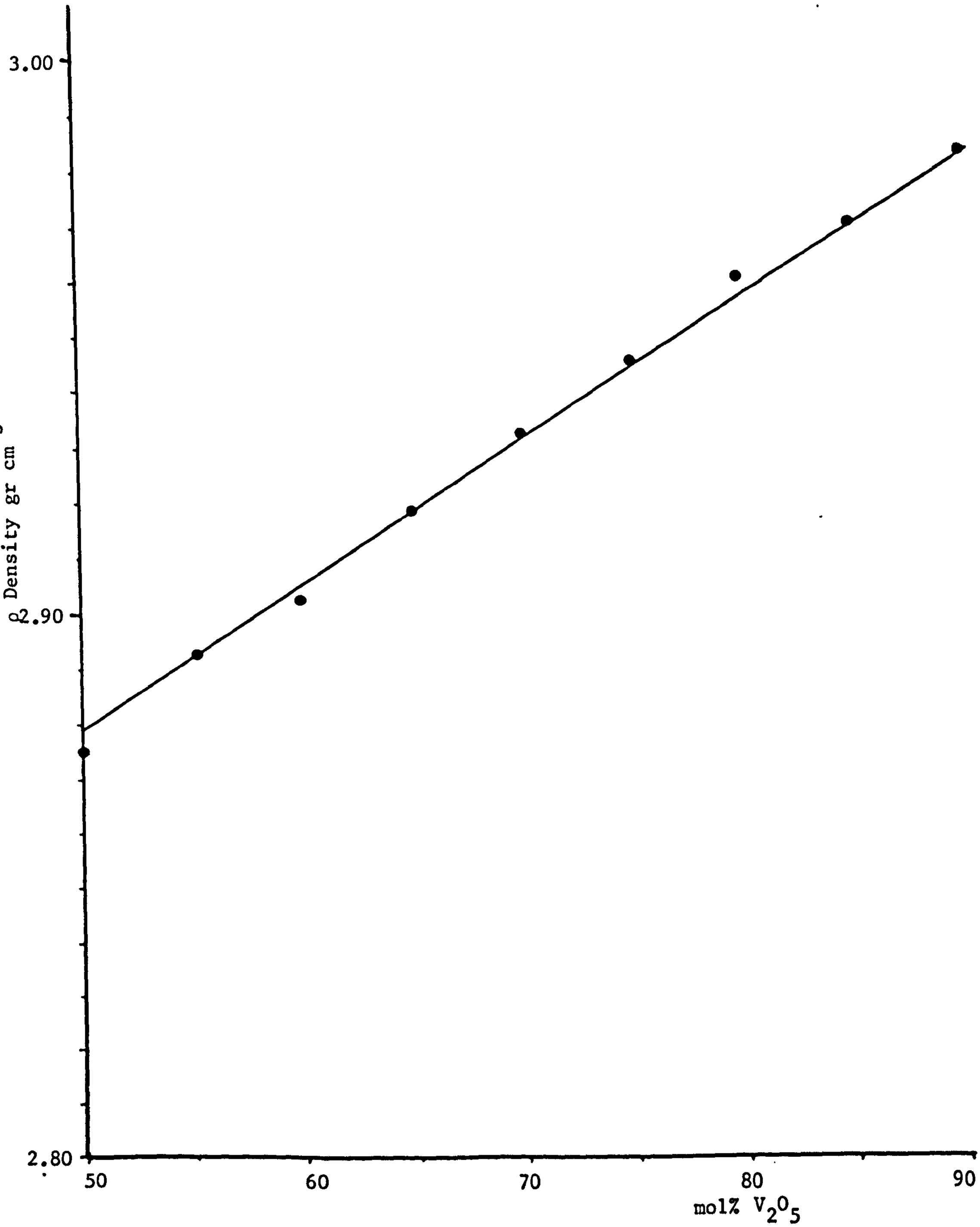

Fig.(5.4) Density of $V_2O_5 - P_2O_5$ Glasses vs. V_2O_5 Content

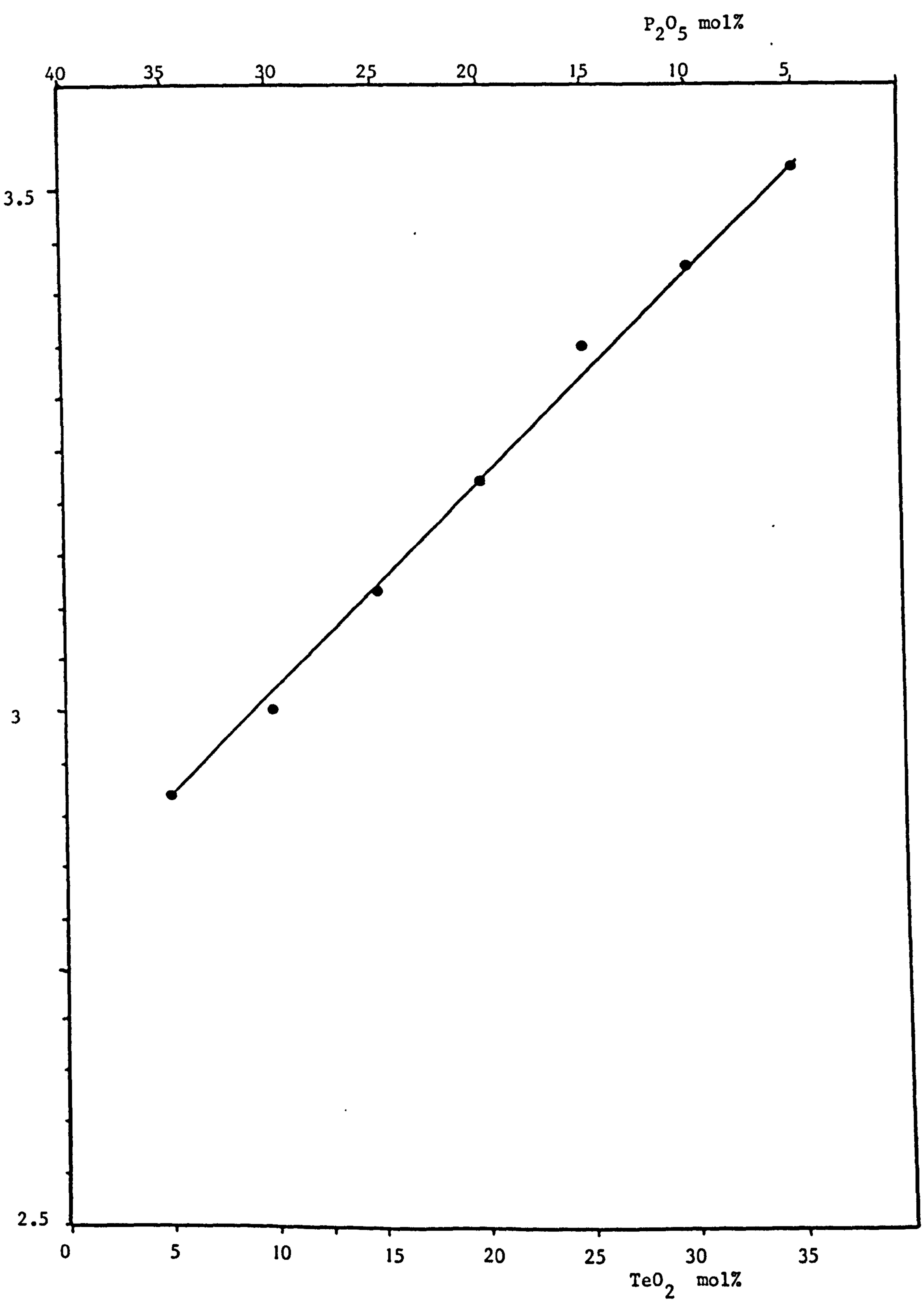

Fig.(5.5) Density of V_2O_5 - P_2O_5 - TeO_2 Glasses vs. TeO_2 Content

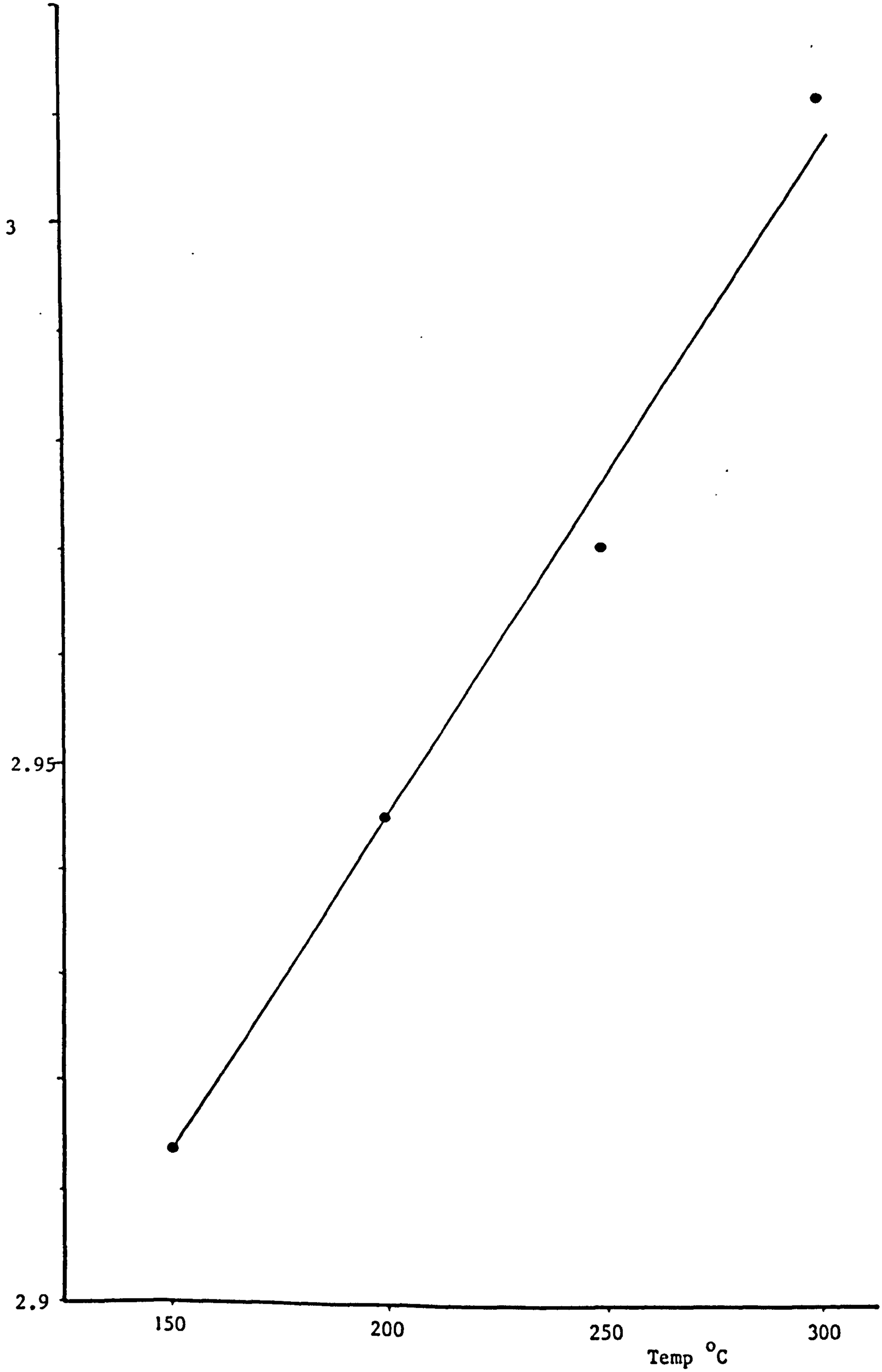

Fig.(5.6) Variation of Density with Annealing Temperature for Glass No.106

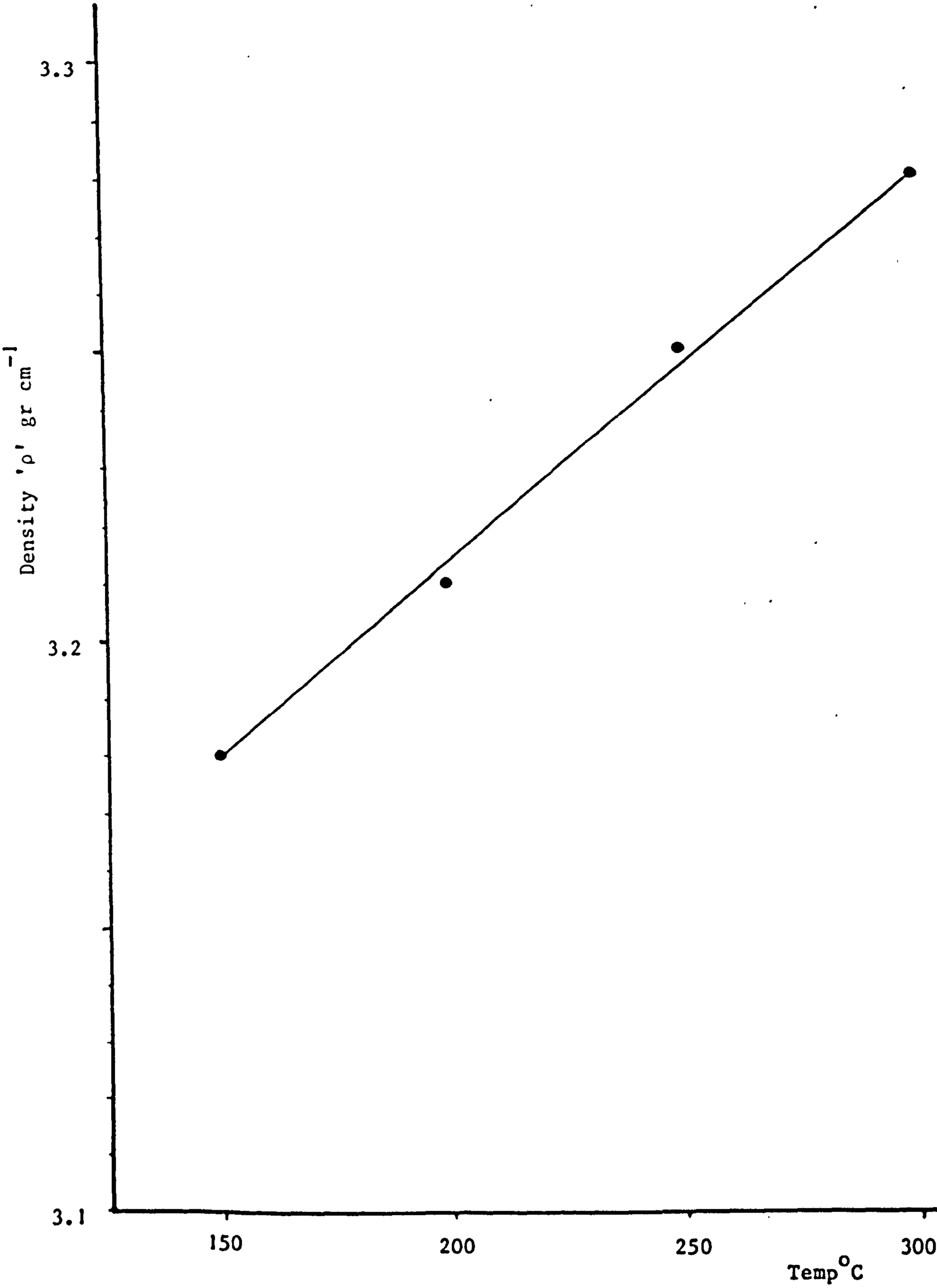

Fig.(5.7) Variation of Density with Annealing Temperatures for Glass No.204

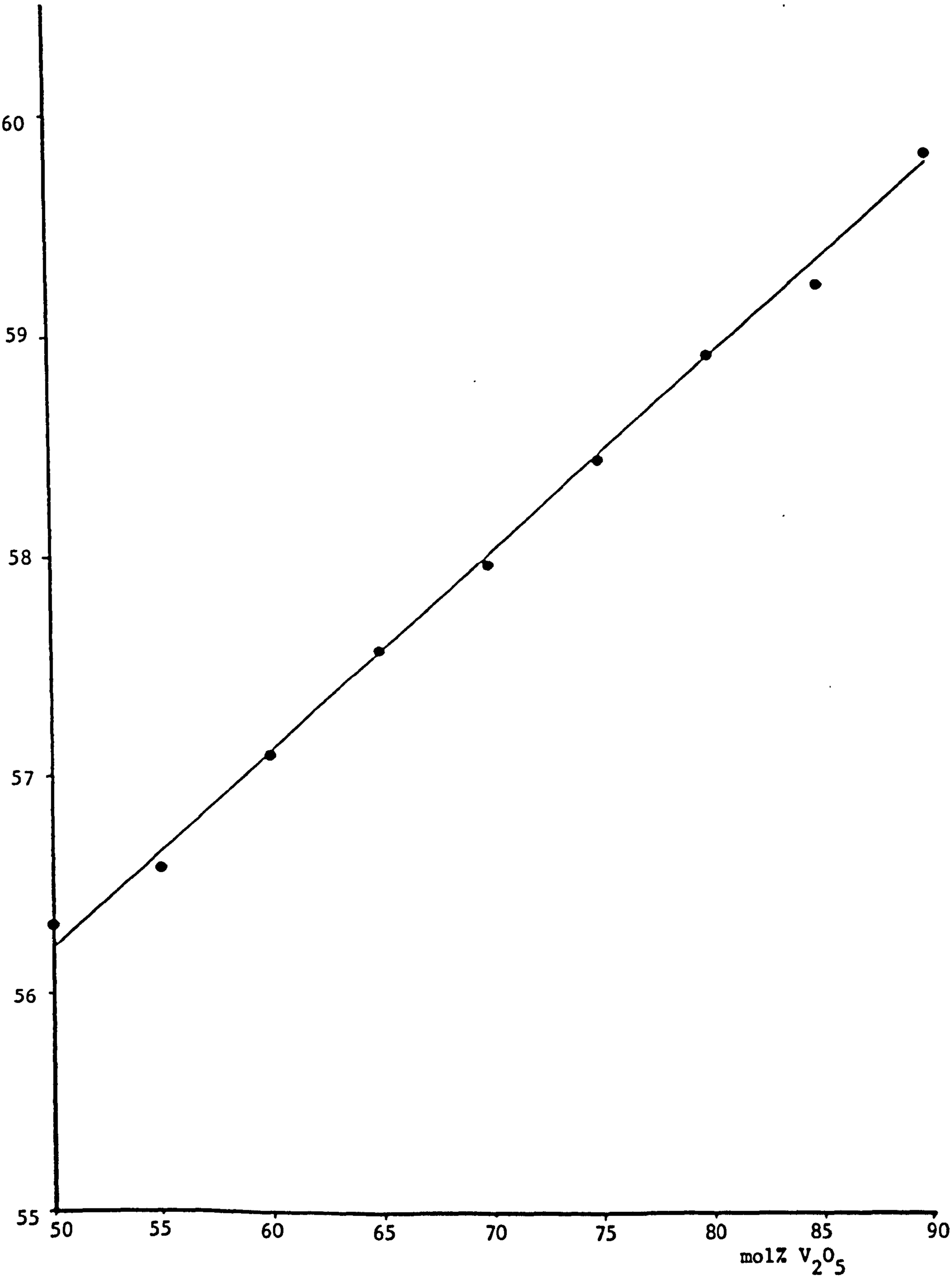

Fig.(5.8) Molar Volume vs. V_2O_5 Content for V_2O_5 - P_2O_5 Glasses

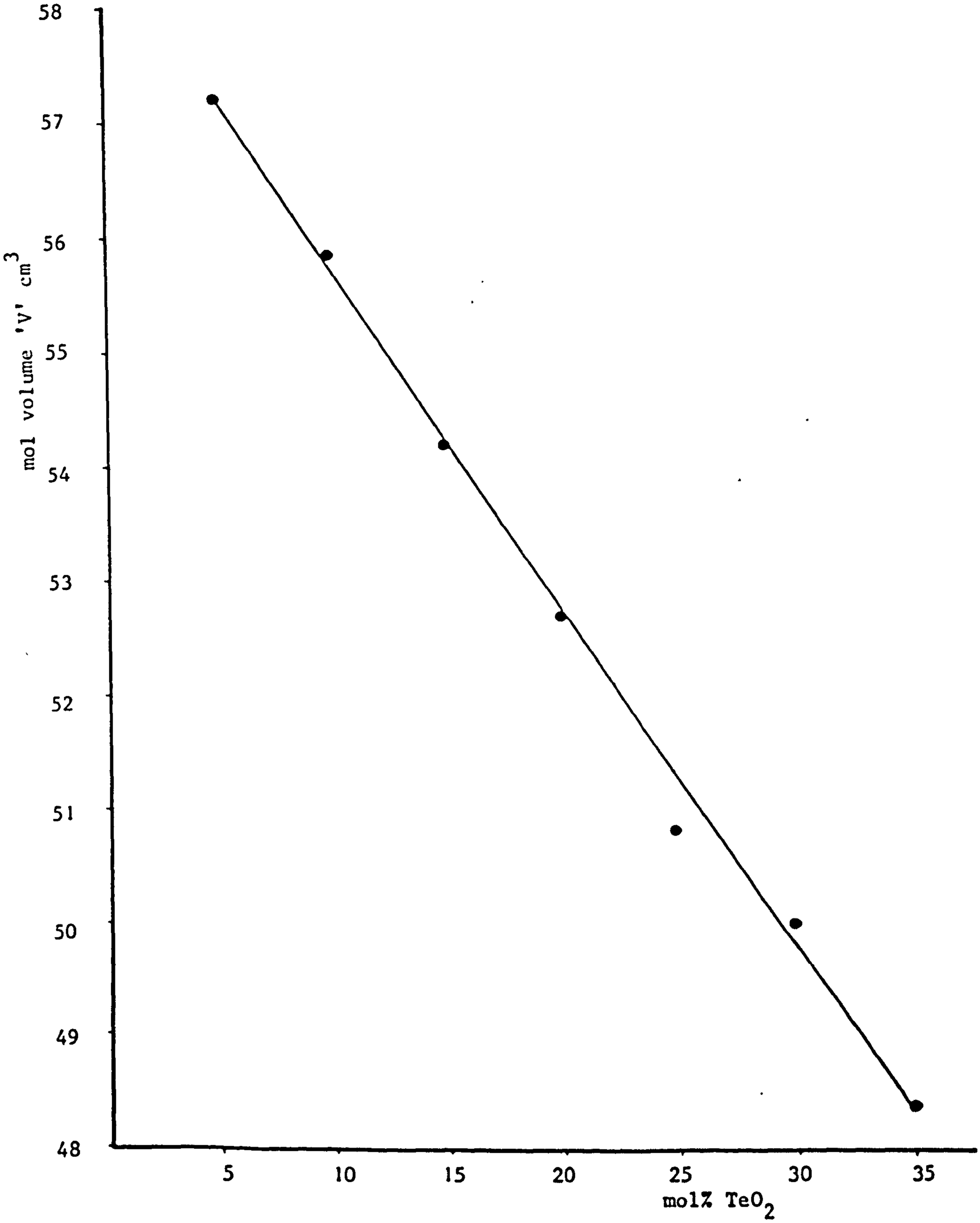

Fig.(5.9) Mol Volume vs. TeO_2 Content for V_2O_5 - P_2O_5 - TeO_2 Glasses

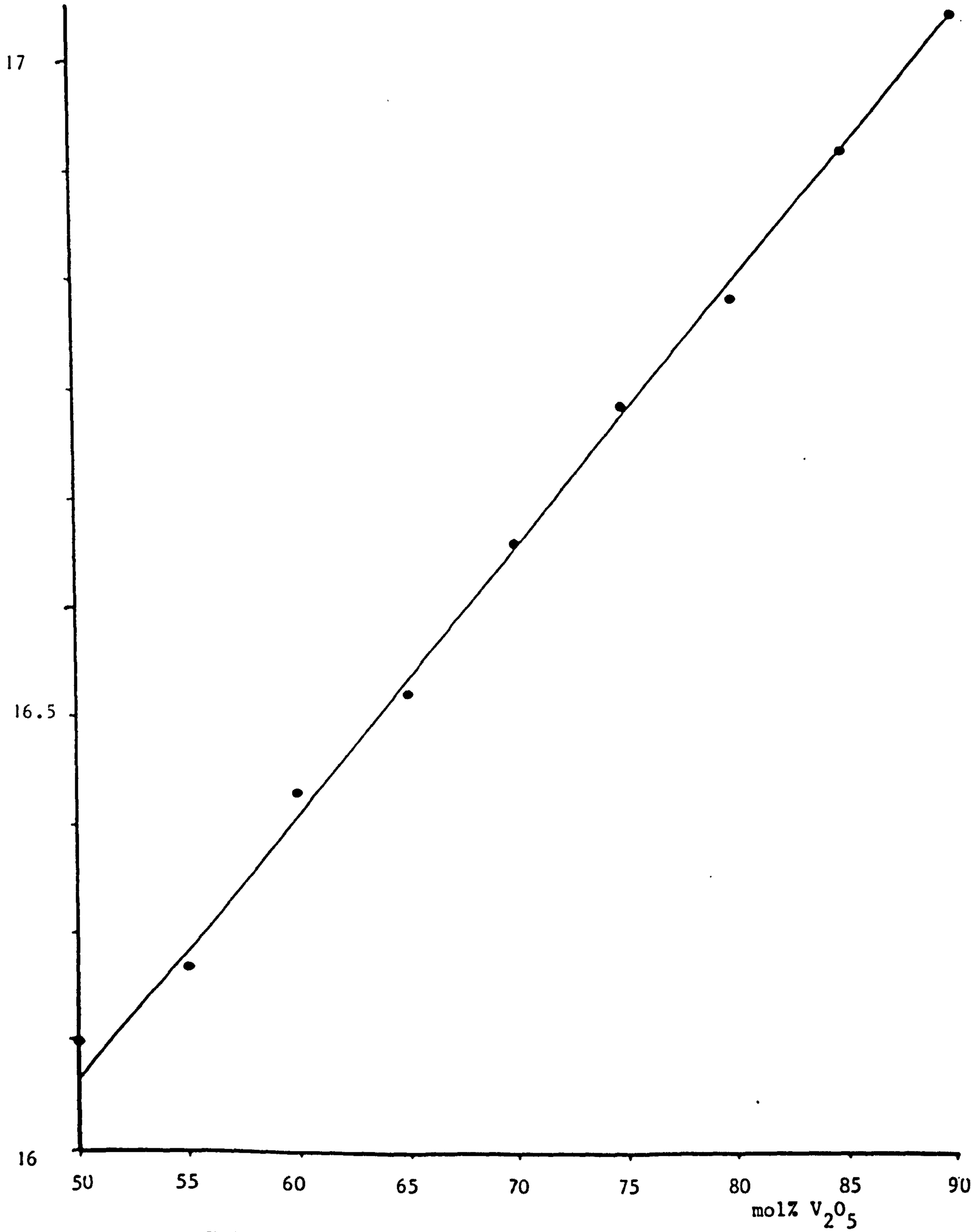

Fig.(5.10) Molar Volume per Ion Pair vs. V_2O_5 Content for V_2O_5 - P_2O_5 Glasses

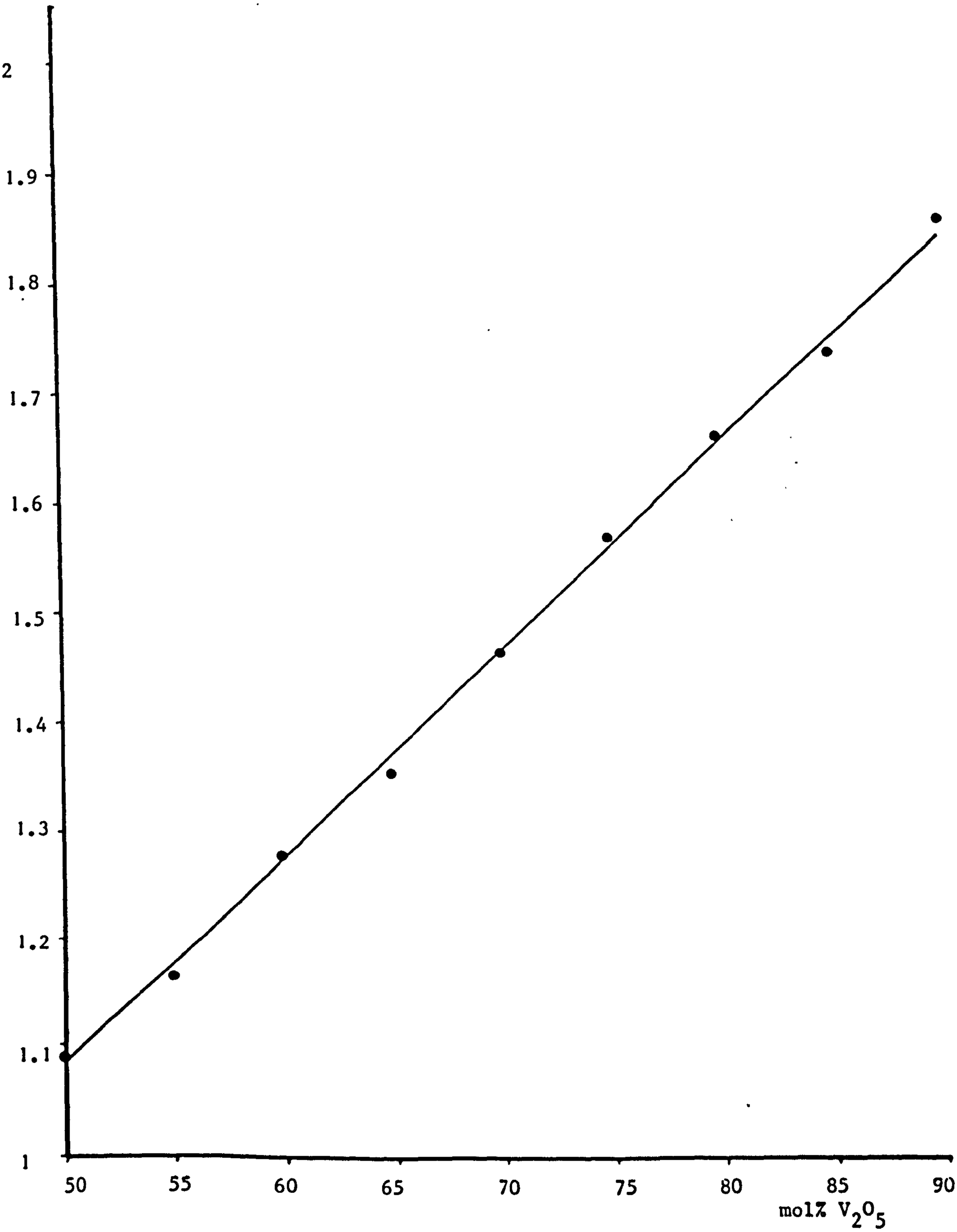

Fig.(5.11) Variation of Transition Metal Ion (T.M.I.) Concentration with V_2O_5 Content for V_2O_5 - P_2O_5 Glasses

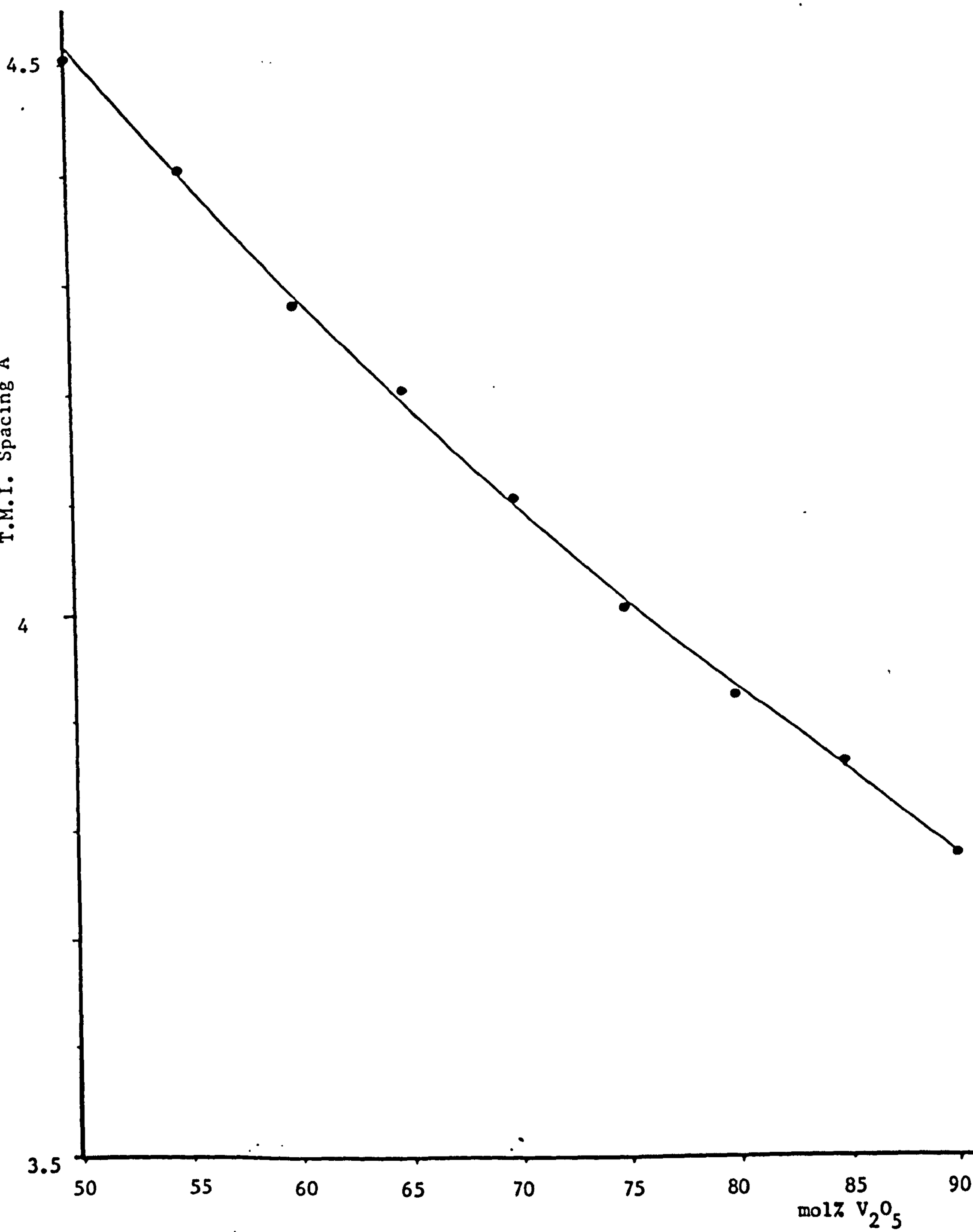

Fig.(5.12) Variation of T.M.I. Spacing with Glass Composition for $V_2O_5 - P_2O_5$ Glasses

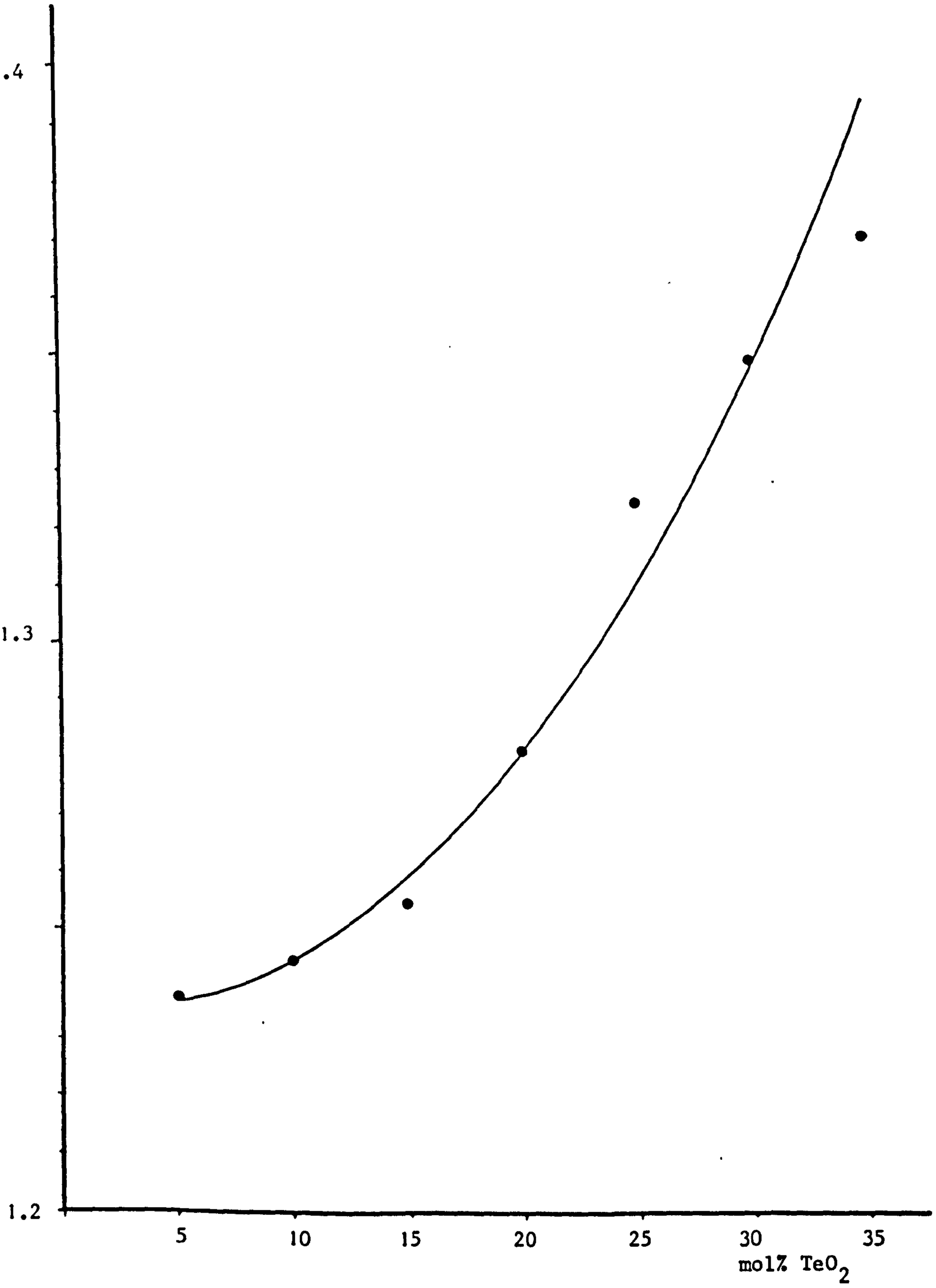

Fig.(5.13) Variation of T.M.I. Concentration with TeO_2 Content for $V_2O_5 - P_2O_5 - TeO_2$ Glasses

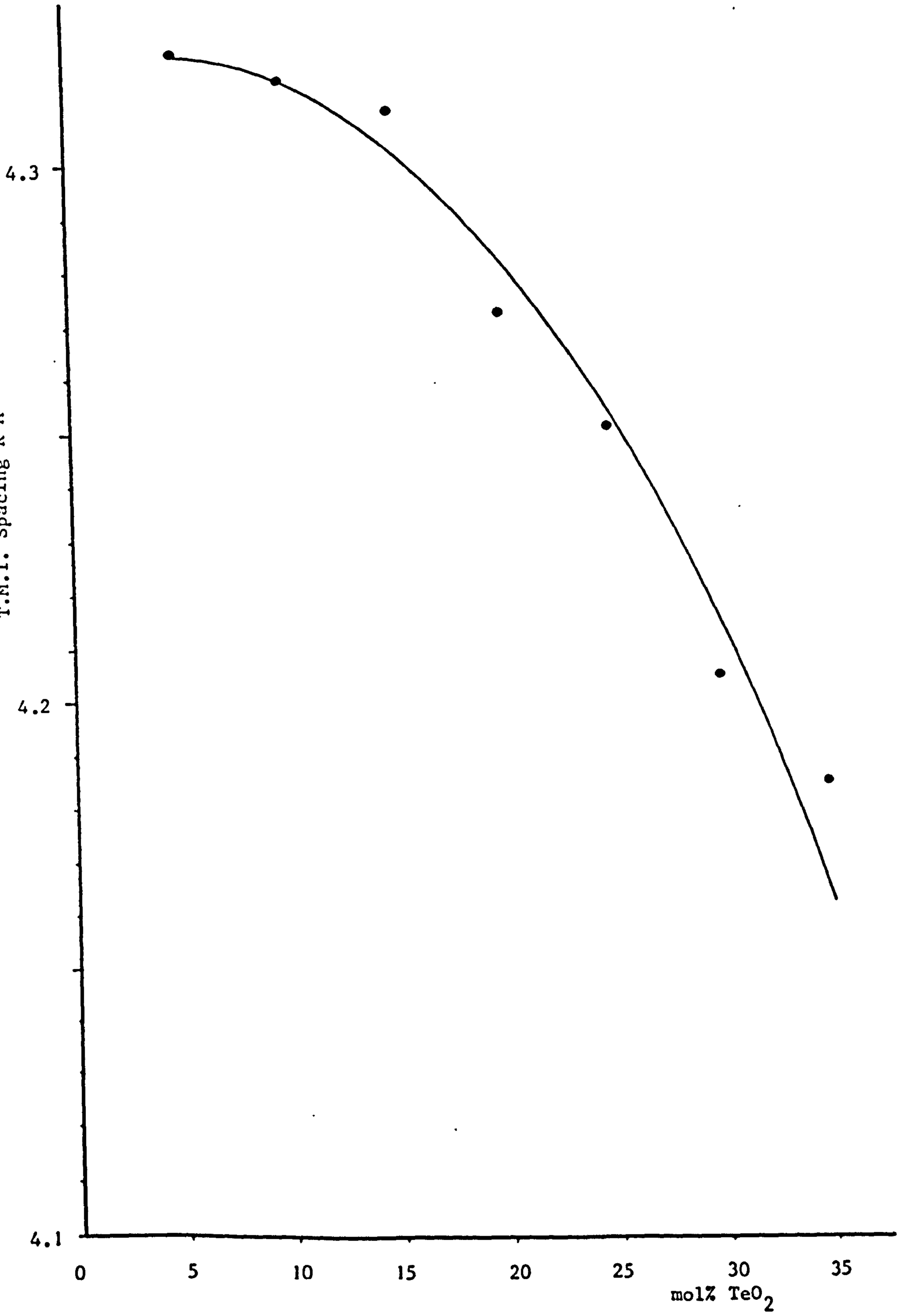

Fig.(5.14) Variations of T.M.I. Spacing with TeO_2 Content for $V_2O_5 - P_2O_5 - TeO_2$ Glasses

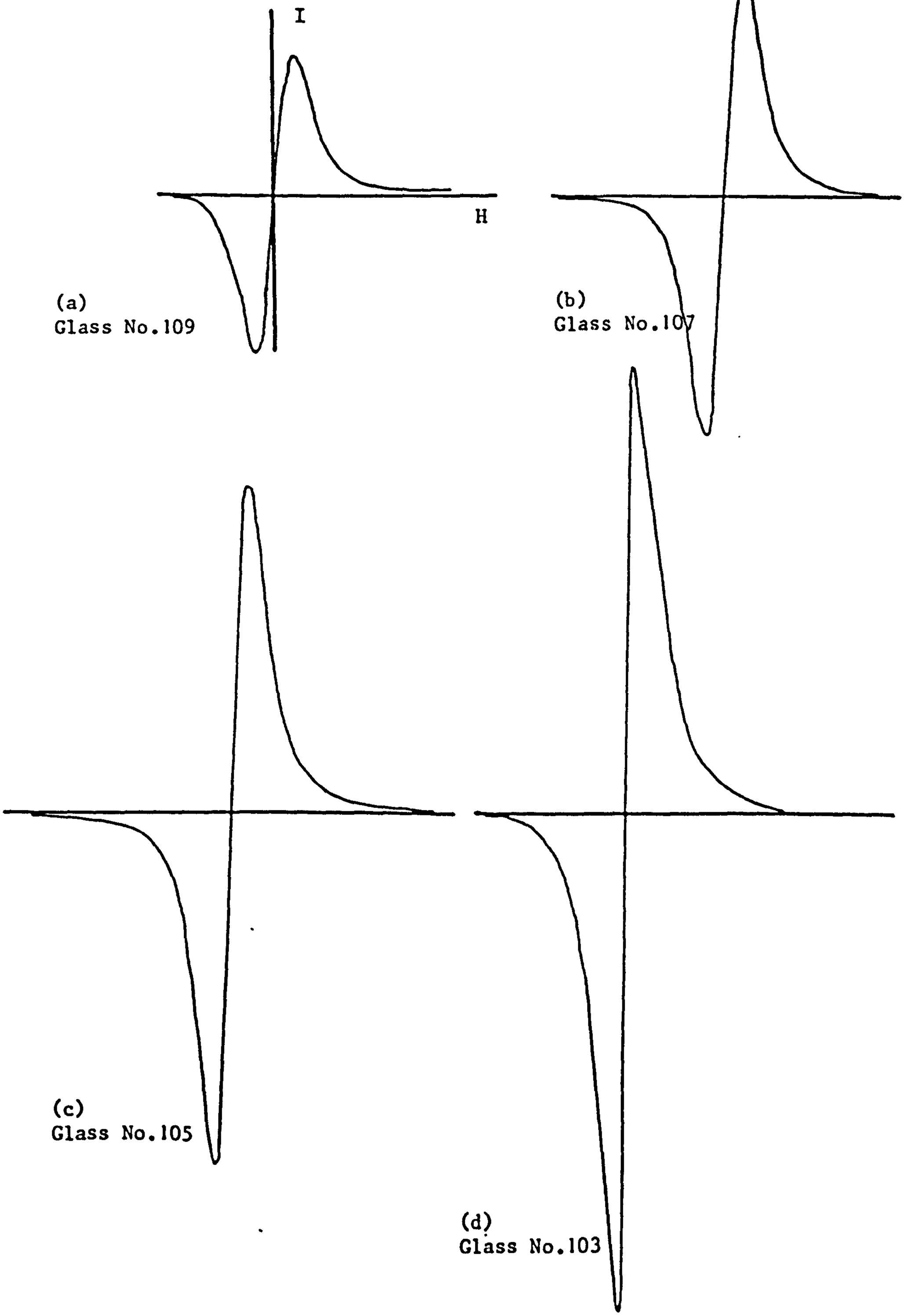

Fig.(5.15) Electron Spin Spectra for $V_2O_5 - P_2O_5$ Glasses with Different mol% of V_2O_5 at Room Temperature

Fig.(5.15,e) Glass No.101

Fig.(5.17) E.S.R. Spectra of Ammonium Vanadyle Oxalite $(NH_4)_2VO(C_2O_4)_2$

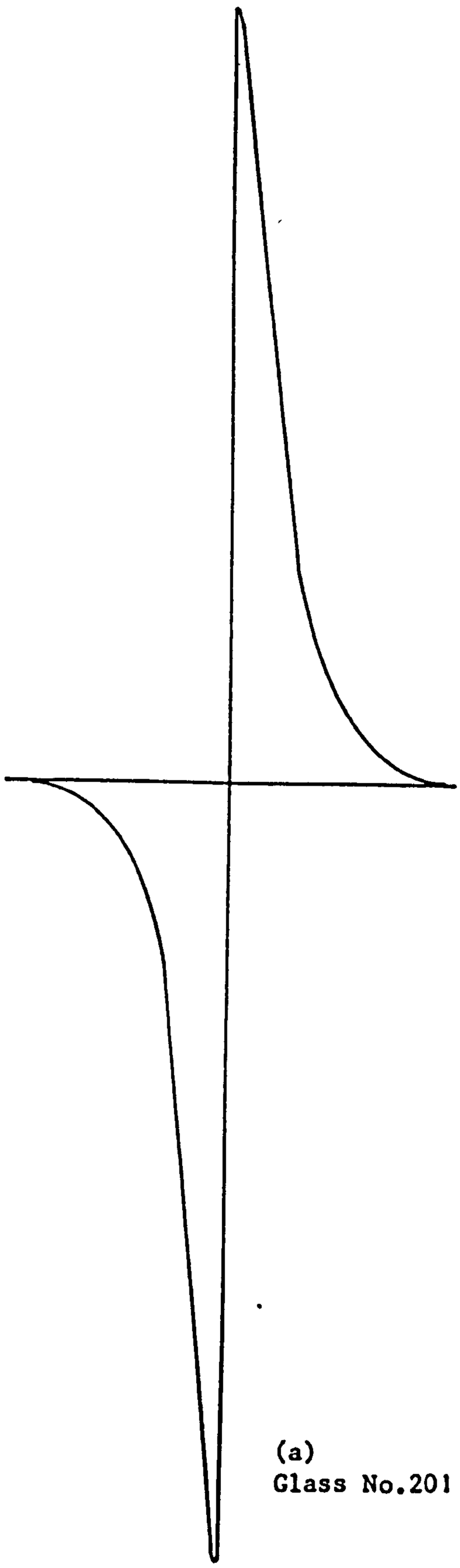

(a)
Glass No.201

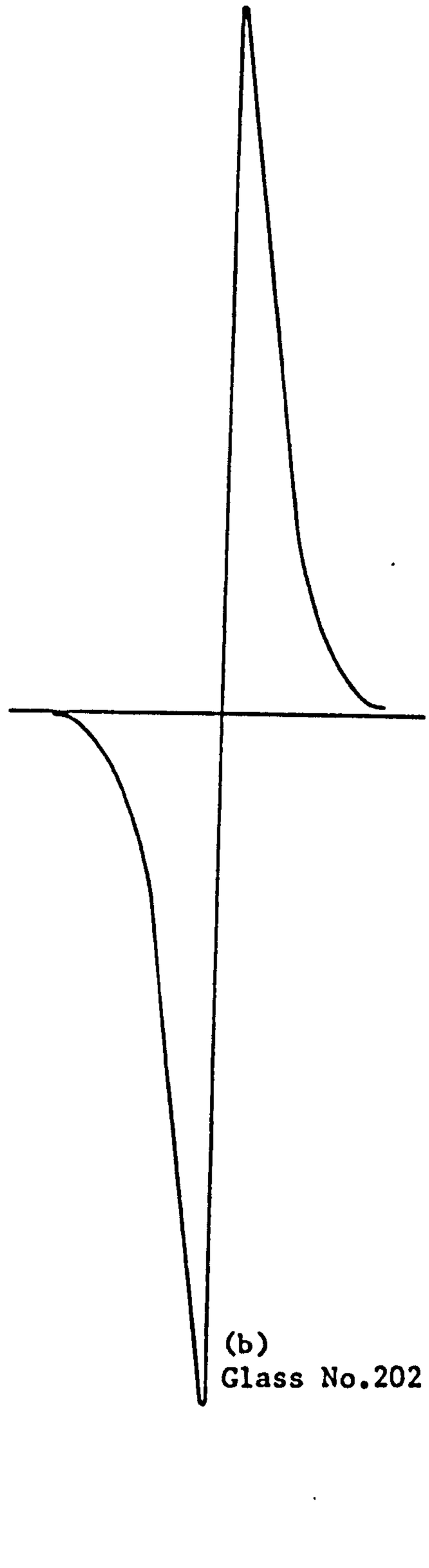

(b)
Glass No.202

Fig.(5.16) E.S.R. Spectra of $V_2O_5 - P_2O_5 - TeO_2$ Glasses with Different Composition at Room Temperature

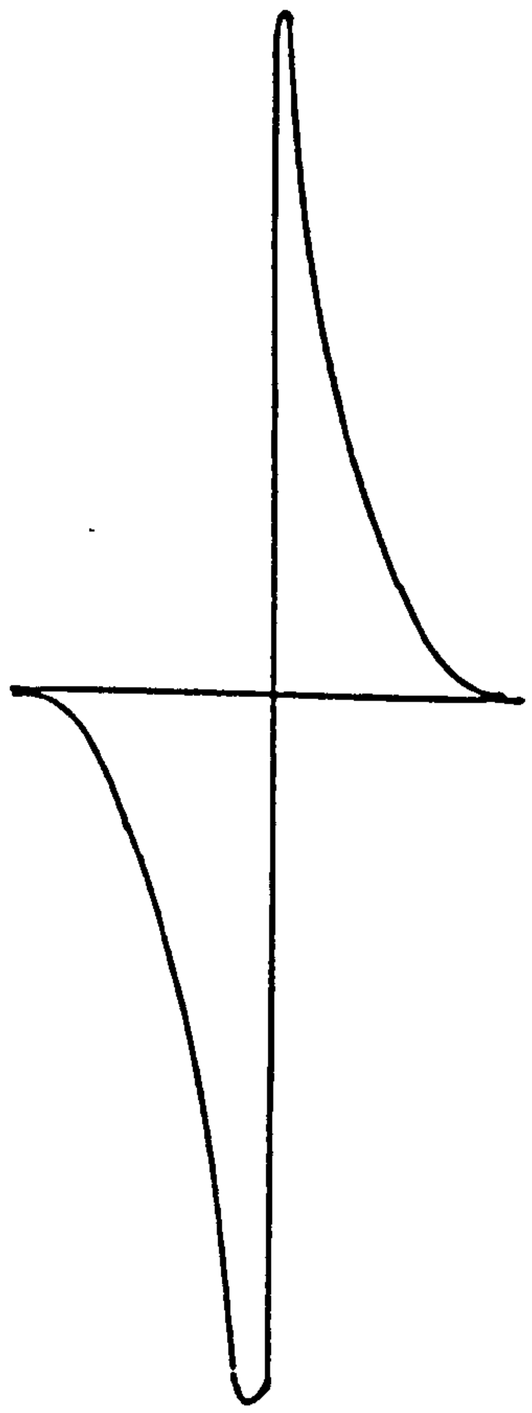

(c)
Glass No.204

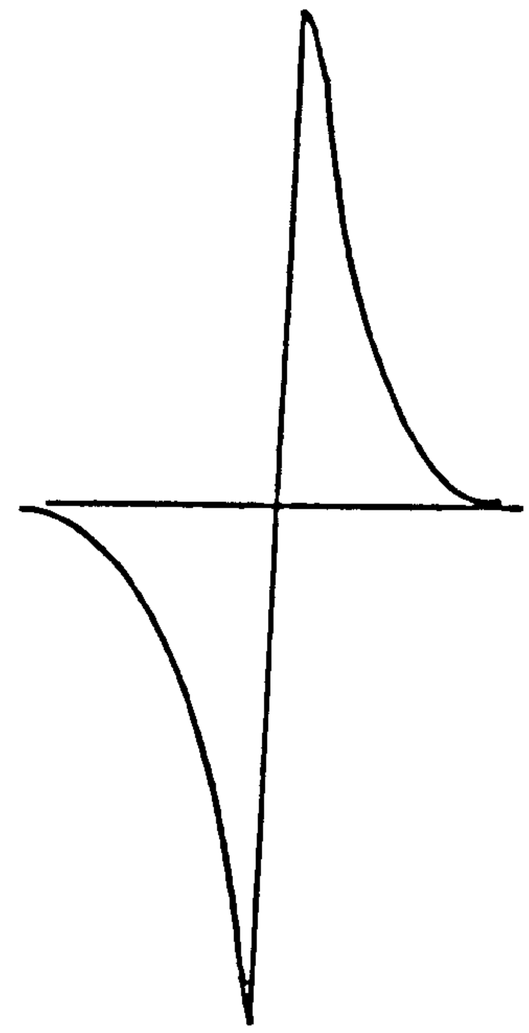

(d)
Glass No.206

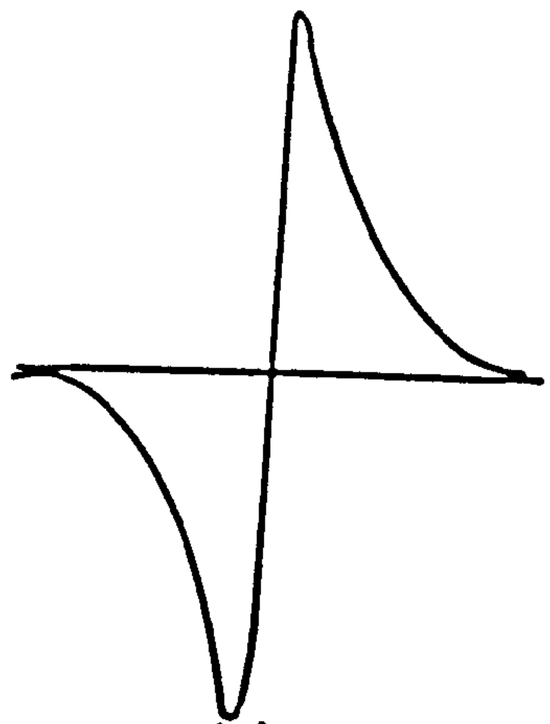

(e)
Glass No.207

Fig.(5.16)

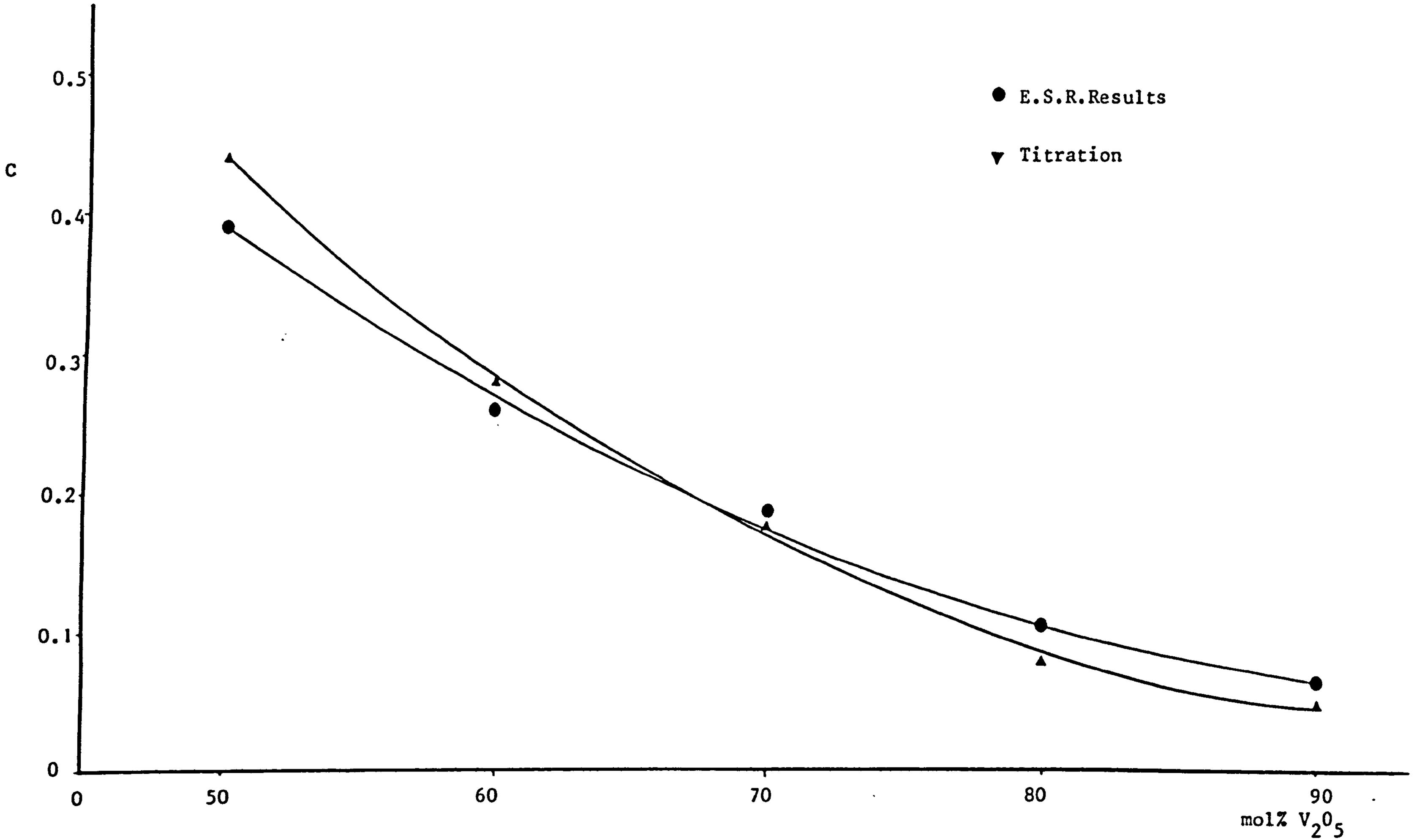

Fig.(5.18) Ratio of Reduced Valence State vs. V_2O_5 Concentration for V_2O_5 - P_2O_5 Glasses

for glass containing 60 mol% V_2O_5

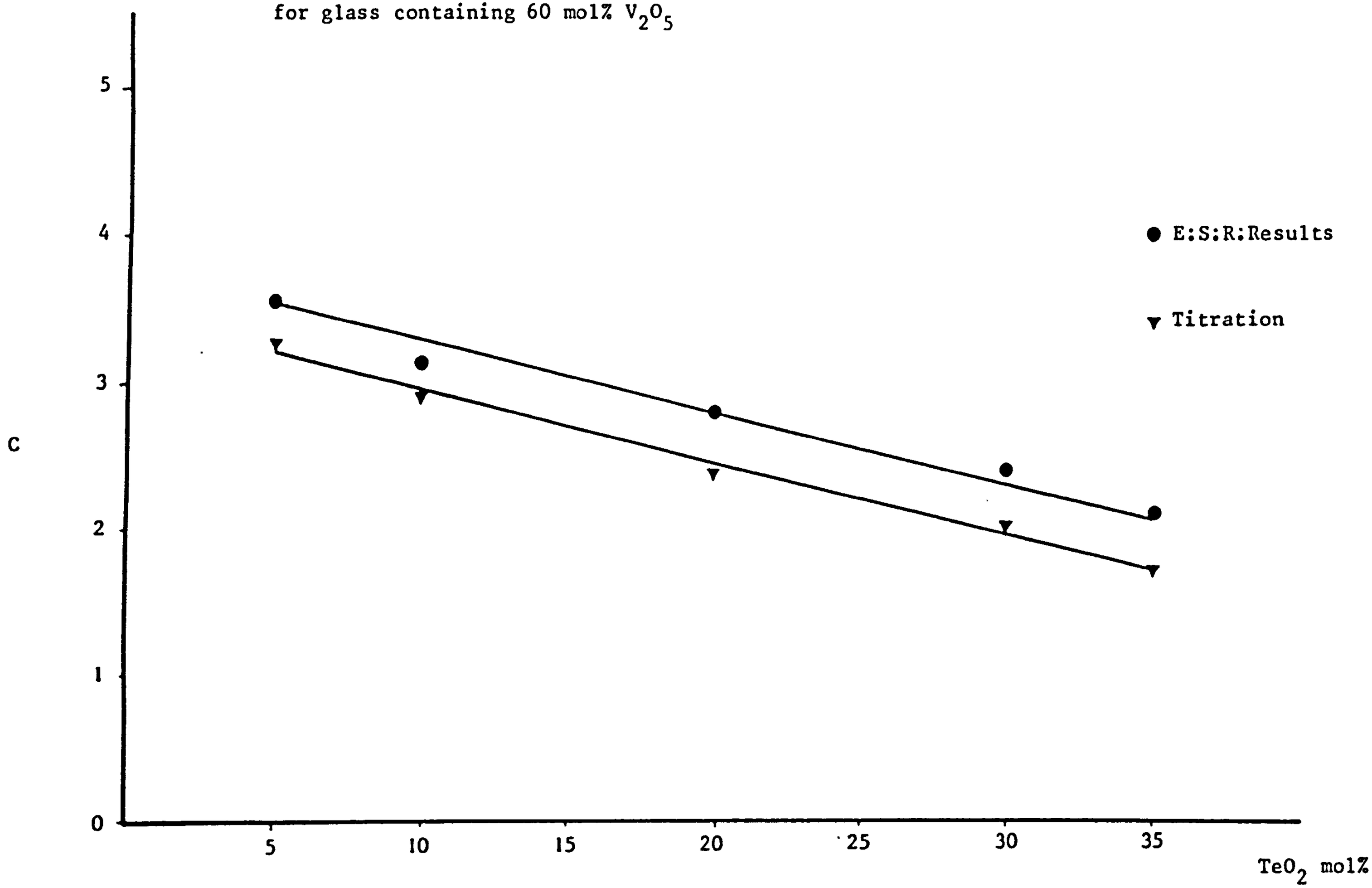

Fig.(5.19) Ratio of Reduced Valence State vs. TeO_2 Concentation for V_2O_5 - P_2O_5 Glasses

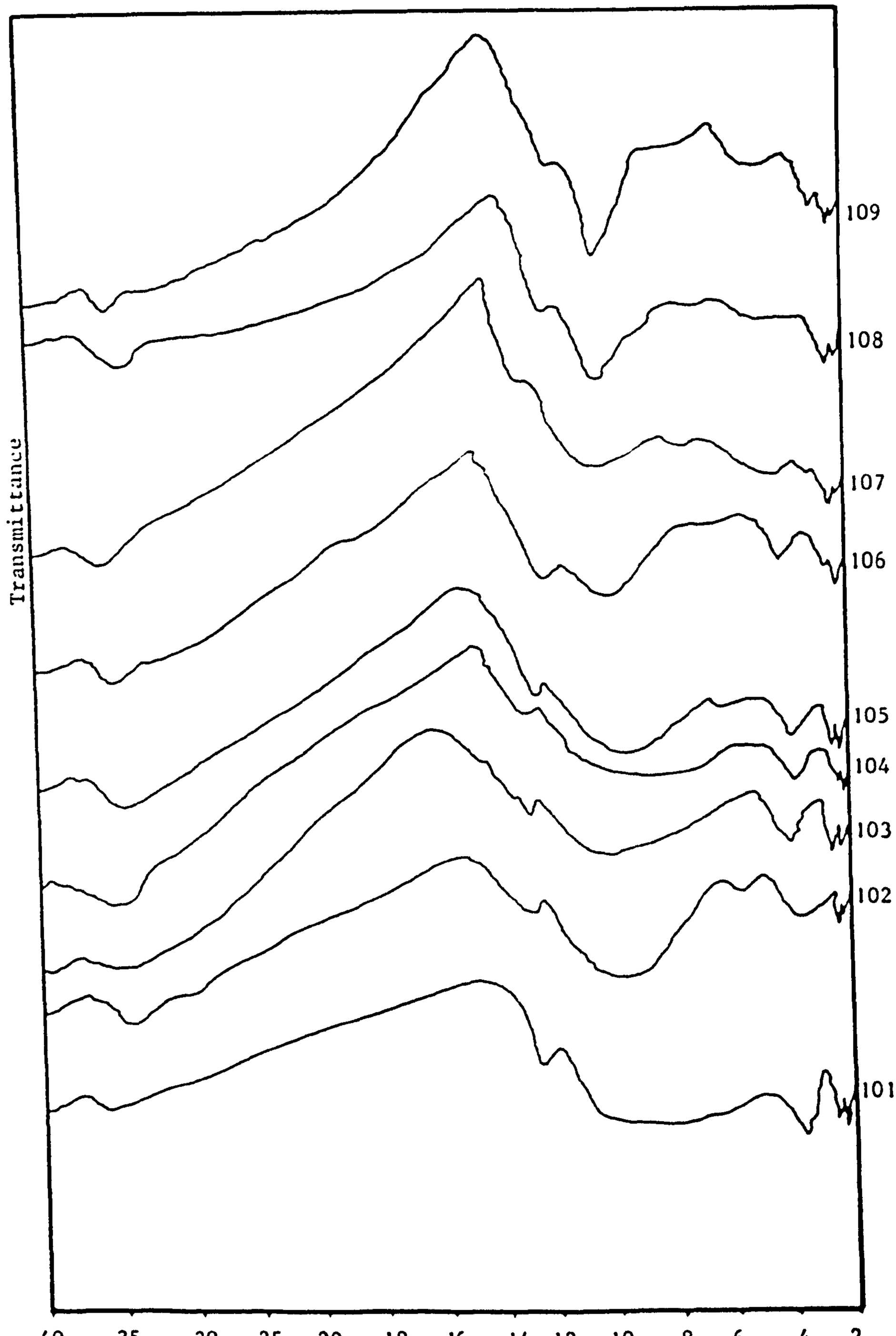

Fig.(6.1) Room Temperature Infra-red Absorption Spectra of V_2O_5 - P_2O_5 Glasses Annealed at 200°C for 2 Hours

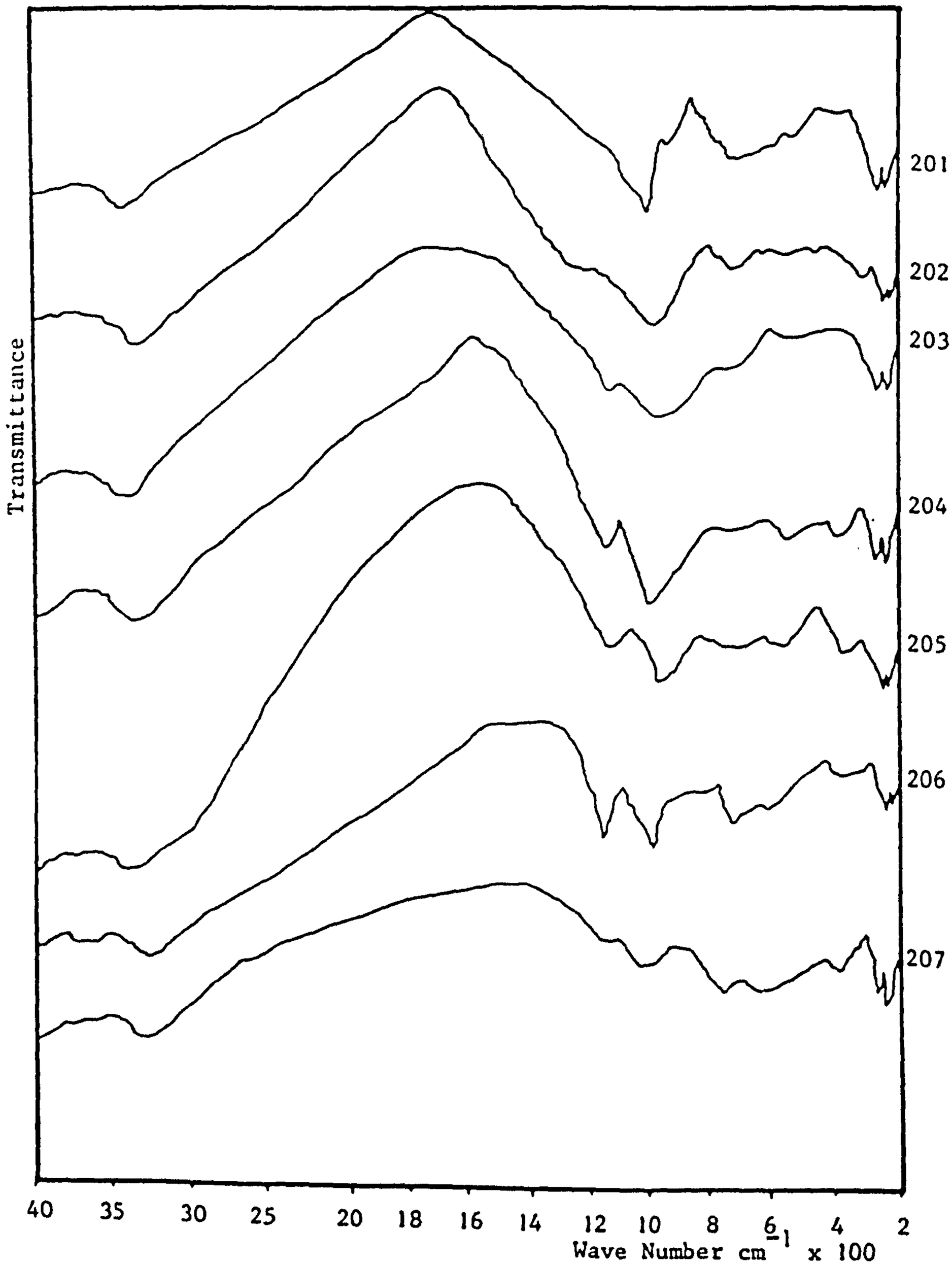

Fig.(6.2) Room Temperature Infra-red Spectra of $V_2O_5 - P_2O_5 - TeO_2$ Glasses Annealed ar 200°C for 2 Hours

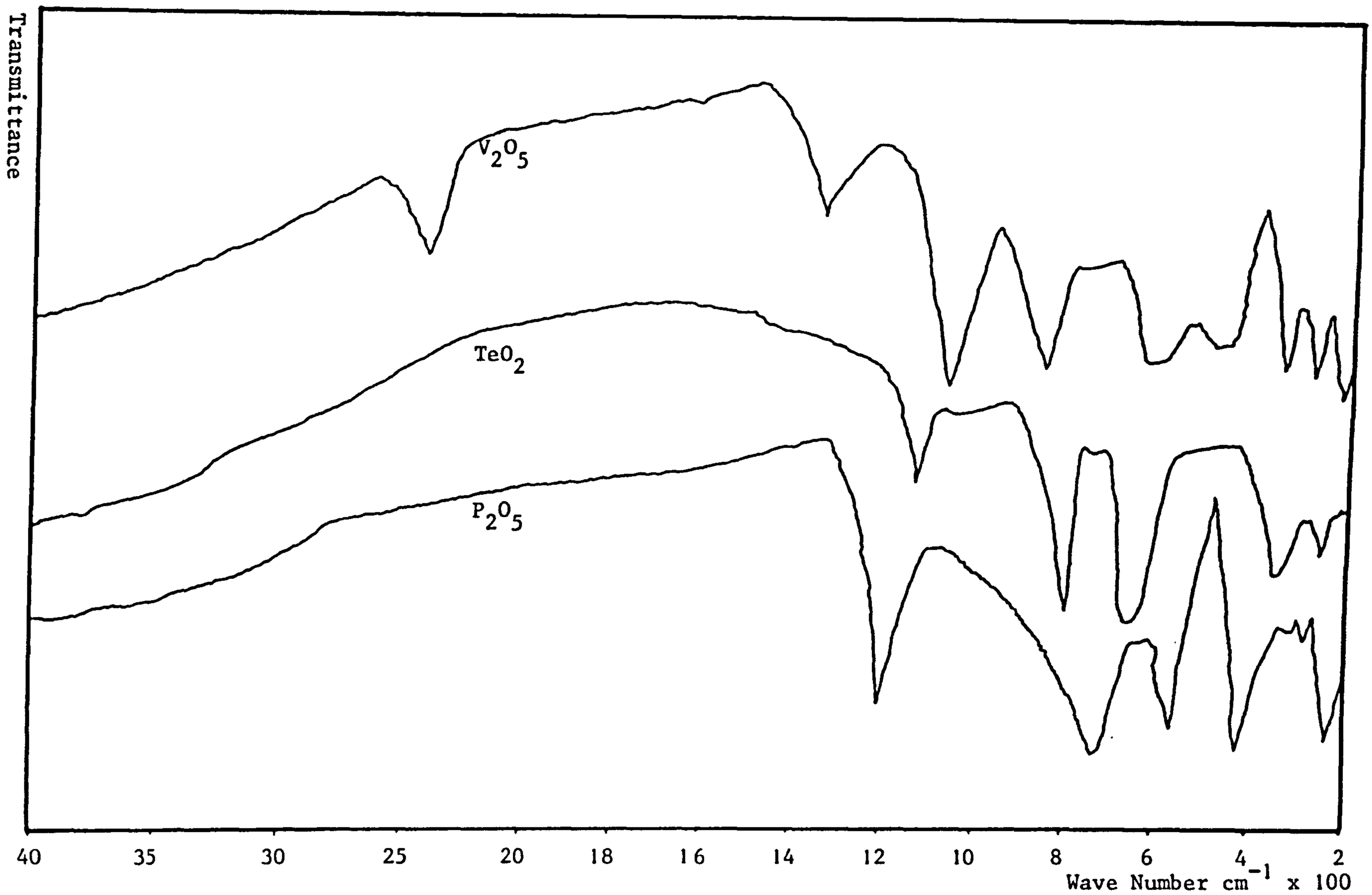

Fig.(6.3) Infra-red Absorption of $V_2O_5^{(113)}$ - $P_2O_5^{(113)}$ and $TeO_2^{(113)}$

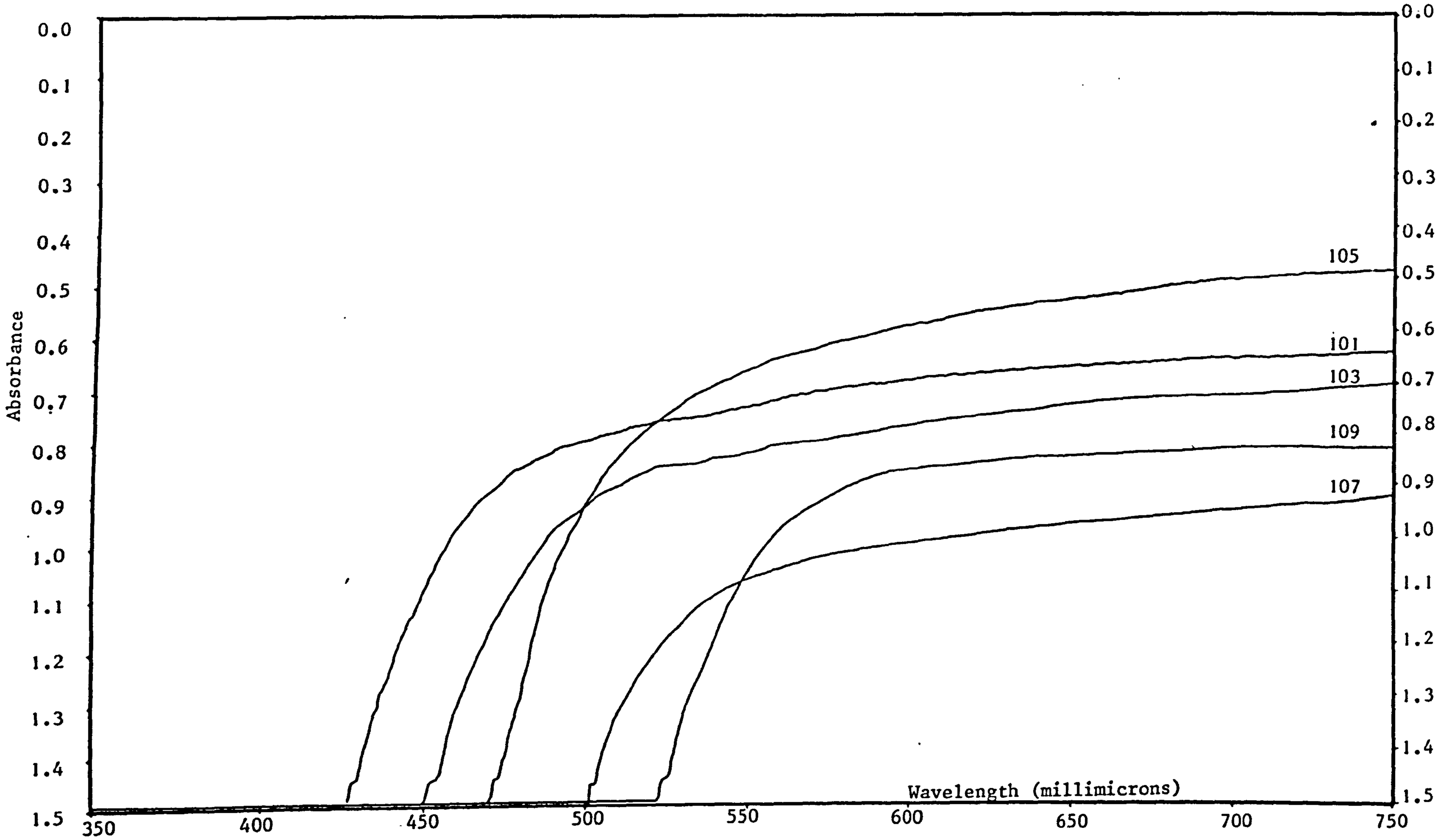

Fig.(6.4) Absorption Edge Characteristic in Visible Range for V_2O_5 - P_2O_5 Glasses

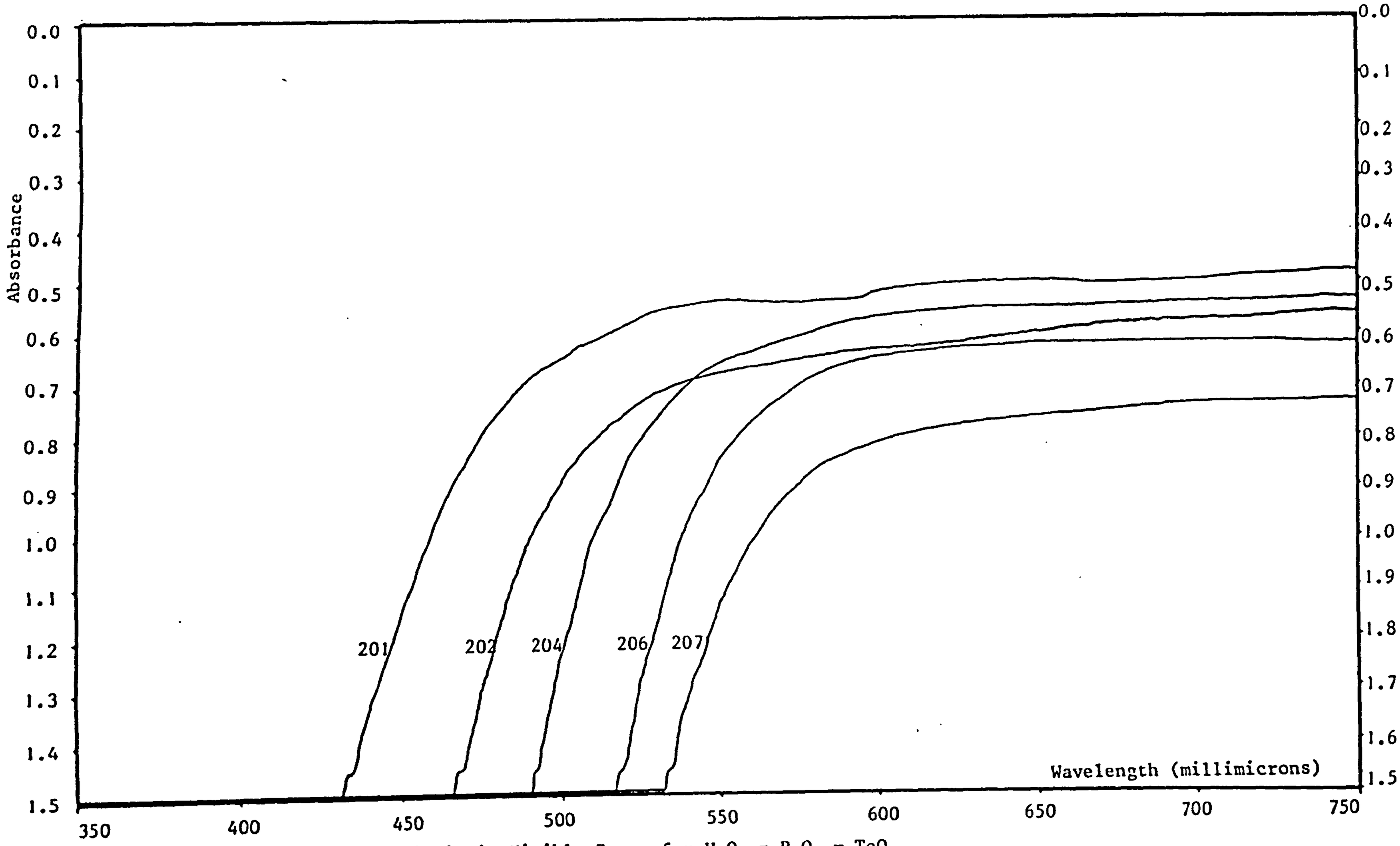

Fig.(6.5) Absorption Edge Characteristic in Visible Range fpr V_2O_5 - P_2O_5 - TeO_2

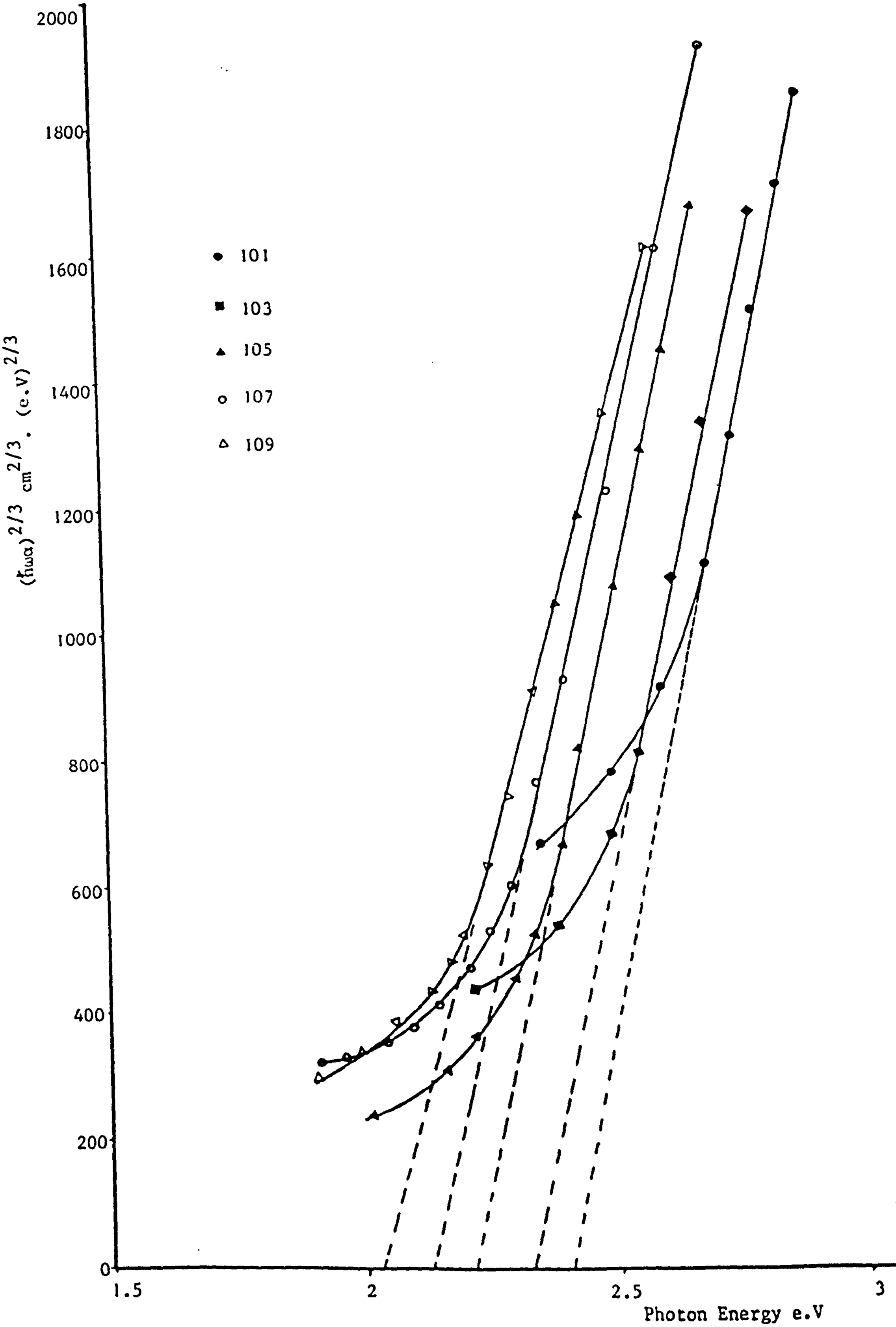

Fig.(6.6) Optical Absoption of V_2O_5 - P_2O_5 Glasses

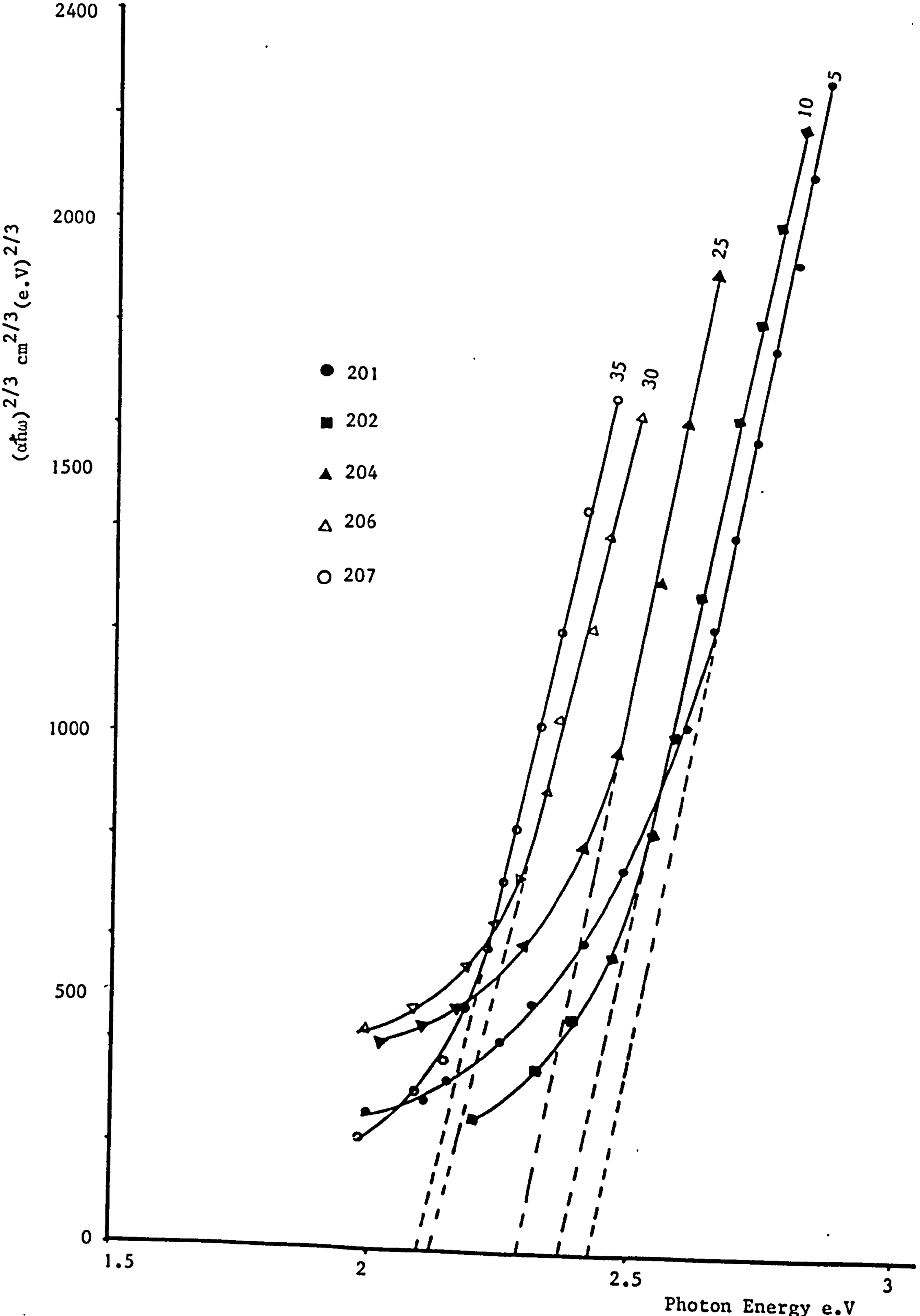

Fig.(6.7) Optical Absorption Edge for $V_2O_5 - P_2O_5 - TeO_2$ Glasses

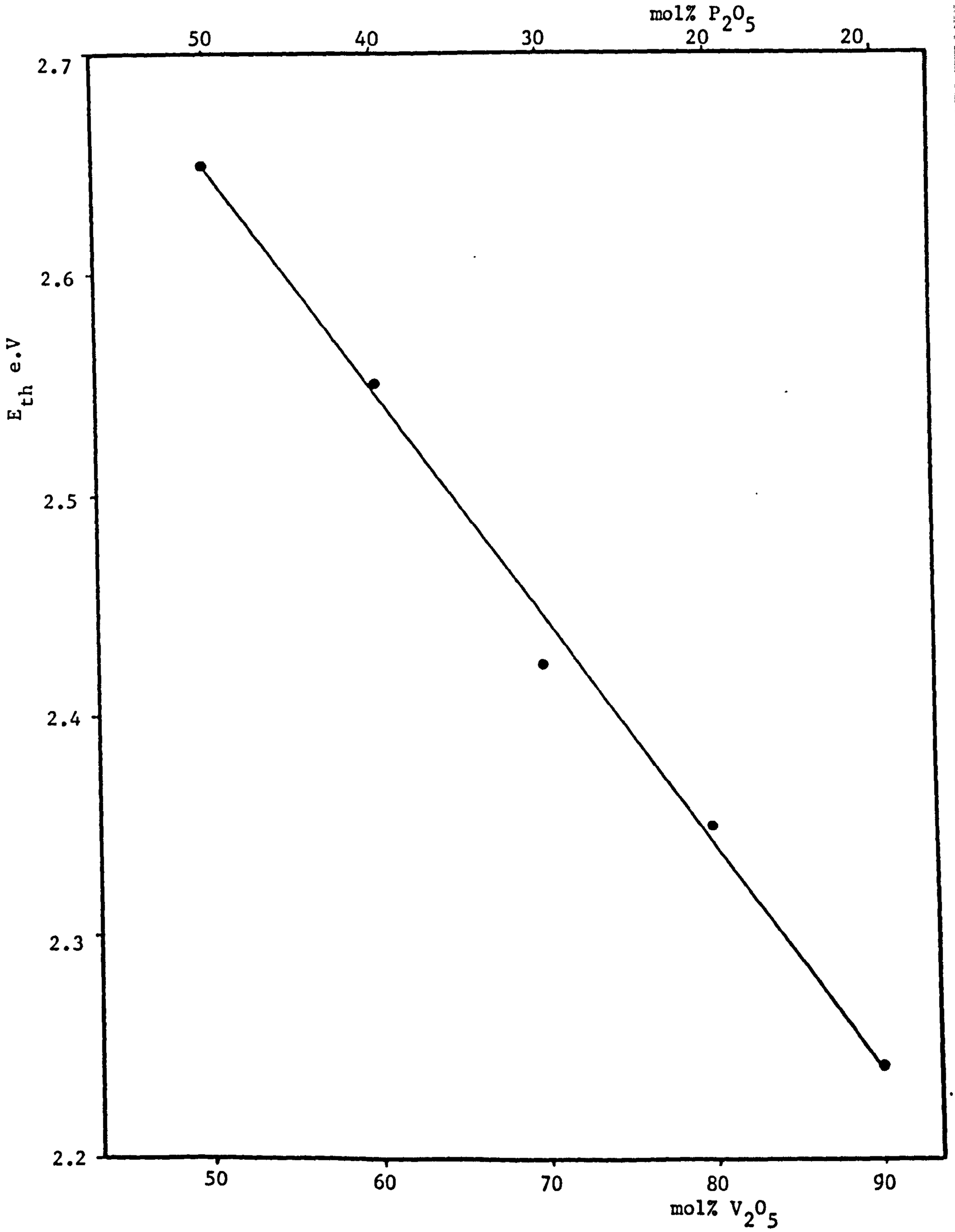

Fig.(6.8) Variation of E_{th} with V_2O_5 Content for V_2O_5 - P_2O_5 Glasses

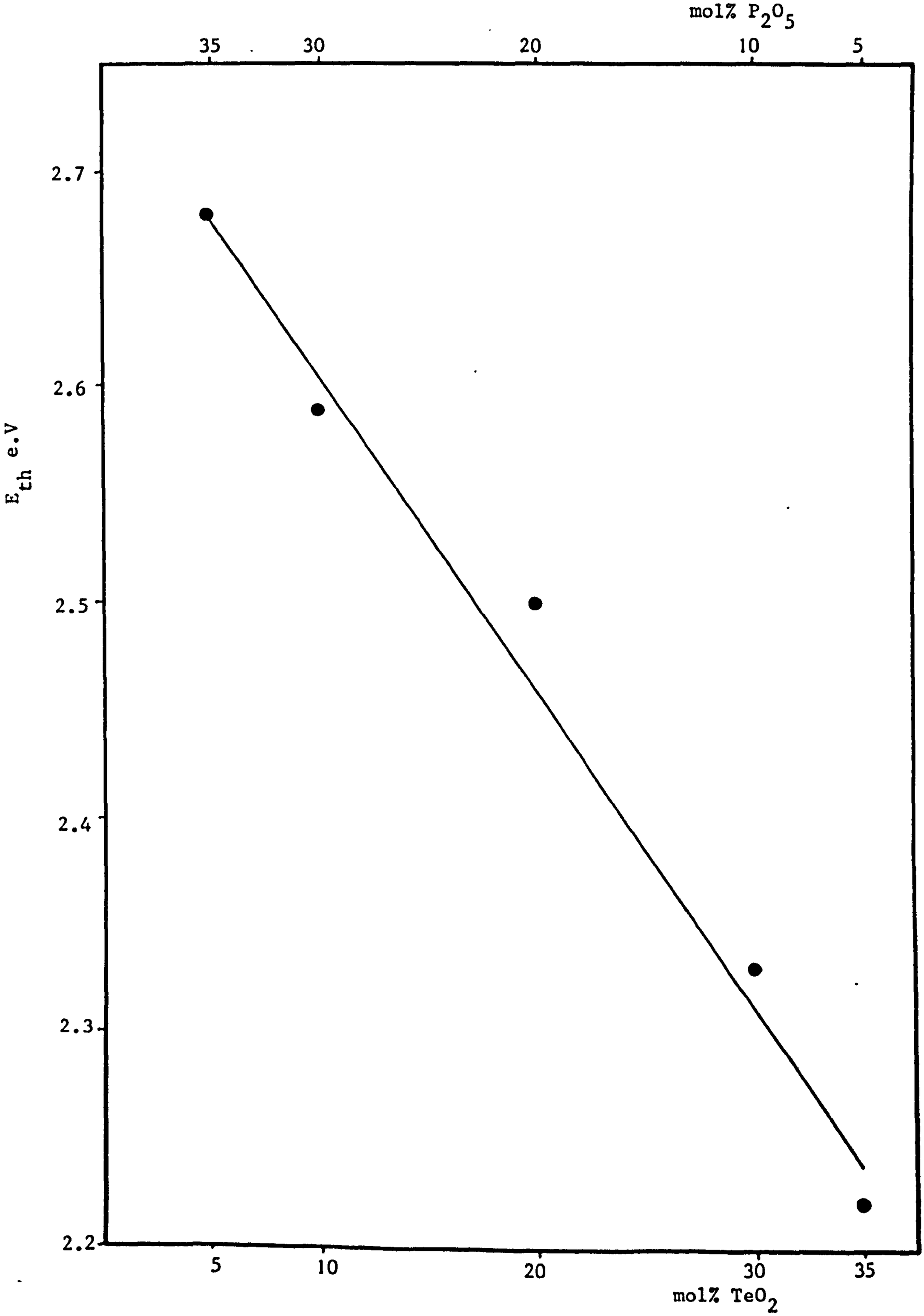

Fig.(6.9) Variation of Thermal Energy with Composition for V_2O_5 - P_2O_5 - TeO_2 Systems

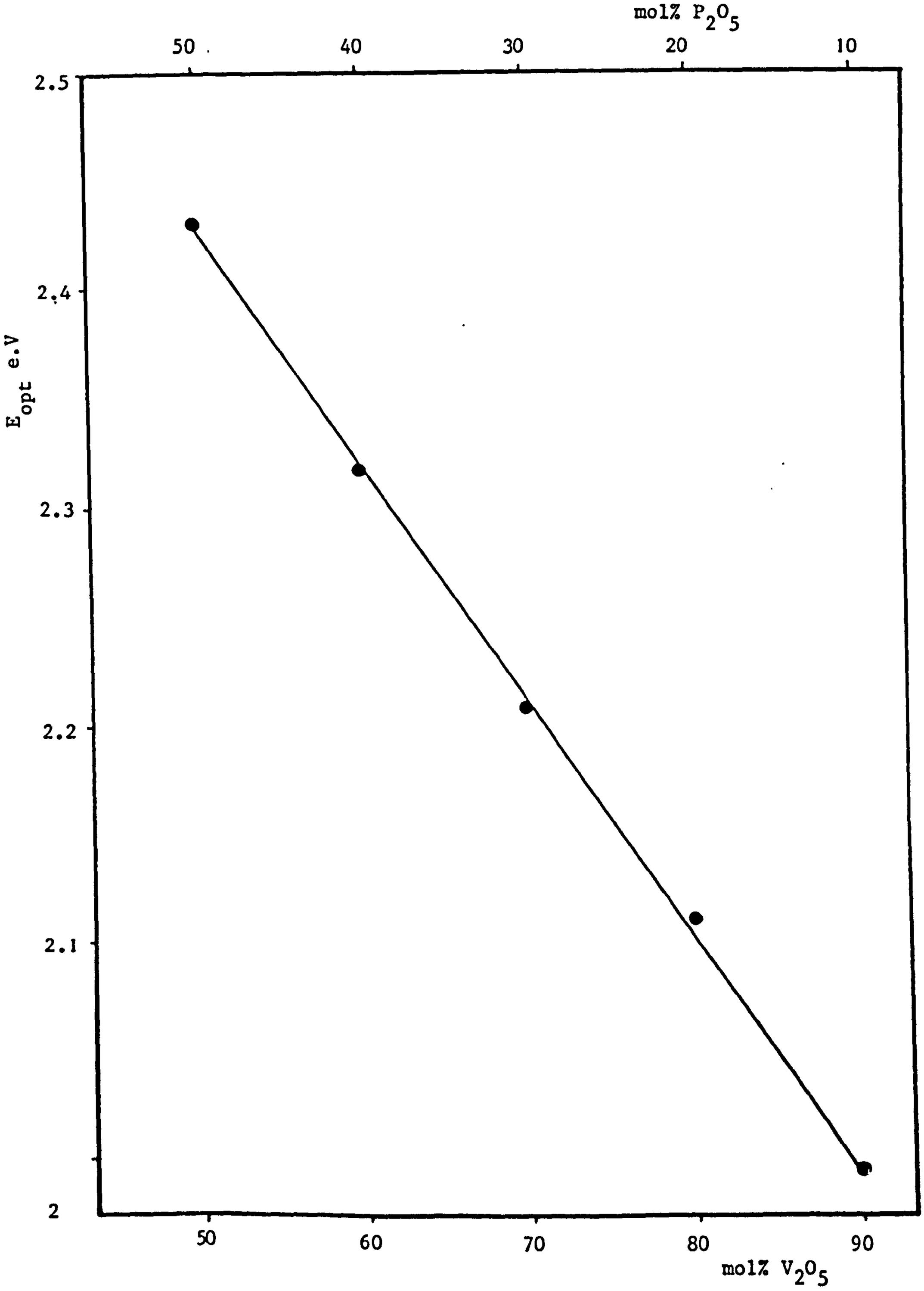

Fig.(6.10) Plot of E_{opt} vs. V_2O_5 Content for V_2O_5 - P_2O_5 Glasses

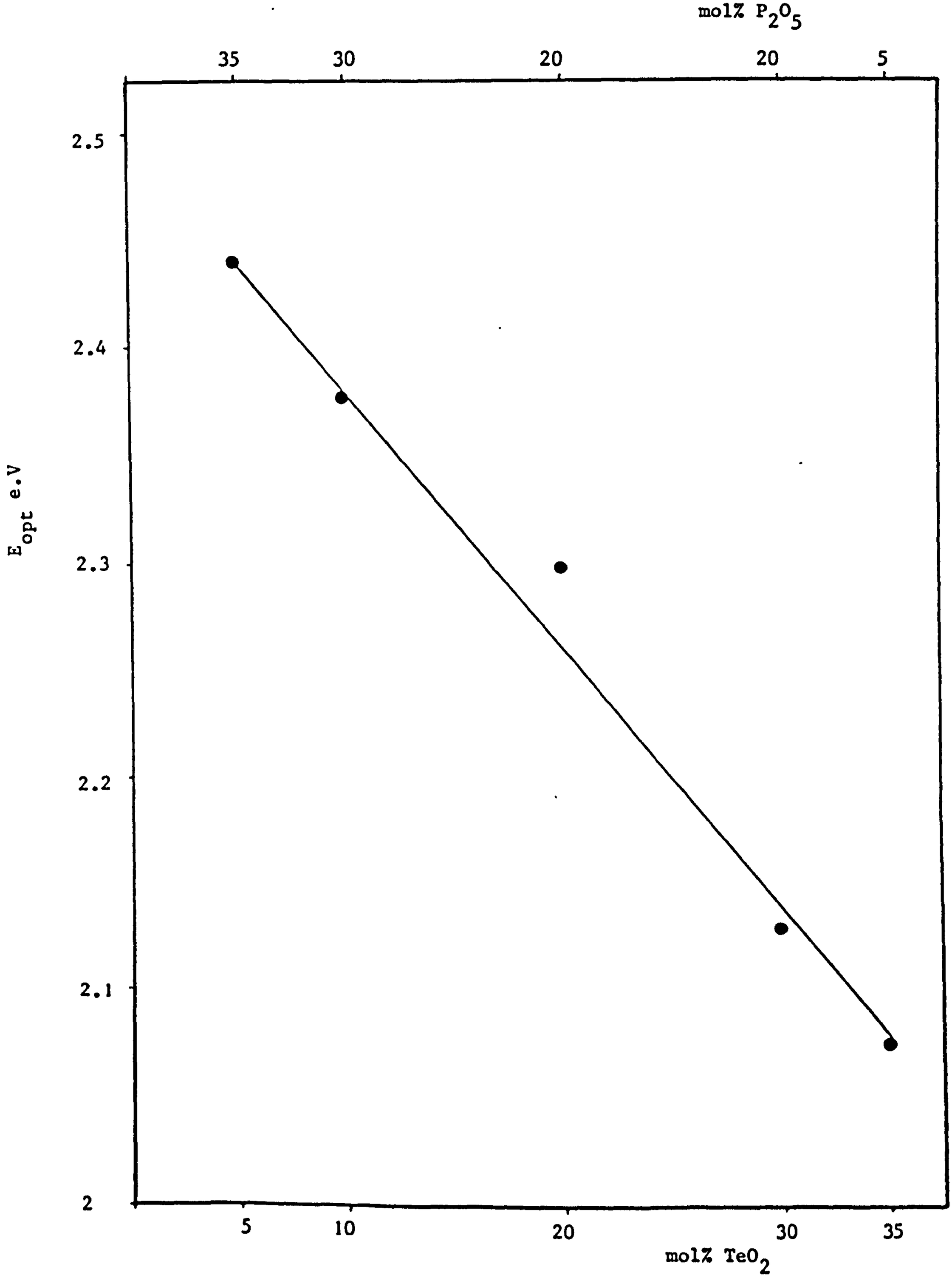

Fig.(6.11) Variation of Optical Gap with Glass Composition for V_2O_5 - P_2O_5 - TeO_2 Glasses

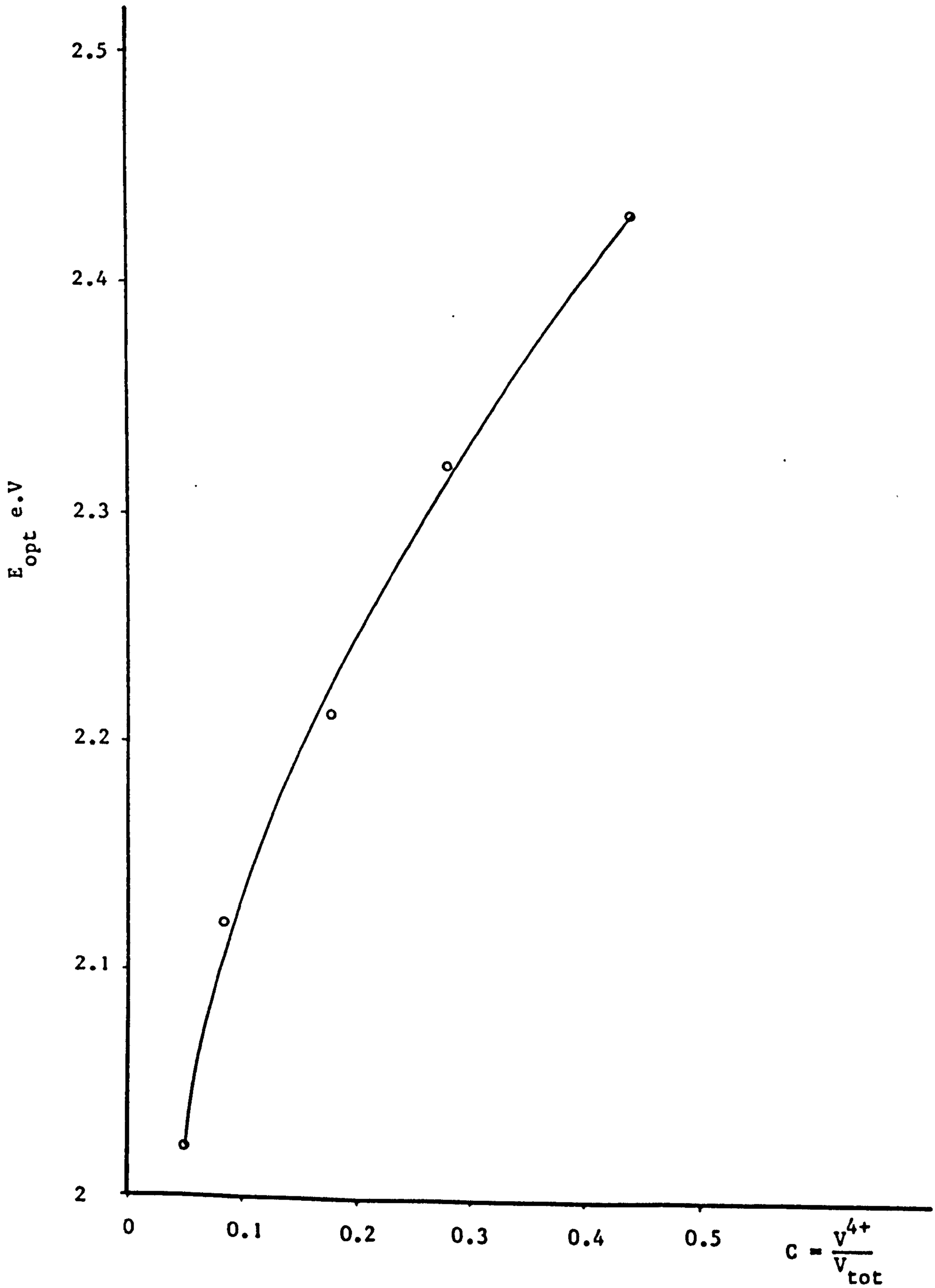

Fig.(6.12) Dependance of Optical Gap on Ratio of Reduced Valence State in $V_2O_5 - P_2O_5$ Glasses

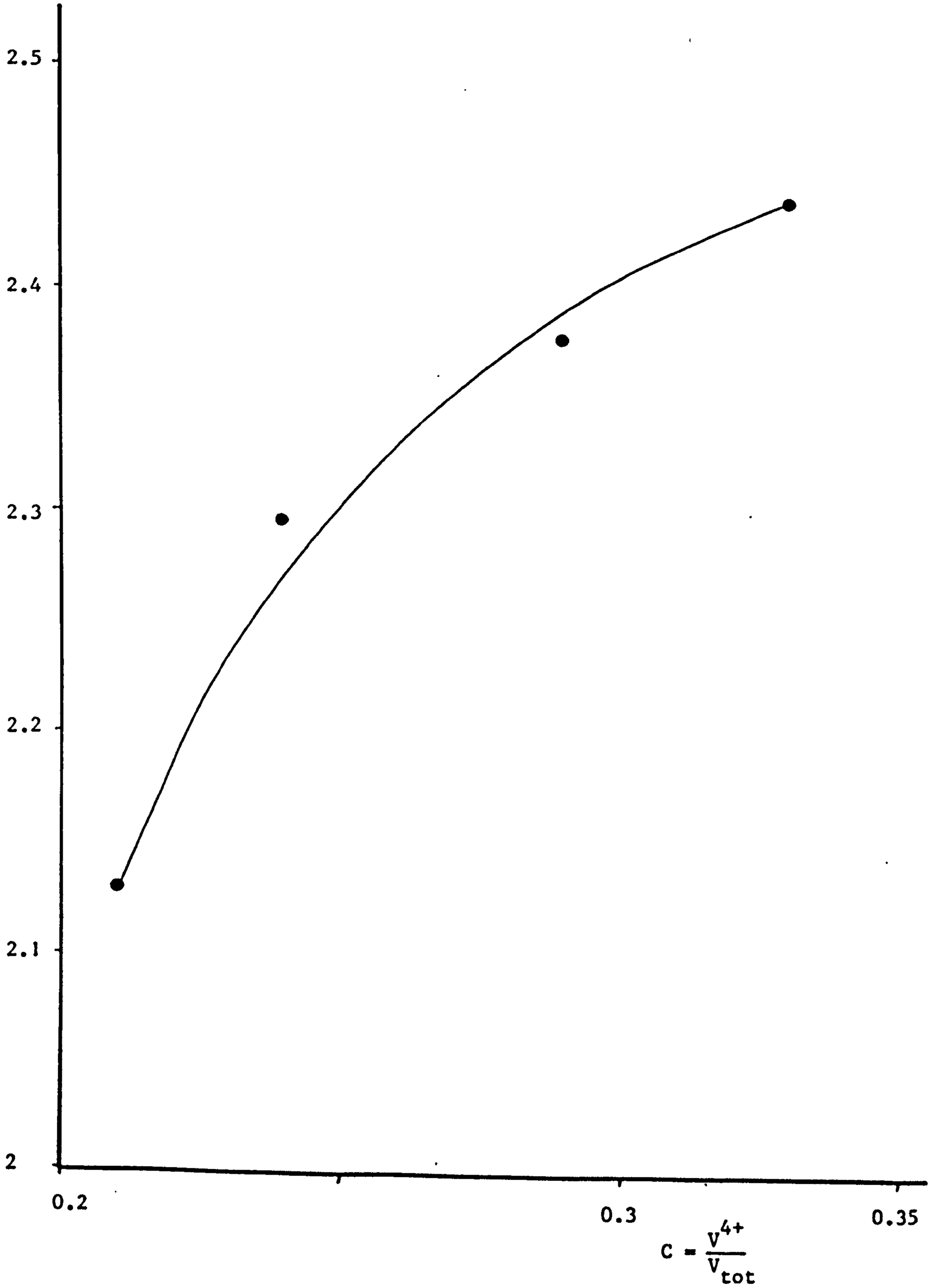

Fig.(6.13 Variation E_{opt} with C for $V_2O_5 - P_2O_5 - TeO_2$ Systems

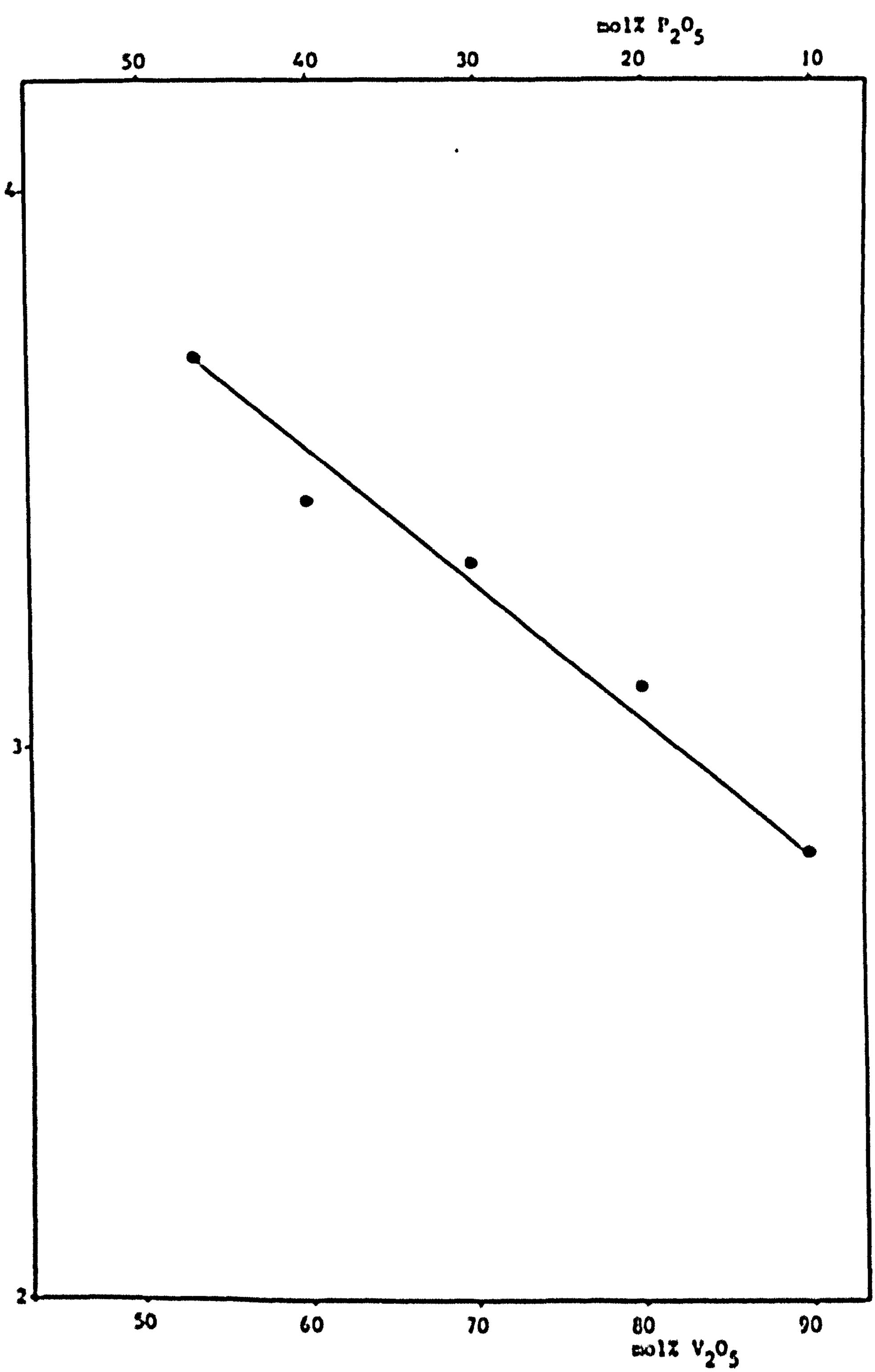

Fig.(6.14 Variation of A (slope of $(\alpha\hbar\omega)^{2/3}$ vs. $\hbar\omega$) with Glass Composition for V_2O_5 - P_2O_5 Glasses

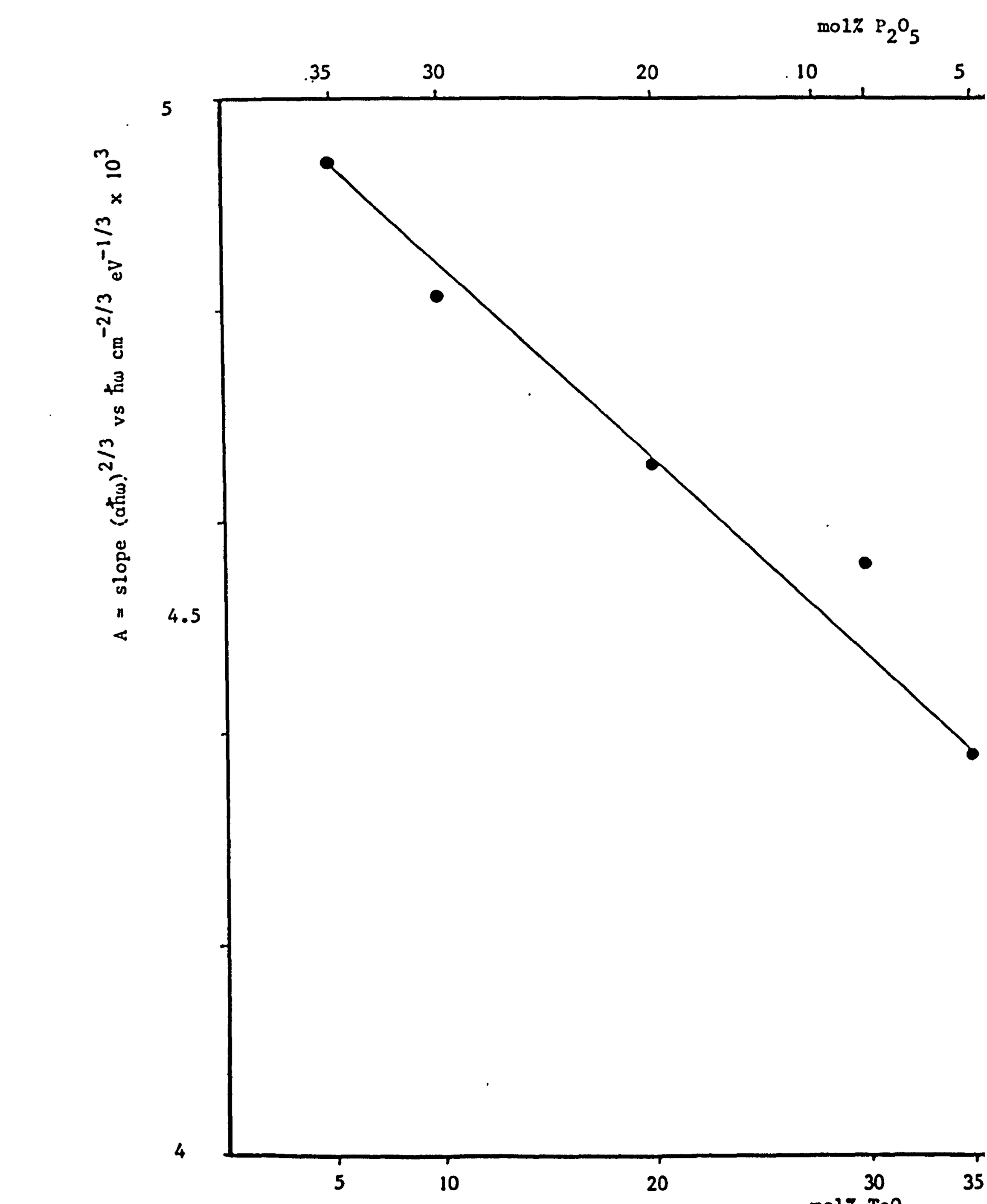

Fig.(6.15) Variation of A with Glass Composition for V_2O_5 - P_2O_5 - TeO_2 Glass Systems

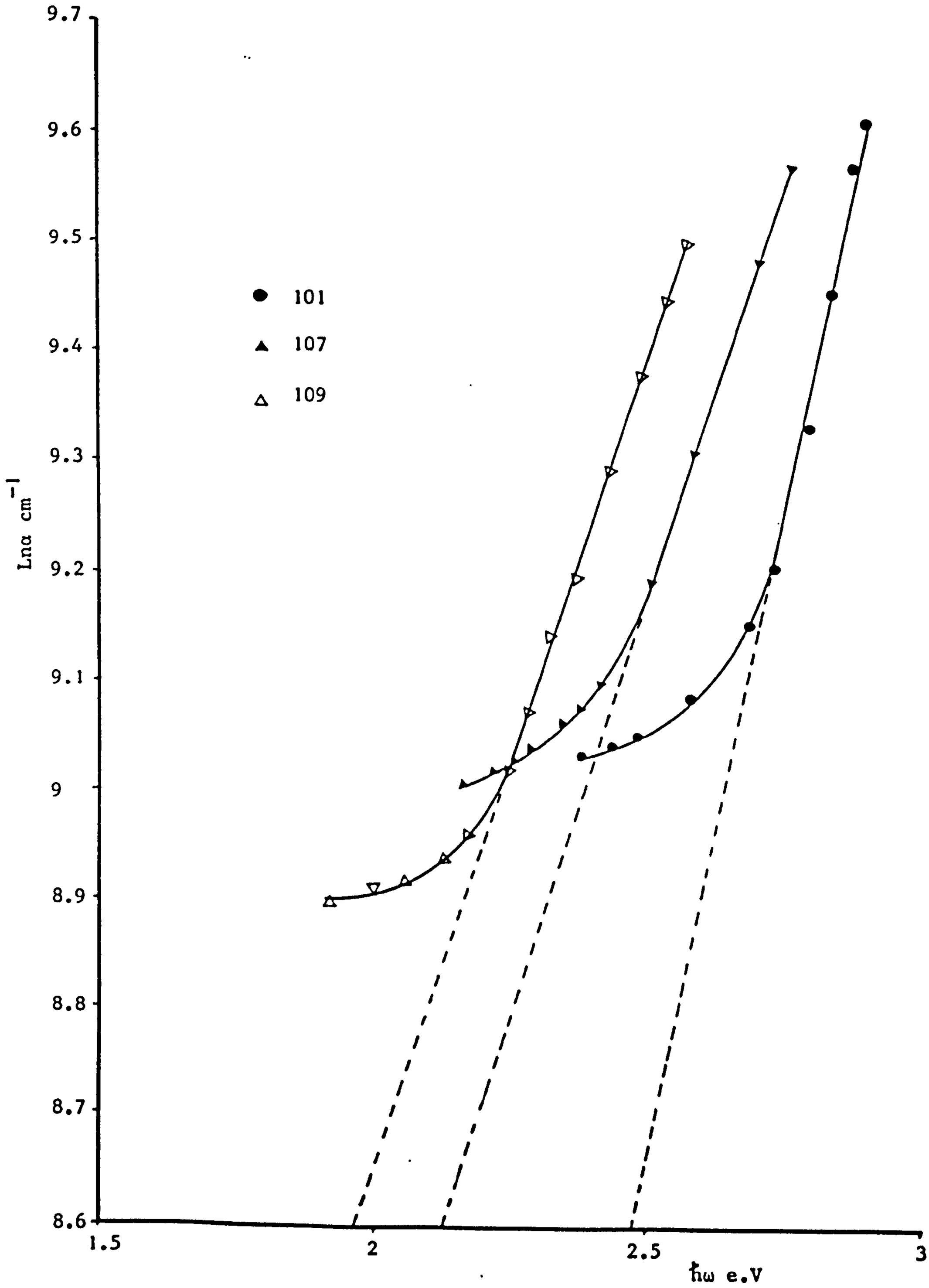

Fig.(6.16) Optical Absorption Coefficient vs. Photon Energy for $V_2O_5 - P_2O_5$ Glasses

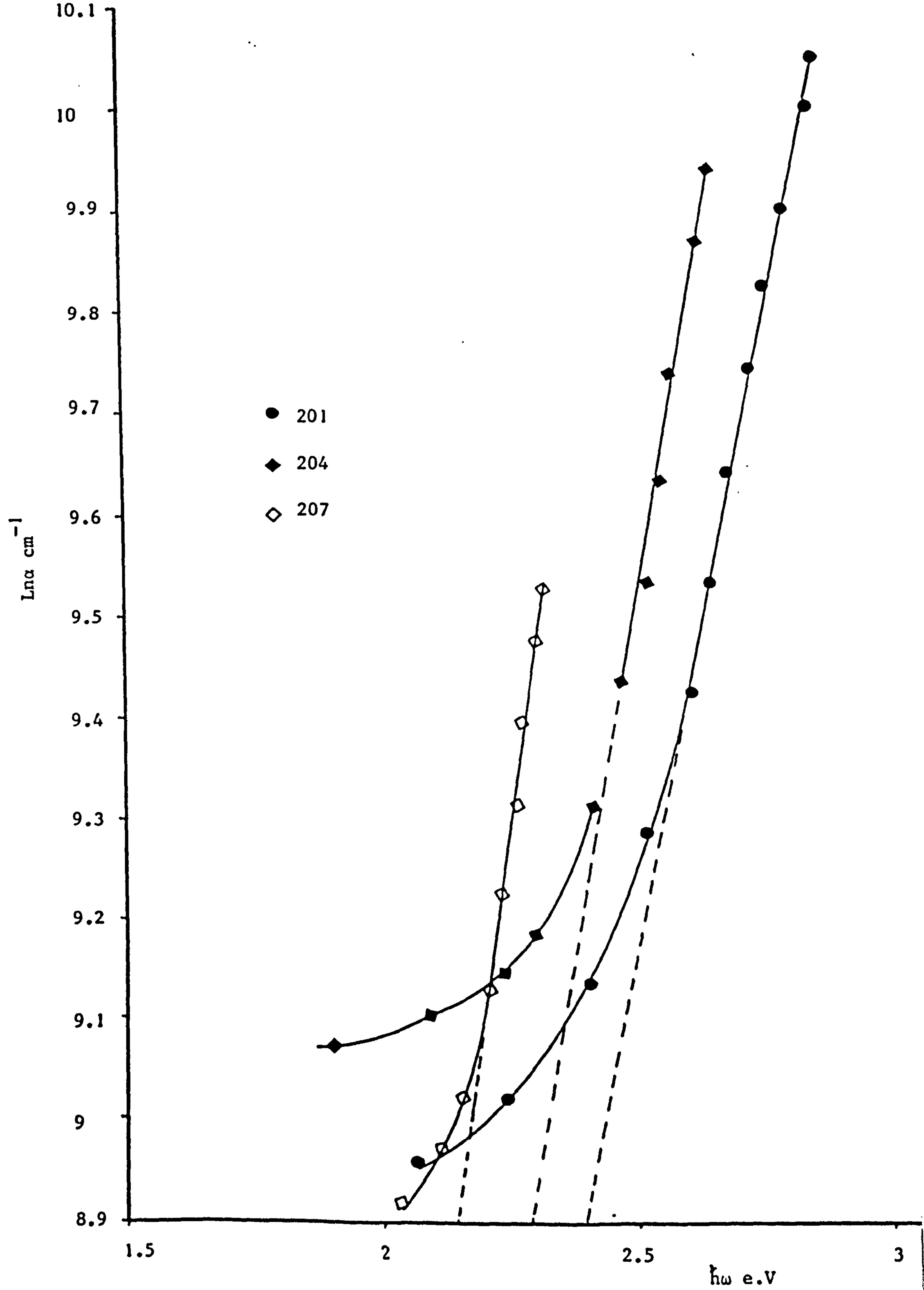

Fig.(6.17) Optical Absorption Coefficient vs. Photon Energy for V_2O_5 - P_2O_5 - TeO_2 Glass

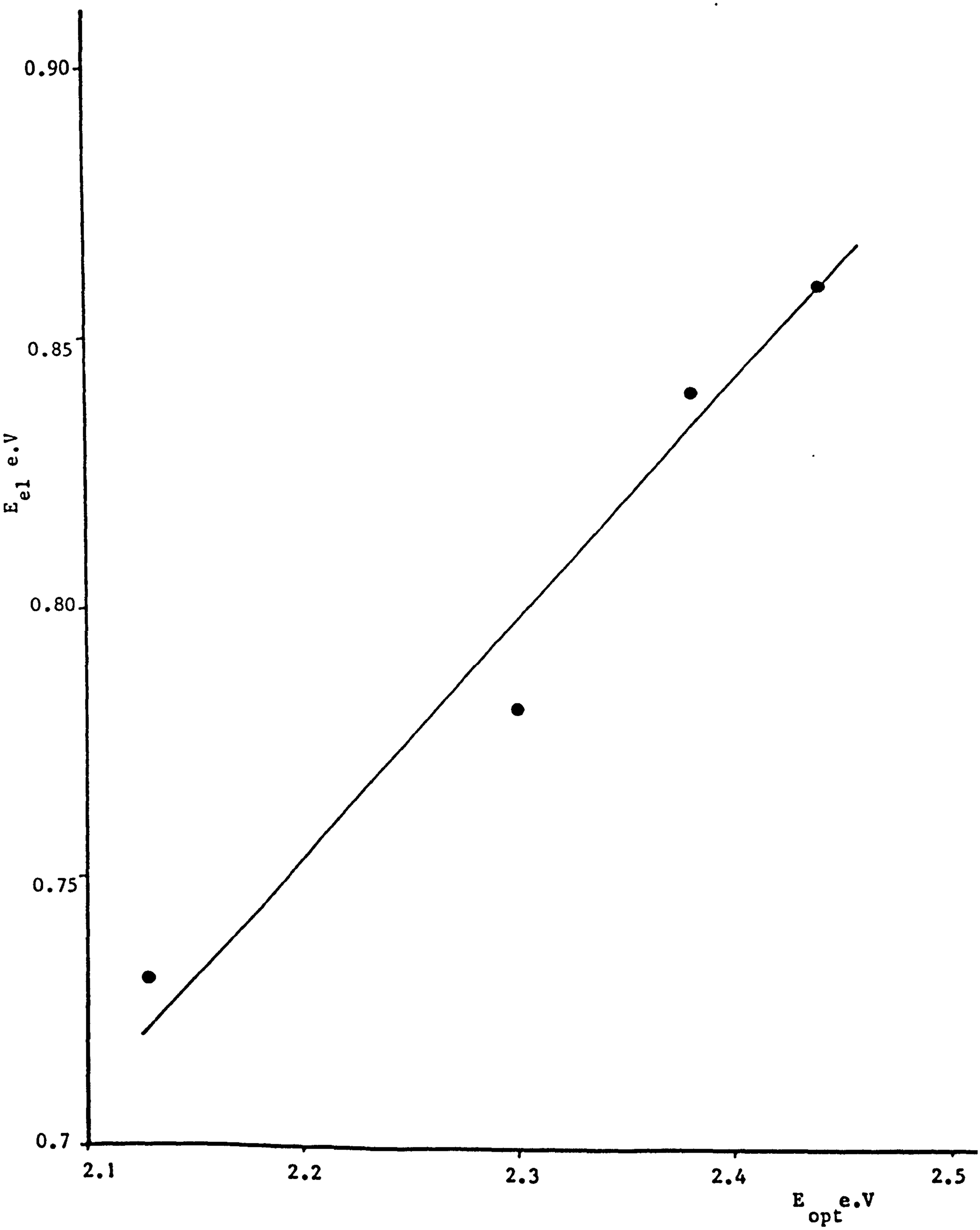

Fig.(6.19) Variation of E_{opt} with E_{el} for V_2O_5 - P_2O_5 -.TeO_2 Glass Systems

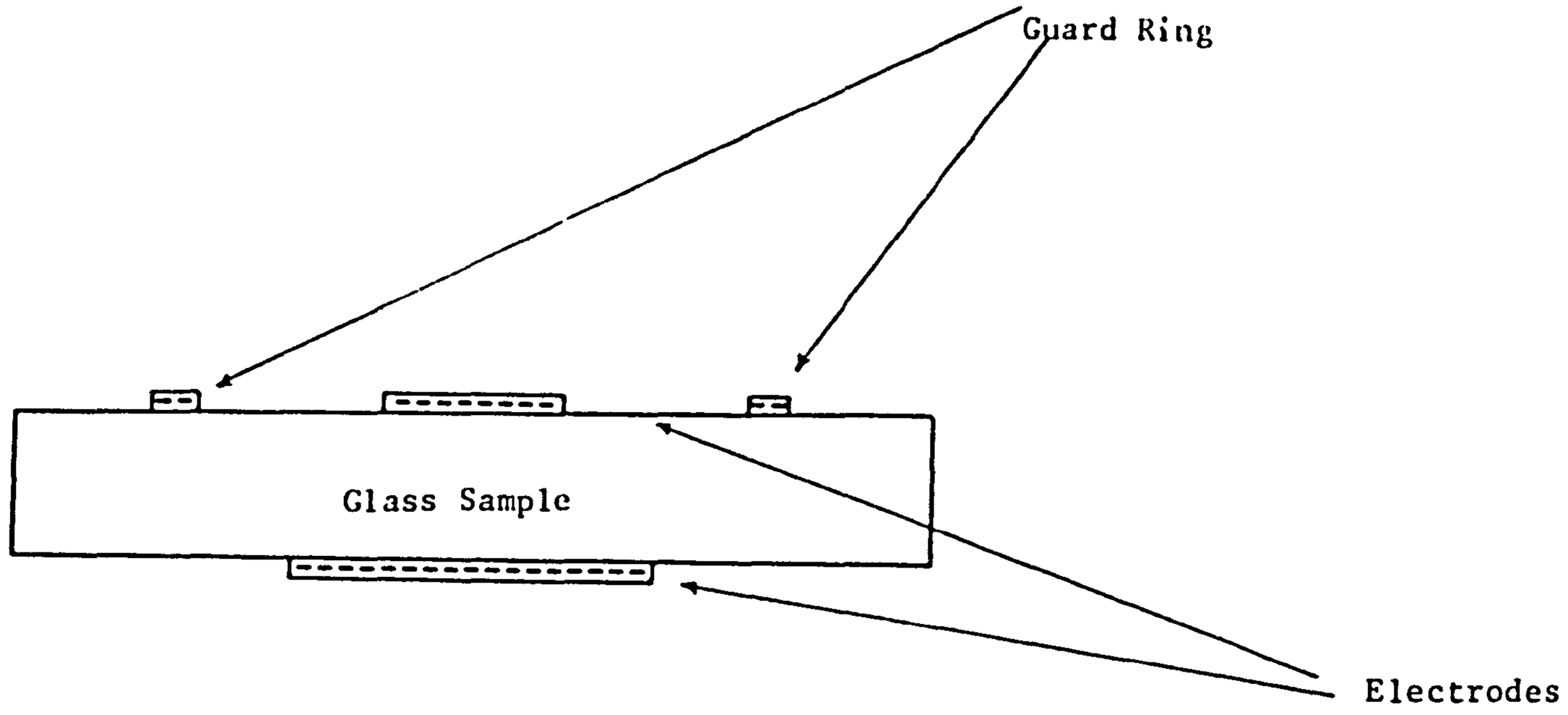

Fig.(7.1) Sample with Electrodes and Guard Ring Deposited for Electrical Measurements

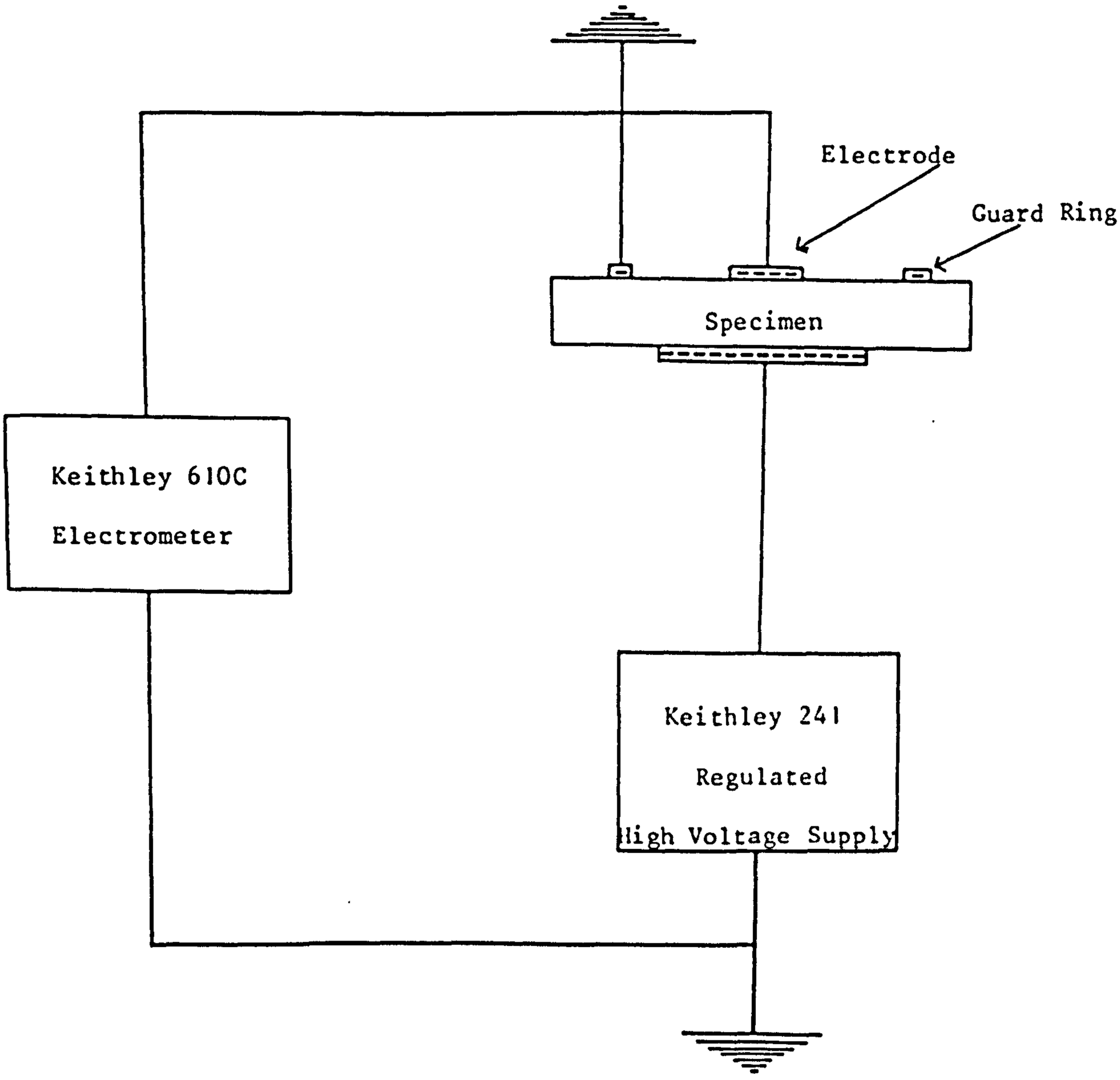

Fig.(7.2) Electrical Circuit used for Conductivity Measurement

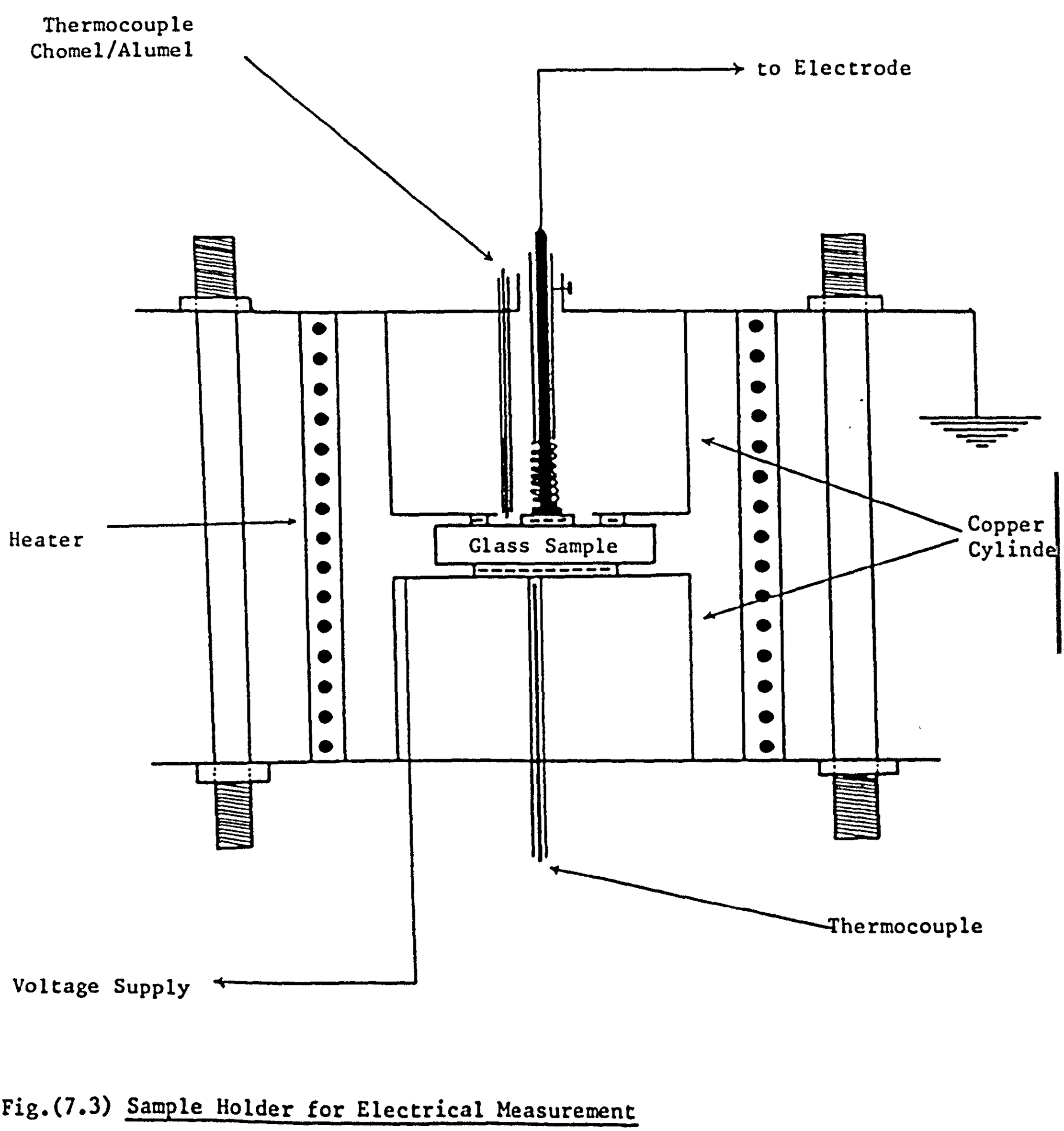

Fig.(7.3) Sample Holder for Electrical Measurement

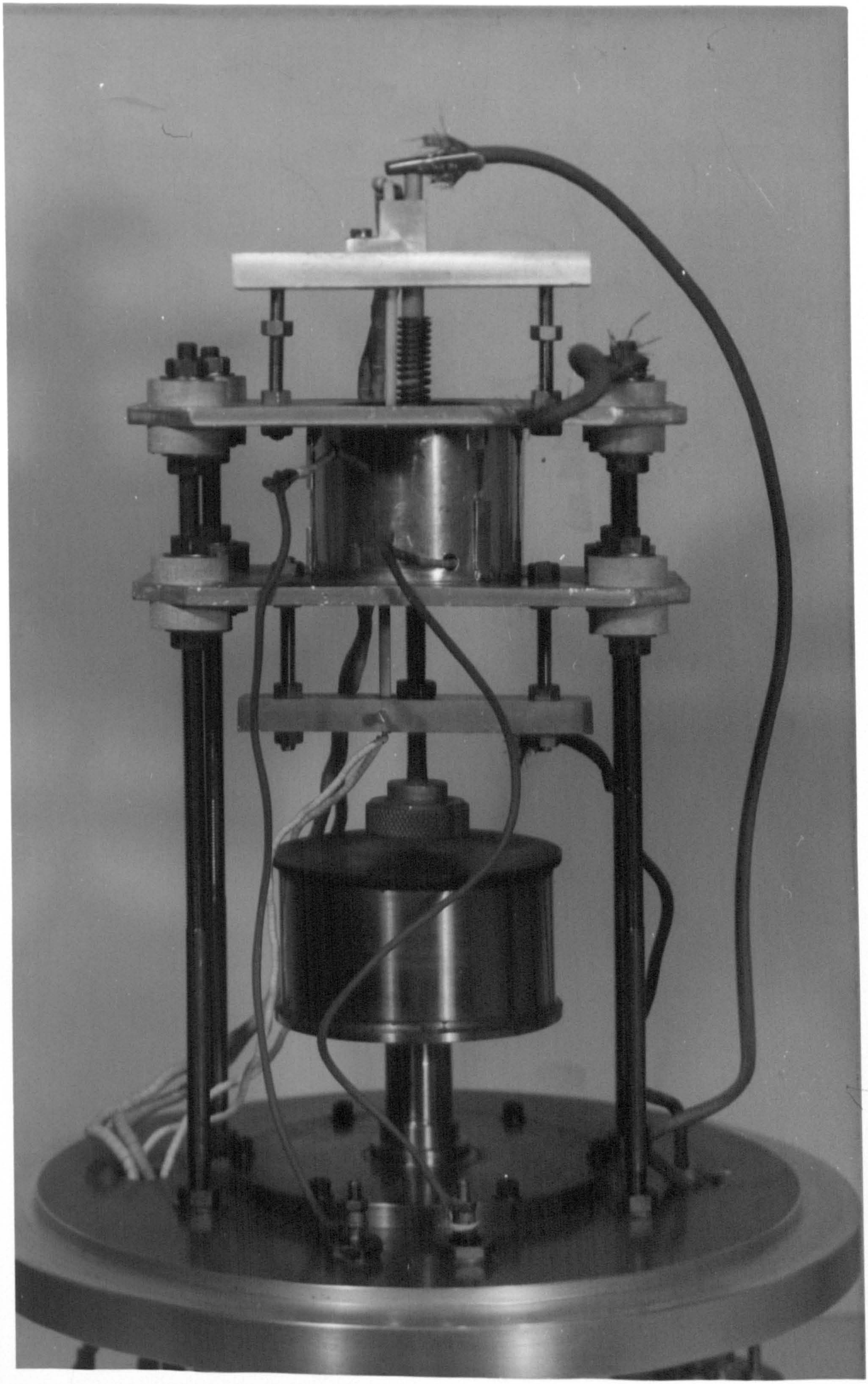

Fig.(7.4) Sample Holder for Conductivity at Low Electric Field

Fig.(7.5) Aparatus used for d.c. Electrical Measurements Under Vacuum

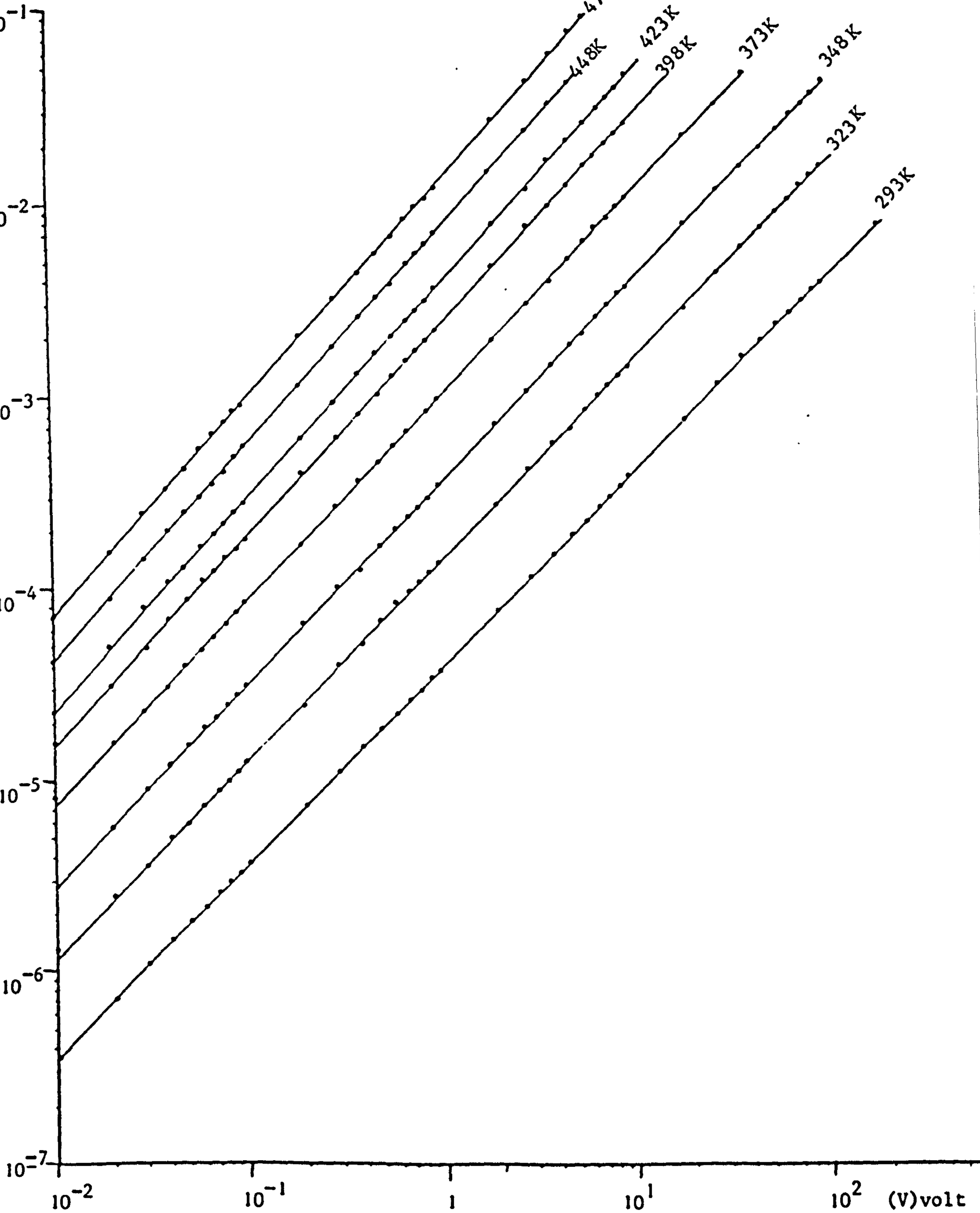

Fig.(7.6) Typical I - V Characteristic for Glass Containing 75 mol% V_2O_5 - 25 mol% P_2O_5 at Low Electric Field at Different Temperatures

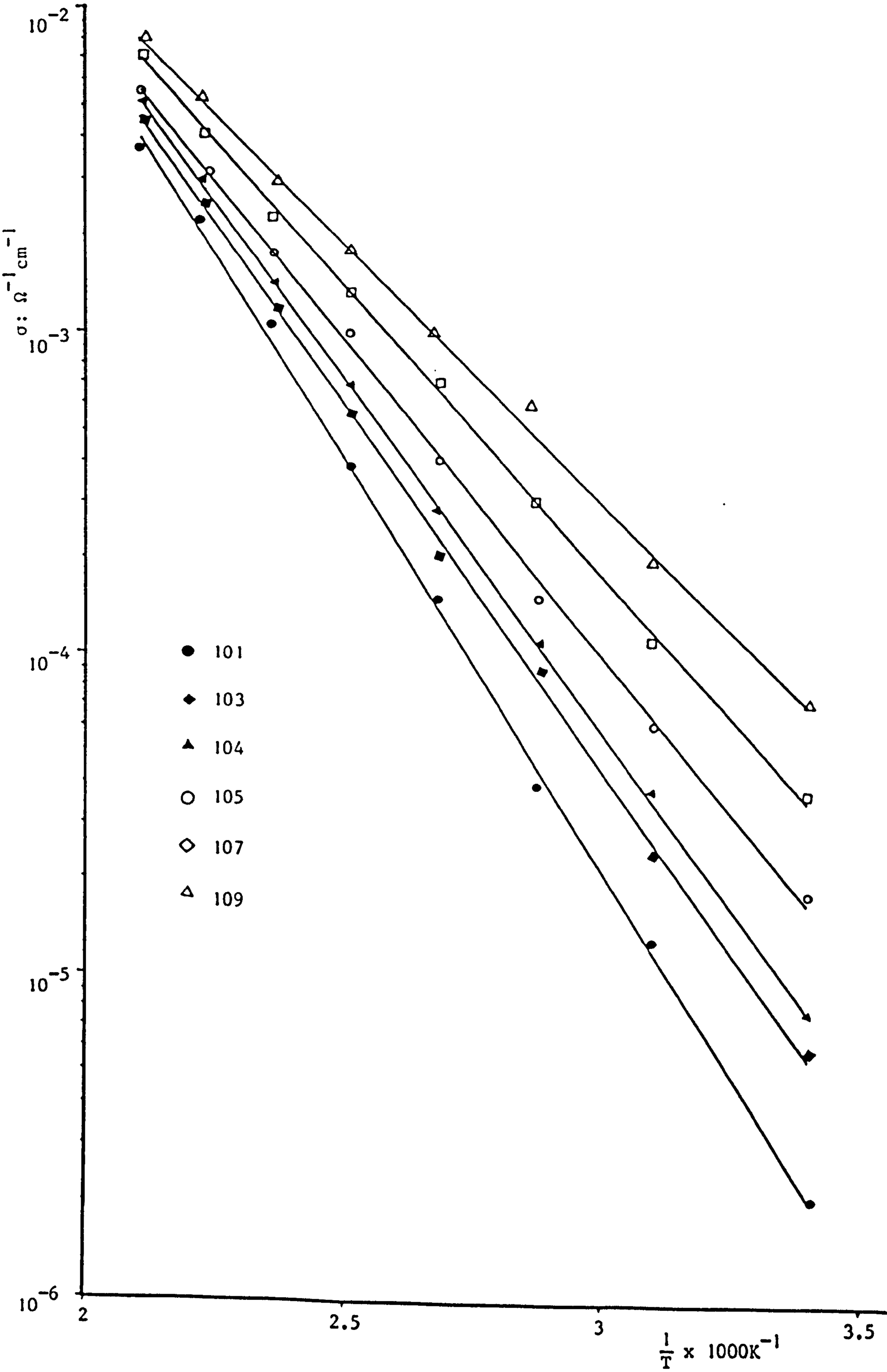

Fig.(7.7) Conductivity of $V_2O_5 - P_2O_5$ Glasses as a Function of $\frac{1}{T}$

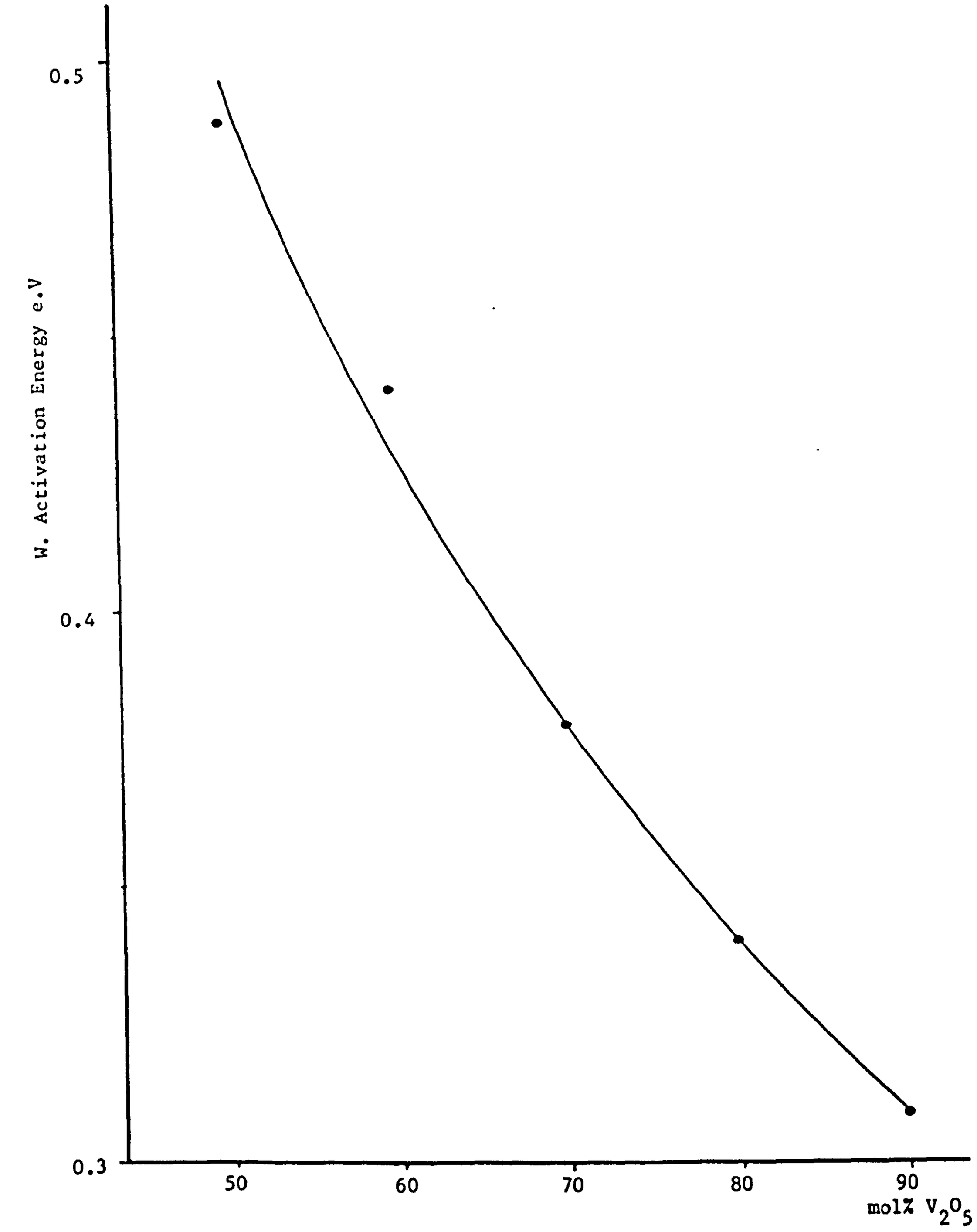

Fig.(7.8) Variation of Activation Energy with T.M.O. Content for $V_2O_5 - P_2O_5$ Glasses

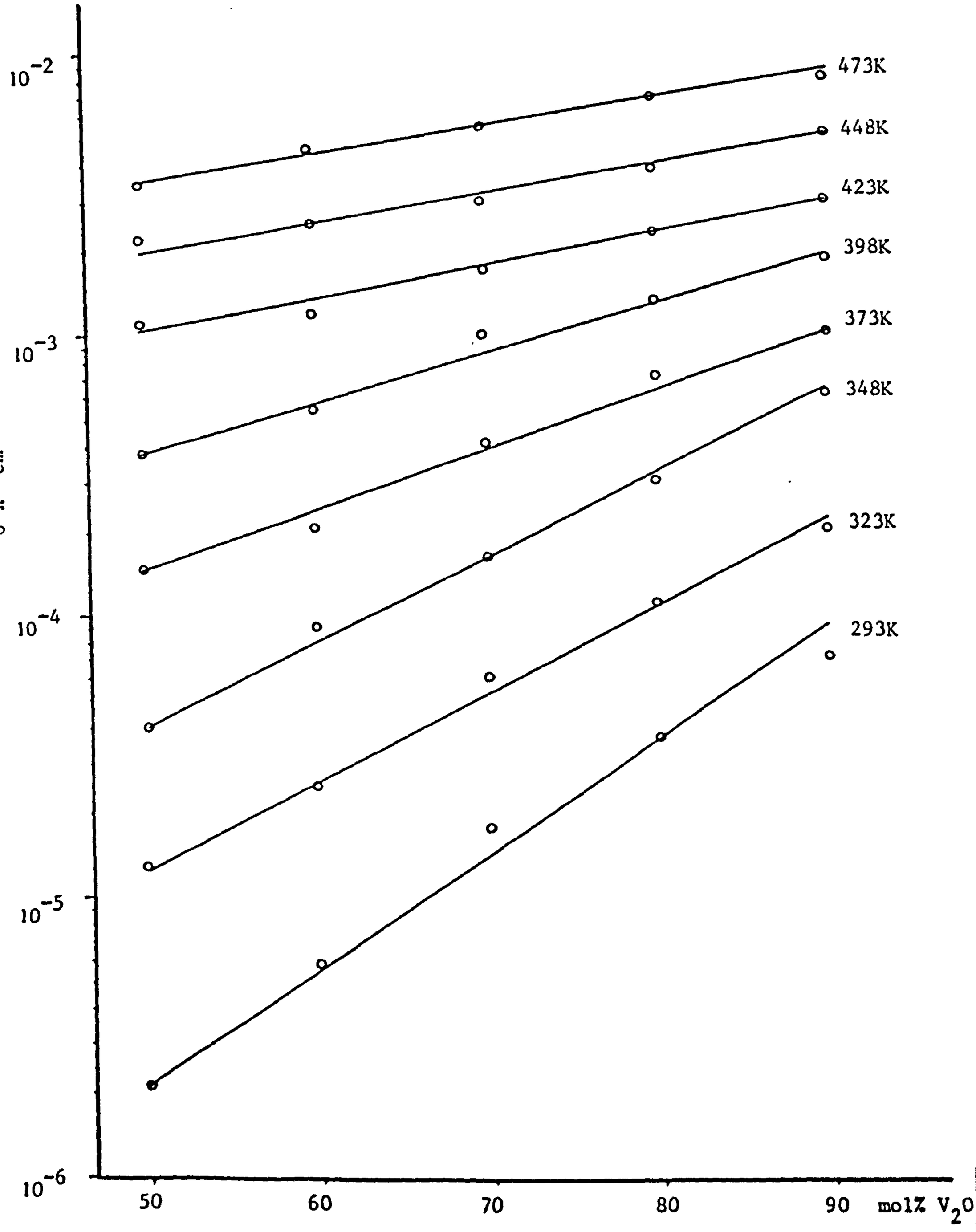

Fig.(7.9) Conductivity vs. Transition-Metal-Oxide Content for V_2O_5 - P_2O_5 Glasses at Different Temperatures

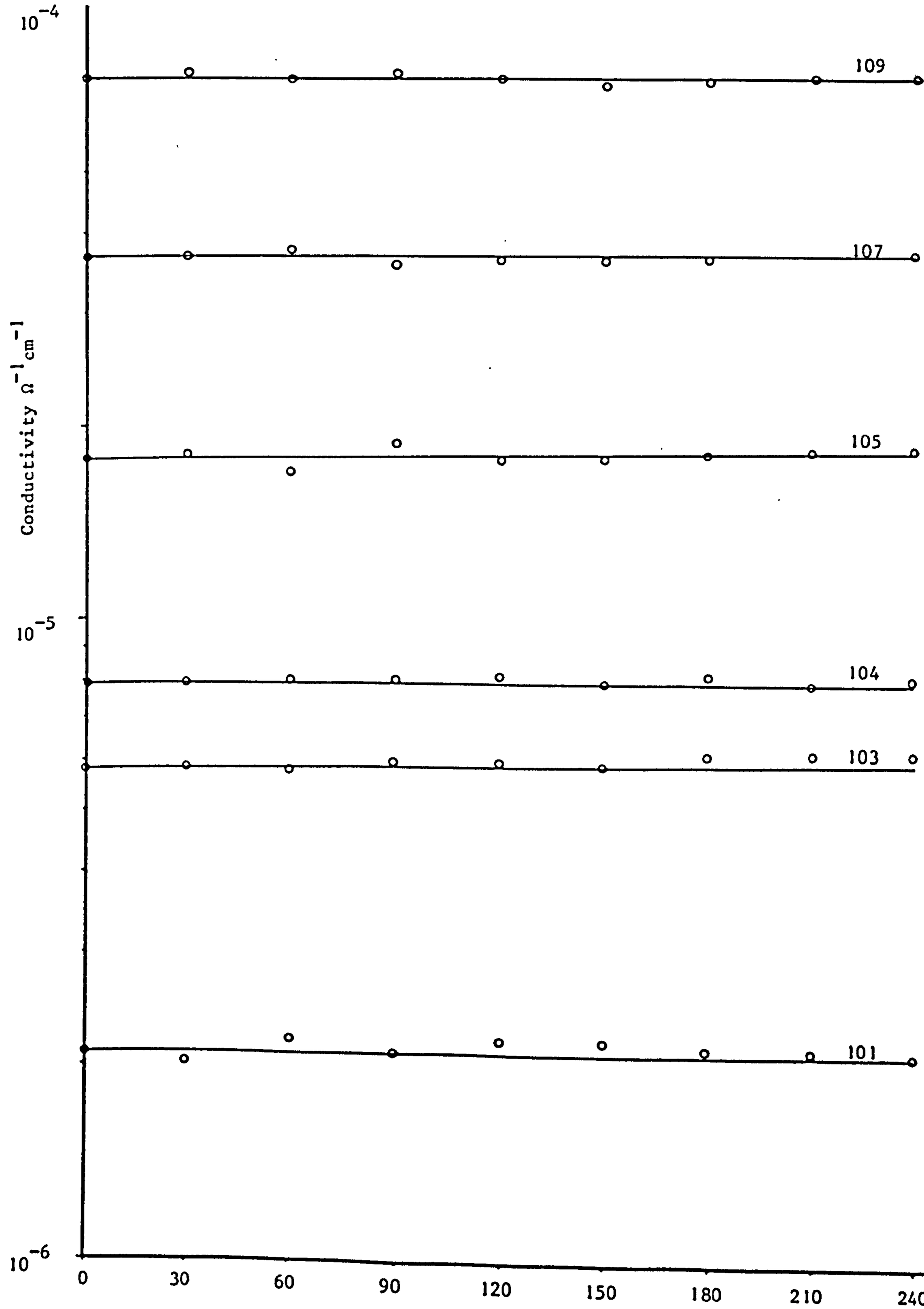

Fig.(7.10) Room Temperature Time Dependence of Conductivity for $V_2O_5 - P_2O_5$ Glasses

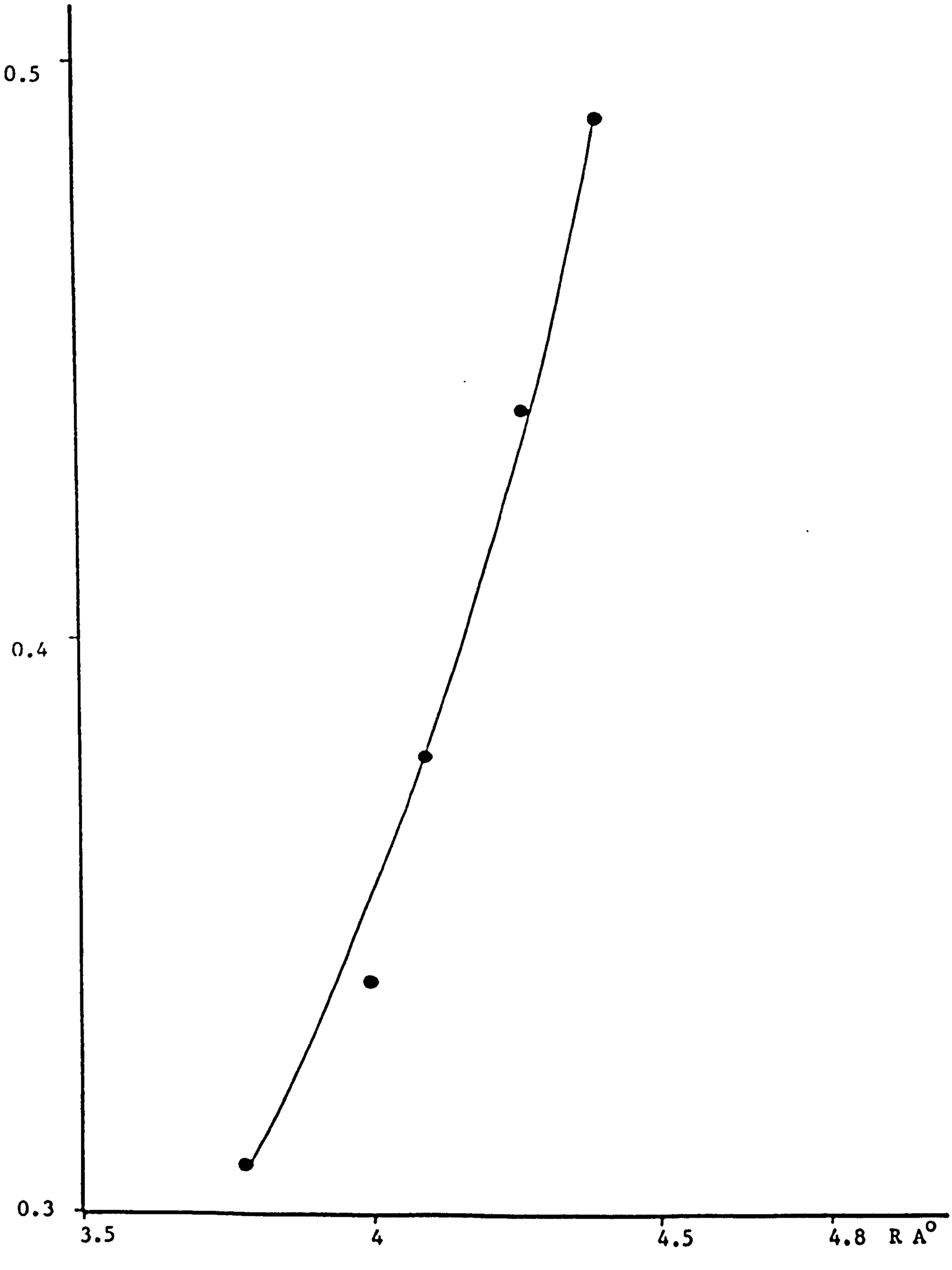

Fig.(7.11) Variation of Activation Energy with T.M.I. Spacing for $V_2O_5 - P_2O_5$ Glasses

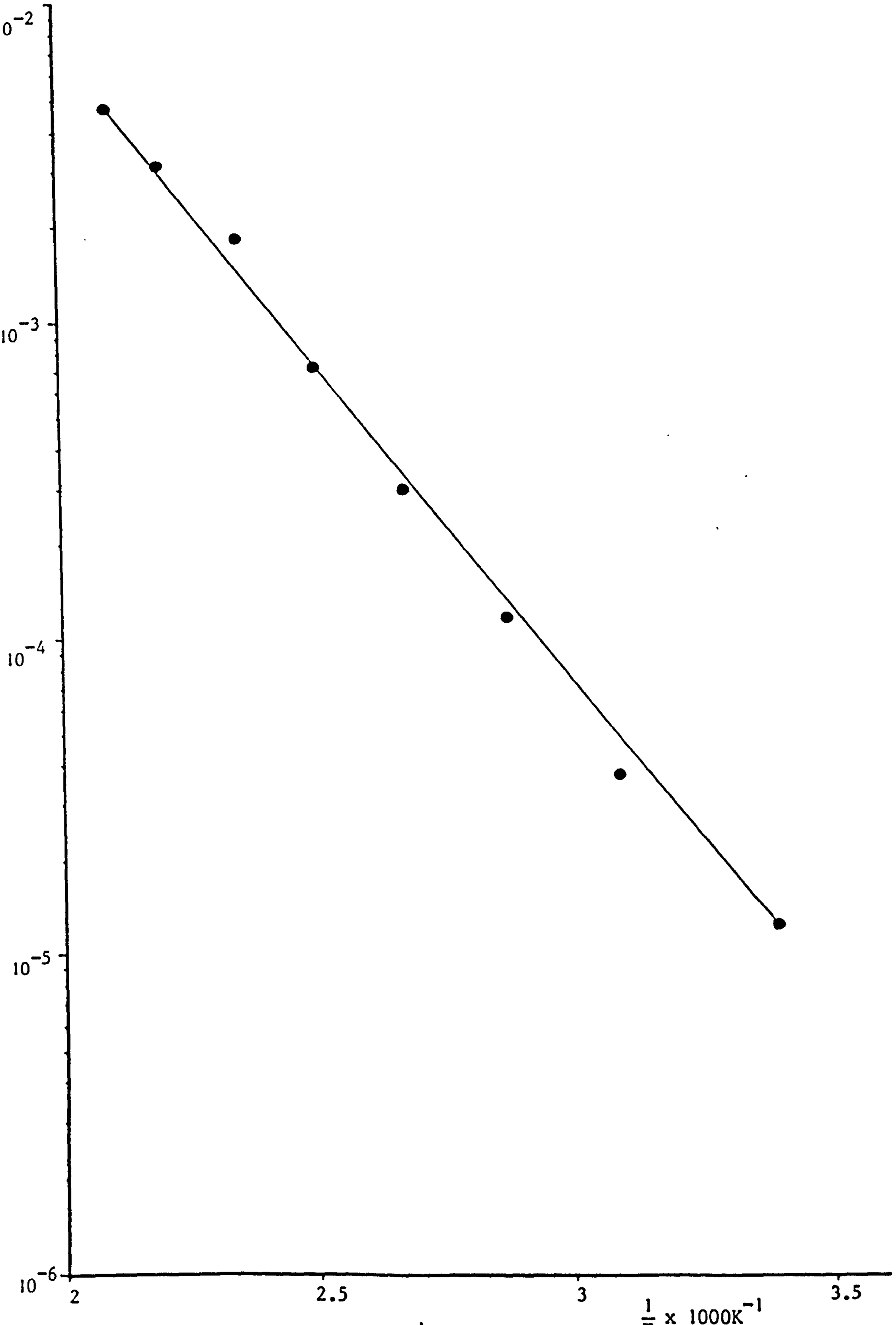

Fig.(7.12) Conductivity as a Function of $\frac{1}{T}$ for Glass No.104 with Silver Electrode

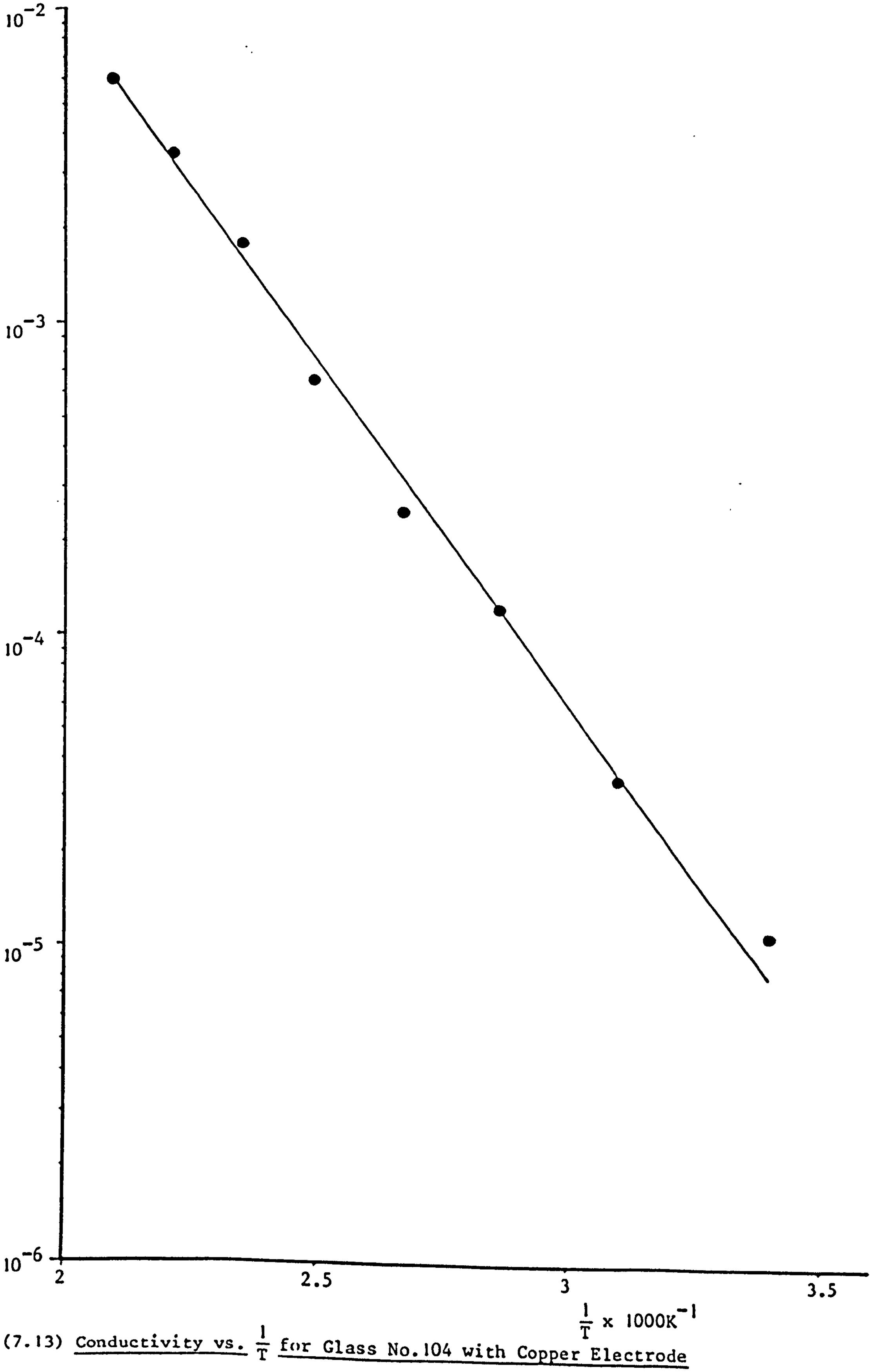

Fig.(7.13) Conductivity vs. $\frac{1}{T}$ for Glass No.104 with Copper Electrode

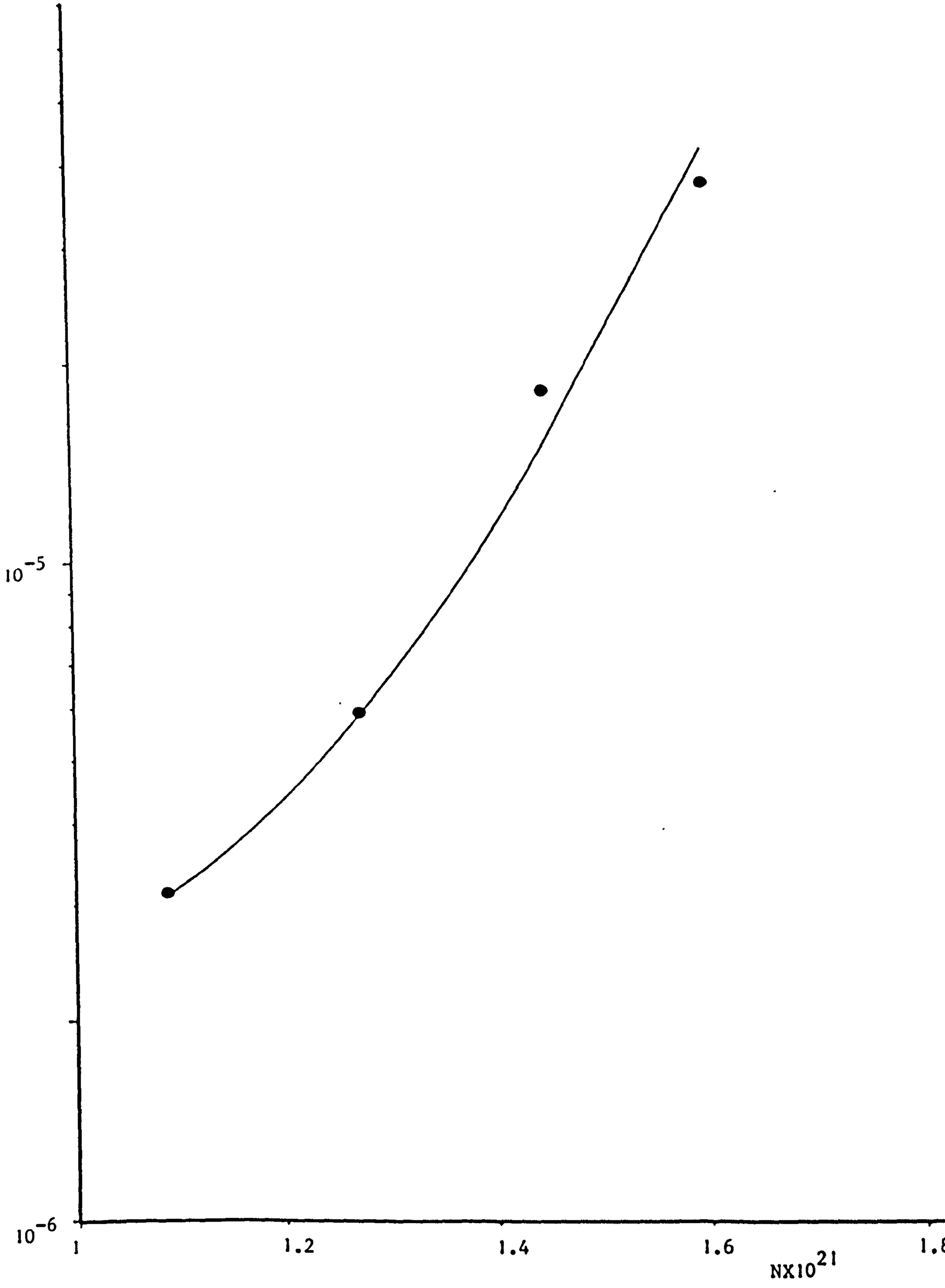

Fig.(7.14) Conductivity as a Function of T.M.I. Concentration for $V_2O_5 - P_2O_5$ Glasses

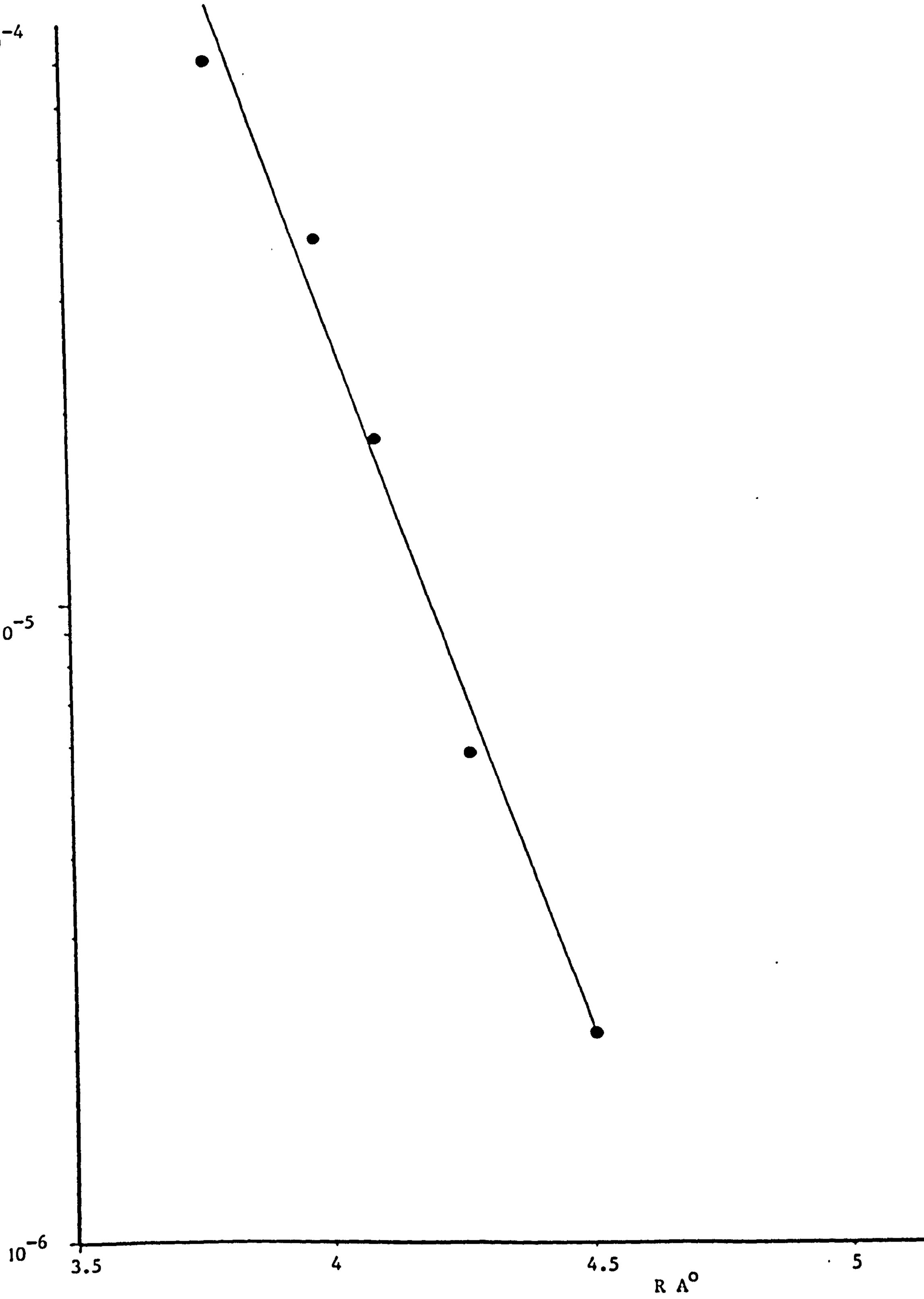

Fig.(7.15) Variation of Conductivity with T.M.I. Spacing (Å) for $V_2O_5 - P_2O_5$ Glasses

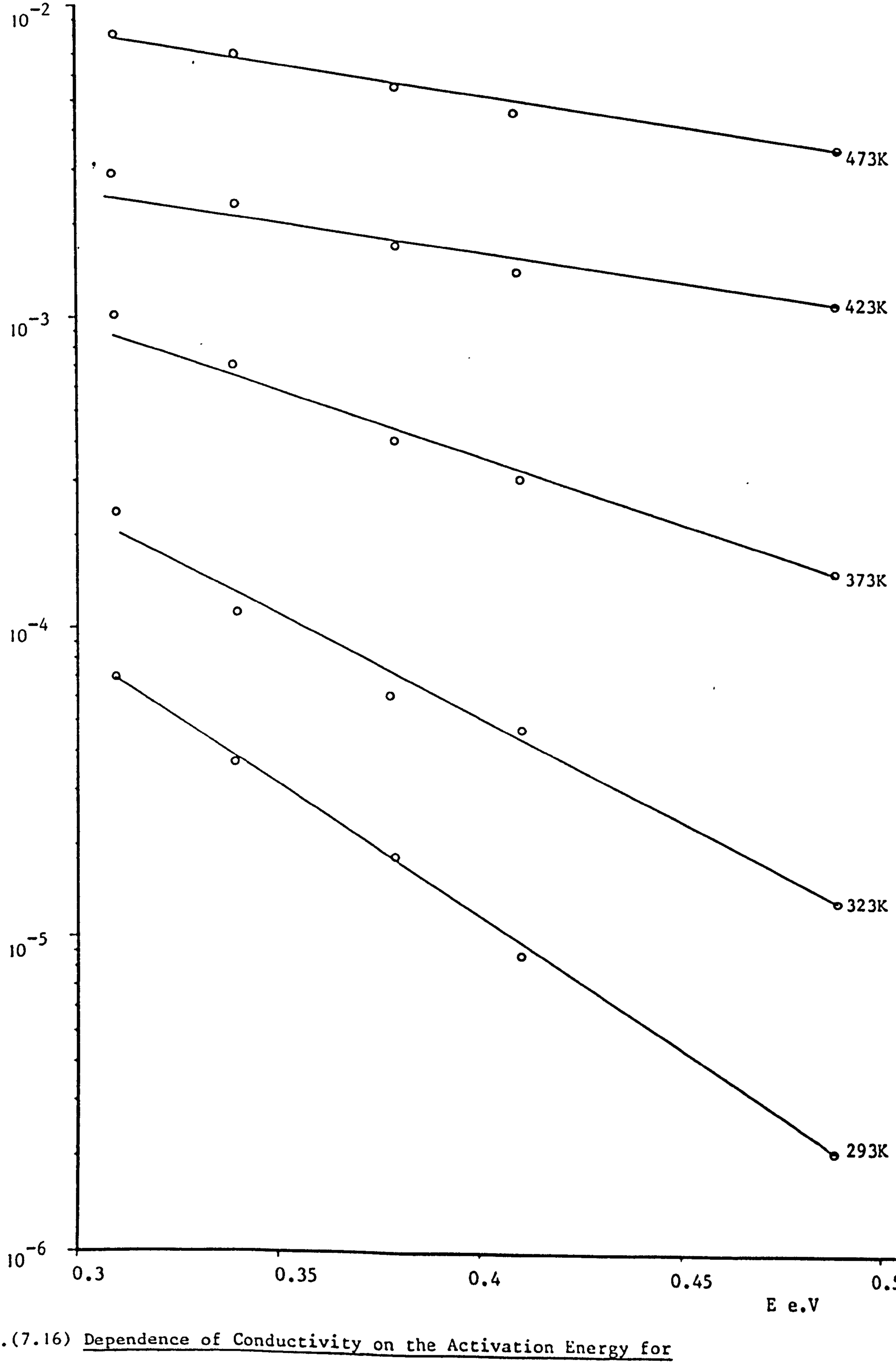

Fig.(7.16) Dependence of Conductivity on the Activation Energy for V_2O_5 - P_2O_5 Glasses at Different Temperatures

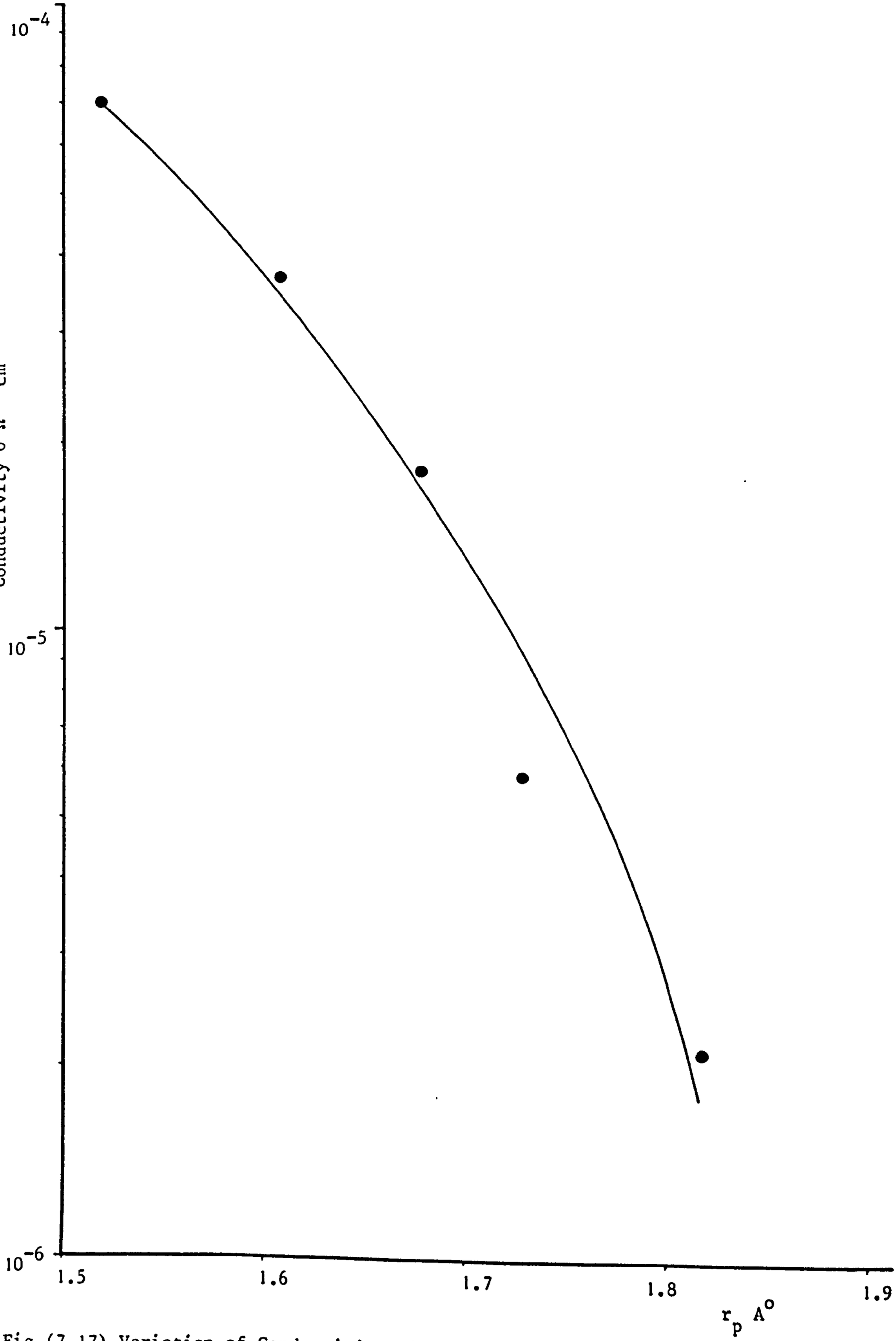

Fig.(7.17) Variation of Conductivity with Polaron Radius for V_2O_5 - P_2O_5 Glasses

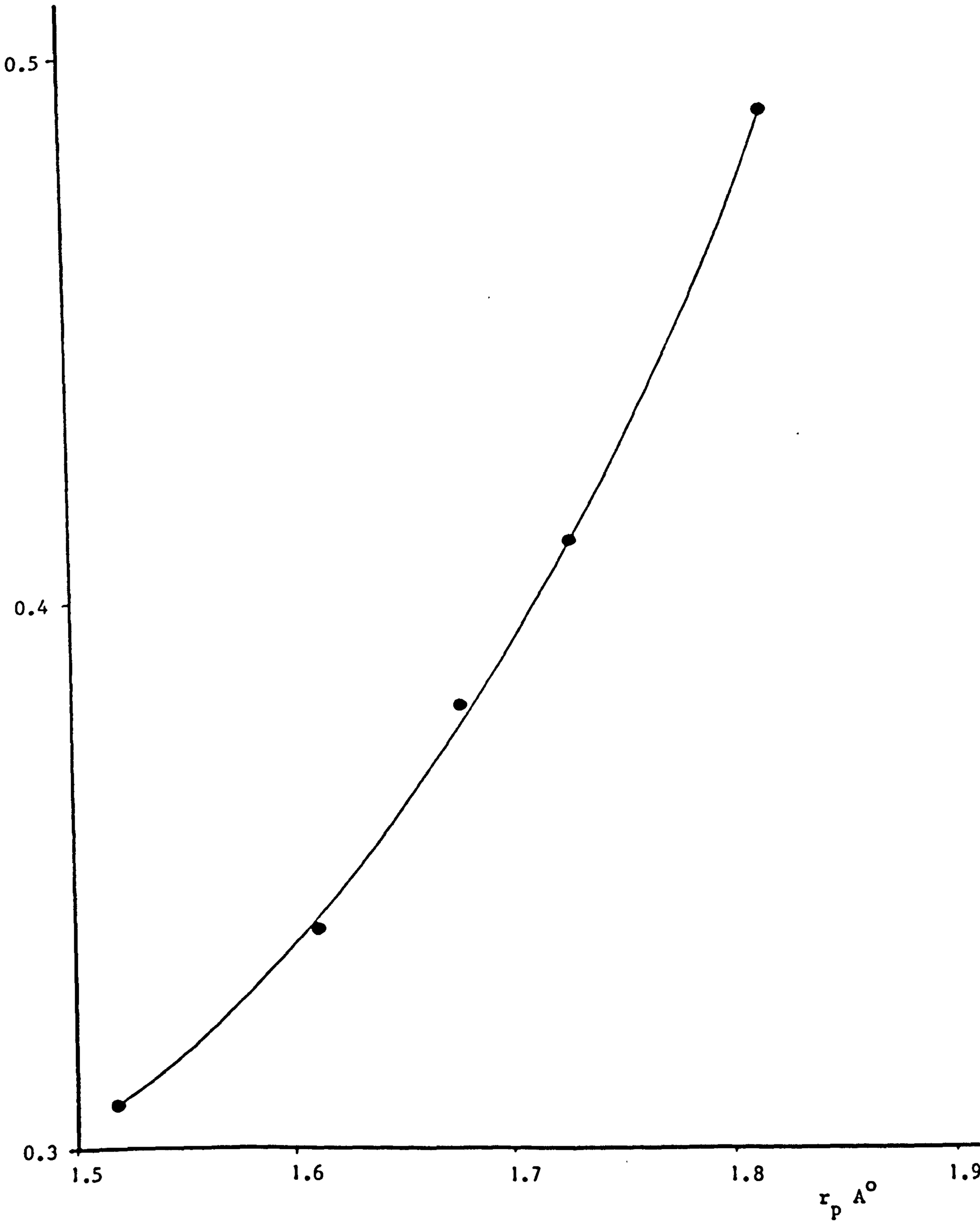

Fig.(7.18) Dependence of Activation Energy on the Polaron Radius for $V_2O_5 - P_2O_5$ Glasses

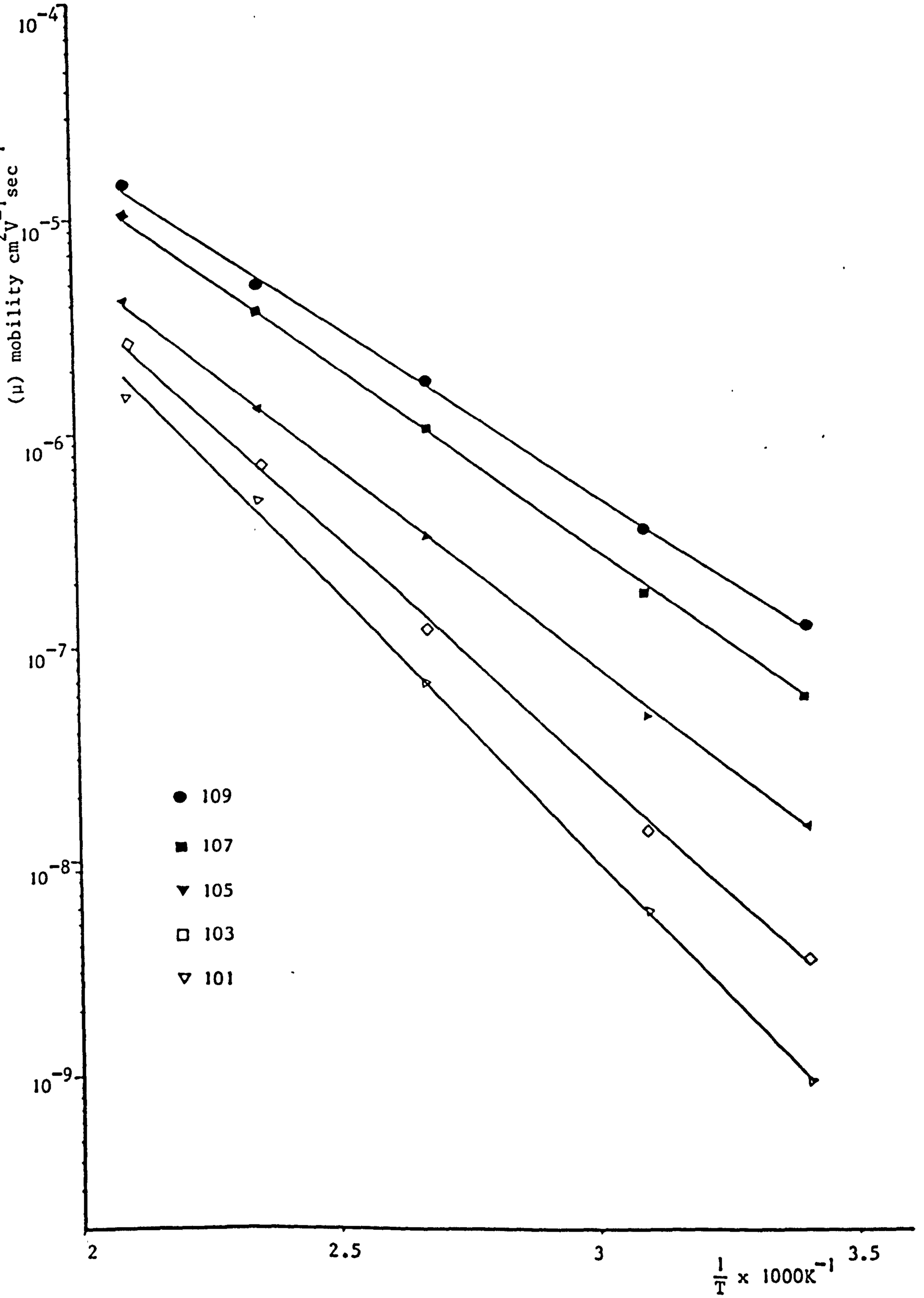

Fig.(7.19) Mobility of the Carriers as a Function of $\frac{1}{T}$ for V_2O_5 - P_2O_5 Glasses

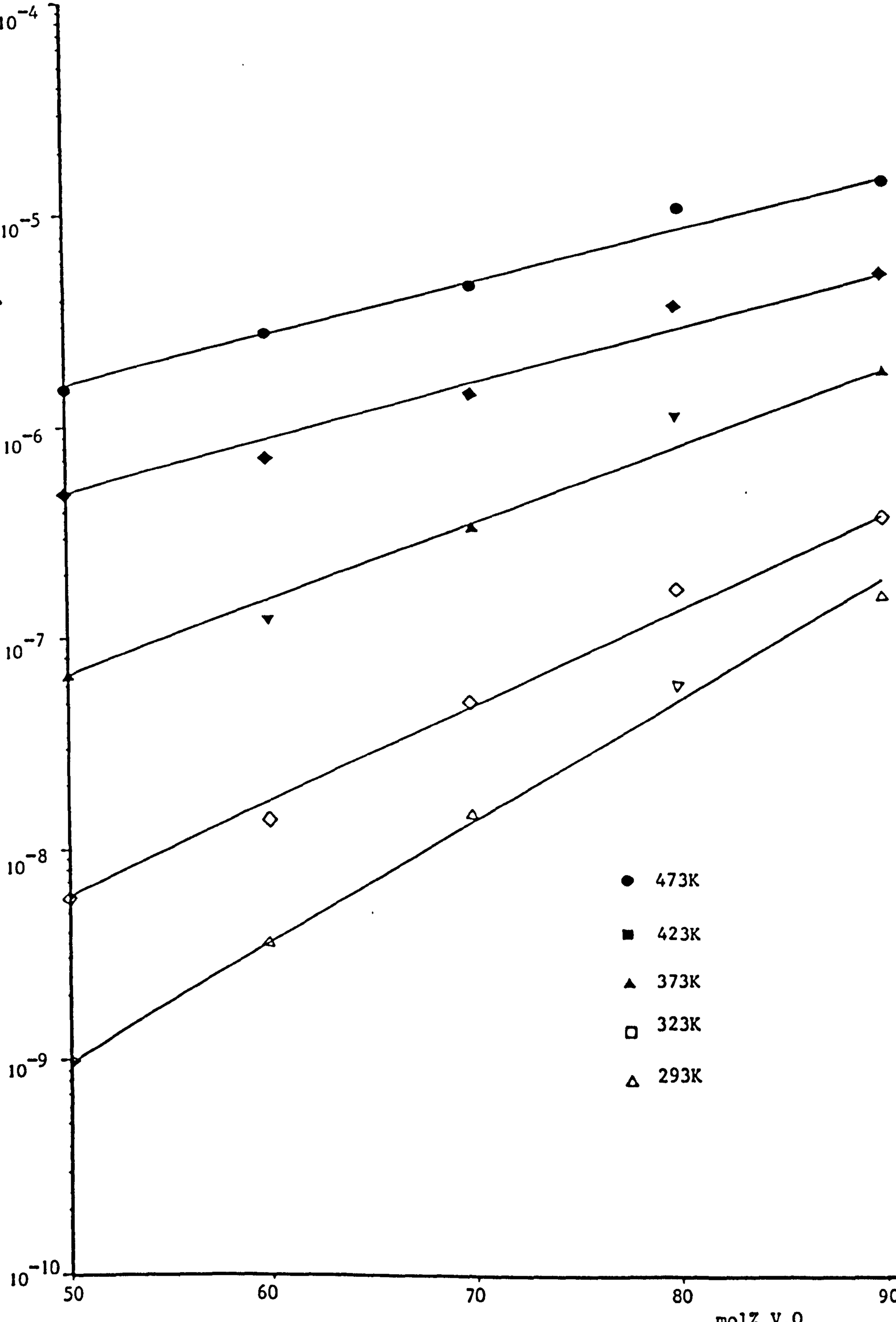

Fig.(7.20) Variation of Mobility with Composition for $V_2O_5 - P_2O_5$ Glasses at Different Temperatures

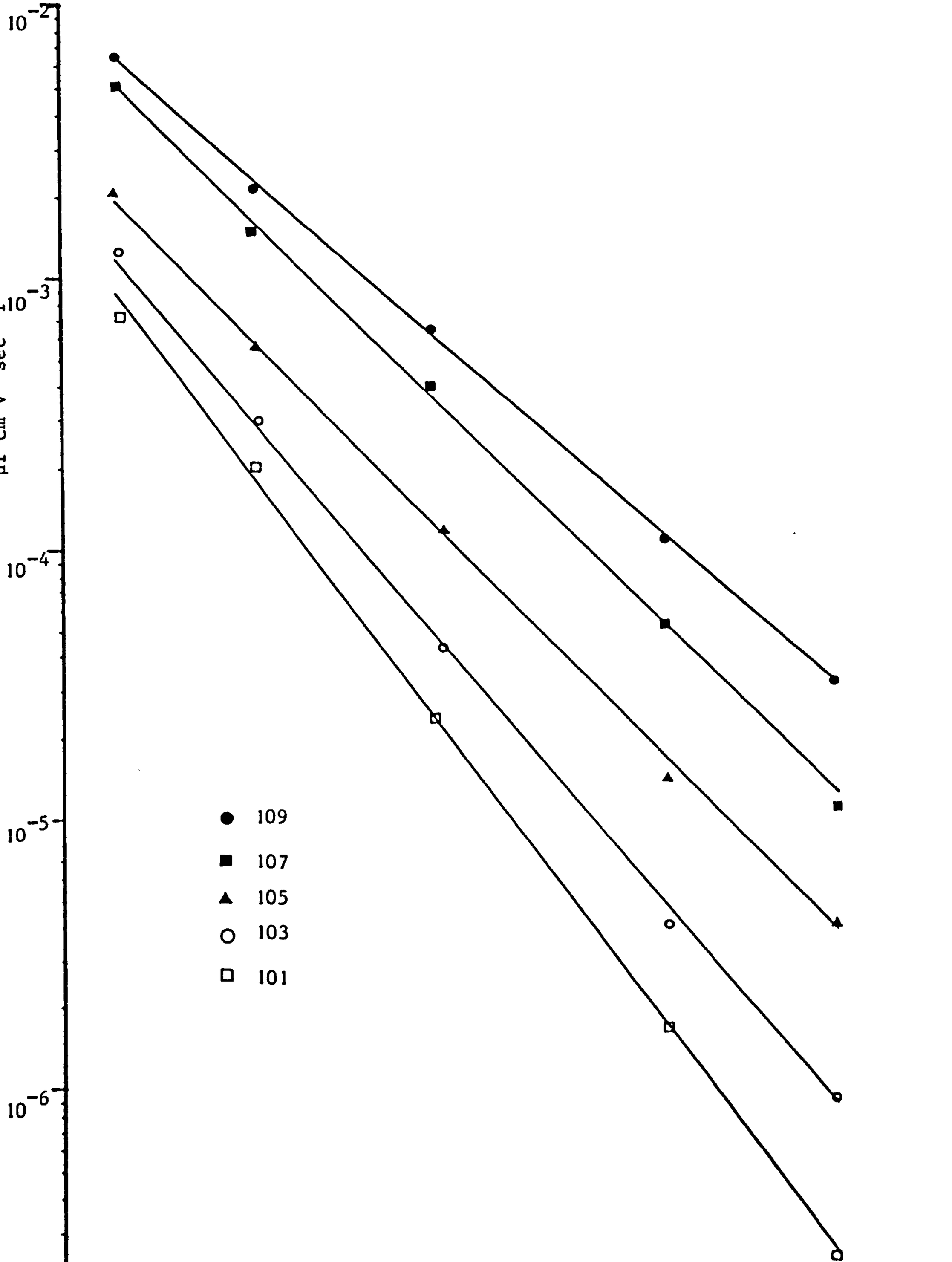

Fig.(7.21) $\mu.T$ vs. $\frac{1}{T}$ for V_2O_5-P_2O_5 Glasses

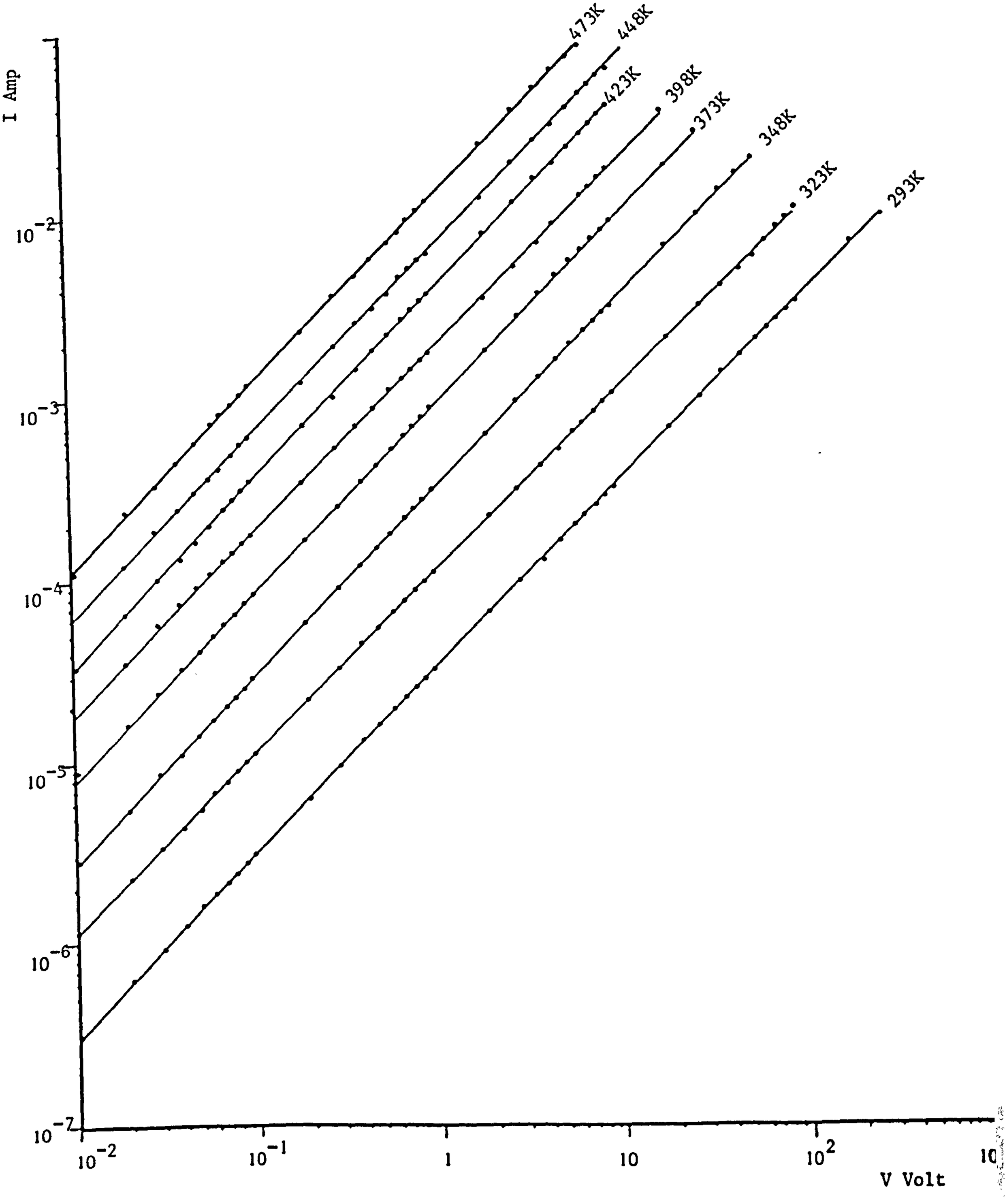

Fig.(7.22) Typical I - V Characteristics at Different Temperatures for $V_2O_5 - P_2O_5 - TeO_2$ Glasses (Glass No.204)

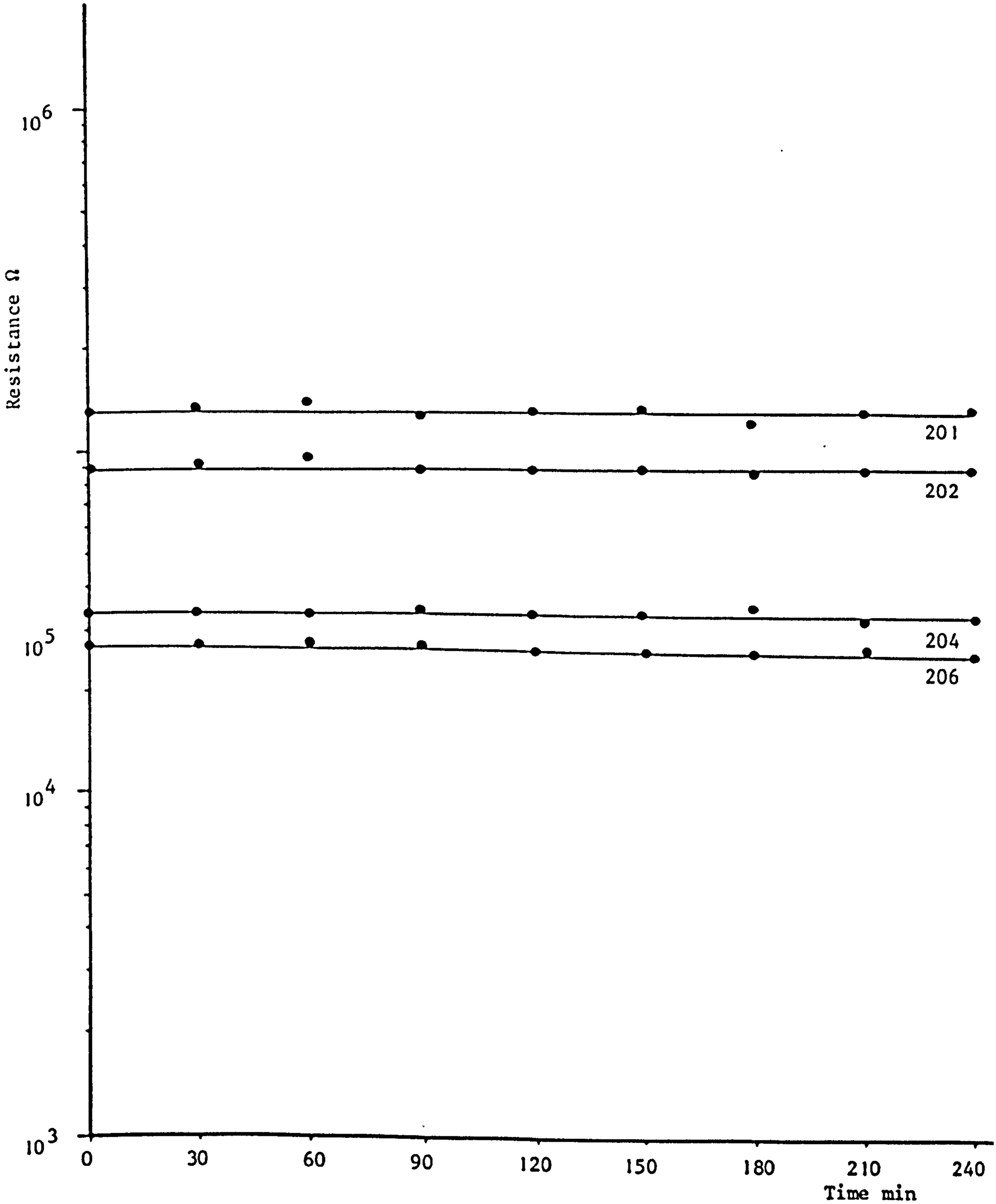

Fig.(7.23) Time Dependence of Resistance at Room Temperature for Glass Containing TeO_2

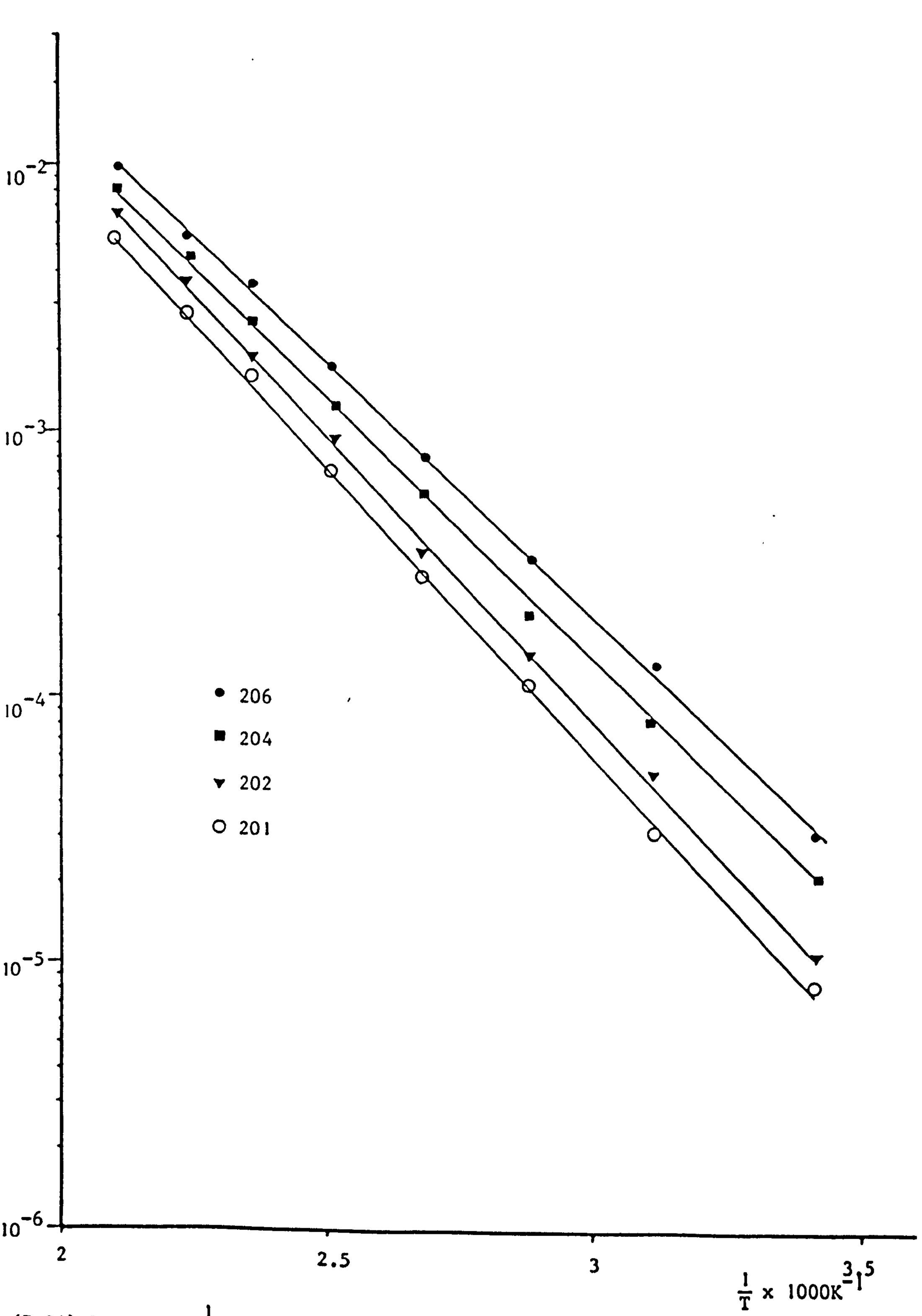

Fig.(7.24) Log σ vs. $\frac{1}{T}$ for Glass Containing TeO_2

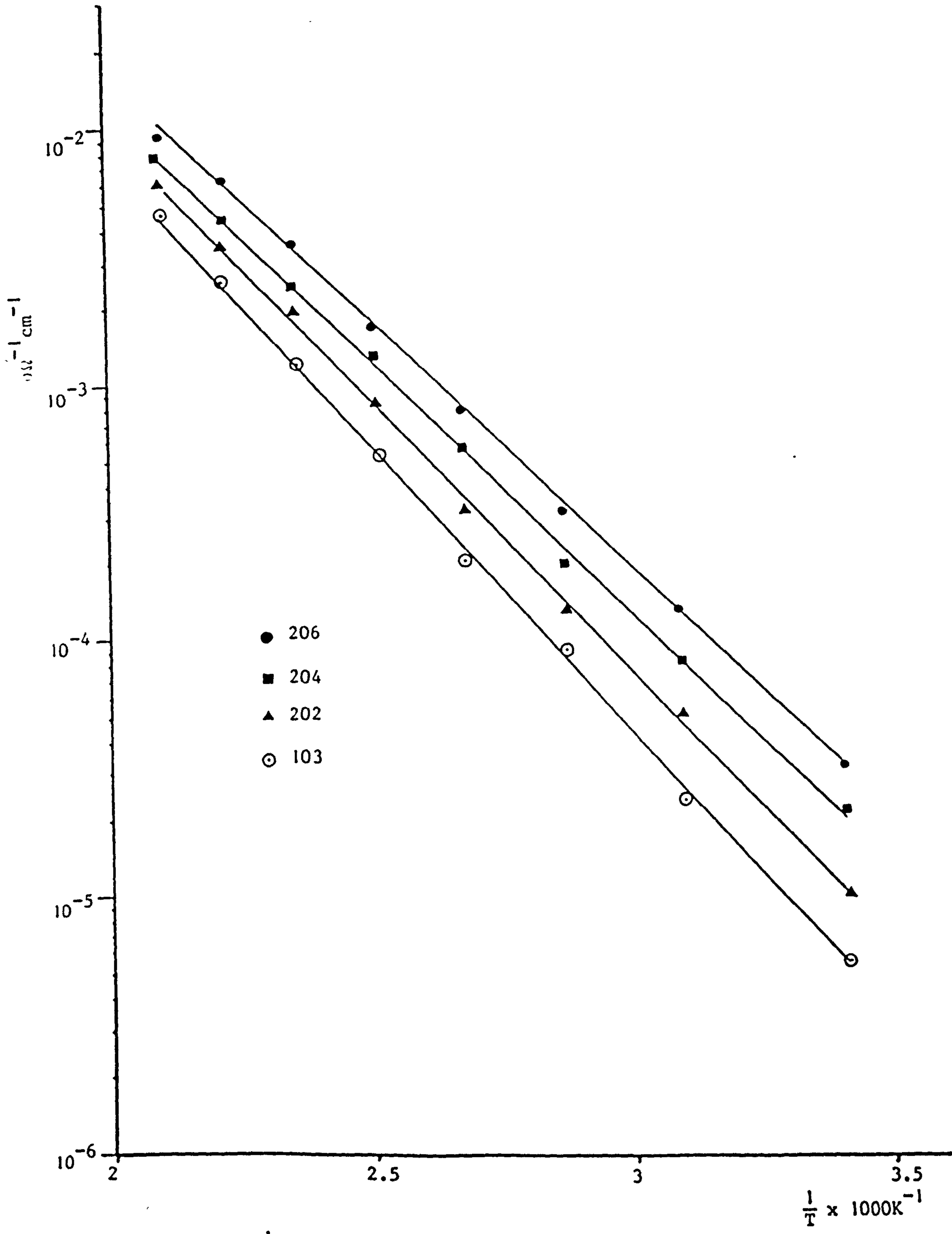

Fig.(7.25) Log σ vs. $\frac{1}{T}$ for some Glasses Containing TeO_2 and Glass No.103 (without TeO_2) for Comparison

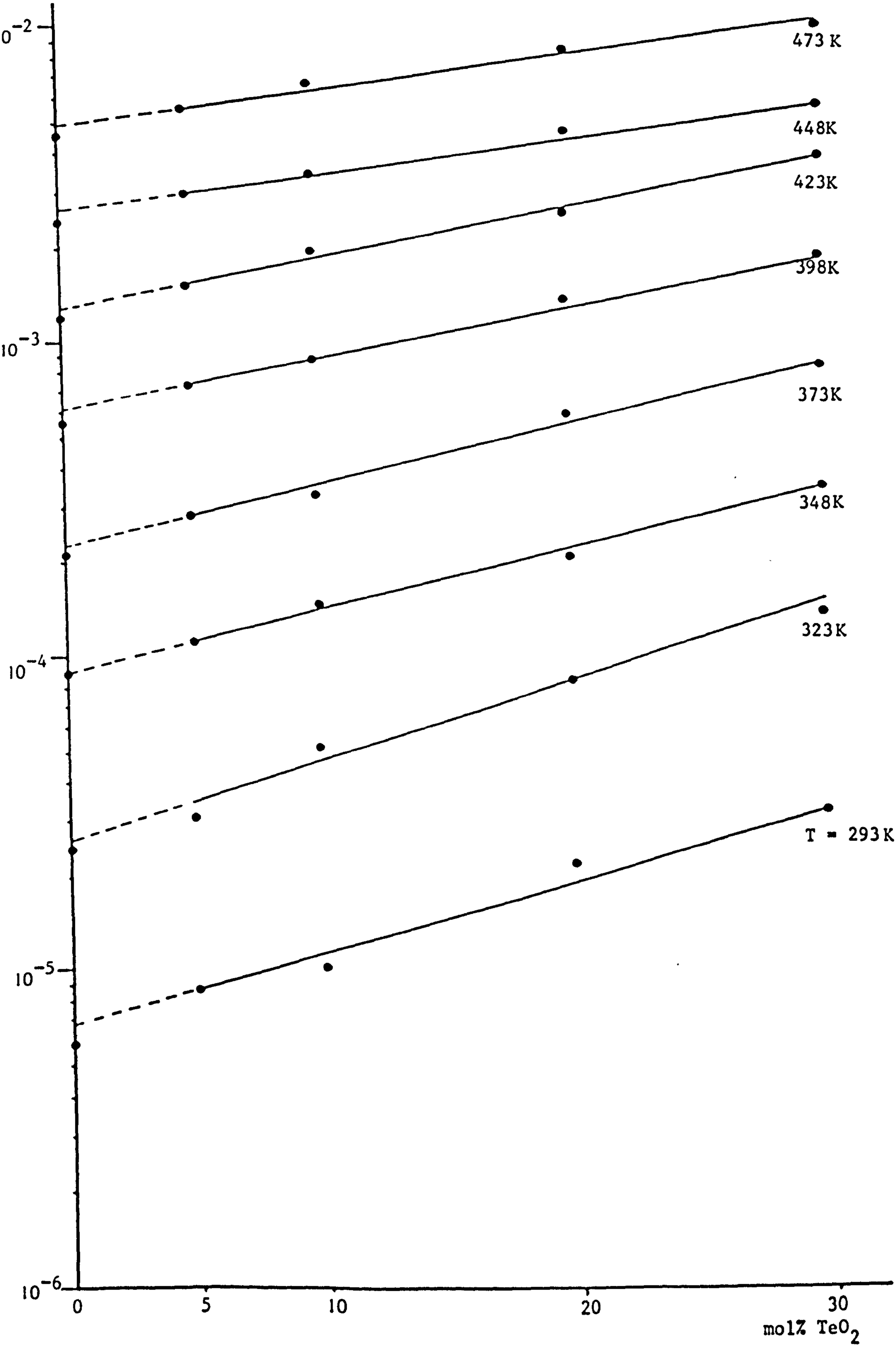

Fig.(7.26) Dependence of Conductivity on TeO_2 Content for V_2O_5 P_2O_5 - TeO_2 Glasses With 60 mol% V_2O_5 at Different Temperatures

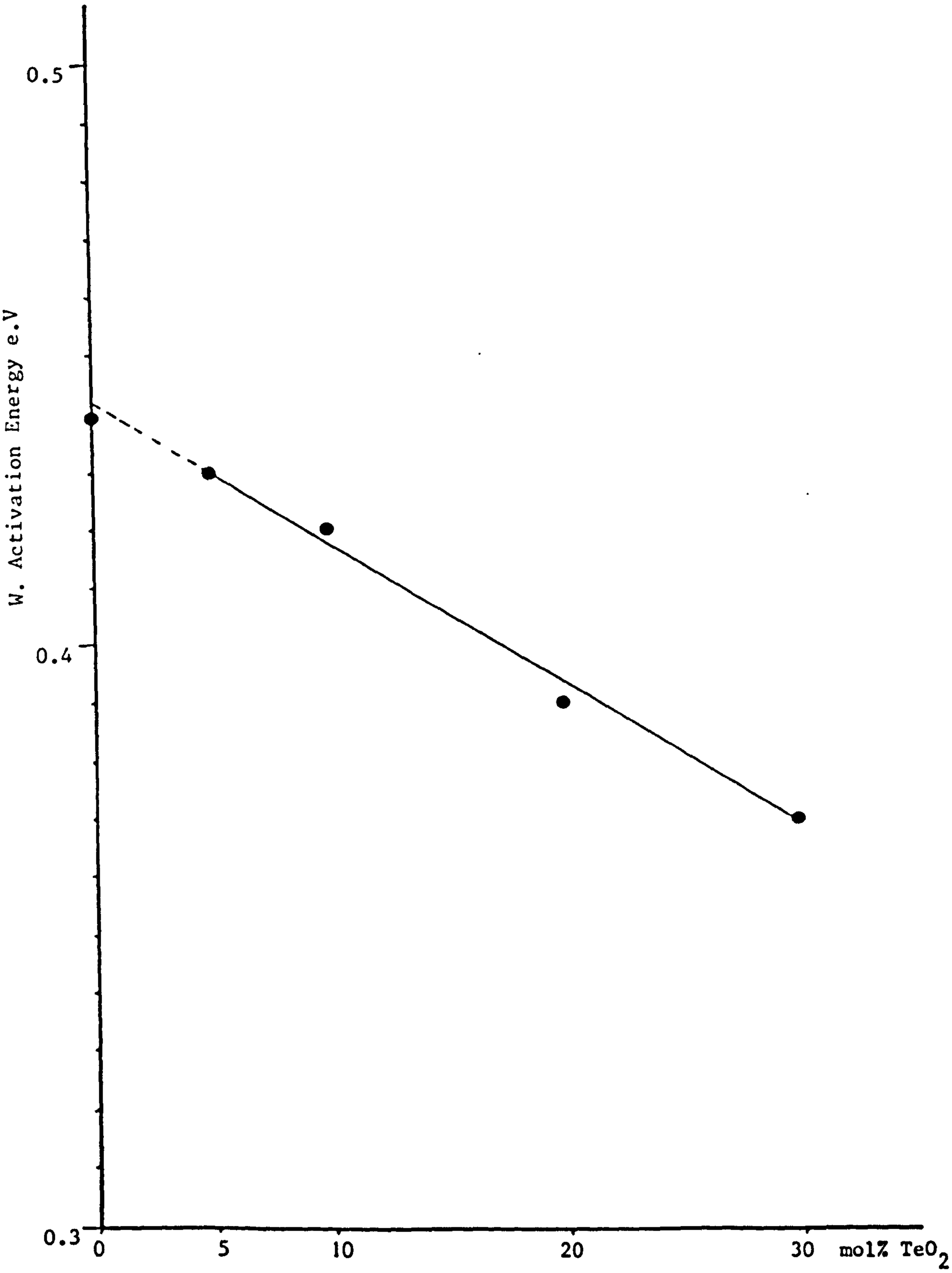

Fig.(7.27) Variation of Activation Energy W with TeO_2 Content for V_2O_5 - P_2O_5 - TeO_2 Glasses

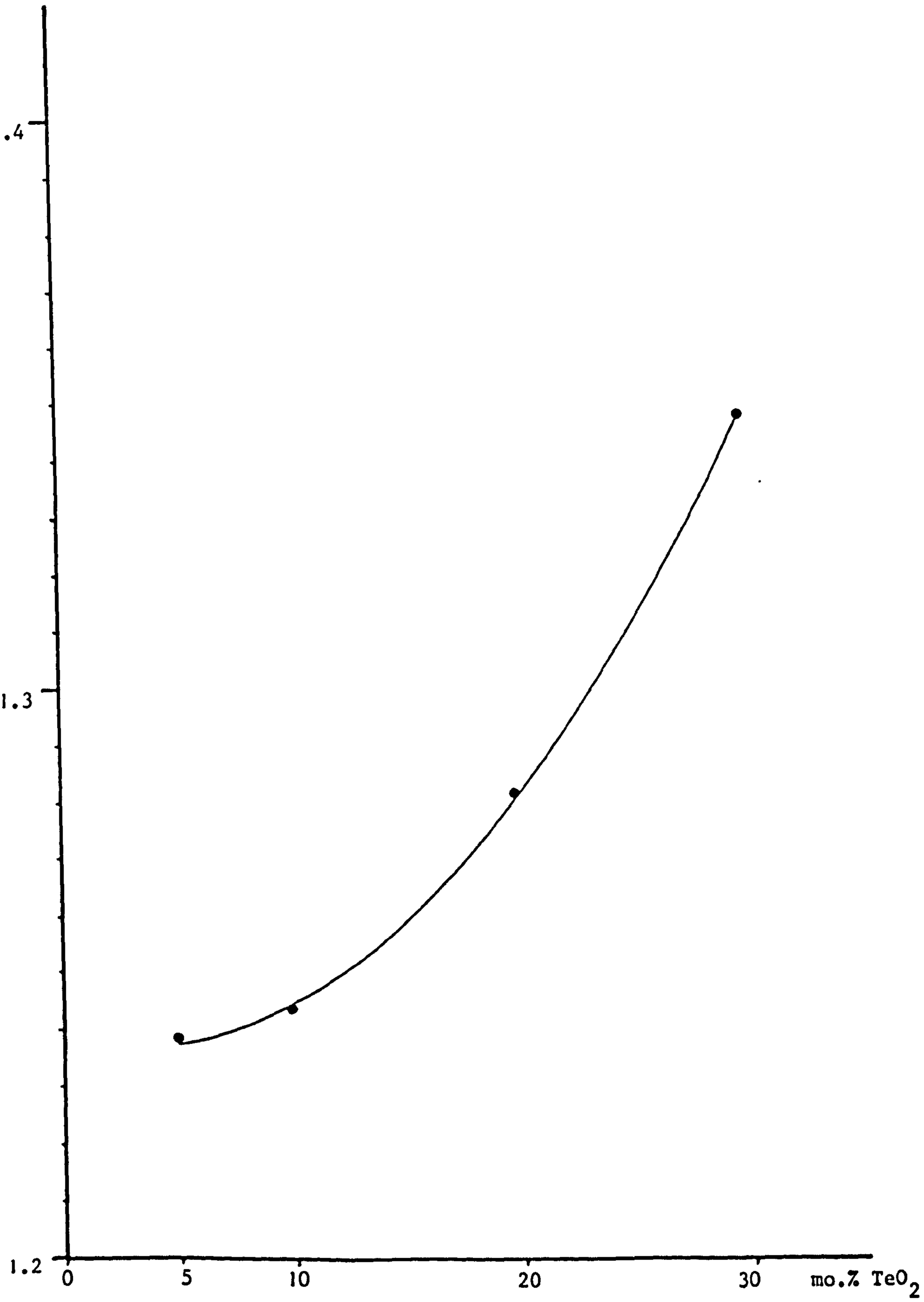

Fig.(7.28) Dependence of T.M.I. Concentration on TeO_2 Content for V_2O_5 - P_2O_5 - TeO_2 Glasses

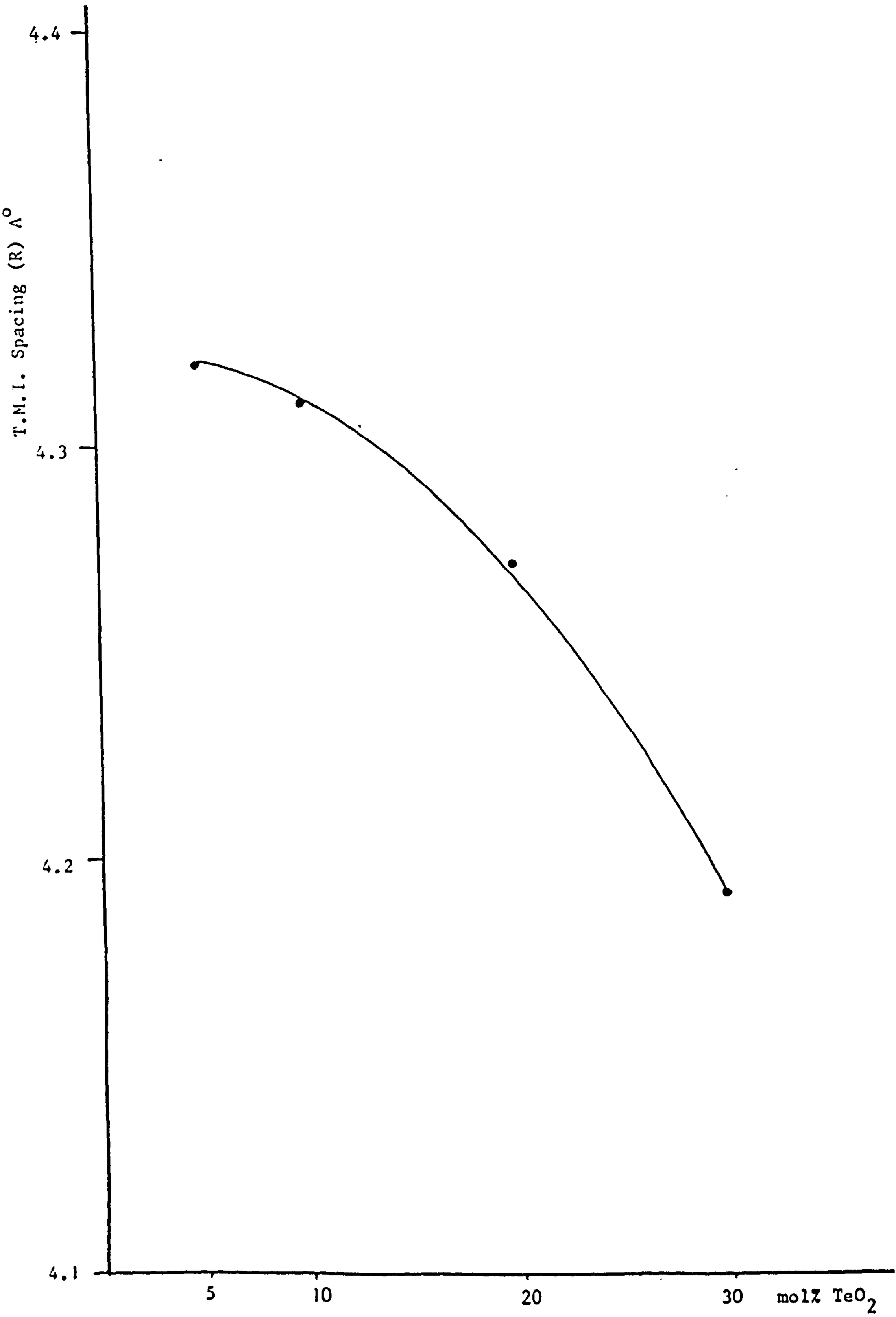

Fig.(7.29) T.M.I. Spacing vs. mol% TeO_2 for V_2O_5 - P_2O_5 - TeO_2 Glasses

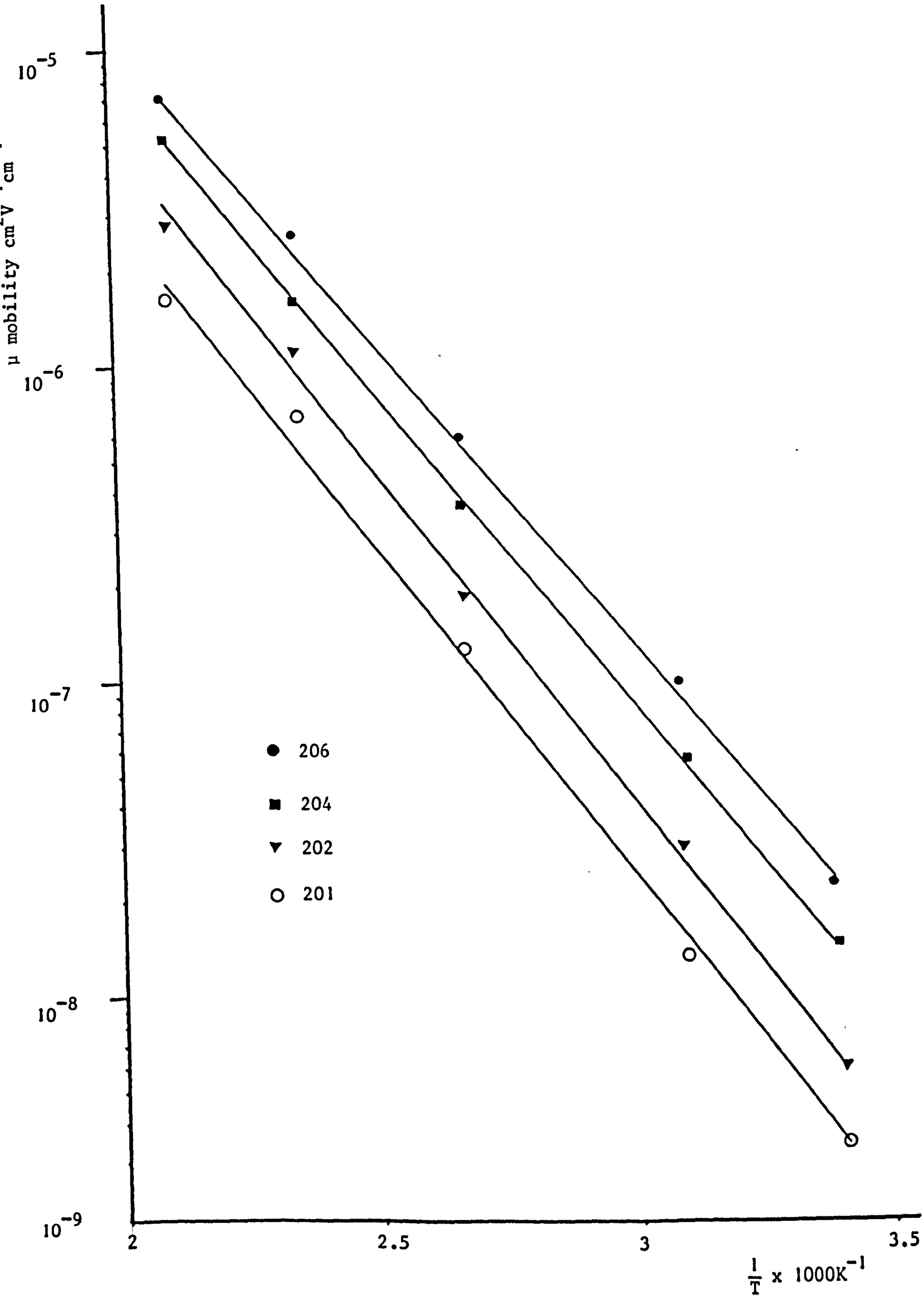

Fig.(7.30) Mobility of Carriers vs. $\frac{1}{T}$ for V_2O_5 - P_2O_5 Glasses

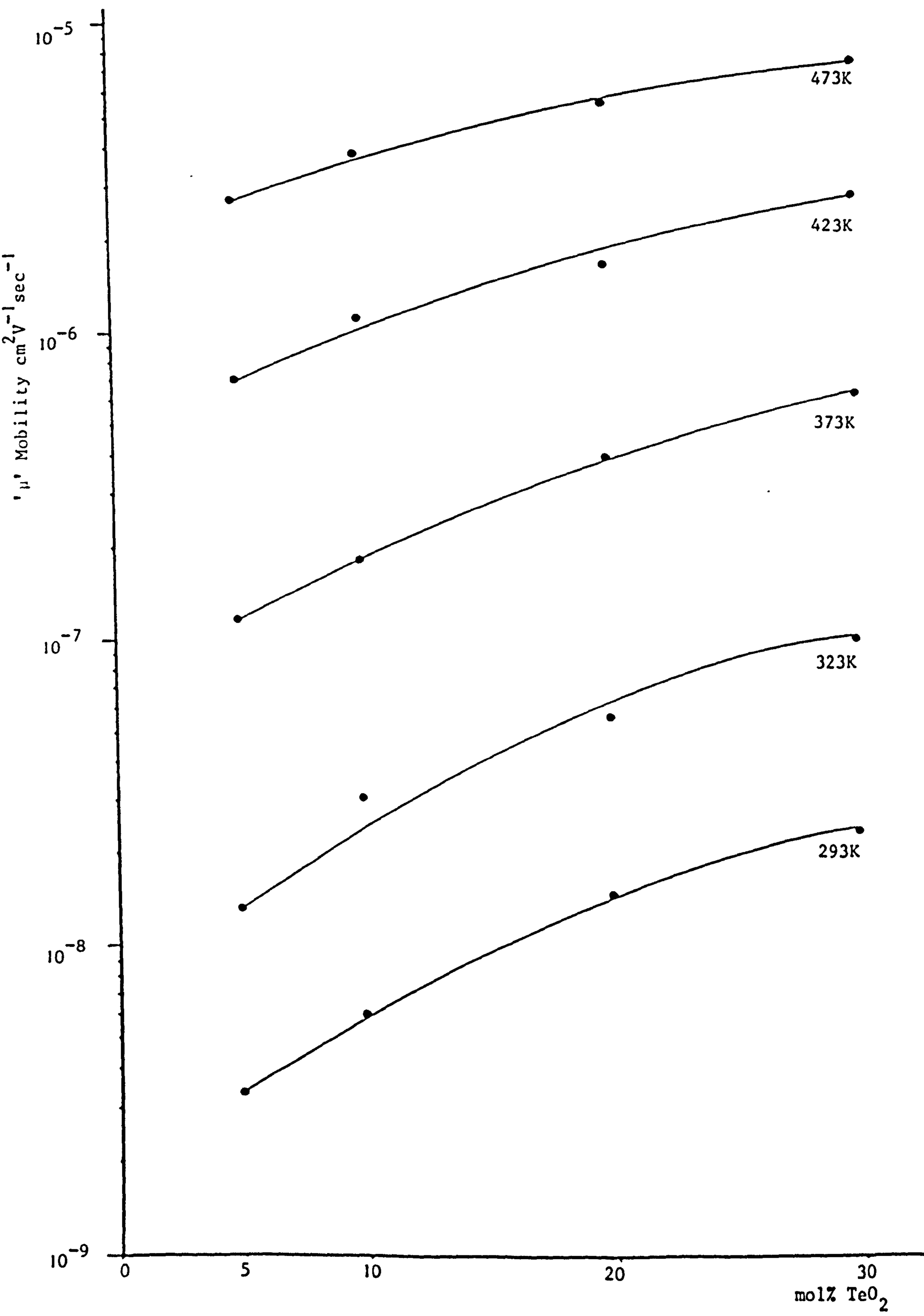

Fig.(7.31) Mobility of Carriers vs. TeO_2 Content for V_2O_5 - P_2O_5 - TeO_2 Glasses

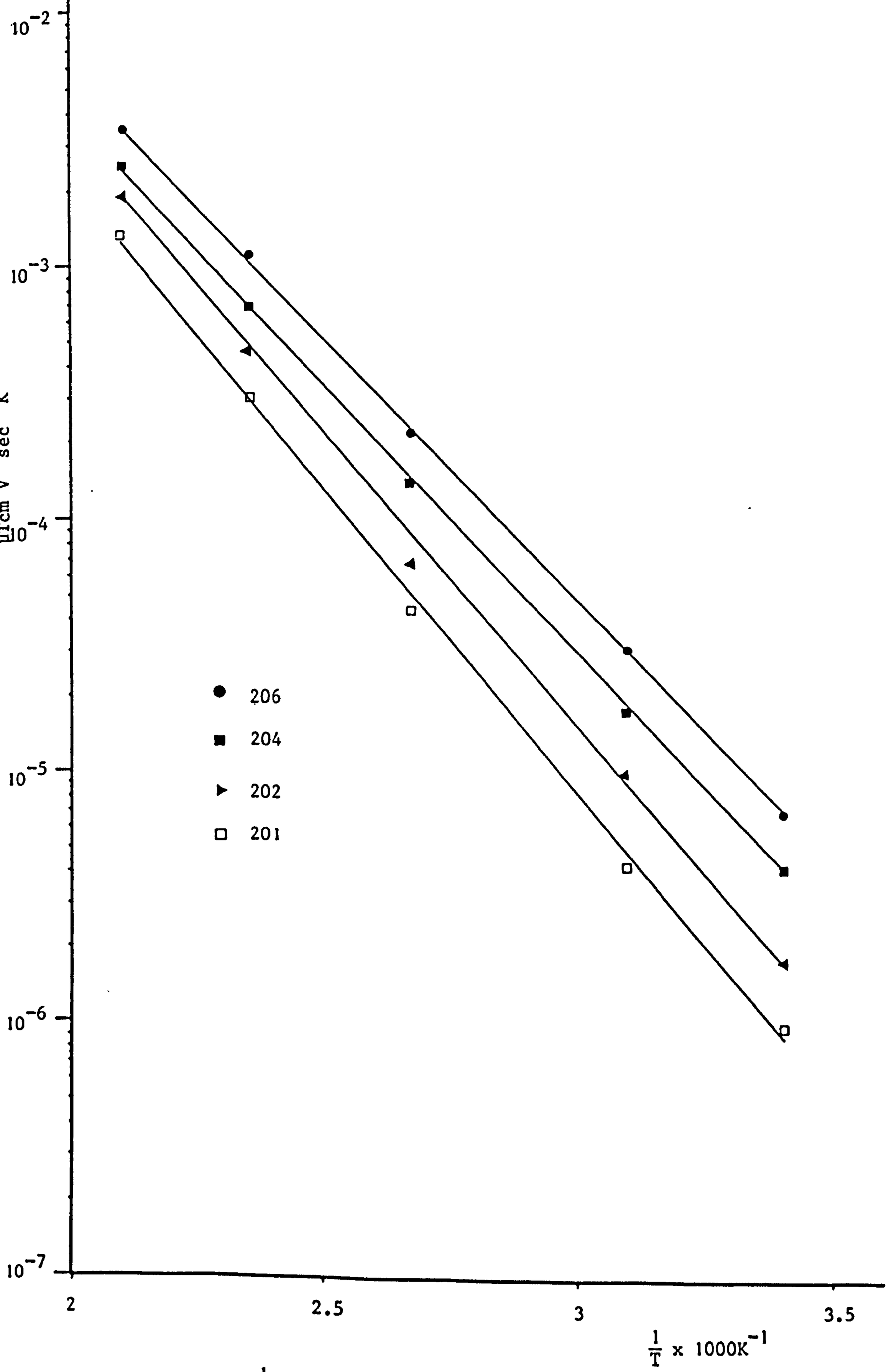

Fig.(7.32) Plot of μT vs. $\frac{1}{T}$ for $V_2O_5 - P_2O_5 - TeO_2$ Glasses

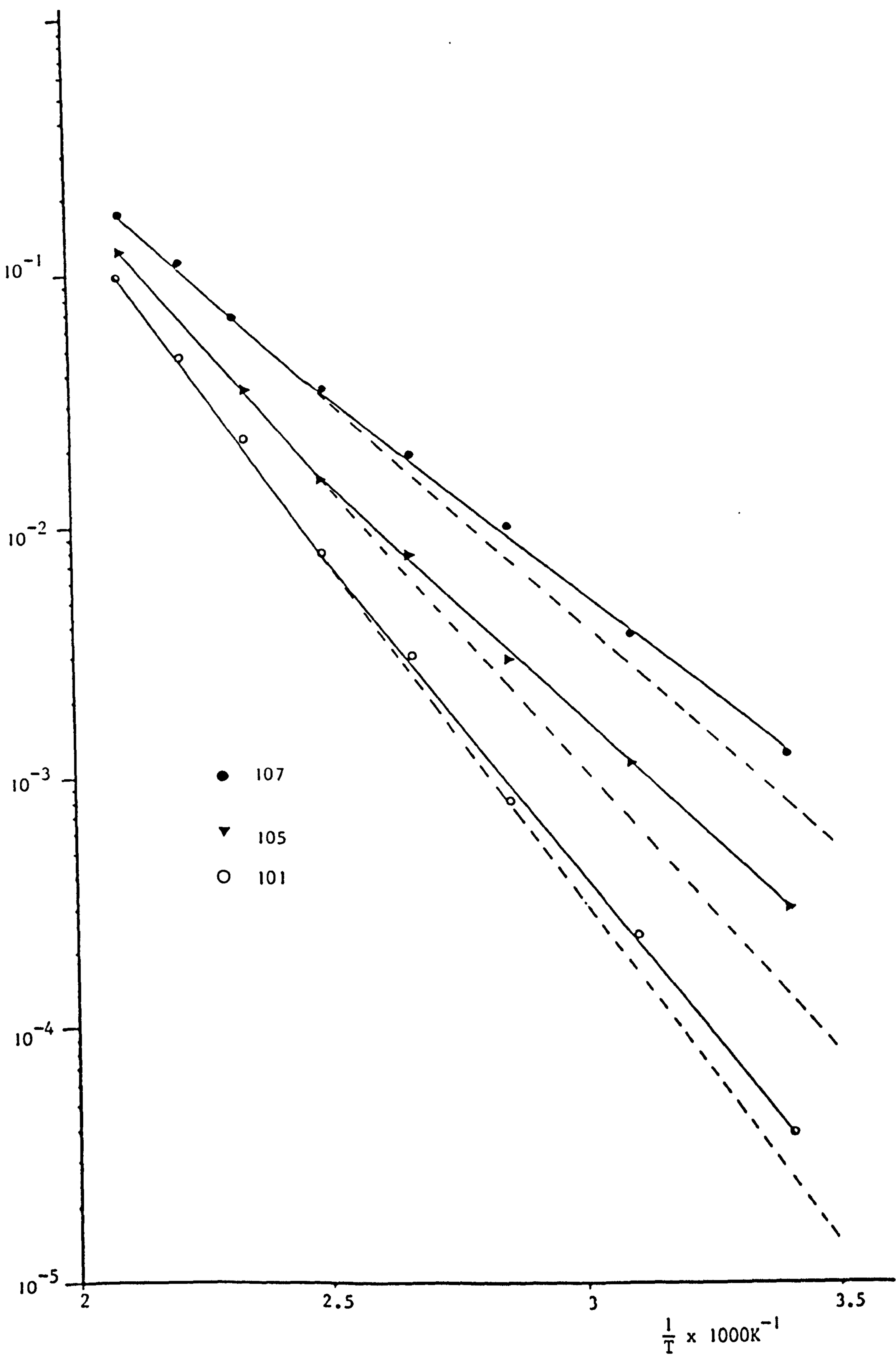

Fig.(7.33) Plot of $\sigma T^{\frac{1}{2}}$ vs. $\frac{1}{T}$ for some $V_2O_5 - P_2O_5$ Glasses

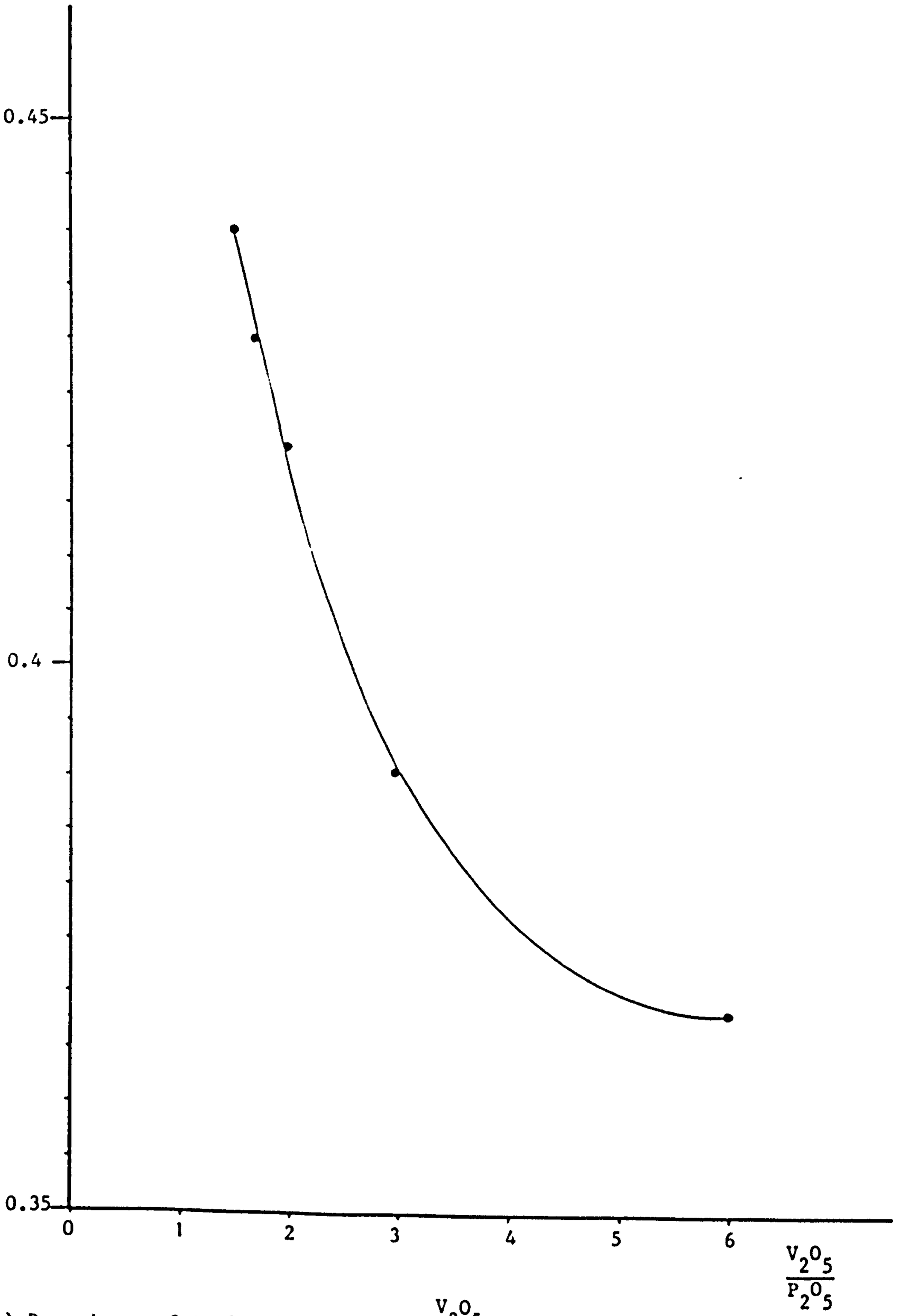

Fig.(7.34) Dependence of Activation Energy on $\frac{V_2O_5}{P_2O_5}$ Ratio for $V_2O_5 - P_2O_5 - TeO_2$ Glasses

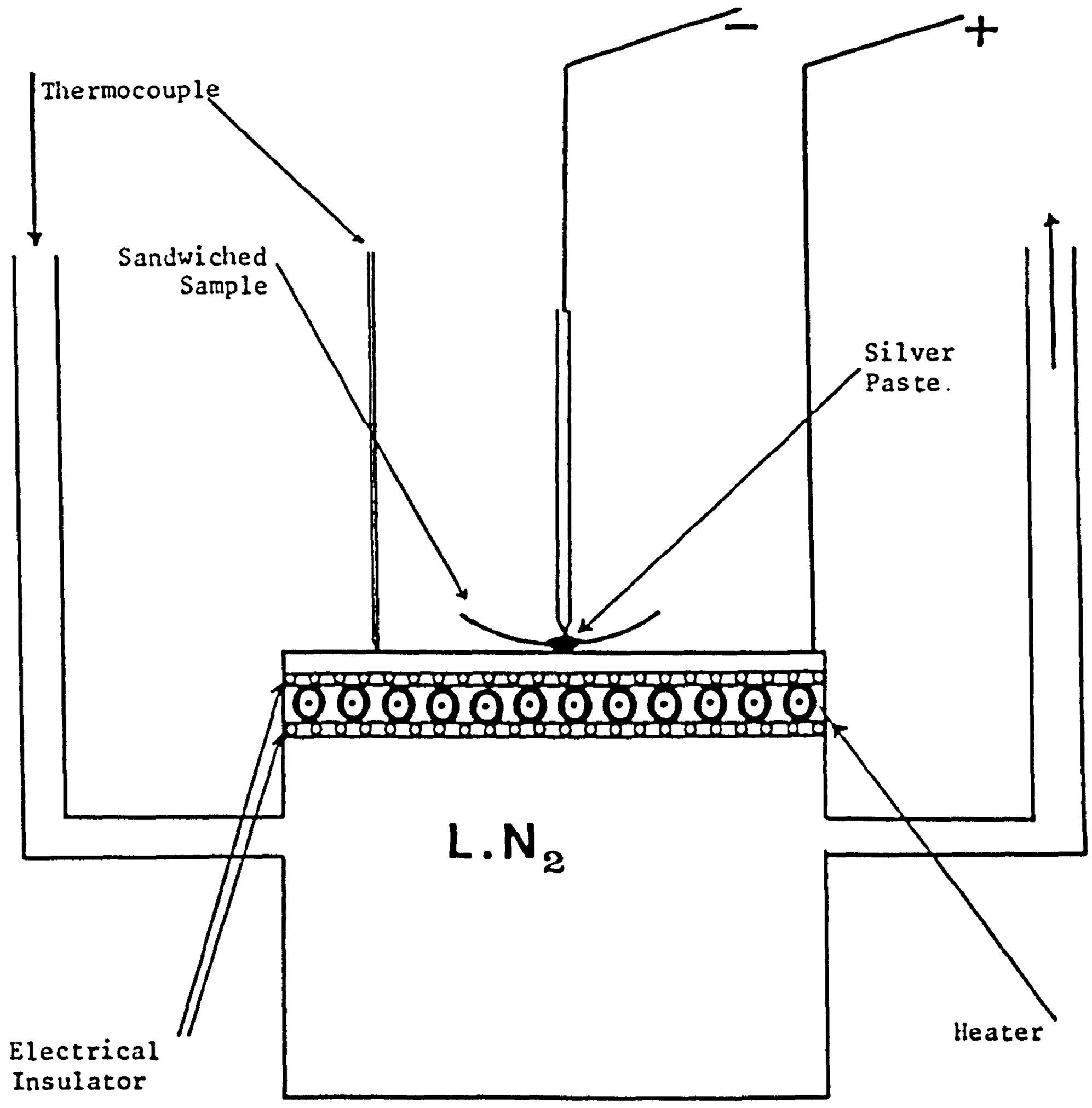

Fig.(8.1) Sample Holder, Cooling and Heating System used for High Electric Field Experiments

Fig.(8.2) Sample Holder used for Electrical Measurements at High Electric Field

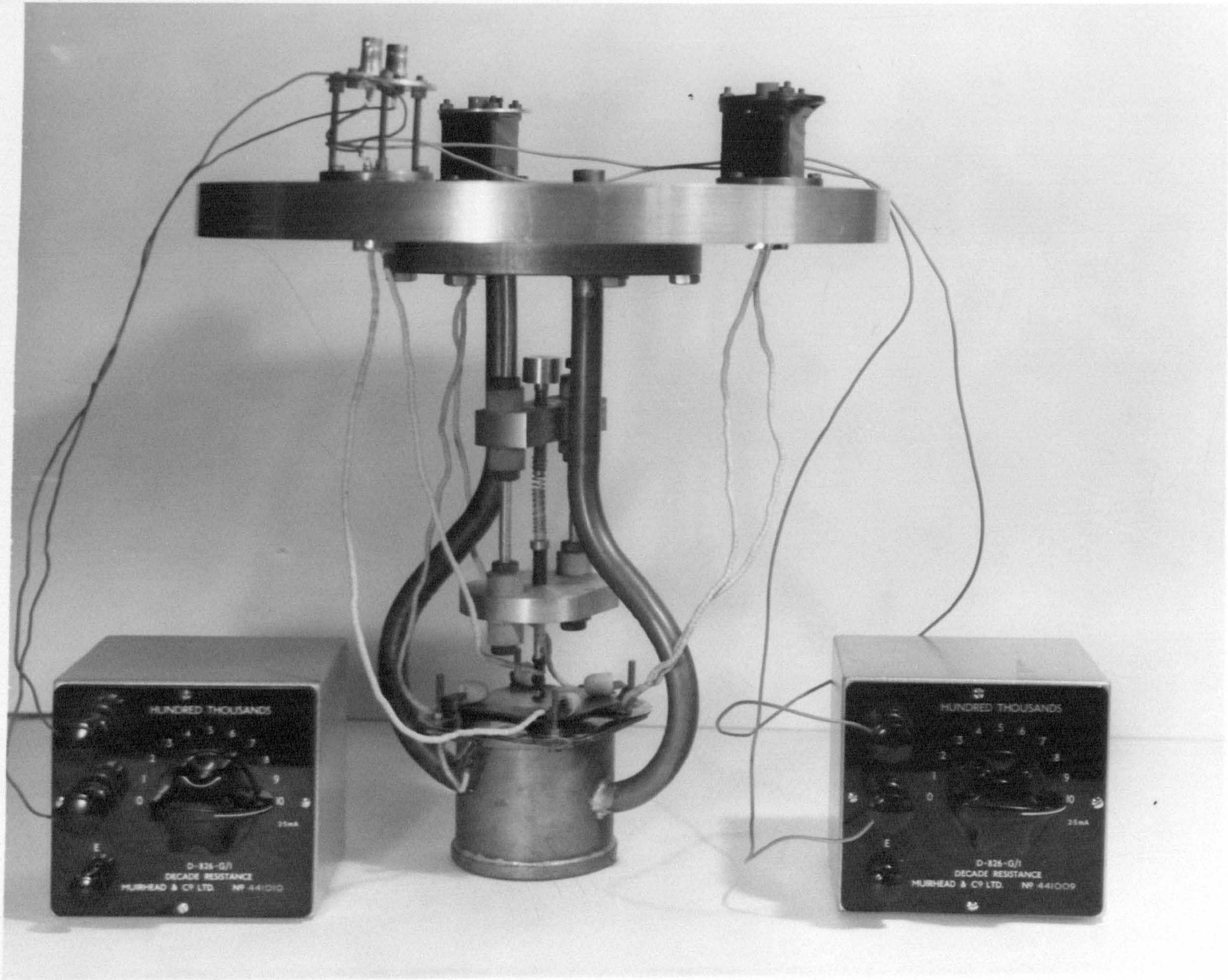

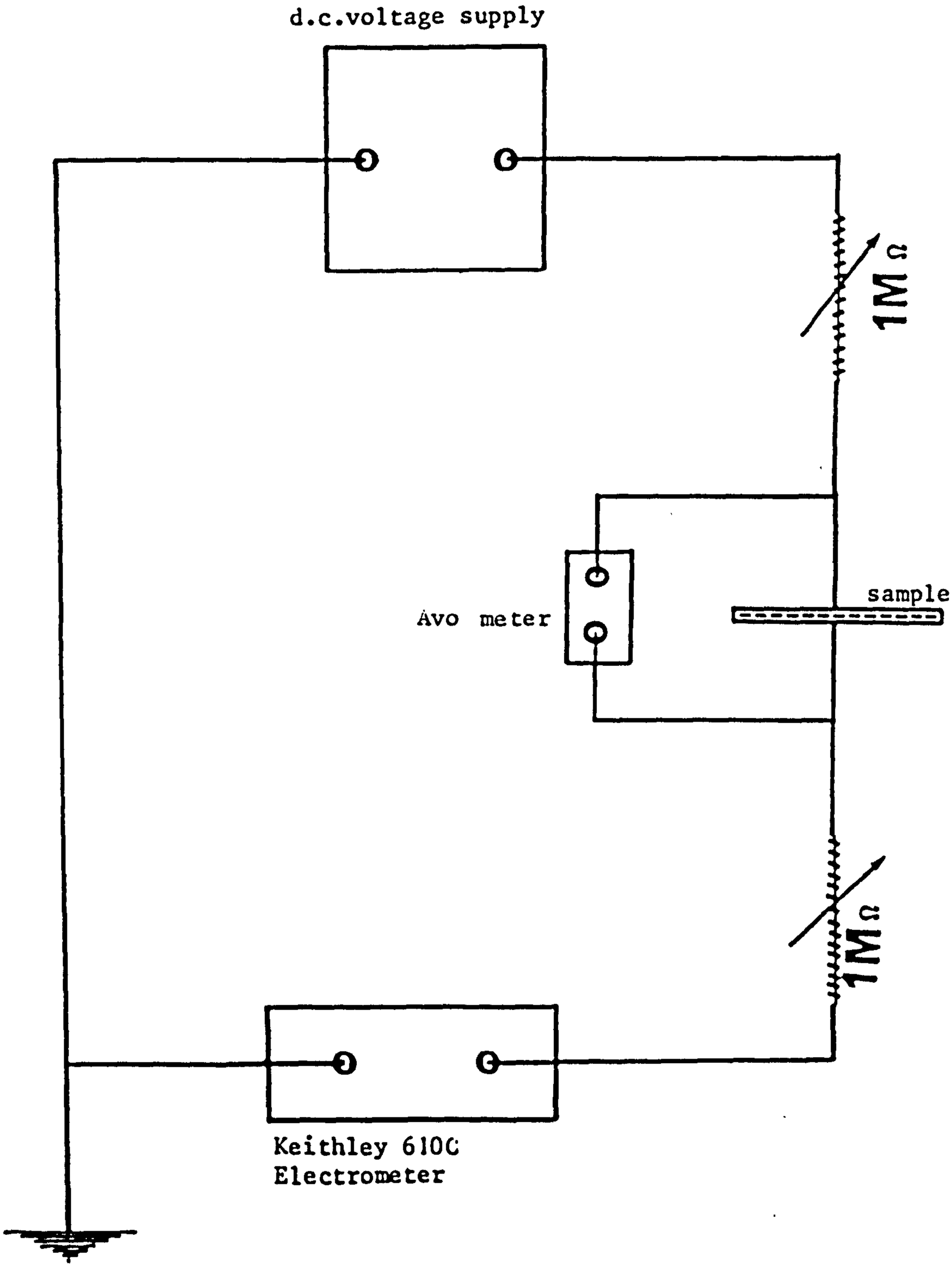

Fig.(8.3) Diagram of the Electrical Circuit for Non-Ohmic Characteristic at High Electric Field and Switching

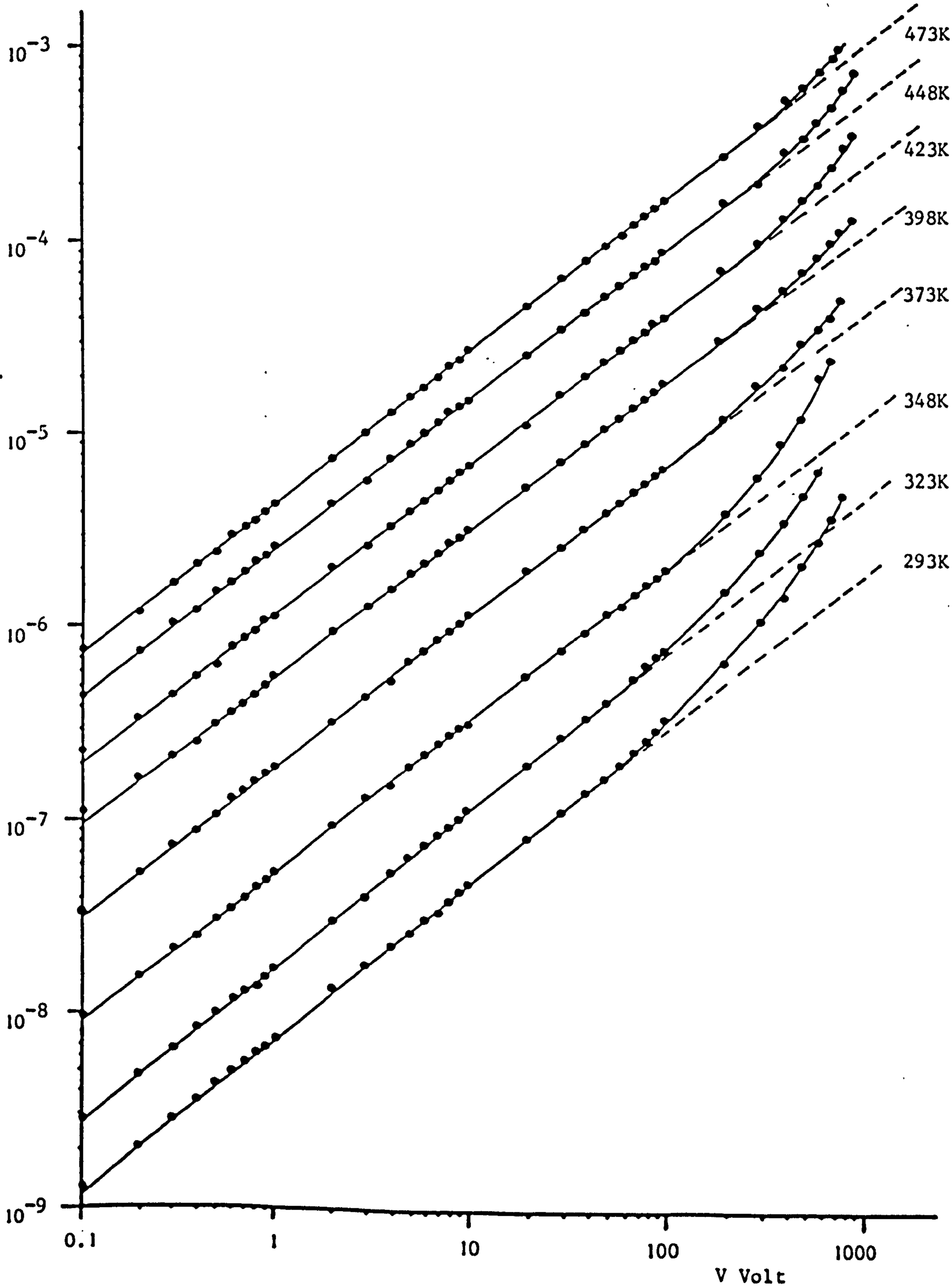

Fig.(8.4) Typical I - V Characteristic at High Electric Field for Glass No.104 at Different Temperatures. Sample Thickness 25μm

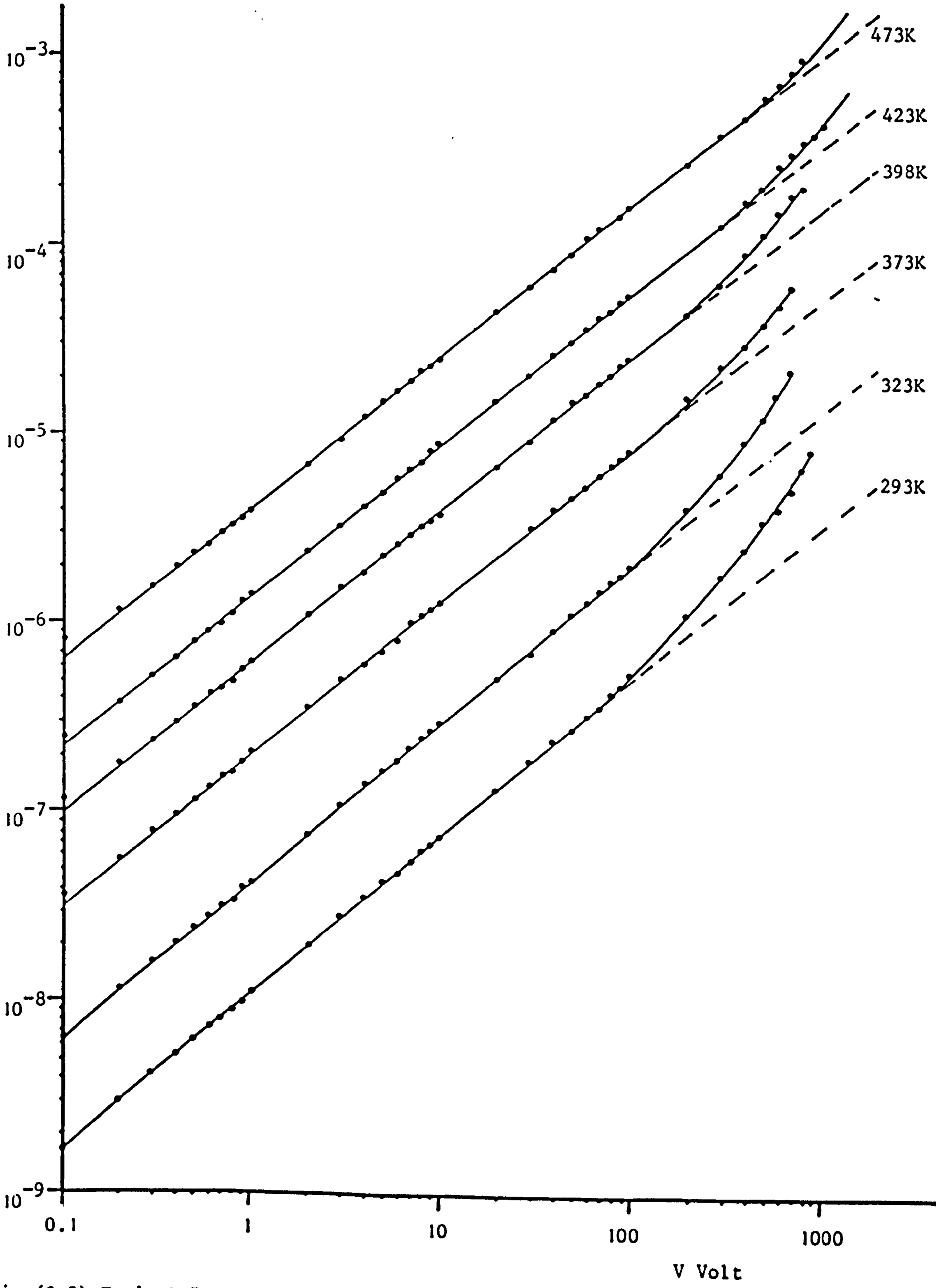

Fig.(8.5) Typical I - V Characteristic at High Electric Field for Glass No.204 at Different Temperatures

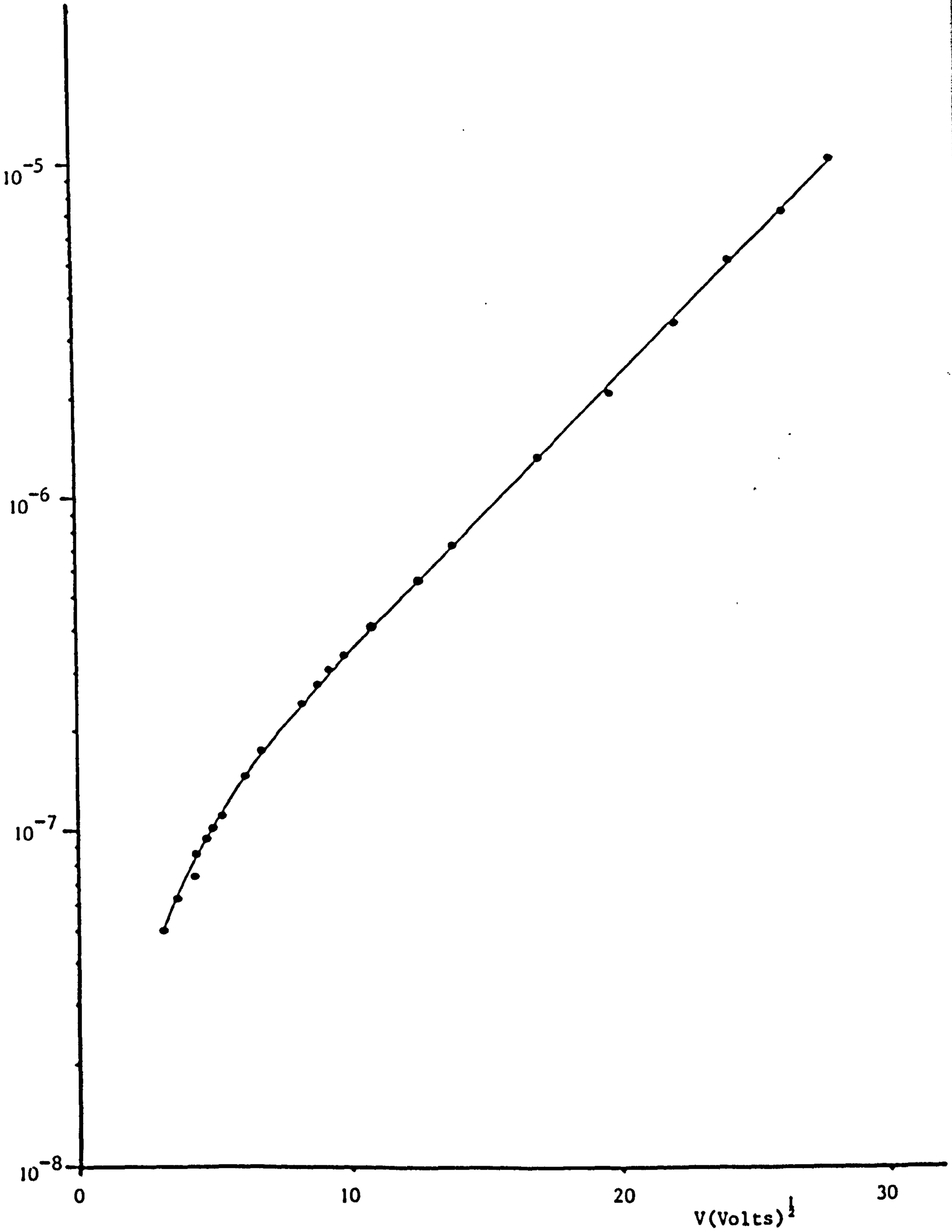

Fig.(8.6) Log I as a Function of $V^{\frac{1}{2}}$ for Glass No.104

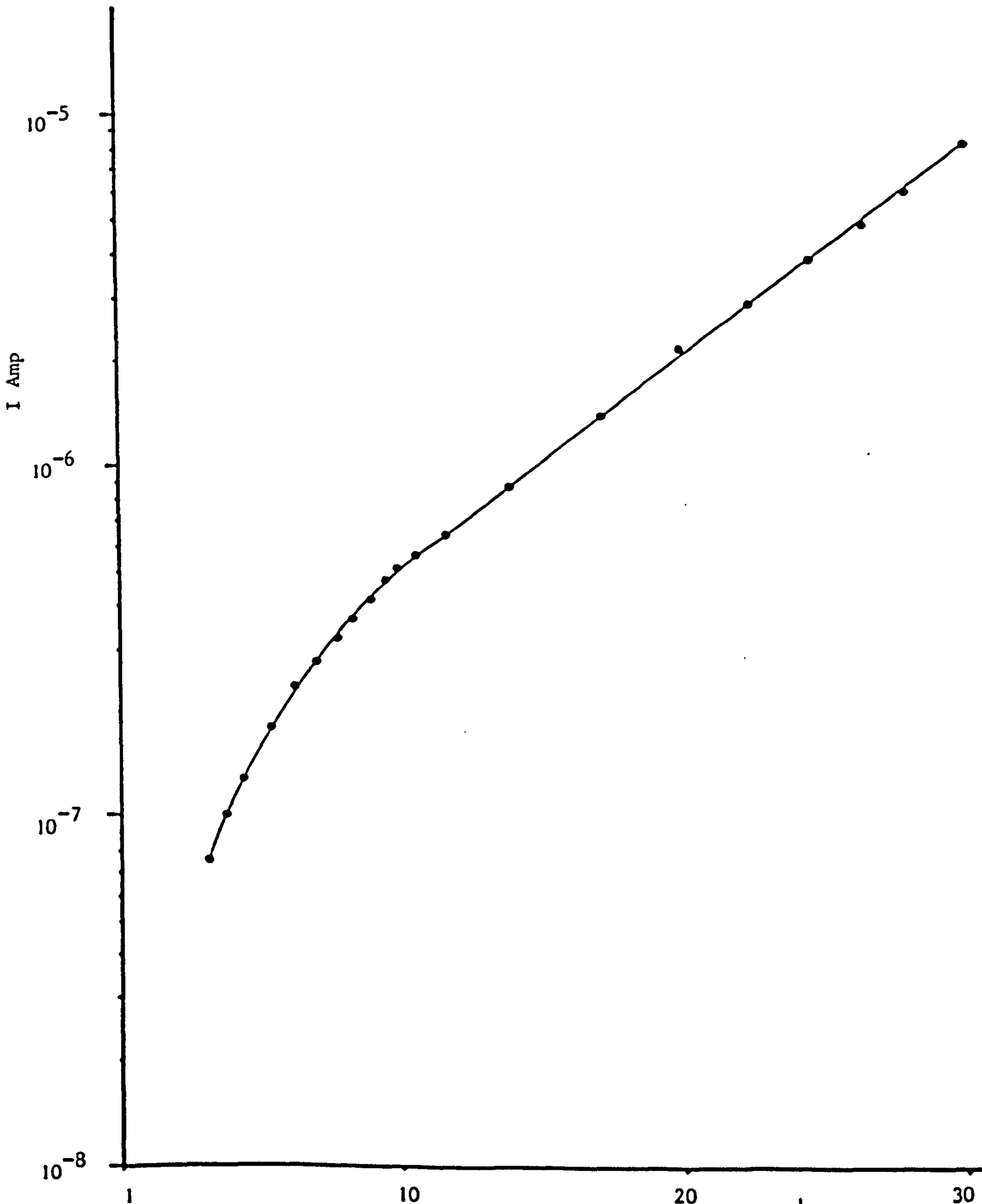

Fig.(8.7) Log I as a Function of $V^{\frac{1}{2}}$ for Glass (204)

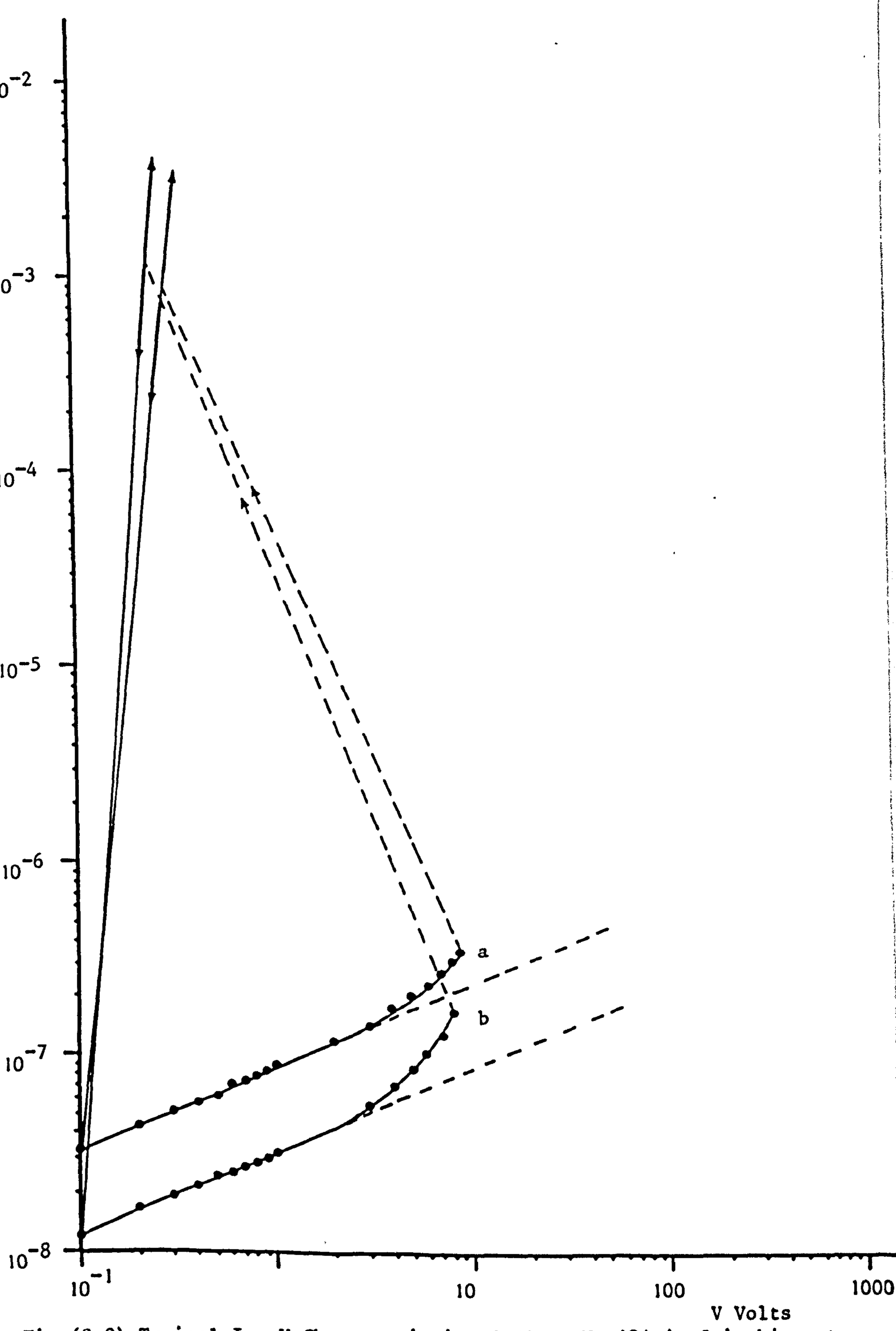

Fig.(8.8) Typical I - V Characteristic of Glass No.104 in Switching at Room Temperature (memory)

a) Sample thickness 12μm b) Sample thickness 19μm

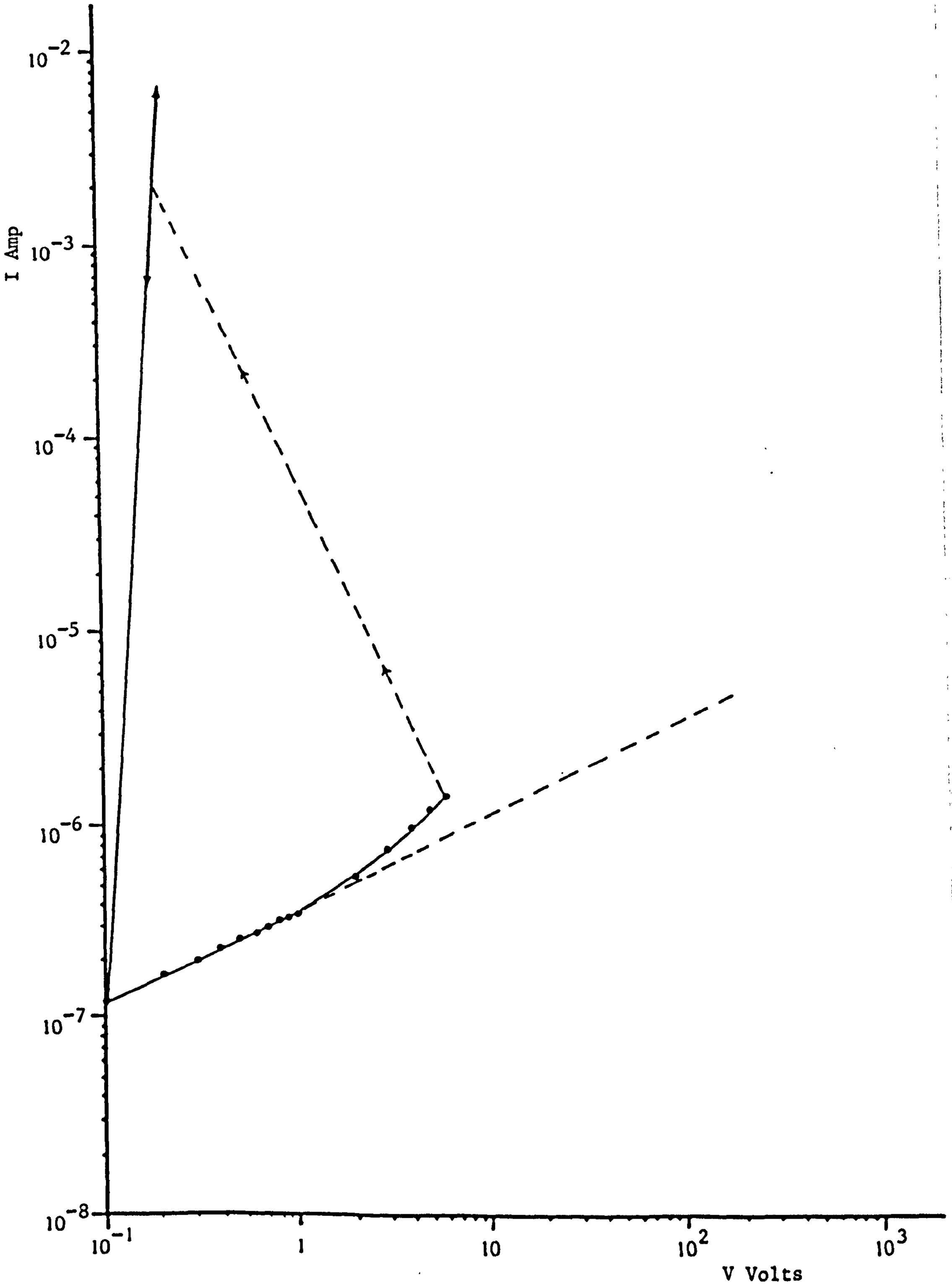

Fig.(8.9) Switching of the Sample No.104 at 40°C (memory)

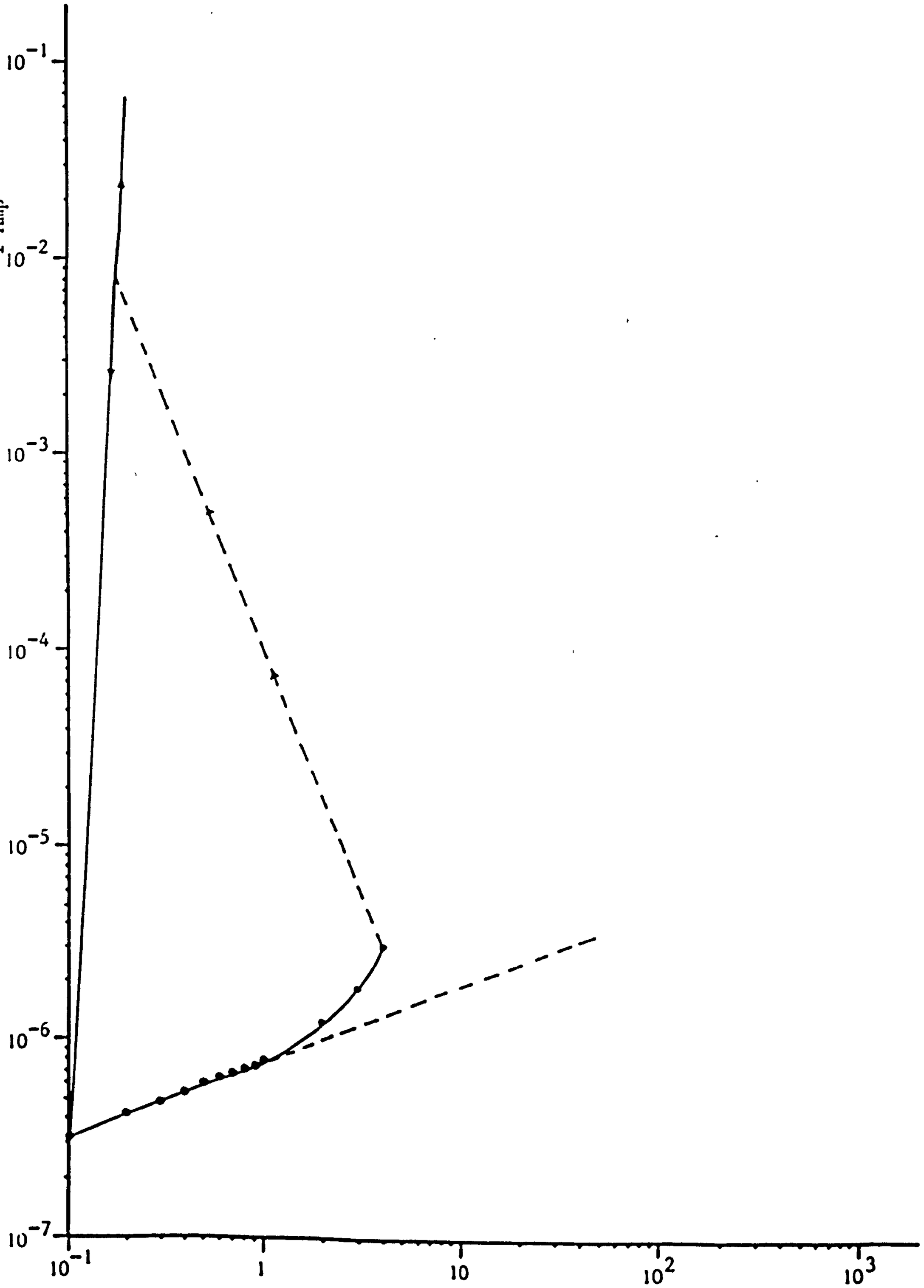

Fig.(8.10) I.V Characteristic of Sample No.104 in Memory Switch at 55°C

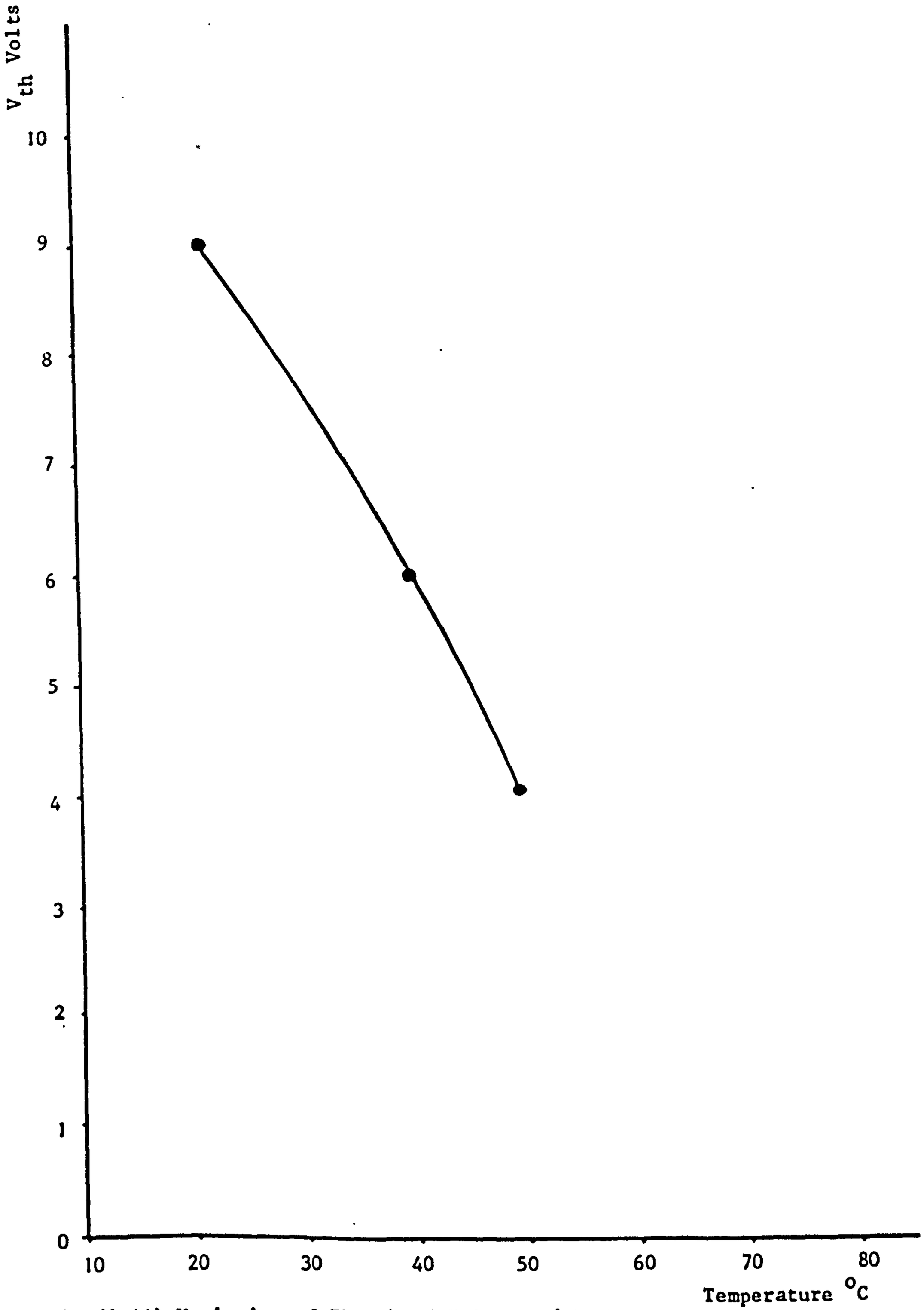

Fig.(8.11) Variation of Threshold Voltage with Temperature for Glass No.104

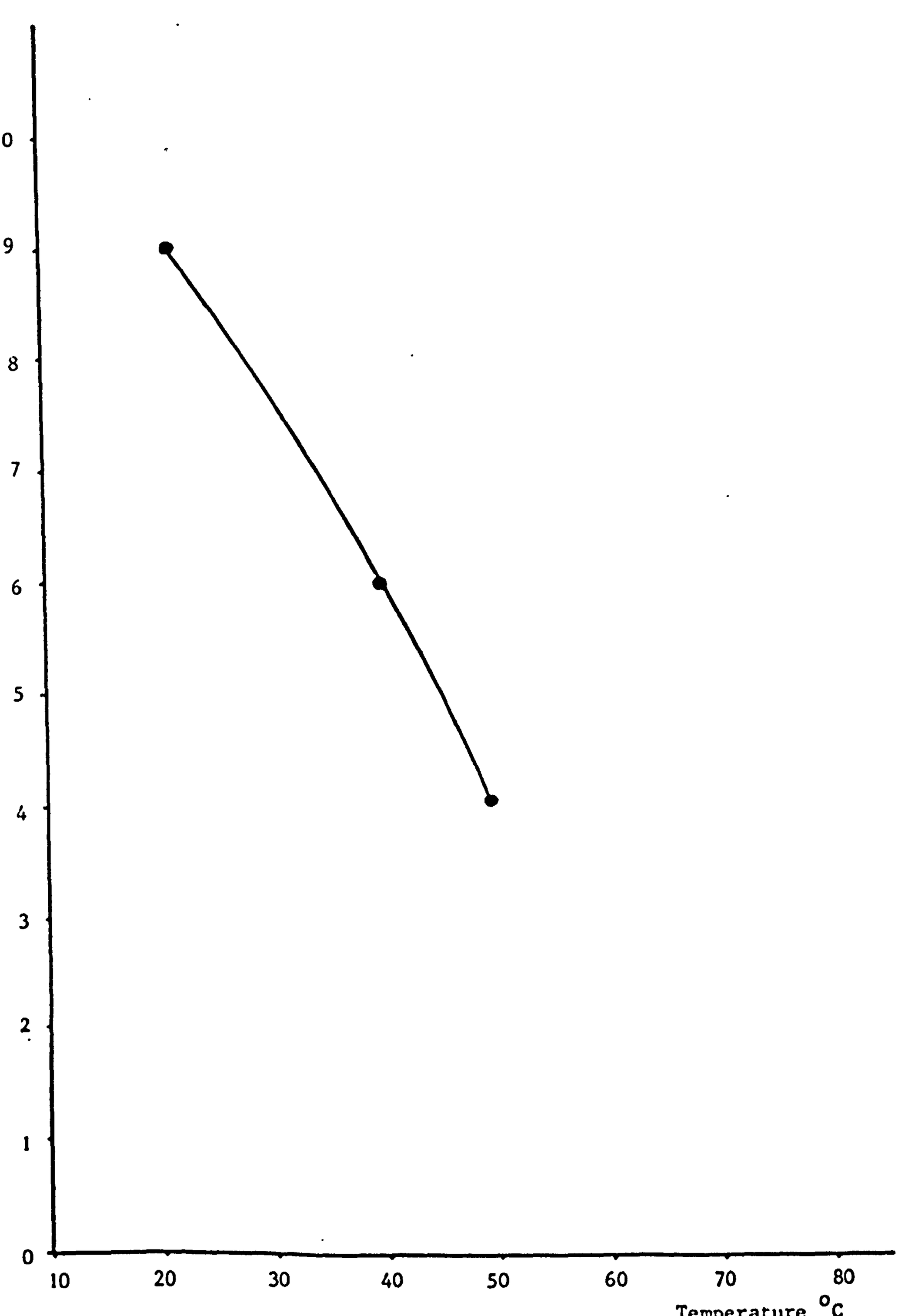

Fig.(8.11) Variation of Threshold Voltage with Temperature for Glass No.104

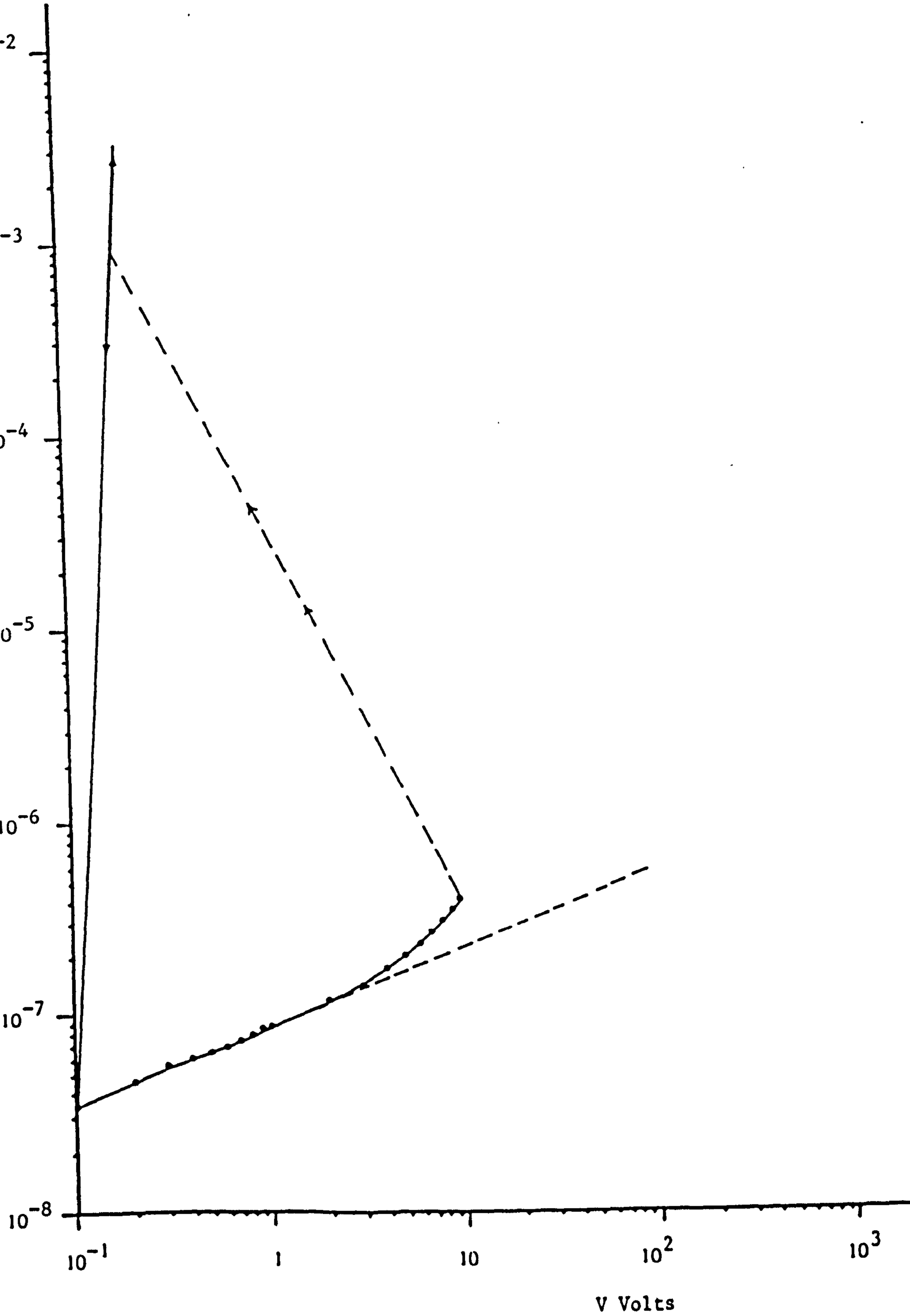

Fig.(8.12) I.V. Characteristics of Memory Switch for Glass No.205 at Room Temperature